Cyclorheniated Azabutadienes and Their Reactions with Unsaturated Molecules

THE UNIVERSITY OF
WAIKATO
Te Whare Wānanga o Waikato

A thesis submitted in partial fulfilment of the requirements for the degree of

Master of Science in Chemistry

at The University of Waikato by

Toshie Asamizu

2009

Abstract

This thesis reports the studies on the reaction of 1-azabutadienes with $PhCH_2Re(CO)_5$ to prepare the cyclometallated azabutadiene tetracarbonyl compounds of the form shown below.

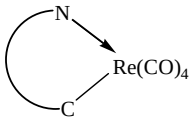

General Form of Cyclorheniated Tetracarbonyl Compound

Three 1-azabutadienes with different reactivity on the N and *C-1* carbons were prepared and their reactions with $PhCH_2Re(CO)_5$ were investigated.

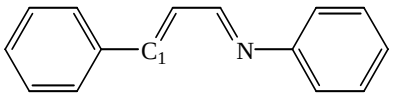

16

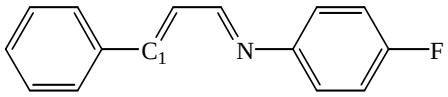

17

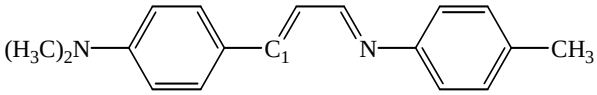

18

All the reactions gave a mixture of the cyclorheniated azabutadienes of the type **24** and the isomers **25a** and **25b** formed by CO substitution of **24** by a second azabutadiene.

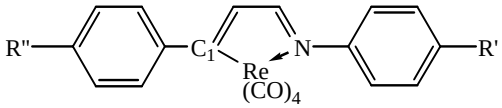

24 **Minor**

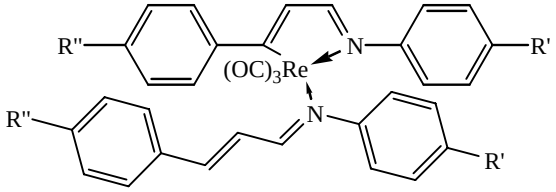

25a

Major

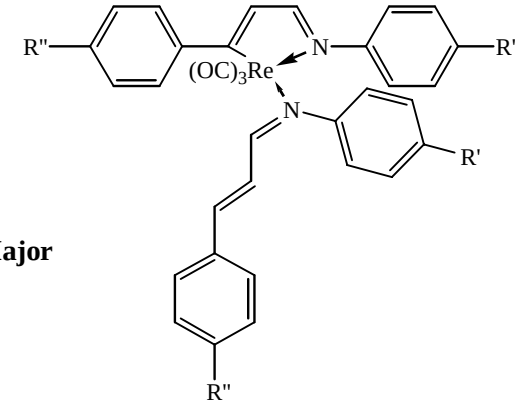

25b

The substituted derivatives **25** as the mixture were always the main products of the reactions and were obtained in good-to-excellent yield even under modified conditions intended to optimise the yield of **24**. The yield of **24** could not be improved beyond 30 %. Isomerisation of the azabutadiene about the N=C bond provided very rare *cis*-azabutadiene metal complexes **25b**. NMR studies on the mixture of the two isomers **25a** and **25b** suggested that the product ratio depended on the molar ratio of $PhCH_2Re(CO)_5$ in the reaction mixtures.

All the compounds were characterised spectroscopically as well as by microanalysis and examples of all three types were structurally determined by X-ray crystallography.

The reactions of the substituted derivative **13** as the mixture of the two isomers with unsaturated molecules including phenyl acetylene, *p*-methoxyphenyl isocyanide, and phenyl isocyanate and methyl acrylate were investigated.

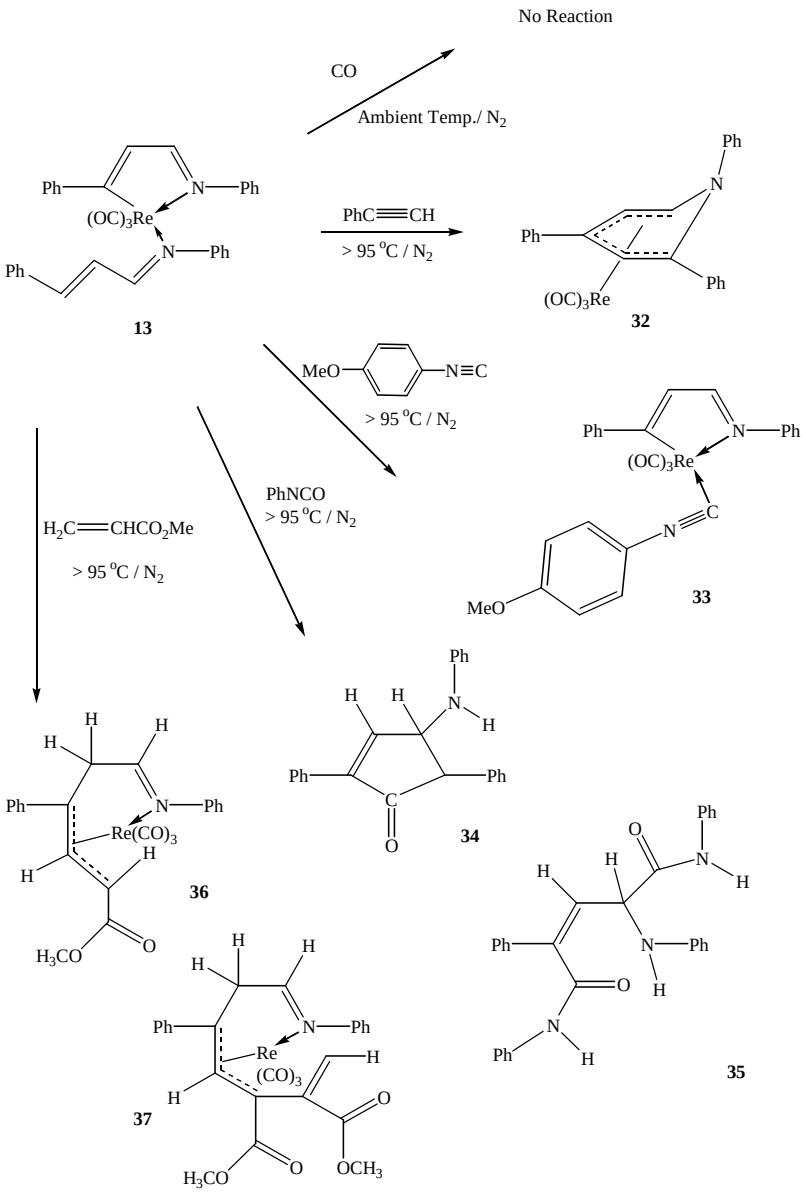

The reactions gave the Re analogues of the products obtained in the corresponding Mn reactions.

Acknowledgements

First of all, I would like to thank my supervisors, Prof. Brian Nicholson and Assoc. Prof. Lyndsay Main, for their guidance, encouragement and help throughout the course of my Masters over the last two years. Without them, it was not possible to learn so much of not only the knowledge and experimental skills, but also things needed in general.

Thank you goes to Wendy and Pat for their help during the course of the Masters in finding things needed for the research as well as the SOP trainings for the Solvent Purification System and ESI-MS spectrometry. Their kind and immediate help kept the research going without any delay.

I would also like to thank Steven, Narendra and John for sharing their knowledge and experimental techniques as the members working in the same area of the chemistry. Preparation of PLC plates and distillation of solvents were always needed in the research. Sharing and preparing them together made the works a lot easier and the research going without any difficulties.

I would like to thank Assoc. Prof. Merilyn Manley-Harris and Prof. Alistair Wilkins for their help with NMR spectroscopy. Their time and help to teach me and solve the problems with the NMR instrument helped me become much familiar with the technique and to use it in the research comfortably, which helped a lot in analysing some of the compounds that could not be characterised with other techniques.

I would also like to thank the C3.04 occupants who kindly helped me with the research to general things that I needed during the course of my Masters.

Last of all, I would like to thank my parents who supported me to do Masters at the Waikato University in New Zealand and are always supportive in everyway. I always appreciate that and hope that I made the efforts that meet your endless support.

All numbered compounds prepared in this study are listed in a fold-out section at the rear of this thesis.

Table of Contents

List of Figures

List of Schemes

List of Tables

List of Abbreviations

M	Metal atom
R	Organic substituent
L	Ligand
Me	Methyl
Ar	Aryl
Ph	Phenyl
Bu^t	*tert*-Butyl
Cy	Cyclohexyl
DMAD	Dimethyl acetylenedicarboxylate
LSR	Lanthanide shift reagent
thf	Tetrahydrofuran
Ether	Diethyl ether
MeOH	Methanol
EtOH	Ethanol
Petroleum spirits	Petroleum spirits 60 – 80 ºC (HPLC grade)
m.p.	Melting point
o	*Ortho-*
m	*Meta-*
p	*Para-*
PLC	Preparative layer chromatography
tlc	Thin layer chromatography
R_F	Retention factor
FTIR	Fourier transform infrared spectroscopy
υ	Frequency in cm^{-1}
str	Stretch
asy	Asymmetric
vs	Very strong
s	Strong
m	Medium

w	Weak
br	Broad
sh	Sharp
ESI-MS	Electrospray ionisation mass spectrometry
HR-MS	High resolution mass spectrometry
M	Molecular ion
m/z	Mass-to-charge ratio
NMR	Nuclear magnetic resonance
DEPT	Distortionless enhancement by polarisation transfer
SELTOCSY	Selective excitation totally correlated spectroscopy
HSQC	Heteronuclear single quantum correlation
HMBC	Heteronuclear multiple bond correlation
1D	One-dimensional
2D	Two-dimensional
δ ppm	Chemical shifts
J	Coupling constant in Hz
s	Singlet
d	Doublet
t	Triplet
q	Quartet
m	Multiplet
br	Broad
SPS	PureSolv solvent purification system model PS-SD-5

Chapter 1 Introduction

1.1 Introduction

1.1.1 C-H Activation and Functionalisation Using Metal Carbonyl Complexes

C-H bond activation and functionalisation using metal carbonyl complexes have been a growing research interest in synthetic organometallic and organic chemistry over the past thirty years. It is now known that C-H bonds, which are, otherwise, relatively unreactive, can be cleaved by intramolecular coordination of a hydrocarbon with a metal[1,3-4]. After cleavage of C-H bond, a new bond forms between the carbon and metal, which often leads to metallocycle or cyclometallated complex[2-4]. Early works on C-H bond activation and functionalisation by metal carbonyl complexes, are reviewed by M. Bruce[2]. Cyclometallated complexes can be useful reagents in a wide range of organic syntheses because they generally further react with organic substrates to yield promising compounds via demetallation and/or functionalisation of the hydrocarbon with the organic substrates[3,4]. Over 1,000 papers describing some aspects of C-H bond activation using metal carbonyl complexes, have been published over the past decade and many preparations of useful compounds in synthetically useful yields have been reported[1]. Transition metal carbonyl complexes are frequently used in C-H activation organic transformations as they are relatively inexpensive, especially the 3d elements, and many interesting compounds have been prepared via the metallated intermediates[5]. Chemistry of this area has advantages in that useful functionalised organic compounds can be synthesised from relatively inexpensive or abundant organic substrates such as alkenes[4].

1.1.2 Cyclometallation and Orthometallation Reactions

1.1.2.1 Cyclometallation

Cyclometallation is a reaction of a metal that undergoes intramolecular coordination with a hydrocarbon followed by cyclisation, leading to a metallocycle or cyclometallated compound[1-3, 6]. Formally, it may be defined as "the reaction of a metal complex in which a C-H bond of the ligand undergoes *Oxidative Addition* to the metal to yield a cyclic alkyl complex"[6]. The new carbon-metal bond is usually σ-bond[7]. Some definitions[7], however, include metal-carbon π-bond as a cyclometallated intramolecular coordination compound. A general cyclometallation reaction[2] is shown in the scheme below.

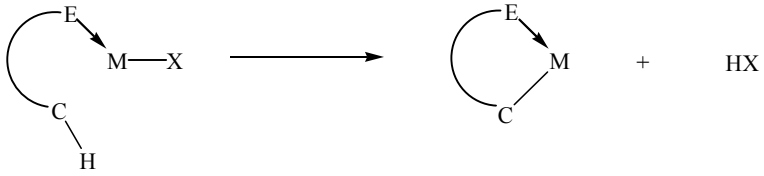

Scheme 1-1: General Cyclometallation Reaction; E = any atom or bond capable of forming a coordinate bond; M = a metal; X = an appropriate leaving group (from Bruce[2]).

Donor ligand, E, coordinates to the metal centre of the complex usually by lone pair donation followed by cyclisation, forming a new bond between the hydrocarbon and metal[2, 7-12]. E can be any atom which is capable of a dative bond to a metal centre and is called "σ-donor"[2, 7-12]. The best studied σ-donor is, probably, N, but O, S and P are also common as σ-donors[2, 7-12]. Examples of cyclometallated compounds from As[13, 14] and Se[15] as a donor atom are also known. Terminal C-H of the ligand preferentially undergoes oxidative addition to the inner C-Hs mainly because of entropic reasons[1] e.g. less steric hindrance.

Cyclometallated rings may have some degree of aromaticity[16]. The favoured ring size is a five-membered mainly due to entropic reasons and is probably the most popular ring size for

cyclometallated compounds[16, 17]. Cyclometallated rings with a non-carbon atom such as phosphorus and nitrogen usually exhibit different properties from those containing only carbon atoms. Heteroaromatic rings may, therefore, sometimes be excluded as a cyclometallated compound[7, 15, 18-19].

1.1.2.2 Orthometallation Reaction

Orthometallation is a reaction in which metal preferentially substitutes at *ortho*-position of the aromatic ring to the other positions and, therefore, also called "o*rtho-directing substitution reaction*"[20]. The ortho-substituent of an aromatic ring, which is usually hydrogen, is removed and replaced with a metal through an *Oxidative Addition* or *β-Elimination* reaction mechanism to usually yield a metallocycle[20]. Orthometallation reactions are well developed for palladium(II) and platinum(II) ions with N-donor aromatic ligands such as azabenzene, benzylamines and 2-phenylpyridines[2, 7, 21]. Little was, however, known about orthometallation of aryl ketones which was an O-donor substrate. Aromatic ketones were known not to normally undergo orthometallation reaction because electophilic substitution at the α-carbon of the ketone preferentially takes place and also the carbonyl is *meta*-directing in electophilic aromatic substitution[5]. Orthometallated aromatic ketones could not be obtained even with the metals which would normally undergo orthometallation with the other donors such as N, S and P[22, 23-26]. In the mid-1970s, however, orthomanganation of aryl ketones such as acetophenones with $MeMn(CO)_5$, was first reported by Kaesz's group, which revealed that orthocyclomanganated aryl ketone complexes could be prepared (Scheme 1-2)[27-32].

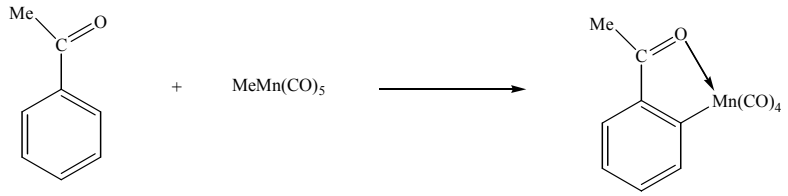

Scheme 1-2: Reaction of Acetophenone with $MeMn(CO)_5$

The reaction was also the first example of a direct preparation of orthometallated aryl ketones. Only rhenium, but no other metals, was known to undergo similar reactions[27].

1.1.3 Cyclomanganation and Orthomanganation of Aromatic and Heteroaromatic Ketones

Kaesz's works inspired the systematic studies on orthomanganation of aromatic, heteroaromatic, and non-aromatic ketones, carried out at the University of Waikato over twenty years, which were reviewed in the literature[5]. The orthomanganation of aryl ketones was of interest because the orthometallated aryl ketones could be used in functionalisation of aryl ketones at the *ortho*-position via displacement of the metal with another metal or coupling to other non-metal substrates[5]. A series of cyclomanganated compounds were prepared from a range of aromatic ketones including acetophenones, benzophenones, quinones, aromatic aldehydes, aromatic esters, *N*-acyl heteroaromatics and heteroaromatic ketones[5]. Orthomanganation of benzamide was also attempted, but no orthomanganated product was obtained. Dimethyl benzamide could, however, be cyclometallated[5].

Kaesz's reaction (Scheme 1-2) was found to be general for a variety of aromatic and heteroaromatic ketones[5]. The reaction also tolerated a wide range of substituents on the benzene rings such as Me, CF_3, OMe, Br, Cl, F, CN, $OSiR_3$[5]. An alternative indirect metallation route has also been reported by Haupt and co-workers (Scheme 1-3)[33].

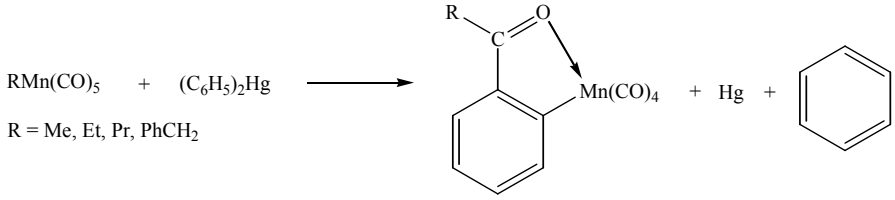

Scheme 1-3: Indirect Route to Orthomanganated Aryl Ketones

General structures of orthomanganated compounds from reactions of $PhCH_2Mn(CO)_5$ with aromatic and heteroaromatic ketones, aromatic aldehydes, aromatic esters, benzamides, *N*-acyl heteroaromatics are listed below.

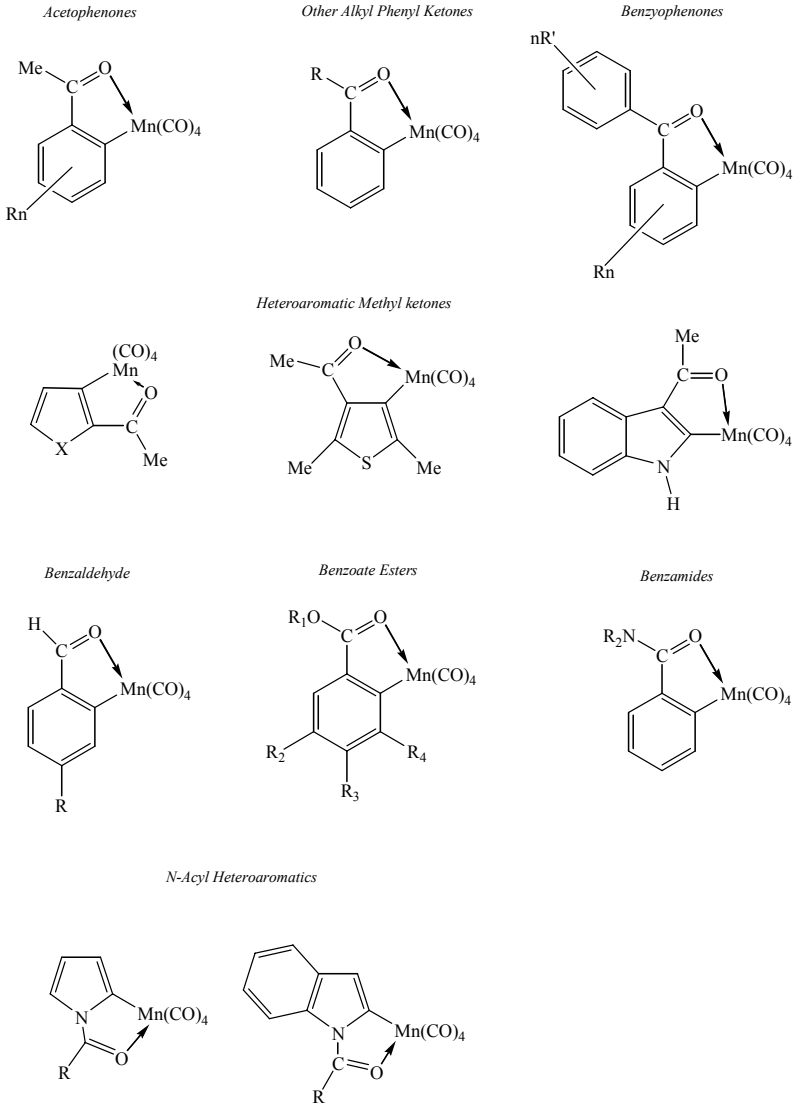

Figure1-1: General Structures of Some Orthomanganated Compounds[5]

All form cyclomanganated rings with the O donor of the ketone[5]. The geometry of the cyclometallated ring is essentially constant in a wide range of derivatives[5]. The metallocycle is essentially planar with some degree of aromaticity indicated by a slightly longer C=O and shorter C-C bond distances than expected for a true double and single bond, respectively[5].

These are also consistent with the results of Fenske-Hall MO calculations[34], which led to a suggestion that the rings can be viewed as a manganafuran species[5].

Heteroaromatic ketones such as various acetyl-thiophenes can also be orthomanganated and obtained in a synthetically useful yield[5]. Those with furans and *N*-methylpyrroles are usually obtained in very low yield[5]. Lower aromaticity of the heterocyclic rings may be responsible for the low yields. Cyclomanganation with *N*-acyl heteroaromatics gives *N*-acetyl-pyrrole and -indole (Figure 1-1) in a good yield, which show different spectroscopic properties from those for the cyclomanganated aryl ketones as expected for the metallocycle with the N incorporated into the ring[5].

1.1.4 Reaction of Cyclomanganated Aromatic and Heteroaromatic Ketones

1.1.4.1 General Properties of Cyclomanganated Compounds

Orthometallated compounds are generally easy to handle, usually stable towards oxidation, very soluble in any organic solvent and would not decompose by normal chromatography on silica or alumina[5]. This makes orthomanganated aromatic ketones a useful reagent in organometallic and organic syntheses and also for investigations into the o*rthofunctionalisation* of aromatic ketones via cyclomanganated compounds[5]. Their reactivity towards organic substrates including alkenes, alkynes and isocyanates, electrophiles, HCl, and oxidising agents has been investigated[5].

1.1.4.2 Reaction with Alkenes

Orthomanganated aromatic ketones undergo coupling reactions with alkenes such as methyl acrylate and methyl vinyl ketone in the presence of Li_2PdCl_4[5]. Arylalkane, arylalkene, and indene can be obtained as the main products in an excellent yield. A minor amount of the parent ketone through demetallation can also be isolated[5].

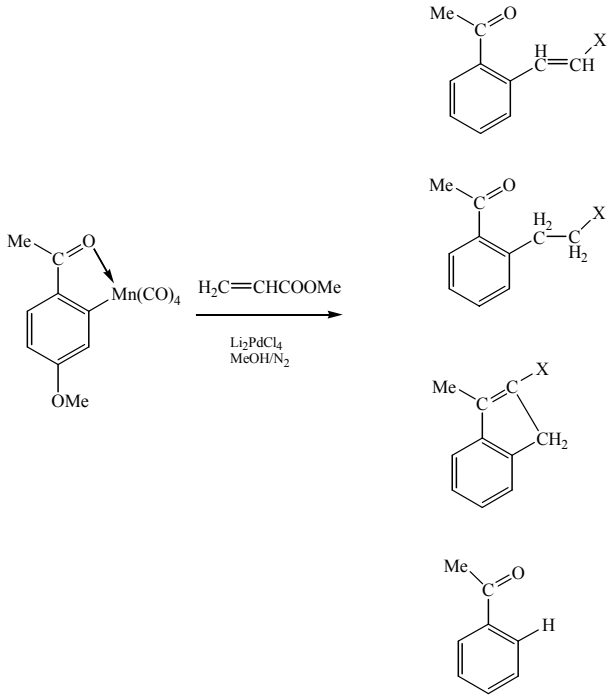

Scheme 1-4: Reaction of an Orthomanganated Aryl Ketone with Methyl Acrylate in the Presence of Li_2PdCl_4[5]

The yield of arylalkane can be improved if orthomanganated esters are used, providing only minor amount of arylalkene which is the favoured product in the reaction of orthomanganated aromatic ketones[5].

Cyclomanganated heteroaromatic ketones such as η^2-(acetylthienyl)tetracarbonyl manganese also undergo coupling reactions with a variety of alkenes in the presence of Li_2PdCl_4/MeOH, leading to a range of coupling products (Scheme 1-5)[5].

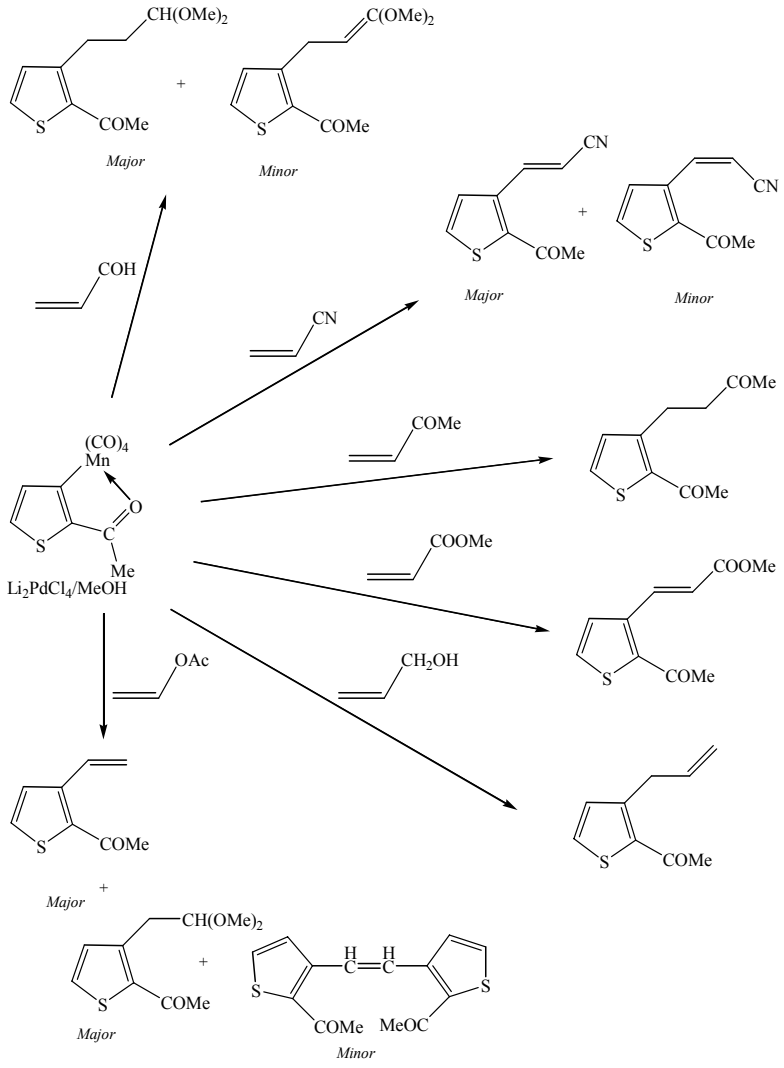

Scheme 1-5: Coupling Reactions of Cyclomanganated Heteroaromatic Ketones with Alkenes in the Presence of Li_2PdCl_4[5]

1.1.4.3 Reaction with Alkynes

Reaction of orthomanganated aromatic ketones with alkynes gives inden-1-ols via thermal or Me_3NO activation methods[5]. Yields can greatly vary with the choice of solvents and alkynes[5].

With unsymmetrical alkynes such as PhCCH, Me_3SiCCH and Pr^nCCMe with a bulky group at the 2-position of the inden-1-ol, yields can significantly be increased[5]. A variety of indenes with different substituents at the 1, 2, 3 positions can be prepared with the appropriate choice of starting ketone and alkyne[5]. The scheme below shows the reaction of η^2-(2-acetylphenyl)tetracarbonyl manganese with PhC≡CPh under thermal condition[5] as an example.

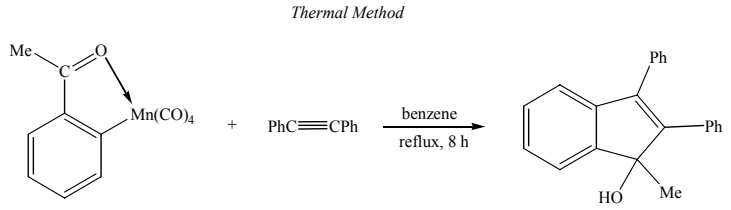

Scheme 1-6: Reaction of η^2-(2-Acetylphenyl)tetracarbonylmanganese with PhC≡CPh Under Thermal Condition[5]

Similarly, reaction of cyclomanganated heteroaromatic ketones with alkynes gives inden-1-ols under thermal condition. The reaction of manganated *N*-acetylindole with dimethyl acetylenedicarboxylate (DMAD) under thermal method provides a tricyclic species (Scheme 1-7) [5].

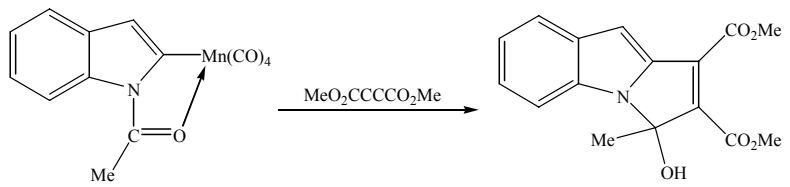

Scheme 1-7: Reaction of Manganated *N*-Acetylindole with DMAD under Thermal Method[5]

The tricyclic product consists of the core of the mitomycin class of antibiotics[35], which may benefit further investigations.

1.1.4.4 Reaction with Isocyanates

Reaction of cyclomanganated aromatic ketones with isocyanates provides 3-alkylidene phthalimidines which is found in a number of isoindole-derived alkaloids via the intermediate 3-methylidene phthalimidines as the core unit. Various substituents can be incorporated into the 3-alkylidene phthalimidines intermediate[36] (Scheme 1-8).

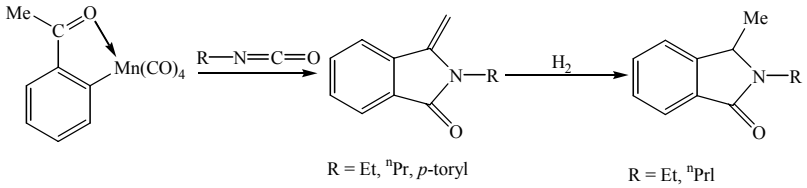

Scheme 1-8: Reaction of η^2-(2-Acetylphenyl)tetracarbonylmanganese with Isocyanates[36]

1.1.4.5 Reactions with Electrophiles

With $HgCl_2$, transmetallation reaction occurs to give the corresponding orthomercurated product[5] (Figure 1-2).

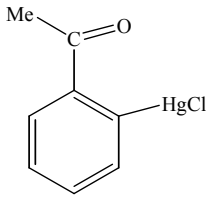

Figure 1-2: Orthomercurated Aryl Ketone

This indirect mercuration of a substrate with a ketone group may have advantages over the other methods in which use of aryl lithium or Grignard reagents may be required, incompatible with C=O[5].

Demetallation of orthomanganated aromatic ketones also occurs with bromine or iodine chloride[5]. Iodine chloride appears to be more selective to substitute the metal than bromine[5]. Bromine also has some other synthetic limitations e.g. fast deprotonation over demetallation and M-C bond resistance etc.[5].

Reaction of orthomanganated acetophenone showed an unexplored potential of cyclomanganated compounds in organometallic and organic syntheses by the unusual *in situ* formation of a P-P bond as the dimanganese complex **2** formed via initial formation of the phosphine-substituted compound **1** which was originally the expected product[5].

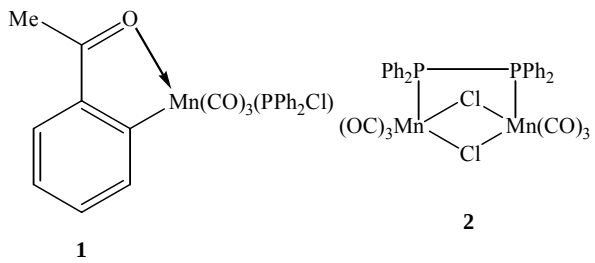

1 **2**

Figure 1-3: Phosphine-substituted Compound **1** and Dimanganese Complex **2**

Orthomanganated aromatic ketones undergo demetallation with HCl in MeCN[37]. A systematic study on demetallation of orthomanganated aryl carbonyl compounds has, however, not been carried out[5].

1.1.4.6 Reactions with SO_2

Orthomanganated triphenylphosphine chalcogenides[38] and aromatic ketones[39] give the S-sulfinato products **3** and **4**, respectively, via insertion of SO_2 into the Mn-C bond (Figure 1-4). The dimanganese product **5** can be obtained as by-product in some cases[38, 39].

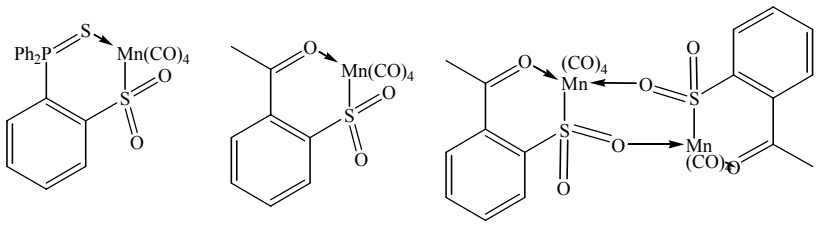

3 **4** **5**

Figure 1-4: S-Sulfinato Products **3**, **4** and **5**

1.1.5 Cyclomanganation of Non-Aromatic Ketones

Cyclomanganated non-aromatic ketones of the type below e.g. enones (Figure 1-5) the structure of which is analogous to that of aromatic ketones, can be prepared directly or indirectly via cyclomanganation reaction[5].

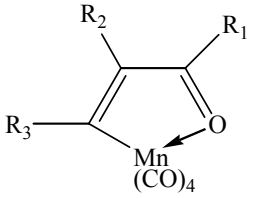

Figure 1-5: General Structure of Cyclomanganated Non-Aromatic Ketones

Cyclomanganated non-aromatic compounds were first prepared indirectly from alkynes in 1968 by Harbourne and Stone (Scheme 1-9)[40].

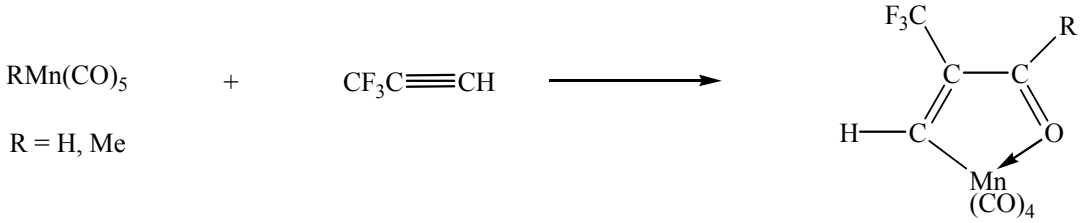

Scheme 1-9: Indirect Route to Non-Aromatic Manganocycle[40]

The further studies carried out by Booth and Hargreaves showed the general reaction of $HMn(CO)_5$ or $RMn(CO)_5$ (R = Me, Ph) with alkynes to give a range of cyclometallated α, β-unsaturated ketones (Scheme 1-10)[41, 42].

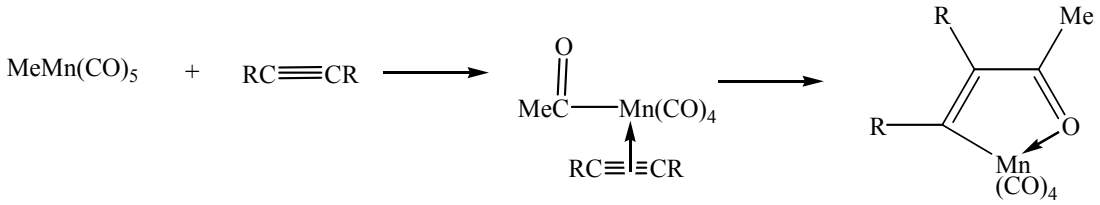

Scheme 1-10: General Route of Cyclomanganated α, β-Unsaturated Ketones [41, 42]

The η^5-by-product **6** can also be isolated from the reactions and assumed to form via double alkyne insertion and cyclisation[5].

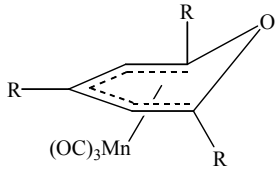

6

Figure 1-6: the By-Product **6**

More recent studies show that these indirect cyclomanganation reactions tolerate $PhCH_2Mn(CO)_5$ as the starting complex and also a wider range of alkynes can be incorporated into the reaction[37]. These indirect reactions have advantages in that relatively unreactive manganese complexes will undergo a reaction under low pressures in the range 2 – 10 kbar[37]. Moreover, unsymmetrical alkynes usually undergo a regiospecific insertion, so only one isomer of the manganocycles can be formed[37] although there are some others which are less regiospecific and give both isomers with either of the isomers slightly favoured[37]. These indirect routes for cyclomanganation of non-aromatic ketones can provide a variety of cyclomanganated α, β-unsaturated ketones using a range of alkynes[37].

Direct cyclomanganation of α, β-unsaturated ketones (chalcones) with $MeMn(CO)_5$ and $PhCH_2Mn(CO)_5$ [5] to give cyclomanganated non-aromatic ketones have also been reported, as shown in the scheme below[5].

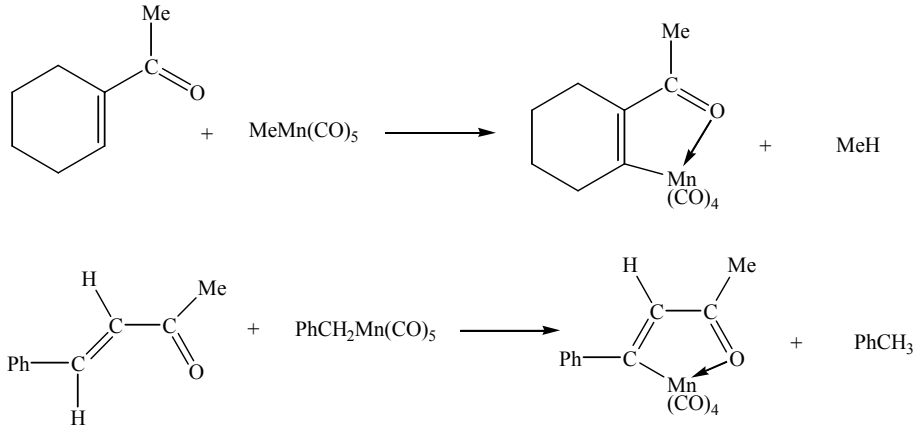

Scheme 1-11: Direct Cyclomanganation Reaction of α, β-Unsaturated Ketones with $MeMn(CO)_5$ and $PhCH_2Mn(CO)_5$[5]

These direct syntheses have advantages of using inexpensive α, β-unsaturated ketones as reagents compared to those from alkynes[5]. A wide range of cyclomanganated non-aromatic ketones can also be prepared via these direct methods[5].

Cyclomanganated compound has also been prepared from dienones[43]. Cyclomanganated dienone complex of the type below can be obtained[43].

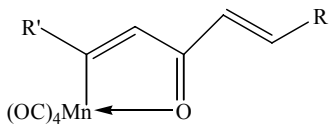

Figure 1-7: Cyclomanganated Dienone

A saturated analogue of cyclomanganated enones of the type below can also be prepared in the corresponding reactions of cyclomanganation of $RMn(CO)_5$ (R = Me, $PhCH_2$) with alkenes under high pressures[37, 44].

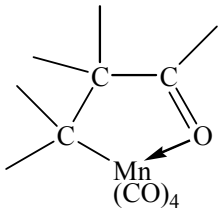

Figure 1-8: Cyclomanganated Complex from Alkenes[5]

1.1.5.1 Reaction of Cyclomanganated Enones and Dienones

Cyclomanganated enones have been shown to undergo interesting reactions involving the M-C bond with unsaturated reagents to yield useful derivatives.

1.1.5.2 Reaction with Alkenes

Reaction of cyclomanganated enones with alkenes such as methyl acrylate and methyl vinyl ketone under thermal conditions gives a different product whether in carbon tetrachloride or acetonitrile as the solvent[45].

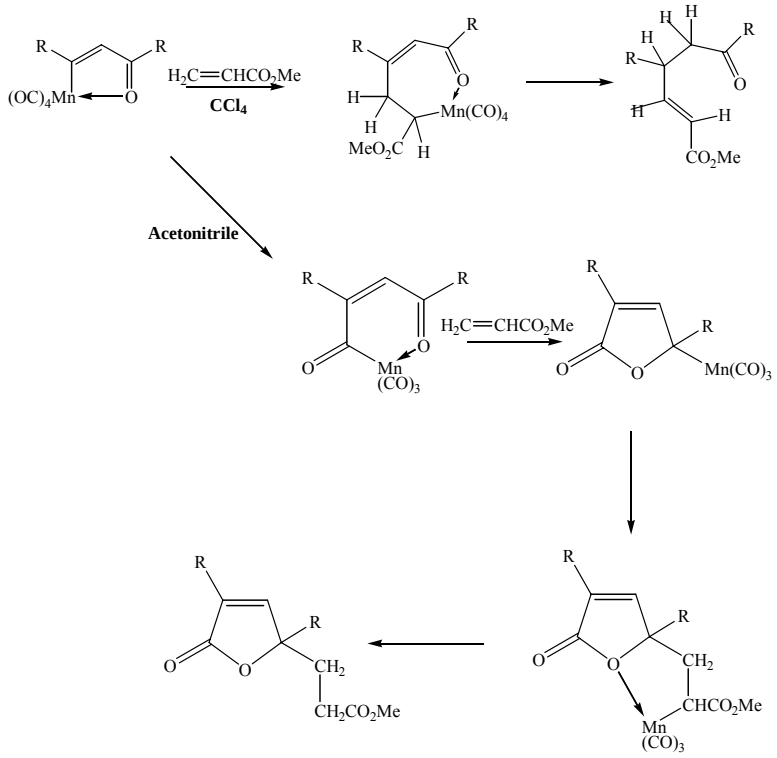

Scheme 1-12: Reaction of Cyclomanganated Enones with Metyl Acrylate in CCl_4 and Acetonitrile

In carbon tetrachloride as the solvent, a methyl acrylate inserts into the M-C bond followed by demetallation to give the insertion and demetallation product in an excellent yield. In acetonitrile, insertion of a CO ligand of the metal into the M-C bond occurs prior to insertion of the alkene. The CO inserted ring undergoes cyclisation to give a furanyl ring followed by insertion of the alkene into the Mn-$C_{furanyl}$ bond to form the cyclopentanol compound (Scheme 1-12)[45]. Substituted furan compounds can be prepared by this route. Other examples of reaction of cyclomanganated enones with alkenes to give the cyclopentenol compound is also shown in the scheme below[45].

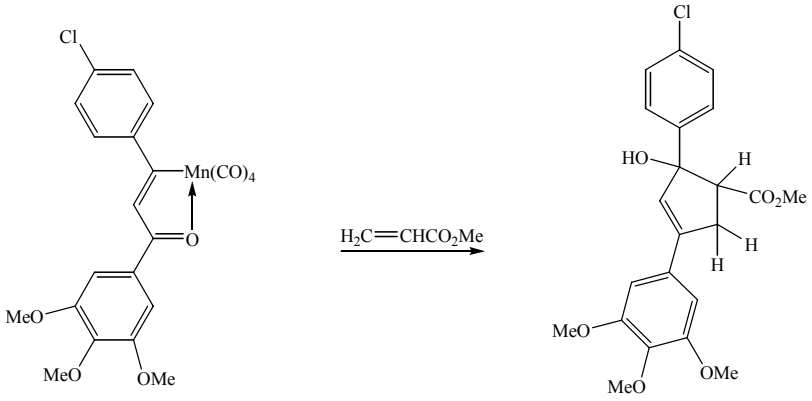

Scheme 1-13: Reaction of Cyclomanganated Enones with Methyl Acrylate in Acetonitrile[45]

1.1.5.3 Reaction with Alkynes

Reaction of cyclomanganated enones with alkynes have been shown to yield a six-membered ring with a $Mn(CO)_3$ group attached to one face of the η^5-pyranyl ring[5] (Scheme 1-14) Other cyclometallated enones and Ph_2C_2 also give similar complexes[5].

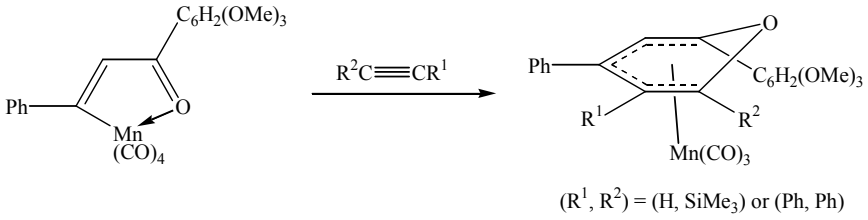

Scheme 1-14: Reaction of Cyclomanganated Chalcone with Alkyne[5]

Initial insertion of the alkyne into the Mn-C bond of the cyclomanganated enones gives a seven-membered ring intermediate **7**, which then undergoes rearrangements to form the six-membered ring, loss of a CO from the $Mn(CO)_4$ and a change of coordination from η^2 to η^5 to give the product[5].

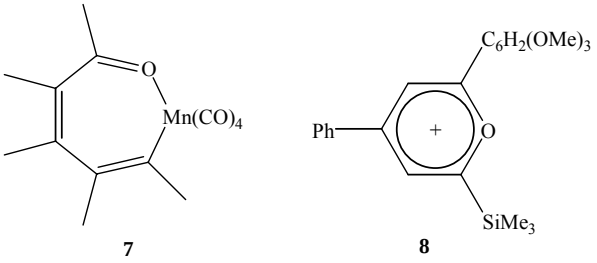

7 **8**

Figure 1-9: Seven-membered Ring Intermediate **7** and Pyrylium Cation **8**

The η^5-pyranyl ring-$Mn(CO)_3$ complex is analogue of the by-products in the preparation of cyclometallated compounds from $RMn(CO)_5$ and alkynes[41-42, 46]. The complex can, however, be obtained in a better yield by this route. A possible application of the complex may be preparation of pyrylium salts **8** e.g. as the PF_6^- salt by treatment of the complex with $AgPF_6$ (1 : 1) in CH_3CN[5].

Other examples of reaction of cyclomanganated enones with alkynes include the substituted (η^5-pyranyl)$Mn(CO)_3$ complexes, which can then undergo oxidative demetallation reaction with excess I_2 to give pyrylium triiodide salts (Scheme 1-15)[43].

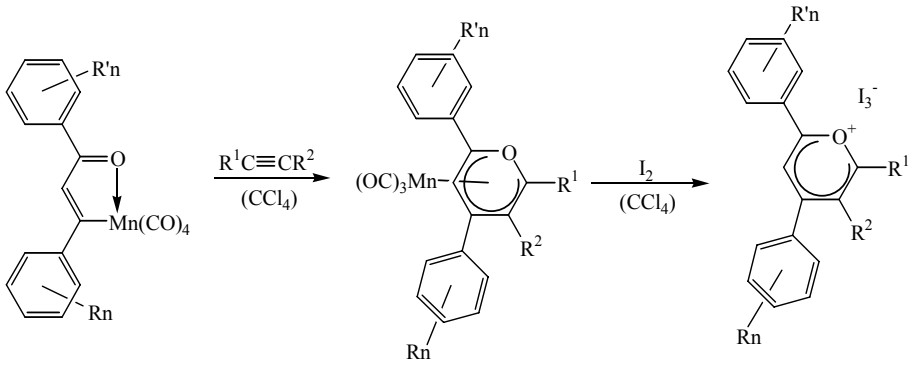

Scheme 1-15: Reaction of Cyclomanganated Enones with Alkyne in CCl_4 to Give Pyrylium Triiodide Salts under Excess I_2[47]

The corresponding reaction of cyclomanganated dienones with alkynes gives another product as well as the analogue of the pyranyl complex. The pyranyl complex is the initial product,

which then undergoes cyclisation of the inserted alkyne with the second alkene carbon rather than the ketone oxygen, leading to the seven-membered ring of the (η^5-oxocycloheptadienyl)$Mn(CO)_3$ complex. The reaction can give specifically either of the products if appropriate conditions are used. The initially formed pyranyl complex under milder condition can then be converted to the oxocycloheptadienyl complex under more forcing conditions[47] (Scheme 1-16)

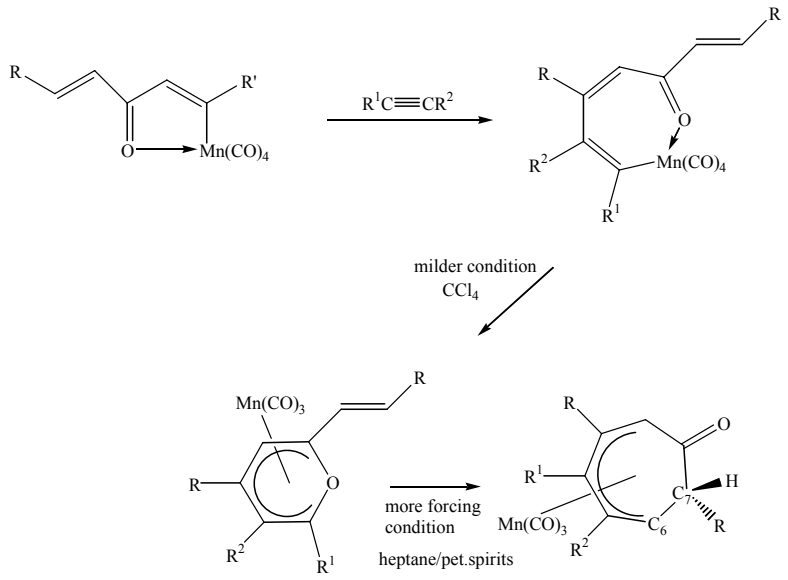

Scheme 1-16: Reaction of Cyclomanganated Dienones with Alkynes

1.1.5.4 Reaction with Electrophiles

Transmetallation with $HgCl_2$ also occurs for cyclometallated enones and gives the corresponding mercurated complexes in a good yield[46].

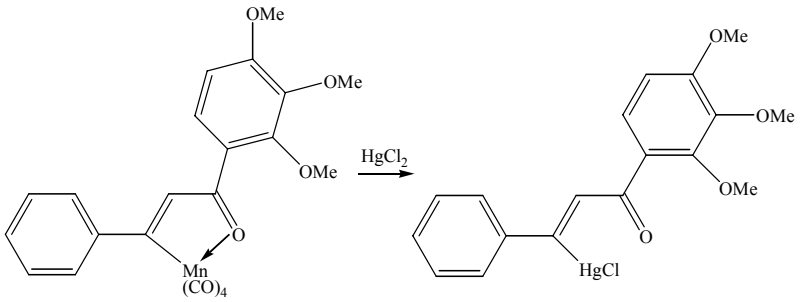

Scheme 1-17: Transmetallation of Cyclometallated Enones with $HgCl_2$[5]

1.1.6 1-Azabutadienes as Ligands

The study of cyclomanganation of non-aromatic ketones was extended to cyclometallation of 1-azabutadienes (Figure 1-10) as a donor ligand[48]. 1-Azabutadienes are pseudo-iso-electronic with α, β-unsaturated ketones (chalcones) and are involved in some important areas of organic chemistry e.g. cycloaddition reactions[49, 50].

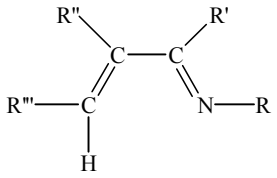

Figure 1-10: 1-Azabuta-1, 3-Diene[48]

1-Azabutadiene is a useful substrate, especially for [4 + 2] and [4 +1] cycloaddition reactions and is extensively used as a building block for various N-heterocycles which plays an important role in synthetic organic chemistry including pharmaceutical purposes[49]. A range of N-heterocyclic compounds including di- and tetrahydropyridines, pyrimidines, quinolines, thiazines, pyrroles, triazinane diones and aziridines, can be prepared from 1-azadienes[49]. The organic chemistry of this type has been reviewed[49]. 1-Azabutadiene, therefore, appears to be a promising substrate for investigations.

1-Azabuta-1, 3-diene compounds can act as a donor ligand to form a variety of transition metal complexes via mono or bidentate coordination through the π-electrons and/or the lone pair donation on the nitrogen[47]. The common coordination modes are summarised in the figure below.

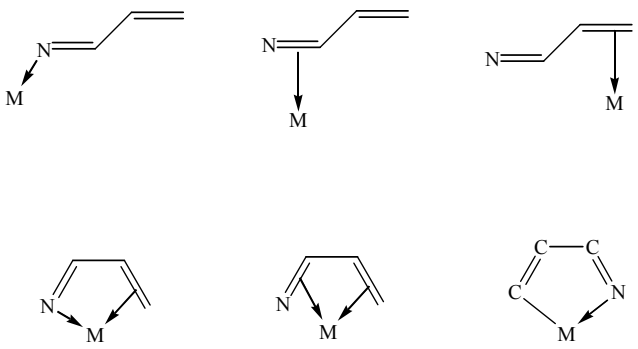

Figure 1-11: Common Coordination Modes of 1-Azabuta-1, 3-Diene with Transition Metal Complexes[47]

Copper (I) salt forms complexes with 1-azabuta-1, 3-diene (Figure 1-12) in which it acts as a simple N-donor ligand[51]. The azabutadiene coordinates to the copper only via the nitrogen lone pair, which differs from enones, and complexes formed all have trigonal planar geometry around the copper atom[51]. Only *trans*-configuration of the azabutadienes can be found[51].

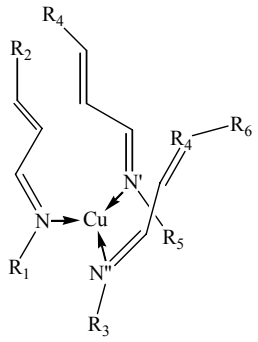

Figure 1-12: Complex of One Cu(I) Salt and Three 1-Azabuta-1, 3-Dienes

There, however, appear to be a very limited number of examples of cyclometallated azabutadienes. Examples of azabutadiene and deprotonated 1-azabuta-1,3-dienyl ligands are limited to Ta, Cr, Mo, Mn, Fe, Ru, Co, Ni and Pt complexes[47]. The first cyclised azabutadiene complex was reported in 1967 and was the iron tricarbonyl species[52] (Figure 1-13). π-Electron donation from the C=C bond and the lone pair donation from the N atom give the cyclised azabutadiene tricarbonyl complex. A few examples of cyclomanganated azabutadienes have also been reported (Figure 1-14).

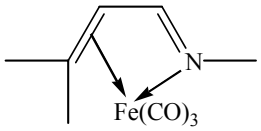

Figure 1-13: Cyclised Azabutadiene-$Fe(CO)_3$ Complex

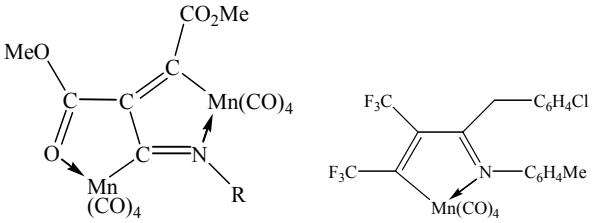

Figure 1-14: Cyclomanganated Azabutadienes

All the species, di-[53] and mono-manganese[54] complexes and also di- and tetra-ruthenium compounds[55], however, were prepared indirectly. The di-manganese compound was synthesised from $Mn_2(CO)_9(CNR)$ and DMAD[53] and the mono-manganese one also from $ClC_6H_4CH_2C(O)Mn(CO)_4(CNC_6H_4CH_3)$ and CH_3CCCF_3[54]. Only examples of cyclometallated azabutadienes via direct method was cyclopalladiated azabutadienes[56] (Scheme 1-18).

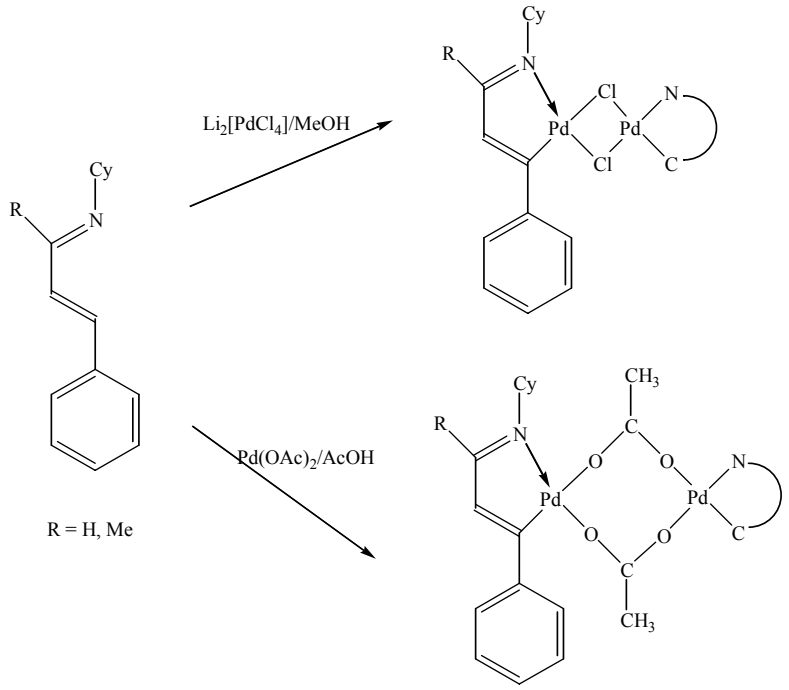

Scheme 1-18: Direct Preparation of Cyclopalladiated Azabutadiene

The 1-azabutadienes undergo cyclopalladiation in the presence of $Li_2[PdCl_4]$/MeOH or $Pd(OAc)_2$/AcOH to give the cyclopalladiated five-membered rings[56] (Scheme 1-18). No other example of direct preparation of cyclometallated azabutadiene appeared to have been known before the work at the University of Waikato[48].

Direct cyclomanganation of the 1-azabutadiene **9** with $PhCH_2Mn(CO)_5$ has been investigated and gives a $Mn(CO)_3$ complex of the pyrrolinonyl ring **10**[48], the reaction of which will be discussed in more detail in Chapter 2.

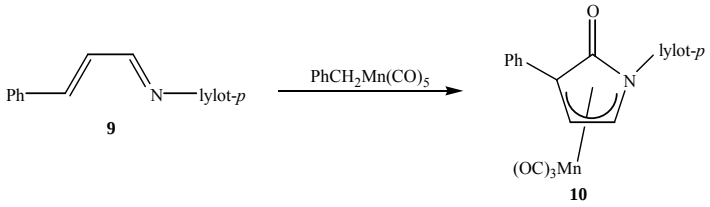

Scheme 1-19: Direct Cyclomanganation of the 1-Azabutadiene **9**[48]

The mechanism was proposed by analogy to chalcone chemistry[5], leading to a proposal of the intermediate cyclomanganated species **11**[48].

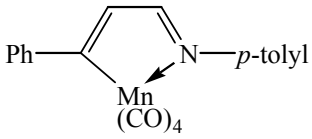

11

Figure 1-15: Intermediate Cyclomanganated Species **11**[48]

The IR evidence which supported the formation of the intermediate **1** could be obtained, but the intermediate never be isolated[48]. One-pot reactions of the 1-azabutadiene **9** and $PhCH_2Mn(CO)_5$ in the presence of the unsaturated reagents which were examined in the investigations into the reactions of cyclomanganated aromatic and heteroaromatic ketones[5], however, showed a series of new intermediates all, presumably, formed via initial formation of the cyclomanganated azabutadiene **11**[48]. This led to further investigations into the isolation of the cyclometallated azabutadiene **11** as the Re analogue **12** using $PhCH_2Re(CO)_5$ as the cyclometallating reagent. Rhenium is a mimic of manganese, but usually reacts more sluggishly than manganese, so it was expected that the Re analogue **12** might be isolated.

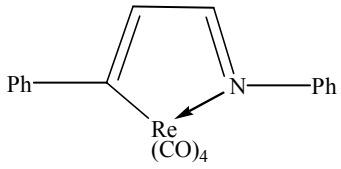

12

Figure 1-16: Cyclorheniated Azabutadiene **12**

1-Azabutadiene has also been shown to react with various alkenes in transition metal-mediated reactions to give pyrrolones and pyrroles[49]. The scheme below shows the Ru-mediated [4 + 1] cycloaddition of 1-azabutadiene with CO and various alkenes to give 1,3-dihydropyrrolone derivative (lactams)[49].

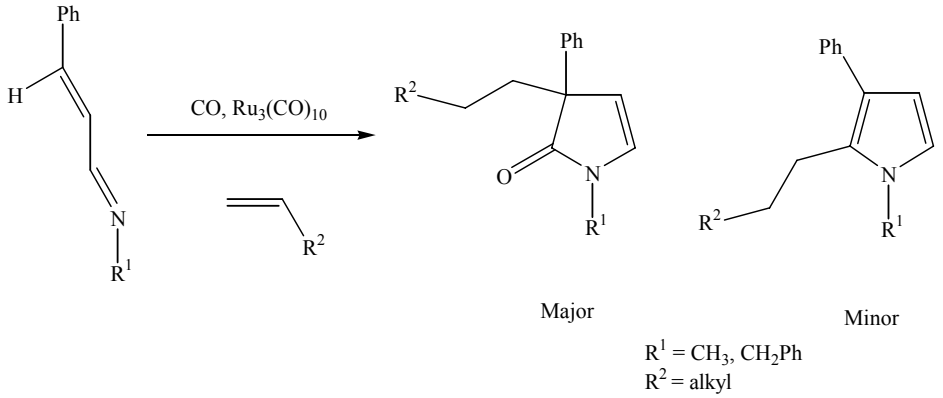

Scheme 1-20: Route to Pyrrolones or Pyrroles via Ru^0-Catalyzed Alkylative [4 + 1] Cycloadditions[49]

Reactions of activated azabutadienes by cyclometallation, therefore, may be of interest for investigations.

This thesis will report the studies of cyclometallation reaction of 1-azabutadienes with $PhCH_2Re(CO)_5$ and also extended investigations into the reactivity of a cyclometallated azabutadiene towards unsaturated reagents. Chapter 2 will report cyclorheniation reaction, and reactions of a cyclorheniated azabutadiene with unsaturated molecules will be discussed in Chapter 3.

Chapter 2 Cyclometallation of 1-Azabutadienes with $PhCH_2Re(CO)_5$

2.1 Introduction

2.1.1 Cyclometallated Azabutadienes

An earlier study[48] showed that reaction of an azabutadiene with $PhCH_2Mn(CO)_5$ under the refluxing-heptane conditions could provide a substituted pyrrolinonyl ring-$Mn(CO)_3$ complex **10** (Scheme 1-19).

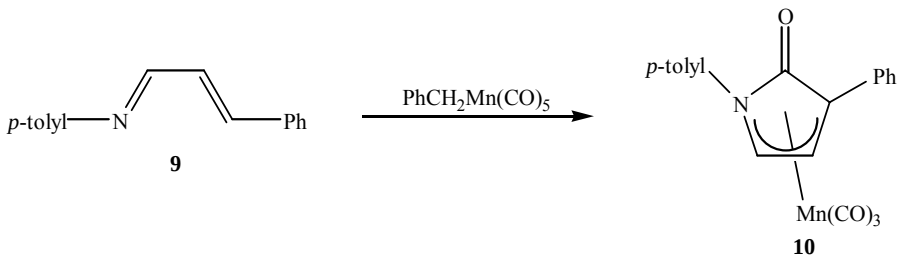

Scheme 1-19: Reaction of an Azabutadiene with $PhCH_2Mn(CO)_5$[48]

The structure of **10** was determined by X-ray crystallography[48]. A substituted pyrrolinonyl ring formed with the $Mn(CO)_3$ group coordinating to one face of the heteroaromatic five-membered ring in a η^4-manner. There appeared to be no previous example of a η^4-pyrrolinonyl complex with a metal carbonyl complex. The reaction was of interest as it could provide a range of pyrrolinonyl rings, which were involved in several areas of organic chemistry[49, 50], with different substituents by choosing the appropriate azabutadienes.

A route to **10** was proposed by analogy to chalcone chemistry[5] and shown in the scheme below[48].

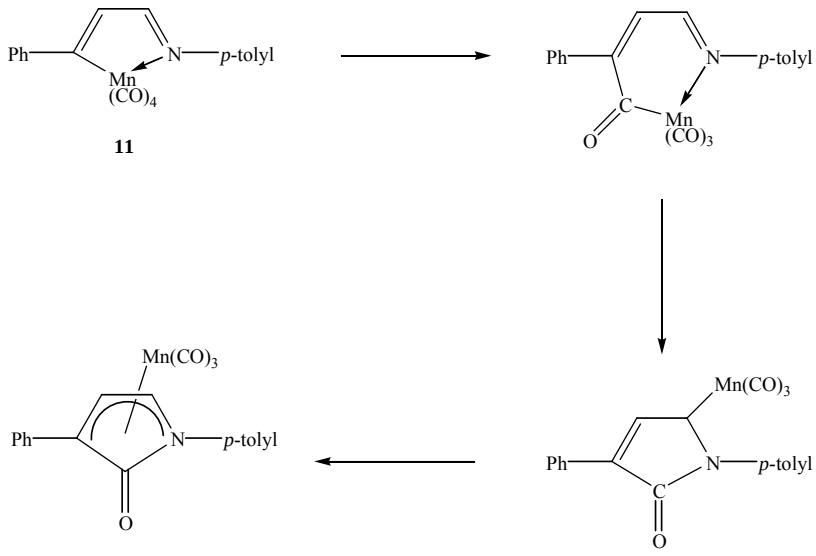

Scheme 2-1: Route to the Pyrrolinonyl Ring-$Mn(CO)_3$ Complex **10**[48]

The complex **10** is formed via cyclometallation of the azabutadiene to give the activated azabutadiene-$Mn(CO)_4$ complex **11**, followed by a rapid insertion of a CO ligand into the Mn-C σ-bond, leading to the six-membered metallocycle. Addition of the new Mn-C bond across the N=C bond followed by cyclisation gives the product[48] (Scheme 2-1).

The cyclomanganated azabutadiene intermediate **11** could, however, not be isolated[48]. The IR spectrum suggested the formation of the intermediate **11** in the reaction, by showing a υ(C≡O) band at 2076 cm^{-1} which was in the expected position for the highest frequency υ(C≡O) band for a $Mn(CO)_4$ complex (cf. ~2081 cm^{-1} for cyclomanganated chalcones[5]). The band, however, never became a major feature during the course of the reaction, nor could the intermediate **11** be obtained[48].

In an attempt to isolate the cyclometallated azabutadiene intermediate, the reaction was carried out with a rhenium carbonyl complex using $PhCH_2Re(CO)_5$ as the cyclometallating reagent[57]. The reaction of 1,4-diphenyl-1-azabuta-1,3-diene with $PhCH_2Re(CO)_5$ under similar conditions to the corresponding Mn reaction, gave a

derivative of the cyclometallated azabutadiene-$Re(CO)_4$ complex **12**[57]. The complex **12** was not obtained, but the substituted derivative **13** could readily be isolated as a red solid[57] (Scheme 2-2).

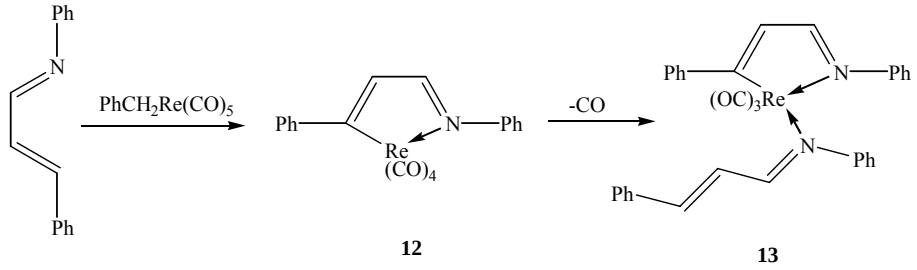

Scheme 2-2: Reaction of an Azabutadiene with $PhCH_2Re(CO)_5$

An X-ray crystal structure determination was carried out and elucidated the structure of **13**[57]. In the complex **13**, the second azabutadiene substitutes to the metal centre of the cyclometallated azabutadiene-$Re(CO)_3$ complex by lone pair donation through the imine nitrogen. It could be assumed that the derivative **13** formed via initial cyclometallation of the azabutadiene with $PhCH_2Re(CO)_5$ to give the cyclorheniated azabutadiene-$Re(CO)_4$ complex **12** (the Re analogue of the unisolated cyclomanganated azabutadiene **11**[48]) which then underwent loss of a CO ligand from Re followed by substitution by a second azabutadiene through the N atom to give the product[57].

There appeared to be no sign of the CO-inserted product in the Re reaction[57] and the Mn system also gave no sign of the substituted product[48]. It, therefore, appeared that the reactions were different.

Further investigations into the Re reaction were, therefore, carried out. The reactions were investigated under alternative reaction conditions with monitoring by IR spectroscopy. The investigations were also extended to cyclorheniation of other 1-azabutadienes in which the reactivity of the imine nitrogen and/or 1-ene carbon were modified by introducing the appropriate substituents on the benzene rings. This chapter will report the investigations into reaction of the 1,4-diphenyl-1-azabuta-1,3-diene with $PhCH_2Re(CO)_5$ and also cyclorheniation reaction of the other 1-azabutadienes.

2.2 Results and Discussion

2.2.1 Preparation of Starting Materials

2.2.1.1 Preparation of $PhCH_2Re(CO)_5$

Benzyl rhenium pentacarbonyl complex **14** was prepared by using the method which was used for the succsesful synthesis of the manganese analogue, $PhCH_2Mn(CO)_5$[5]. The product was characterised by IR, ^1H and ^{13}C NMR and ESI-MS analyses and the spectroscopic data were consistent with the expected product.

2.2.1.1.1 IR

IR analysis was carried out in hexane. The table below summarises the C≡O frequencies for $PhCH_2Re(CO)_5$ **14**, $PhCH_2Mn(CO)_5$[5] and also the earlier prepared $PhCH_2Re(CO)_5$[57] for comparison.

Table 2-1: C≡O Frequencies for **14**, $PhCH_2Re(CO)_5$[57] and $PhCH_2Mn(CO)_5$[5]

υ(C≡O) / cm^{-1}			
14	2127 (m)	2018 (s, br)	1986 (s)
$PhCH_2Re(CO)_5$[57]	2127 (w)	2018, 2014 (m)	1986 (s)
$PhCH_2Mn(CO)_5$[5]	2105 (s)	2010 (vs, br)	1990 (vs)

A characteristic CO pattern at 2127, 2018, 2014 and 1986 cm^{-1} is expected[57]. Bands were observed at 2127, 2018 and 1986 cm^{-1} in the υ(C≡O) region and were consistent with those for the earlier prepared one[57]. The 2018 cm^{-1} band did not resolve, but appeared as a broad band containing the two unresolved bands. The overall pattern of the bands was also consistent with that for the Mn analogue[5]. The higher frequency υ(C≡O) bands were, however, shifted by ~8 – 22 cm^{-1} to higher frequencies and the lowest one by ~4 cm^{-1} to a lower frequency for the Re complexes from the corresponding bands for the Mn complex.

2.2.1.1.2 ^{1}H and ^{13}C NMR

NMR experiments were carried out on samples in $CDCl_3$. ^{1}H and DEPT experiments were carried out at 400 MHz and ^{13}C NMR experiment was carried out at 300 MHz. The purity of the product was determined by the NMR experiments and the spectra showed that the product was reasonably pure although it was a dark-yellow solid, while it should be white solid if pure. The table below summarises the assignments and the corresponding protons and carbons can be referred to in the figure below.

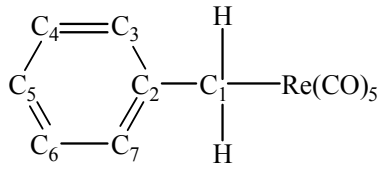

Table 2-2: NMR Assignments for $PhCH_2Re(CO)_5$ and $PhCH_2Mn(CO)_5$[5]

δ ppm	**$PhCH_2Re(CO)_5$**	**$PhCH_2Mn(CO)_5$**[5]
^{1}H NMR		
H-1	2.44 (s, 2 H)	2.45 (s, 2 H)
H-3, 7	7.07 – 7.10 (m, 2 H)	7.28 (s, 2 H)
H-4, 6	7.18 – 7.23 (m, 2 H)	7.28 (s, 2 H)
H-5	6.86 – 6.90 (m, 1 H)	7.28 (s, 1 H)
^{13}C NMR		
C-1	–2.20 (CH_2)	11.31 (CH_2)
C-2	155.04 (C)	152.01 (C)
C-3, 7	125.44 (2 CH)	126.03 (2 CH)
C-4, 6	128.33 (2 CH)	128.84 (2 CH)
C-5	122.44 (CH)	123.68 (CH)
Axial C≡O	180.98 (C≡O)	210.34 (C≡O)
Equatorial C≡O	185.01 (4 C≡O)	212.51 (4 C≡O)

One singlet and three multiplets were observed in the ^{1}H NMR spectrum. The singlet at 2.44 ppm was assigned for the CH_2 protons and could also integrate as two protons. The signal was consistent with the corresponding proton signal for the Mn analogue, which appeared at 2.45 ppm. The three multiplets were observed in the aromatic region. The multiplets at 7.08 and 7.20 ppm could integrate as two protons and the

one at 6.88 ppm as one proton. The $CH_2Re(CO)_5$ may be expected to have a similar electronic effect on the *ortho*- and *para*-protons. The 7.08, 7.20 and 6.88 ppm proton signals were, therefore, assigned as *H-3, 7*, *H-4, 6*, and *H-5*, respectively. All the five aromatic protons appear as one signal of a singlet at 7.28 ppm for the Mn analogue[5]. Since the signals for the *ortho*-, *meta*- and *para*-substituted protons could be distinguished for the Re analogue, it appears that Re has a stronger and longer range influence than Mn.

Seven carbon signals were observed in the ^{13}C NMR spectrum. The secondary carbon signal at δ –2.20 ppm was assigned as *C-1*. The *C-1* signal was shifted by 13 cm^{-1} up-field from the corresponding signal at 11.31 ppm for the Mn analogue[5], suggesting Re is more strongly shielding than Mn. The three tertiary carbon signals of 1 : 2 : 2 intensity in the aromatic region at 122.44, 125.44 and 128.33 ppm were assigned as *C-5*, *C-3*, *7* and *C-4*, *6*, respectively. The intensity of the *para*-carbon signal may be expected to be smaller than those of the *ortho*- and *meta*-carbon signals as only one carbon contributes to the signal, while two carbons to each of the other two signals. The quaternary carbon signal at 155.04 ppm was assigned as *C-2*. The chemical shifts of the aromatic carbon signals were consistent with those for the Mn analogue.

Metal carbonyl carbons generally appear at 180 – 200 ppm[61]. Two quaternary carbon signals were observed at 185.01 and 180.98 ppm with ~4 : 1 intensity, respectively. The four equatorial carbonyl carbons are all chemically equivalent, so may be expected to appear as one signal. The 185.01 ppm signal was, therefore, assigned as the *equatorial* C≡O carbons and the 181.98 ppm signal as the *axial* C≡O carbon. The carbonyl carbon signals for the Re complex were shifted by 30 ppm up-field from the corresponding signals for the Mn analogue, which, again, suggests that Re is more strongly shielding than Mn.

2.2.1.1.3 ESI-MS

ESI-MS analysis was carried out in MeOH/NaOMe. The parent molecule was observed at *m/z* 448 as $[M + OMe]^-$ in the negative ion mode. A sequential loss of CO ligands could be observed with increase in a cone voltage, which is quite common for rhenium carbonyl complexes in ESI-MS conditions. The loss of COs was also

observed for the tetracarbonyl complexes **12**, **19** and **21**, which will be discussed later in this section.

2.2.1.2 By-Product 15

A small amount of the by-product **15** was also isolated as a red solid in the preparation of $PhCH_2Re(CO)_5$. It was characterised by ESI- and HR-MS only because of the small amount. The solid was soluble in MeOH and could easily be detected by ESI- and HR-MS with a great intensity of the peak corresponding to the parent molecule of **15**. The compound would decompose with time even if stored at -20 ºC.

2.2.1.2.1 ESI- and HR-MS

ESI-MS analysis was carried out at cone voltage of 20 V in MeOH with NaOMe. The parent molecule was observed at *m/z* 633 as $[M - H]^-$ in the negative ion mode with the characteristic isotope pattern for two rhenium atoms. The accurate mass of 632.957 obtained on HR-MS in MeOH closely agreed with the mass of 632.948 calculated for the chemical formula of $Re_2O_6C_{13}H_9$ which could be assigned as $[M - H]^-$ where M = $Re_2O_6C_{13}H_{10}$. This led to a proposal of structure for **15** (Figure 2-1). Eight electrons from the four carbonyl carbons and four from the σ-bonding with three hydrogenes and one carbon, and six electrons from the π-electron system of the aromatic ring and four from the carbonyl carbons and two from the σ-bonding with two hydrogenes satisfy the 18 electron configurations of the $Re(CO)_4$ and $Re(CO)_2$ metal centres, respectively, supporting the structure below which is in a stable configuration. Further characterisations may, however, be needed to confirm this structure.

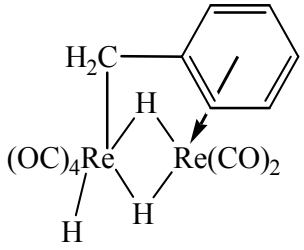

Figure 2-1: Possible Structure of **15**

2.2.1.3 Preparation of Azabutadienes

2.2.1.3.1 Preparation

Three azabutadienes **16**, **17** and **18** were prepared. In the azabutadiene **17**, the basicity of the imine nitrogen was reduced by substitution of fluoride, which is electron-withdrawing, at the *para*-site of the aniline ring. Those of the imine nitrogen and also *C-1* carbon were increased by substitution of the electron-donating methyl and dimethylamine groups at the *para*-sites of the aniline and cinnamaldehyde rings, respectively, in the azabutadiene **18**.

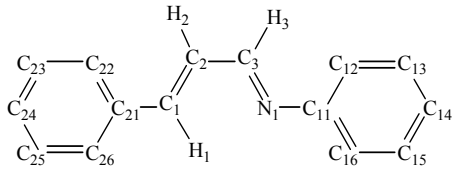

16

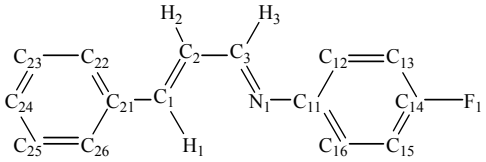

17

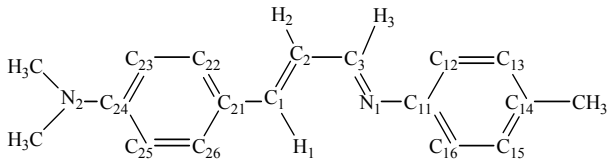

18

The azabutadienes **16** and **17** could be prepared in a reasonable yield e.g. >50 % using the literature method[58]. The syntheses were carried out both under nitrogen as in the literature and normal atmospheres in order to see if yield would be affected. The yields were, however, the same under both conditions. It, therefore, appeared that the reactions did not need to be carried out under an inert atmosphere. The azabutadiene **18** was prepared from two alternative literature methods[58, 59] due to the very low yield e.g. 5 % obtained from the method used for the preparation of the azabutadienes **16** and **17**. The overall yields from both routes were, however, the same e.g. ~5 %. The alternative method[59], nevertheless, appeared to give a better yield than the other as 25 % crude yield could be obtained, which reduced to ~5 % during the recrystallisation process.

2.2.1.3.2 Characterisation

The azabutadienes **16**, **17**, and **18** were obtained as pale-yellow needles, a pale-white powder and yellow powder, respectively. They undergo decomposition in the air with time unless stored in the freezer. The products were characterised by IR and ^{1}H and ^{13}C NMR spectroscopy and ESI- and HR-MS spectrometry.

2.2.1.3.2.1 IR

IR analysis was carried out as a KBr disc. The table below summarises the selected IR frequencies for the azabutadienes **16**, **17** and **18**. The data for the azabutadiene **16** were adapted from the literature[58].

Table 2-3: Selected IR Frequencies for the Azabutadienes **16**, **17** and **18**

IR (KBr / cm^{-1})	**16**	**17**	**18**
-N-CH_3 str			2739 (m)
-C=C- str	1630 (v)	1627 (m)	1665 (vs, sh)
Aryl-C-C- str	1605 (v), 1505	1607 (m), 1502 (s)	1605 (vs, sh)
-C=N- str or Aryl-C-C- str	1551*(s, sh,)	1586 (w)	1528 (m)
Trans-C=C-H alkenes	986 (s)	981 (m)	972 (m)
Two neighbouring aryl-C-H		837 (m)	810 (m)
Five neighbouring aryl-C-H	720 (s)	747 (m), 692 (m)	
-CH_3 asy			1449 (w)
-N-($\underline{CH_3}$)$_2$			1374 (m)
Monofluorinated benzene, aryl-C-F str		1240 (m, br)	

* In heptane/CH_2Cl_2

Alkene bond stretching vibrations give a band of variable intensity in the range from 1690 – 1635 cm^{-1} [60]. If conjugated with a phenyl group, the band could be shifted to ~1630 cm^{-1} [60]. The bands at 1630 and 1627 (m) cm^{-1} in the spectrum of the azabutadienes **16** and **17**, respectively, were, therefore, assigned as *-C=C-* bond stretches. In the same region, a band was observed at 1665 (s, sh) cm^{-1} in the spectrum of the azabutadiene **18**. The frequency was higher by ~35 cm^{-1} than the C=C bond frequencies for the azabutadienes **16** and **17**. In the azabutadiene **18**, the $N(CH_3)_2$

group at the *para*-site of the cinnamaldehyde ring is strongly electron-donating which might reduce the electron-withdrawal from the alkene bond by the ring and, therefore, increase the C=C bond order and, hence, the frequency. The 1665 cm^{-1} band was, therefore, assigned as -*C=C*- bond stretch for the azabutadiene **18**. The influence of the $N(CH_3)_2$ group on a long range e.g. to the *C-2* carbon, could also be indicated by the NMR experiment.

Alkenyl C-H out of plane vibrations exhibit a number of bands in the range from 1005 – 675 cm^{-1} [60]. *Trans*-alkenyl C-H out of plane vibrations expect in the range from 990 – 960 cm^{-1} [60]. The bands at 986, 981 and 972 cm^{-1} in the spectrum of the azabutadienes **16**, **17** and **18**, respectively, were, therefore, assigned as *trans*-alkenyl C-H out of plane vibrations.

Imine C=N bond stretching vibrations normally give a strong band in the region from 1690 – 1580 cm^{-1} [60]. Conjugation at either or both sides may lower the frequency[60]. In a similar compound of the C=N bond type, $CH_3COCH=NPh$[60], the C=N bond stretching vibration appears at 1555 cm^{-1} [60]. The band at 1551 (s, sh) cm^{-1} in the spectrum of the azabutadiene **16** was, therefore, assigned as *C=N* bond stretch. At a similar frequency, a band was observed at 1586 (w) and 1528 (m) cm^{-1} in the spectrum of the azabutadienes **17** and **18**, respectively. In the azabutadiene **17**, the aniline ring is substituted with an electro-withdrawing fluoride at the *para*-site and that is an electro-donating methyl group in the azabutadiene **18**. The frequency of the C=N bands for the azabutadienes **17** and **18** may, therefore, be expected to shift from the corresponding frequency for the azabutadiene **16**. The 1586 and 1528 cm^{-1} bands were, therefore, assigned as *C=N* stretch.

Aromatic C-C bond stretching vibrations may produce two bands of a medium intensity, often doublet, and weak in benzene derivatives with a centre of symmetry in the ring, in the region from 1625 – 1575 and 1525 – 1475 cm^{-1} [60]. Two bands were observed at 1605 and 1505, 1607 (m) and 1502 (s) in the spectrum of the azabutadienes **16** and **17**, respectively, and one at 1605 (s) cm^{-1} in the azabutadiene **18**. The bands were, therefore, assigned as aromatic *C-C* stretches.

Aromatic five neighbouring C-H out of plane vibrations expect a strong band in the region from 720 – 760 cm^{-1} [60]. A band was observed at 720 (s) and 747 (w) cm^{-1} in the spectrum of the azabutadienes **16** and **17**, respectively, and each was, therefore, assigned as aromatic five neighbouring C-H out of plane vibrations. Aromatic two-neighbouring C-H out of plane vibrations is expected for a band near 800 – 850 cm^{-1} [60]. The bands at 837 and 810 cm^{-1} in the spectrum of the azabutadienes **17** and **18**, respectively, were, therefore, assigned as aromatic two-neighbouring C-H out of plane vibrations.

2.2.1.3.2.2 ESI-MS

ESI-MS analysis was carried out at a cone voltage of 20 V in MeOH. The three azabutadienes were all soluble in MeOH and could easily be detected by ESI-MS spectrometry. The parent molecules all appeared with a great intensity in the positive ion mode at the respective *m/z* as $[M + H]^+$ and/or $[M + Na]^+$. The table below summarises the accurate *m/z* obtained on HR-MS in MeOH for the azabutadienes **16**, **17** and **18** for the confirmation of the assignments.

Table 2-4: Accurate *m/z* Obtained on HR-MS for the Azabutadienes **16**, **17** and **18**

(MeOH, +ve ion)	**16**	**17**	**18**
$[M + H]^+$	*m/z* 208.1129 (calcd. *m/z* 208.1121)	*m/z* 226.1021 (calcd. *m/z* 226.1027)	*m/z* 265.1701 (calcd. *m/z* 265.1699)
$[M + Na]^+$			*m/z* 287.1524 (calcd. *m/z* 287.1519)

The observed *m/z* all closely agreed with the calculated masses.

2.2.1.3.2.3 ^1H and ^{13}C NMR

NMR experiments were carried out on samples in $CDCl_3$ at 400 MHz. The assignments for the azabutadiene **16** were made in accordance with the NMR data including ^1H, ^{13}C, SELTOCSY, DEPT, HSQC and HMBS experiments. The *J* value of 160 Hz was used to optimise signals for aromatic and other sp^2 and sp carbons in

the DEPT, HSQC and HMBS experiments. Full assignment for the azabutadiene **16** is summarised in the table below and the ^{1}H-^{1}H couplings in the SELTOCSY experiment (d9 = 0.03 seconds) and the $^{2\text{-}3}J_{CH}$ correlations in the HMBC experiment, in the azabutadiene **16** were shown in the figures below.

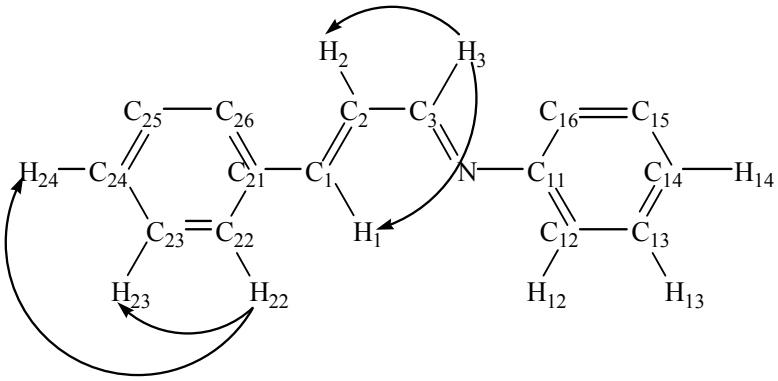

Figure 2-2: ^{1}H-^{1}H Couplings in the Azabutadiene **16**

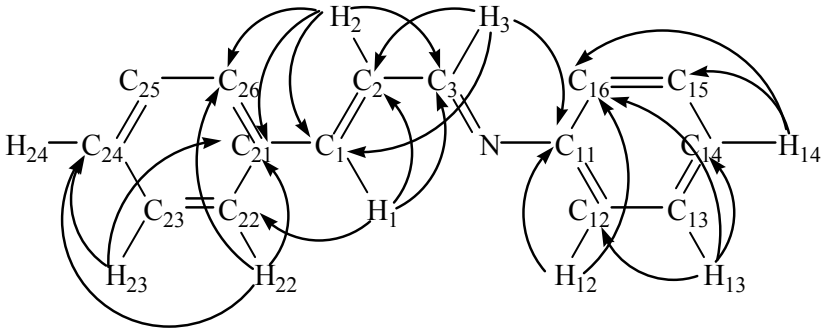

Figure 2-3: $^{2\text{-}3}J_{CH}$ Correlations in the Azabutadiene **16**

Table 2-5: Full NMR Assignment for the Azabutadiene **16**

^{1}H NMR	δ ppm	**^{13}C NMR**	δ ppm
H-1	7.19 (m)	*C-1*	144.01 (CH)
H-2	7.15 (m)	*C-2*	128.70 (CH)
H-3	8.28 (dd, $^{3,4}J_{HH}$ = 7.02, 1.12 Hz), 1 H	*C-3*	161.63 (CH)
		C-11	151.82 (C)
H-12, 16	7.39 (m)	*C-12, 16*	120.95 (CH)
H-13, 15	7.20 (m)	*C-13, 15*	129.21 (CH)
H-14	7.24 (m)	*C-14*	126.14 (CH)
		C-21	135.67 (C)
H-22, 26	7.55 (m), 2 H	*C-22, 26*	127.54 (CH)
H-23, 25	7.41 (m), 2 H	*C-23, 25*	128.96 (CH)
H-24	7.20 (m)	*C-24*	129.62 (CH)

The signal for the *H-3* proton appeared at 8.28 ppm as a doublet of doublet with a $^{3,4}J_{HH}$ coupling constant of 7.02 and 1.12 Hz, respectively. The *H-3* proton signal showed a $^{1}J_{CH}$ correlation to the tertiary carbon signal at 161.63 ppm in the HSQC experiment, which was, therefore, assigned as *C-3*. The SELTOCSY experiment, irradiating at the *H-3* proton signal, showed strong and weak ^{1}H-^{1}H couplings with the proton signals at 7.15 and 7.19 ppm, respectively. The 7.15 and 7.19 ppm signals showed a $^{1}J_{CH}$ correlation in the HSQC experiment to the tertiary carbon signals at 128.70 and 144.01 ppm, respectively. The 7.15 ppm signal showed $^{2,3}J_{CH}$ correlations in the HMBC experiment to the carbon signals at 161.63, 144.01 and 135.67 ppm and the 7.19 ppm signal to those at 161.63 and 128.70 ppm (Figure 2-3). The *H-3* signal also showed $^{2,3}J_{CH}$ correlations in the HMBC experiment to the carbon signals at 128.70, 144.01 and 151.82 ppm (Figure 2-3). These correlations suggested that the 7.15 and 7.19 ppm signals could be assigned as *H-2* and *H-1* and the corresponding carbon signals at 128.70 and 144.01 ppm as *C-2* and *C-1*, respectively.

The proton signal at 7.55 ppm was irradiated in the SELTOCSY experiment and ^{1}H-^{1}H couplings with the proton signals at 7.41 and 7.20 ppm were observed. The 7.41 and 7.20 ppm signals showed a $^{1}J_{CH}$ correlation to the carbon signals at 127.54 and 128.96 ppm, respectively, in the HSQC experiment. In the HMBC experiment, the 7.55 ppm signal showed $^{2\text{-}3}J_{CH}$ correlations to the carbon signals at 135.67, 127.54 and 129.62 ppm and the 7.41 ppm to those at 135.67 and 129.62 ppm (Figure 2-3). The 135.67 ppm carbon signal could be correlated to the *H-2* proton signal, suggesting that the carbon signal was within $^{2,3}J_{CH}$ distances from the *H-2* proton. The 135.67 ppm signal was, therefore, assigned as *C-21* and the 127.54 ppm carbon signal as *C-22, 26* and the corresponding proton signal at 7.55 ppm as *H-22, 26* by the $^{2,3}J_{CH}$ correlation between the *C-22, 26* carbon and the *H-1* (and also *H-2*) proton signals (Figure 2-3). These left the 128.96 and 129.62 ppm signals to be assigned as *C-23*, *25* and *24* and the corresponding proton signals at 7.41 and 7.20 ppm as *H-23, 25* and *24*, respectively. The $^{3}J_{CH}$ correlation between the 7.41 ppm proton and the *C-21* carbon signals and no $^{2,3}J_{CH}$ correlation between the *C-21* and the *H-24* signals because of the beyond $^{3}J_{CH}$ distance, further support the assignments.

The *H-3* proton signal showed a $^{2,3}J_{CH}$ correlation to the quaternary carbon signal at 151.82 ppm, which could, therefore, be assigned as *C-11*. The 151.82 ppm signal also

showed a $^{2,3}J_{CH}$ correlation to the proton signals at 7.39 and 7.20 ppm, which also showed a $^{1}J_{CH}$ correlation in the HSQC experiment to the carbon signals at 120.95 and 129.21 ppm, respectively. The 7.20 ppm proton signal showed $^{2,3}J_{CH}$ correlations to the tertiary carbon signals at 120.95 and 126.47 ppm and the 126.47 ppm carbon signal showed the corresponding proton at 7.24 ppm in the HSQC experiment. The 7.24 ppm proton signal showed $^{2,3}J_{CH}$ correlations to the carbon signals at 120.95 and 129.21 ppm. According to these correlations, the 7.39, 7.20 and 7.24 ppm proton signals could be assigned as *H-12, 16*, *H-13, 15* and *H-14*, respectively, and the corresponding carbons as *C-12, 16*, *C-13, 15* and *C-14* (Table 2-5).

The assignments for the azabutadienes **17** and **18** were made in accordance with that for the azabutadiene **16** with the help of the additivity rule for substituted benzene derivatives[60]. The azabutadienes **16**, **17** and **18** are analogues, so the chemical shifts of the aromatic proton and carbon signals can be estimated by using the additivity rule[60]. The values of the substituent increaments[60] used in the assignments are summarised in the table below. NMR experiments, including ^{1}H and ^{13}C and DEPT experiments were carried out on samples of the azabutadienes **17** and **18** in $CDCl_3$ at 400 MHz. The *J* value of 145 Hz was used in the DEPT experiments. The table below summarises the assignments for the azabutadienes **16**, **17** and **18** and the corresponding protons and carbons in the azabutadienes **17** and **18** can be referred to in the figures below.

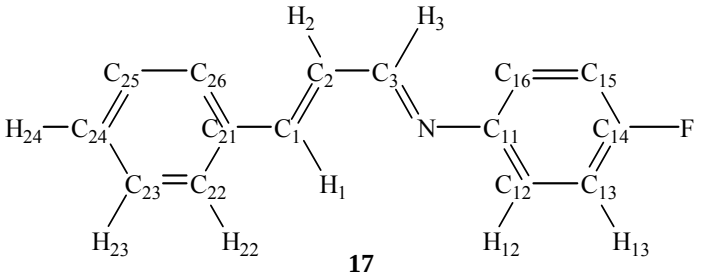

17

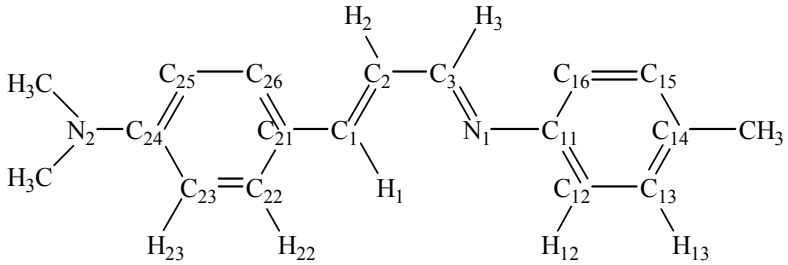

18

Figure 2-4: Proton and Carbon Correspondences in the Azabutadienes **17** and **18**

Table 2-6: NMR Assignments for the Azabutadienes **16**, **17** and **18**

δ ppm	**16**	**17**	**18**
^{1}H NMR			
H-1	7.19 (m)	7.20 – 7.07 (m, 5 H)	7.16 – 7.04 (m, 6 H)
H-2	7.15 (m)	7.20 – 7.07 (m, 5 H)	7.16 – 7.04 (m, 6 H)
H-3	8.28 (dd, $^{3,4}J_{HH}$ = 7.02, 1.12 Hz), 1 H	8.25 (d, $^{3}J_{HH}$ = 8.08 Hz, 1 H)	8.24 (d, $^{3}J_{HH}$ = 8.84 Hz, 1 H)
H-12, 16	7.39 (m)	7.43 – 7.35 (m, 4 H)	7.16 – 7.04 (m, 6 H)
H-13, 15	7.20 (m)	7.20 – 7.07 (m, 5 H)	7.16 – 7.04 (m, 6 H)
H-14	7.24 (m)	-	-
H-22, 26	7.55 (m), 2 H	7.56 – 7.54 (m, 2 H)	7.43 (d, $^{3}J_{HH}$ = 8.84 Hz, 2 H)
H-23, 25	7.41 (m), 2 H	7.43 – 7.35 (m, 4 H)	6.70 (d, $^{3}J_{HH}$ = 8.88 Hz, 2 H)
H-24	7.20 (m)	7.20 – 7.07 (m, 5 H)	-
N(CH_3)$_2$			3.02 (s, 6 H)
CH_3			2.36 (s, 3 H)
^{13}C NMR			
C-1	144.01 (CH)	144.11	144.35 (CH)
C-2	128.70 (CH)	128.51	124.25 (CH)
C-3	161.63 (CH)	161.34	161.57 (CH)
C-11	151.82 (C)	147.86 (d, $^{4}J_{CF}$ = 3.00 Hz)	149.68 (C)
C-12, 16	120.95 (CH)	122.30 (d, $^{3}J_{CF}$ = 8.21 Hz)	120.84 (2 CH)
C-13, 15	129.21 (CH)	115.90 (d, $^{2}J_{CF}$ = 22.59 Hz)	129.74 (2 CH)
C-14	126.14 (CH)	161.35 (d, $^{1}J_{CF}$ = 245.06 Hz)	135.32 (C)
C-21	135.67 (C)	135.60	123.87 (C)
C-22, 26	127.54 (CH)	127.53	129.00 (2 CH)
C-23, 25	128.96 (CH)	128.97	112.09 (2 CH)
C-24	129.62 (CH)	129.67	151.31 (C)
N(CH_3)$_2$			40.21 (2 CH_3)
CH_3			20.99 (CH_3)

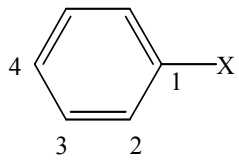

Table 2-7: Substituent Increments for -F, -CH_3 and -$N(CH_3)_2$ Groups

^{1}H NMR				
X	Z_2	Z_3	Z_4	
-F	-0.26	0.00	-0.20	
-CH_3	-0.20	-0.12	-0.22	
-$N(CH_3)_2$	-0.66	-0.18	-0.67	
^{13}C NMR				
	Z_1	Z_2	Z_3	Z_4
-F	34.8	-13.0	1.6	-4.4
-CH_3	9.2	0.7	-0.1	-3.0
-$N(CH_3)_2$	22.5	-15.4	0.9	-11.5

The *H-3* proton signals for the azabutadienes **17** and **18** appeared at 8.2 ppm as a doublet with a $^3J_{HH}$ coupling constant of 8 Hz. The chemical shifts and coupling constants were both consistent with those for the azabutadiene **16**. The *H-1* and *2* proton signals for the azabutadienes **17** and **18** appeared as a multiplet due to overlap with other signals in the aromatic region. The exact chemical shifts of the signals could, therefore, not be determined. They can, however, be determined by SELTOCSY experiment irradiating at the *H-3* proton signal. The proton signals for the azabutadiene **17** appeared to be consistent with those for the azabutadiene **16**, but those for the azabutadiene **18** appeared to have shifted by ~0.03 ppm up-field from the corresponding signals for the azabutadiene **16**. The *C-3, 2* and *1* carbon signals for the azabutadienes **17** and **18** were consistent with those for the azabutadiene **16** (Table 2-6), except for the *C-2* carbon signal for the azabutadiene **18**, which shifted by 4 ppm up-field from the corresponding signals for the azabutadienes **16** and **17**. This may be due to the $N(CH_3)_2$ group at the *para*-site of the cinnamaldehyde ring as the long range influence was also observed by the higher frequency of the C=C bond stretching vibrations in the IR spectrum of the azabutadiene **18**.

The aromatic ring proton signals appeared as multiplets of overlapped signals. A detailed assignment was, therefore, not made for the aromatic proton signals. The

table shows the range of the signals in which the corresponding proton signal might appear. The ring carbon signals, on the other hand, appeared as individual signals, which could, therefore, be assigned for each carbon (Table 2-6). The assignments for the cinnamaldehyde ring proton and carbon signals for the azabutadiene **17** were made with reference to those for the azabutadiene **16** as the signals could be expected to be consistent with those for the azabutadiene **16** because of the equivalent chemical environments of the rings. Those for the azabutadiene **18** may, on the other hand, be expected to shift by the substituent increments for the $N(CH_3)_2$ group (Table 2-7), from the corresponding signals for the azabutadienes **16** and also **17**. The ring proton and carbon signals for the azabutadienes **17** and **18** were observed at the expected shifts and, therefore, assigned accordingly (Table 2-6).

The chemical shifts of the aniline ring proton and carbon signals for the azabutadienes **17** and **18** are also expected to shift by the substituent increments for -F and $-CH_3$ (Table 2-7), respectively, from the corresponding shifts for the azabutadiene **16**. For the azabutadiene **17**, the signals for the *H-13, 15* protons were shifted by ~0.2 ppm up-field and no shift was observed for the *H-12, 16* proton signals as expected. The corresponding carbon signals were also observed at the estimated shifts by using the values in the table. ^{13}C-^{19}F couplings (I = ½, 100 % natural abundance) were observed in the aniline ring carbon signals and the assignments for the ring carbon signals could also be confirmed by the couplings which showed $^{1}J_{CF}$, $^{2}J_{CF}$, $^{3}J_{CF}$ and $^{4}J_{CF}$ coupling constants of 245.06, 22.59, 8.21 and 3.00 Hz for the *C-14, C-13, 15, C-12, 16,* and *C-11* carbon signals, respectively, (cf. general J_{CF} coupling constants[60]; $^{1}J_{CF}$ = 245.1 Hz; $^{2}J_{CF}$ = 21.0 Hz; $^{3}J_{CF}$ = 7.8 Hz; $^{4}J_{CF}$ = 3.2 Hz). The observed and estimated chemical shifts of the aniline ring proton and carbon signals for the azabutadiene **18** were also consistent and the assignments were also further supported by the DEPT experiment.

2.2.2 Reaction of $PhCH_2Re(CO)_5$ with Azabutadienes

2.2.2.1 Reaction of $PhCH_2Re(CO)_5$ with the Azabutadiene *16*

2.2.2.1.1 Reaction

The scheme below shows the reaction of $PhCH_2Re(CO)_5$ with the azabutadiene **16**.

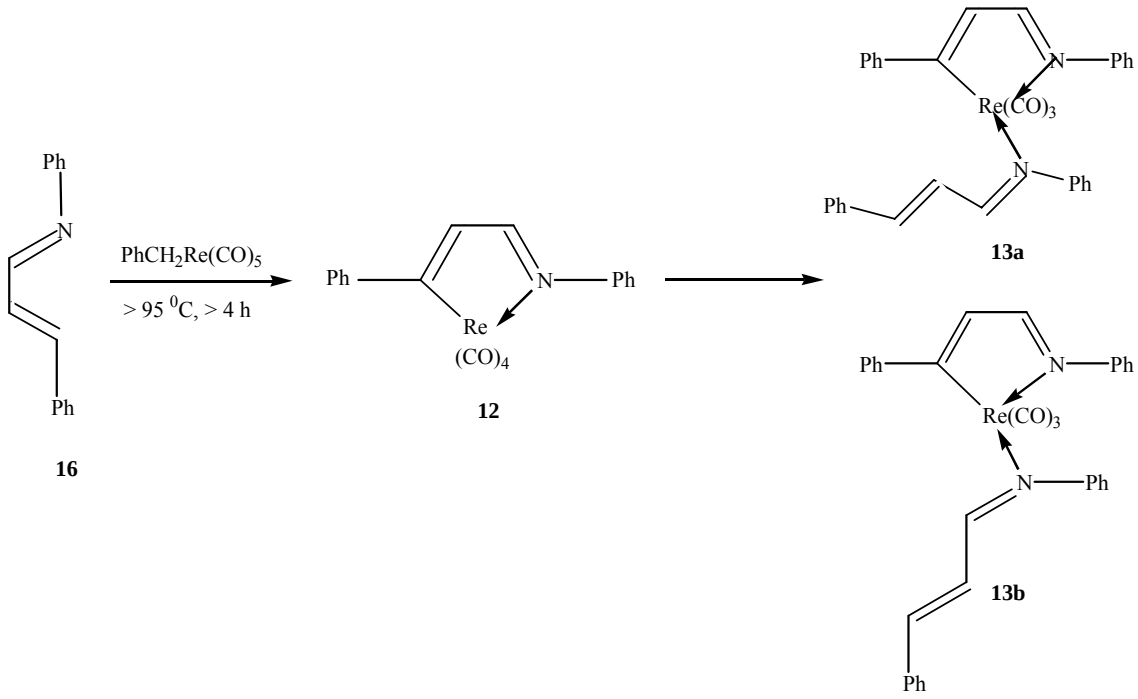

Scheme 2-3: Reaction of $PhCH_2Re(CO)_5$ with the Azabutadiene **16**

When a mixture of $PhCH_2Re(CO)_5$ and the azabutadiene **16** in distilled heptane was heated above 95 °C for 4 hours a under nitrogen atmosphere, a mixture of the cyclorheniated azabutadiene complex **12** and the substituted derivatives **13a** and **13b** could be obtained.

The IR spectrum of the reaction mixture in heptane/CH_2Cl_2 showed the initiation of the reaction at 95 °C by the development of a broad peak at 1896 and 1890 cm^{-1}. In the υ(C≡O) region, new peaks developed at 2091 (w), 2004 (s, sh), 1992 (s), 1896, 1890 (s, br) and 1944 (m) cm^{-1} on 1 : 1 mole ratio reaction and only the 2004, 1896 and 1890 cm^{-1} peaks could be observed on 1 : > 2 mole ratio reaction ($PhCH_2Re(CO)_5$

: azabutadiene). On 1 : > 2 mole ratio reaction, the other peaks might also appear, but would disappear as the reaction proceeded. The mixture turned intense red and precipitation of red (major) and yellow (minor) solids could be observed during the course of the reaction.

The products could easily be purified by PLC, eluting with CH_2Cl_2/petroleum spirits. Chromatography on a PLC plate, eluting with CH_2Cl_2/petroleum spirits (2 : 3) gave strong yellow and orange bands at R_F 0.86 and 0.57, respectively, from which the crystals of **12**, **13a** and **13b** as yellow plates and a mixture of red plates and needles, respectively, could be isolated by fractional crystallisation or vapour diffusion from CH_2Cl_2/petroleum spirits at –20 °C. X-ray crystal structure determinations on the single crystals elucidated the structures of **12**, **13a** and **13b** and the yellow plate **12** was determined to be the Re analogue of the cyclomanganated azabutadiene tetracarbonyl complex **11** and also the red plate and needles **13a** and **13b** were the isomers of the substituted derivatives.

There was no sign of Re analogues of the CO-inserted product **10**[48], and the Mn system[48] also gives no sign of analogues of the substituted derivatives **13**. The initial aim of the present study to isolate the cyclorheniated azabutadiene tetracarbonyl complex **12** was achieved and the isolation may also support the proposed mechanism for the corresponding Mn reaction[48] (Scheme 1-19) in which the initial step of the reaction was cyclometallation of azabutadiene to give the cyclomanganated azabutadiene tetracarbonyl species **11**. The reactions appear to proceed differently in the Re or Mn system after the initial cyclometallation step. In the Mn system, insertion of a CO ligand into the new metal-carbon σ-bond takes place, leading to the pyrrolinonyl five-membered ring by cyclisation and demetalation[48], while the Re system gives the substituted derivatives formed via loss of a CO ligand from the pre-formed complex **12** followed by substitution of a second azabutadiene to the vacant coordination site through the N atom.

Insertion and loss of a CO ligand both appear to take place very rapidly, suggesting that the cyclometallated azabutadiene species is unstable and fairly reactive. The cyclomanganated azabutadiene **11** could never be isolated in the Mn system[48] and,

although the Re analogue could be isolated in the Re system, the further reacted products of the substituted derivatives were always the main products in the reaction. The yield of **12** was always minor and could not be optimised with alternative mole ratios or reaction conditions. The yields of **12** and **13** are shown in the figures below. The yields from 1 : < 1 and 1 > 2 mole reactions were calculated based on the number of moles of the azabutadiene **16** and $PhCH_2Re(CO)_5$, respectively.

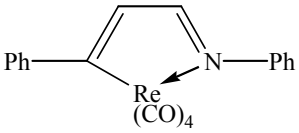

Minor

12

7 - 29% Yield

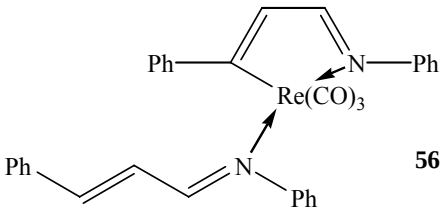

13a **Major**

56 - 98% Yield (Combined)

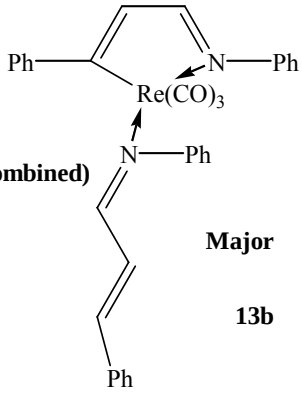

Major

13b

The substituted derivative **13** as combined of the two isomers were always obtained in good-to-excellent yield e.g. > 95%, while the yield of the cyclorheniated azabutadiene **12** could never be beyond 30%. The substituted derivative could be obtained with >50% yield even on 1 : 1 mole ratio in which there was a deficit of the azabutadiene to give the substituted derivatives. The yield of **12** could significantly be reduced to ~7 % in 1 : > 2 mole ratio reaction. These all appear to suggest that loss of a CO ligand is quite fast and substitution of a second azabutadiene takes place to give the substituted derivatives as always the favoured products. The reactions were also carried out at milder conditions e.g. ~85 – 95 ºC. It did, however, not affect the product ratio.

The IR studies of the reaction also support the rapid loss of a CO and substitution reactions in the Re system. The highest frequency υ(C≡O) band at 2091 cm^{-1}

corresponding the complex **12** was always minor feature throughout the course of the reaction as observed in the Mn system[48] and the υ(C≡O) bands at 2091 (w), 1990 (s) and 1941 (m) cm^{-1} corresponding to the complex **12** were not observed until after 3 – 4 hours at > 95°C on 1 : < 1 mole ratio reaction by the time the υ(C≡O) bands corresponding to the substituted derivative **13** had already dominated in the υ(C≡O) region of the spectrum. The υ(C≡O) bands corresponding to the complex **12** were not usually observed at all in 1 : > 2 mole ratio reaction. These may suggest that the complex **12** could be remained unreacted in the mixture (so that it can be isolated) only when there is no more azabutadienes to undergo the subsequent substitution reaction to yield the substituted derivative **13**.

In addition, so as to improve the yield of **12**, the reaction solvent should be removed under vacuum as removal by a syringe could reduce the yield significantly e.g. ~7% (syringe) cf. 15% (under vacuum). It appeared that the complex **12** tended to stay in the solvent rather than to precipitate out as the substituted derivative **13** as a red solid, which may be due to concentration effect.

Isomerisation of azabutadiene with respect to the N=C bond occurs in the reaction. Lanthanide metals as a Lanthanide Shift Reagent (LSR) e.g. $Eu(fod)_3$ are known to induce c*is-trans* isomerisation of *N*-benzylidene-alkyl or aryl amines[62]. Single crystals of the substituted derivative **13** were obtained in two different shapes, plates and needles. X-ray crystal structure determinations elucidated that, in the plate, the *trans*-isomer of the azabutadiene **16** substituted to the rhenium and it was the *cis*-isomer in the needle. The presence of the two isomers was also indicated by ^{1}H and ^{13}C NMR spectroscopy, showing two sets of NMR signals corresponding to each isomer. The two sets of the signals appeared with 3 : 1 intensity. Isomerisation of azabutadiene can naturally occur during the preparation process[62]. The NMR study of the *N*-cinnamylidene-alkyl-anilines, for example, showed 96 – 99 % of one isomer and 4 – 1 % of the other and change of the ratio after addition of LSR to induce isomerisation[62]. The simple ^{1}H and ^{13}C NMR spectra of the azabutadiene **16** under the same experimental conditions as for the mixture of **13a** and **13b** showed only one set of the signals that could be assigned for one isomer, suggesting the presence of one isomer in abundance, which may be *trans*-isomer as is a stable isomer. Therefore, the 3 : 1

ratio of the two sets of the signals in the NMR spectrum of the derivatives **13a** and **13b** may only be accounted by the isomerisation induced in the present system. The same literature[62] also stated that *cis/trans* ratio depends on the molar ratio of the lanthanide metal added in the mixture. This may also explain that the different intensity ratio of the sets of the signals observed in the NMR spectrum of the derivatives prepared from alternative mole ratio reactions. The reaction was interesting as there appear to be no example of metal complexes in which *cis*-azabutadiene coordinates to the metal acting as a ligand.

Separation of the two isomers by PLC was not possible. They are also indistinguishable by IR spectroscopy and ESI-MS spectrometry. NMR, XRD and the shape of their single crystal can, however, determine either of the isomers.

The cyclorheniated azabutadiene **12** and the substituted derivatives **13a** and **13b** were all air-stable and would not easily undergo decomposition if stored in the freezer e.g. over a year.

2.2.2.1.2 Characterisation

2.2.2.1.2.1 IR

IR analysis was carried out in CH_2Cl_2. The table below summarises the υ(C≡O) frequencies for the complexes **12** and **13**.

Table 2-8: υ(C≡O) Frequencies for the Complexes **12** and **13**

υ(C≡O) / cm^{-1}			
12 (CH_2Cl_2)	2092 (w)	1992 (s)	1934 (m)
(KBr)	2093 (w)	1998 (s), 1981 (vs)	1916 (s)
13* (**CH_2Cl_2**)	2002 (s, sh)	1897 (s, br)	1891 (s, br)
13a (Single Crystal FTIR in transmission mode)		1983 (vs)	1875 (vs, br)

*As the mixtures of the two isomers

Cis-$L_2Re(CO)_4$ molecules expect four carbonyl bands[61]. In the IR spectrum of the complex **12**, three bands were observed at 2092 (w), 1992 (s), and 1934 (m) cm^{-1} in the υ(C≡O) region with the strong 1992 cm^{-1} band containing two unresolved peaks. The IR spectroscopy was also carried out in hexane and heptane in an attempt to resolve the peaks. The 1992 cm^{-1} band could, however, not be resolved in either of the solvents. The solid state IR as a KBr disc, however, clearly showed the four carbonyl bands at 2093 (w), 1998 (s), 1981 (vs) and 1916 (s) cm^{-1}. The highest frequency υ(C≡O) band was observed at a higher frequency by 16 cm^{-1} than the corresponding band for the Mn analogue at ~2076 cm^{-1} [48].

Symmetrical $LRe(CO)_3$ molecules expect a_1 and e bands and, for asymmetry, the splitting of the e band is also expected[61]. In the IR spectrum of the mixture of the derivatives **13a** and **13b**, the a_1 and e bands were observed at 2002 (s), 1897 and 1891 (s, br) cm^{-1}, respectively. Single crystal FTIR in transmission mode using a microscope attachment was also carried out on the single crystal of the derivative **13a**. The υ(C≡O) bands were observed at 1983 and 1875 (vs, br) cm^{-1} with the latter containing the unresolved e bands. The FTIR spectrum of the single crystal showed unusually strong overtone peaks of the υ(C≡O) bands at 3984 (m), 3860 (m) and 3756 (m) cm^{-1} which were not observed in the normal IR spectrum.

2.2.2.1.2.2 ESI-MS

ESI-MS analysis was carried out at a cone voltage of 20 V in MeOH and also with NaOMe to enhance ionisation. The table below summarises the ESI-MS data for the complexes **12** and **13**.

Table 2-9: ESI-MS Data for the Complexes **12** and **13**

cv 20 V / *m/z* (%)	**12** (MeOH)	**13** (MeOH)	(MeOH/NaOMe)
(+ve)			
$[M + H]^+$	505(3)	685(100)	
$[M + Na]^+$		707(3)	707 (83)
$[2M + Na]^+$			1391(7)
(-ve)			
$[M]^-$		684(65)	
$[M + OMe]^-$	535(100)	715(5)	715(100)
$[M + OMe - CO]^-$	507(30)		
$[M + OMe - 2\ CO]^-$	479(10)		

For the complex **12**, the parent molecule was observed at *m/z* 505 and 535 as $[M + H]^+$ and $[M + OMe]^-$ (M = **12**), respectively, in the positive and negative ion mode. In the negative ion mode at a cone voltage of 20 V, the peaks corresponding to the loss of CO ligands from the parent molecule were observed at *m/z* 507 and 479. The former was *m/z* 28 and the latter was *m/z* 56 apart from the parent molecule at *m/z* 535 as $[M + OMe]^-$. The peaks were, therefore, assigned as $[M + OMe - CO]^-$and $[M + OMe - 2\ CO]^-$, respectively. These may suggest that the CO ligands in the complex **12** are quite labile, so can easily be removed at such a relatively low cone voltage.

The parent molecule for the complex **13** was observed at *m/z* 1391, 707 and 685 as $[2M + Na]^+$, $[M + Na]^+$ and $[M + H]^+$ in the positive and at *m/z* 715 and 684 as $[M + OMe]^-$ and $[M]^-$ in the negative ion mode, respectively. The *m/z* 707 and 715 peaks can be enhanced by addition of NaOMe e.g. 100 % intensity in the respective ion mode. The accurate mass of *m/z* 707.1372 was also obtained on HR-MS in MeOH/NaOMe and closely agreed with the mass of 707.1315 calculated for the formula of $C_{33}H_{25}N_2NaO_3Re$, which could be assigned as $[M + Na]^+$.

2.2.2.1.2.3 ^{1}H and ^{13}C NMR

NMR experiments were carried out on samples in $CDCl_3$ at 400 MHz. The *J* value of 160 Hz was used in the DEPT, HSQC and HMBC experiments to optimise signals for aromatic and other sp^2 and sp carbons.

The assignments for the complex **12** are summarised in the table below and the figures show the ^{1}H-^{1}H couplings in the SELTOCSY experiment (d9 = 0.03 seconds) and the $^{2,3}J_{CH}$ correlations in the HMBC experiment in the complex **12**.

Table 2-10: NMR Assignments for the Complex **12**

δ / ppm		**12**	
^{1}H NMR		**^{13}C NMR**	
		C-1	218.45 (C)
H-2	7.24 (d, $^{3}J_{HH}$ = 2.24 Hz)	*C-2*	137.03 (CH)
H-3	8.26 (d, $^{3}J_{HH}$ = 2.28 Hz)	*C-3*	177.85 (CH)
		C-11	153.62 (C)
H-12, 16	7.23 (m)	*C-12, 16*	122.25 (2 CH)
H-13, 15	7.44 (m)	*C-13, 15*	129.38 (2 CH)
H-14	7.31 (m)	*C-14*	127.27 (CH)
		C-21	151.28 (C)
H-22, 26	7.38 – 7.45 (m)	*C-22, 26*	128.28 (2 CH)
H-23, 25	7.43 (m)	*C-23, 25*	126.64 (2 CH)
H-24	7.38 – 7.45 (m)	*C-24*	128.15 (CH)
		CO-Re-CO	187.49 (2 C)
		N-Re-CO	191.69 (C)
		C-Re-CO	191.05 (C)

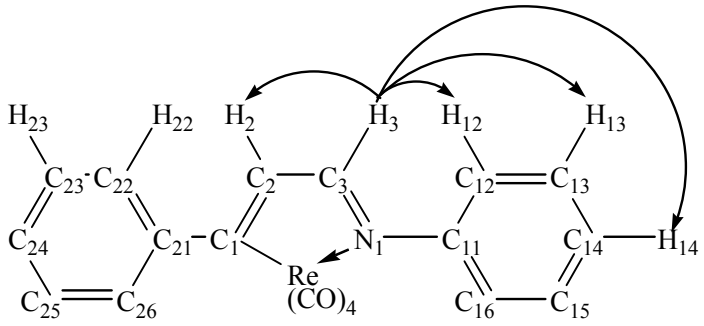

Figure 2-5: ^{1}H-^{1}H Couplings in the Complex **12**

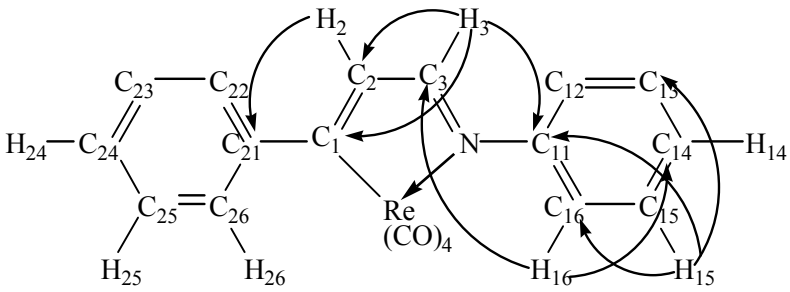

Figure 2-6: $^{2-3}J_{CH}$ Correlations in the Complex **12**

The signal for the *H-3* proton appeared at 8.26 ppm as a doublet with a $^{3}J_{HH}$ coupling constant of 2.28 Hz. The chemical shift was consistent with the corresponding signal for the free azabutadiene **16** and the coupling constant was decreased upon cyclisation which was expected[60]. The *H-3* signal showed a $^{1}J_{CH}$ correlation in the HSQC experiment to the tertiary carbon signal at 177.85 ppm, which was, therefore, assigned as *C-3*. In the SELTOCSY experiment, the *H-3* proton signal showed a ^{1}H-^{1}H coupling with the proton signal at 7.24 ppm. The 7.24 ppm signal showed a $^{1}J_{CH}$ correlation in the HSQC experiment to the tertiary carbon signal at 137.03 ppm. In the HMBC experiment, the *H-3* proton signal showed a correlation to the 137.03 ppm carbon signal, which was, therefore, assigned as *C-2* and the corresponding 7.24 ppm proton signal as *H-2*. The *H-3* proton signal also showed a $^{2,3}J_{CH}$ correlation to the quaternary carbon signal at 218.45 ppm. Signals for rheniated carbons can be expected to appear at ~200 ppm[63]. The 218.45 ppm carbon signal was, therefore, assigned as *C-1*.

The *H-2* proton signal showed a $^{2,3}J_{CH}$ correlation to the quaternary carbon signal at 151.28 ppm, which was assigned as *C-21*. The *C-21* carbon signal showed a correlation with the proton signals at ~7.38 and 7.43 ppm. Their corresponding carbon signals at 128.28 and 126.64 ppm, respectively, were determined by HSQC experiment. The DEPT experiment suggested that both carbon signals were tertiary carbon signals. By reference to the corresponding signals for the complexes **13a** and **13b**, the 128.28 and 126.64 ppm signals were assigned as *C-22, 26* and *C-23, 25*, respectively, and the corresponding proton signals as *H-22, 26* and *H-23, 25*. Further confirmations by HMBC experiment could, however, not be obtained due to overlap of the signals. The signals for the *H-24* proton and the *C-24* carbon were also overlapped with the other signals in the aromatic region and no supporting $^{2-3}J_{CH}$ correlations could, therefore, be obtained. The *H-24* and *C-24* signals may, however, be assigned for the proton signal at 7.38 – 7.45 and the carbon signal at 128.15 ppm, respectively, by reference to those for the complexes **13a** and **13b**. The intensity of the 128.15 ppm carbon signal was the half of that of the carbon signals corresponding to two tertiary aromatic carbons, which may suggest that the signal can be assigned for one tertiary carbon.

The *H-3* proton signal showed a $^{2,3}J_{CH}$ correlation to the quaternary carbon signal at 153.62 ppm, which was, therefore, assigned as *C-11*. The *H-3* proton signal showed ^{1}H-^{1}H couplings with the proton signals at 7.23, 7.44 and 7.31 ppm in the SELTOCSY experiment. Their corresponding carbons were determined at 122.25, 129.38 and 127.27 ppm, respectively, by HSQC experiment. The 7.23 ppm proton signal showed a $^{2,3}J_{CH}$ correlation to the *C-3* carbon signal. The proton signal and the corresponding carbon were, therefore, assigned as *H-12, 16* and *C-12, 16*, respectively. The intensity of the 122.25, 129.38 and 127.27 ppm signals was 2 : 2 : 1, respectively, suggesting that the former of those can be assigned for two tertiary carbons and the latter for one. The 129.38 and 127.27 ppm carbon signals were, therefore, assigned as *C-13, 15* and *C-14*, respectively. The assignments were further supported by the $^{2-3}J_{CH}$ correlations in the HMBC experiment (Figure 2-6). The *H-13, 15* proton signals showed $^{2-3}J_{CH}$ correlations to the *C-11* and *C-12, 16* carbon signals and the *H-12, 16* proton signals to the *C-13, 15* carbon signals. The ^{1}H-^{1}H couplings of the *H-3* proton signal with the *H-12, 16, 13, 15* and *14* proton signals were not observed in the corresponding SELTOCSY spectrum of the azabutadiene **16**. The couplings in the complex **12** may, therefore, be due to incorporation into the rigid structure of the cyclometallated five-membered ring.

The carbonyl quaternary carbons appeared at 191.69, 191.05 and 187.49 ppm with 1 : 1 : 2 intensity, respectively. The two *axial* C≡O carbons can be expected to appear as one signal as are chemically equivalent. One *equatorial* CO carbon, on the other hand, is *trans* to nitrogen and the other to carbon, so they expect two signals. The signal for the former is expected to appear at a higher chemical shift than that for the latter as nitrogen is more deshielding than carbon. The 191.69, 191.05 and 187.49 ppm signals were, therefore, assigned as *N-Re-CO*, *C-Re-CO*, and *CO-Re-CO*, respectively.

For the substituted derivatives **13a** and **13b**, the NMR experiments were carried out on the mixture of the two isomers in $CDCl_3$. Two sets of the signals with 3 : 1 intensity were observed. Each can be assigned for the *trans*- **13a** or the *cis*-isomer **13b**. By inspection, there appeared to be more of the plate-shaped single crystals than the needles formed. The set of the signals with a greater intensity was, therefore, assigned to the *trans*- **13a** and the other to the *cis*-isomer **13b**. A full assignment of the ^{1}H and ^{13}C signals was not possible, especially the aromatic protons and carbons,

due to overlap of the signals. The table below, therefore, summarises the selected assignments. The figures illustrate the ^{1}H-^{1}H coupling in the SELTOCSY experiment (d9 = 0.03 seconds) and the $^{2\text{-}3}J_{CH}$ correlations in the HMBC experiment in the *trans*-isomer **13a**.

Table 2-11: Selected NMR Assignments for the Complexes **13a** and **13b**

δ / ppm	**13a**	**13b**		**13a**	**13b**
^{1}H NMR			**^{13}C NMR**		
			C-1	200.71 (C)	200.11 (C)
H-2	7.28 (d, $^{3}J_{HH}$ = 2.16 Hz)	7.10 (d, $^{3}J_{HH}$ = 2.44 Hz)	*C-2*	135.25 (CH)	135.90 (CH)
H-3	8.40 (d, $^{3}J_{HH}$ = 2.28 Hz, 1 H)	8.15 (d, $^{3}J_{HH}$ = 2.40 Hz, 0.3 H)	*C-3*	176.31 (CH)	176.04 (CH)
H-4	8.17 (d, $^{3}J_{HH}$ = 10.00 Hz, 1 H)	7.88 (d, $^{3}J_{HH}$ = 9.80 Hz, 0.3 H)	*C-4*	171.82 (CH)	174.57 (CH)
H-5	6.25 (m, 1 H)	6.87 (m)	*C-5*	120.69 (CH)	122.70 (CH)
H-6	6.98 (d, $^{3}J_{HH}$ = 15.65 Hz, 1 H)	6.98 (d, $^{3}J_{HH}$ = 15.65 Hz, 0.3 H)	*C-6*	147.55 (CH)	150.42 (CH)
			C-11	153.30 (C)	152.62 (C)
			C-12, 16	122.61 (2 CH)	120.71 (2 CH)
			C-21	151.73 (C)	151.91 (C)
H-22, 26	7.46 (dd, $^{3,4}J_{HH}$ = 7.00, 1.14 Hz)	7.53 (dd, $^{3,4}J_{HH}$ = 7.08, 1.28 Hz)	*C-22, 26*	126.73 (2 CH)	127.02 (2 CH)
			C-31	151.54 (C)	156.07 (C)
			C-41	134.29 (C)	134.54 (C)
			C-Re-CO	193.67 (C)	193.67 (C)
			N-Re-CO	199.45 (2 C)	193.95 (2 C)

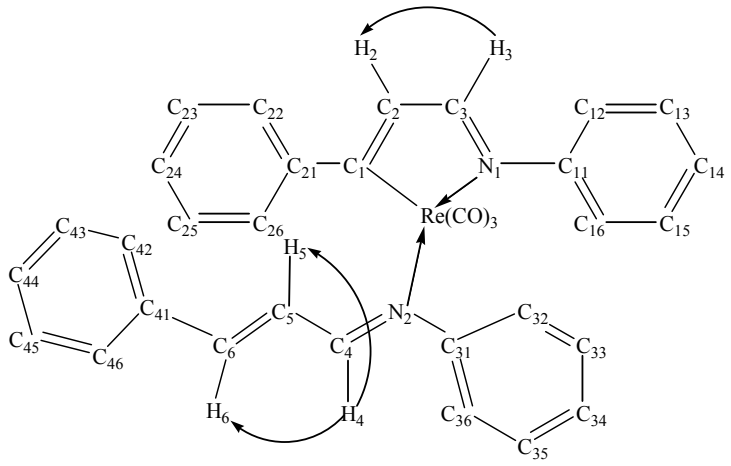

13a

Figure 2-7: Selected ^{1}H-^{1}H Couplings in the *trans*-Isomer **13a**

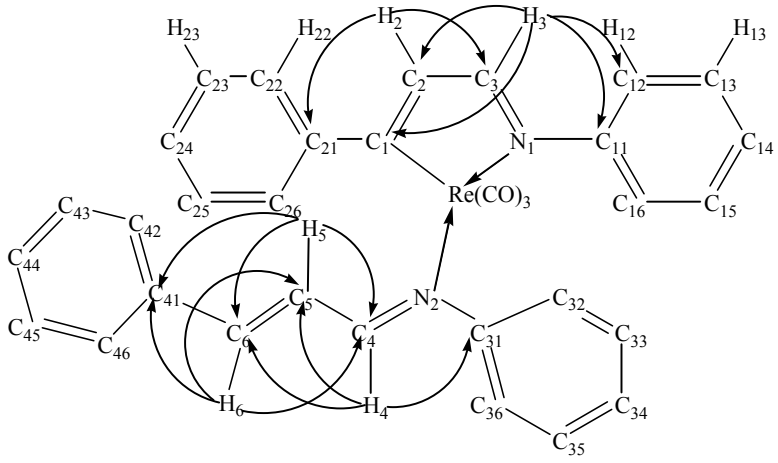

13a

Figure 2-8: Selected $^{2,3}J_{CH}$ Correlations in the *trans*-Isomer **13a**

For the *trans*-isomer **13a**, the *H-3* proton signal appeared at 8.40 ppm as a doublet with a $^{3}J_{HH}$ coupling constant of 2.28 Hz. The signal was shifted by 0.12 ppm down-field from the corresponding signal for the complex **12** upon substitution of a second azabutadiene. The coupling constants were, however, consistent. The *H-3* signal showed a $^{1}J_{CH}$ correlation in the HSQC experiment to the tertiary carbon signal at 176.31 ppm, which was, therefore, assigned as *C-3*. In the SELTOCSY experiment, the *H-3* proton signal showed a ^{1}H-^{1}H coupling with the proton signal at 7.28 ppm and this signal showed a $^{1}J_{CH}$ correlation in the HSQC experiment to the tertiary carbon signal at 135.25 ppm. The HMBC experiment showed a $^{2\text{-}3}J_{CH}$ correlation between the 135.25 ppm carbon and the *H-3* proton signals and also between the 7.28

proton and the *C-3* carbon signals (Figure 2-8). The 7.28 ppm proton signal was, therefore, assigned as *H-2* and the corresponding carbon as *C-2*.

The *H-3* proton signal showed a $^{2,3}J_{CH}$ correlation to the quaternary carbon signal at 200.71 ppm, which was in the position expected for rheniated carbon signals (cf. 218.45 ppm for the complex **12**) and, therefore, assigned as *C-1*. The *C-1* carbon signal was shifted by 18 ppm up-field upon substitution of a second azabutadiene from the corresponding signal for the complex **12**.

The *H-4* proton signal appeared at 8.17 ppm as a doublet with a $^{3}J_{HH}$ coupling constant of 10.00 Hz and showed a $^{1}J_{CH}$ correlation in the HSQC experiment to the tertiary carbon signal at 171.82, which was, therefore, assigned as *C-4*. The signal was shifted by 0.11 ppm up-field from the corresponding signal at 8.28 ppm for the free azabutadiene **16**. The *H-4* signal showed ^{1}H-^{1}H couplings with the proton signals at 6.25 and 6.98 ppm in the SELTOCSY experiment and the proton signals showed a $^{1}J_{CH}$ correlation in the HSQC experiment to the tertiary carbon signals at 120.69 and 147.55 ppm, respectively. In the HMBC experiment, the $^{2,3}J_{CH}$ correlations (Figure 2-8) suggested that the 6.25 and 6.98 ppm signals could be assigned as *H-5* and *6* and the corresponding carbons as *C-5* and *6*, respectively.

The signals for the aromatic ring protons and carbons were difficult to assign because of overlap of the signals. The signals for the ring quaternary carbons could, however, be assigned by the $^{2,3}J_{CH}$ correlations in the HMBC experiment (Figure 2-8). The quaternary carbon signals at 153.30, 151.73, 151.54 and 134.29 ppm were assigned as *C-11*, *21*, *31* and *41*, respectively.

The C≡O carbon signals appeared at 193.67 and 199.45 ppm with 1 : 2 intensity, respectively. The signals for the two C≡O carbons *trans* to nitrogen may be expected to appear as one signal due to the similar chemical environments. The former was, therefore, assigned as *C-Re-C≡O* and the latter as *N-Re-C≡O*. A correlation was observed in the HMBC experiment between the C≡O carbon and the *H-2, 3* and *4* proton signals. The *H-3* and *4* proton signals showed a correlation to the *C-Re-C≡O* carbon signal and the *H-2* signal to both the *N-Re-CO* and *C-Re-CO* carbon signals. These correlations are all beyond the $^{3}J_{CH}$ distances, so may, therefore, arise from the

geometry of the molecule in which the configurations of the protons and carbons are appropriate to show a correlation in the HMBC experiment.

The overall pattern of the chemical shifts for the cyclorheniated five-membered ring and diene protons and carbons were consistent with the corresponding shifts for the complex **12** and the free ligand **16**, respectively. For the substituted derivative **13a**, however, the signals for the five-membered ring protons and carbons were shifted slightly down-field from the corresponding signals for the complex **12** and those for the ligand were, on the other hand, observed at slightly up-field than the corresponding signals for the free azabutadiene **16**.

The figure below shows the selected ^{1}H-^{1}H couplings in the SELTOCSY and $^{2,3}J_{CH}$ correlations in the HMBC experiments in the complex **13b**.

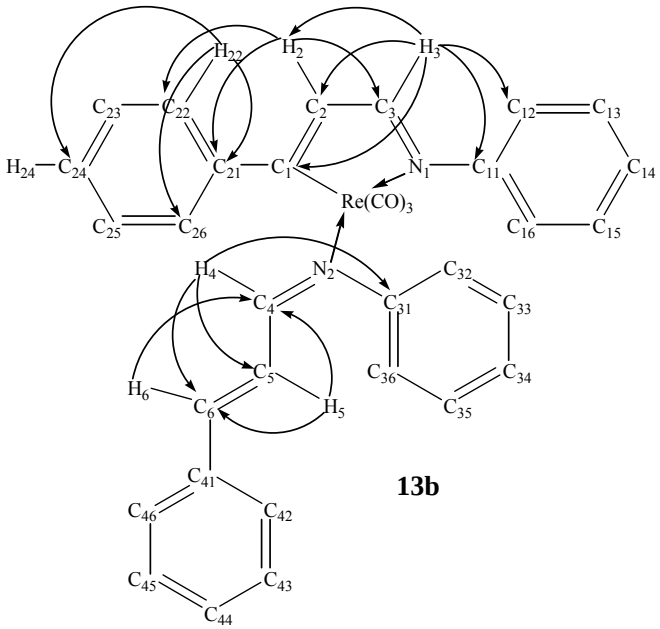

13b

Figure 2-9: Selected ^{1}H-^{1}H Couplings and $^{2,3}J_{CH}$ Correlations in the *Cis*-Isomer **13b**

The *H-3* proton signal appeared at 8.15 ppm as a doublet with a $^{3}J_{HH}$ coupling constant of 2.4 Hz. The coupling constant was consistent, but the signal was shifted by 0.13 – 0.25 ppm up-field from the corresponding signals for the *trans*-isomer **13a** and also the complex **12**, respectively. In the SELTOCSY experiment, the *H-3* proton signal showed a ^{1}H-^{1}H coupling with the proton signal at 7.10 ppm, which was, therefore, assigned as *H-2*. The *H-2* proton signal also appeared as a doublet with a

$^{3}J_{HH}$ coupling constant of 2.4 Hz, which agreed with the coupling constant of the *H-3* signal. As for the *H-3* proton signal, the *H-2* proton signal was also shifted up-field by 0.14 – 0.18 ppm from the corresponding signals for the *trans*-isomer **13a** and the complex **12**, respectively. The *H-3* and *2* proton signals showed a $^{1}J_{CH}$ correlation to the tertiary carbon signals at 176.04 and 135.90 ppm in the HSQC experiment, which were, therefore, assigned as *C-3* and *2*, respectively. These could be further confirmed by the $^{2,3}J_{CH}$ correlations in the HMBC experiment (Figure 2-9), which showed the correlations between the *H-3* proton and the *C-2* carbon signals, and also the *H-2* proton and the *C-3* carbon signals. The chemical shifts of the *C-3* and *2* carbon signals were consistent with the corresponding signals for the *trans*-isomer **13a** and slightly shifted by 2 ppm down-field from those for the complex **12**. The *H-3* proton signal also showed a $^{2,3}J_{CH}$ correlation to the quaternary carbon signal at 200.11 ppm in the HMBC experiment, which was assigned as *C-1*. The chemical shift was consistent with the corresponding shift for the *trans*-isomer **13a** and shifted by 18 ppm up-field from the corresponding signal for the complex **12** as for the *trans*-isomer **13a**.

The *H-4* proton signal appeared at 7.88 ppm as a doublet with a $^{3}J_{HH}$ coupling constant of 9.80 Hz and showed a $^{1}J_{CH}$ correlation to the tertiary carbon signal at 174.57 ppm in the HSQC experiment, which was, therefore, assigned as *C-4*. In the SELTOCSY experiment, the *H-4* proton showed a ^{1}H-^{1}H coupling with the proton signals at 6.87 and 6.98 ppm, which showed a $^{1}J_{CH}$ correlation to the tertiary carbon signals at 122.70 and 150.42 ppm, respectively, in the HSQC experiment. The $^{2,3}J_{CH}$ correlations in the HMBC experiment (Figure 2-9) suggested that the 6.87 and 6.98 ppm proton signals could be assigned as *H-5* and *6* and the corresponding carbons as *C-5* and *6*, respectively. The *H-4* proton signal was shifted by 0.29 ppm up-field and the $^{3}J_{HH}$ coupling constant was also decreased by 0.2 Hz from the corresponding signal and coupling constant for the *trans*-isomer **13a**. The *H-5* proton signal was, on the other hand, shifted by 0.62 ppm down-field from the corresponding signal for the *trans*-isomer **13a**. The chemical shift of the *H-6* proton signal was consistent with the corresponding signal for the *trans*-isomer **13a**. The *C-4, 5* and *6* carbon signals were all shifted by ~3 ppm down-field from the corresponding signals for the *trans*-isomer **13a**. These shifts may be accounted by the *trans*- or *cis*-configurations of the coordinating azabutadiene **16**.

The *H-2* proton signal showed a $^{2,3}J_{CH}$ correlation to the quaternary carbon signal at 151.91 ppm and also to the tertiary carbon signal at 127.02 ppm in the HMBC experiment (Figure 2-9), which were, therefore, assigned as *C-21* and *C-22*, *26*, respectively. The *C-22, 26* carbon signals showed a $^{1}J_{CH}$ correlation to the proton signal at 7.46 ppm, which was, therefore, assigned as *H-22, 26*. In the HMBC experiment, the proton signal at 6.87 ppm showed $^{2,3}J_{CH}$ correlations to the *C-21*, *C-22, 26* and the tertiary carbon signals at 128.55 and 130.73 ppm. The 130.73 ppm carbon signal showed a $^{1}J_{CH}$ correlation to the proton signal at 7.35 ppm and the 128.55 ppm signal to the 6.87 ppm proton signal in the HSQC experiment. The 6.87 and 7.35 ppm proton signals were, therefore, assigned as *H-23, 25* and *H-24* and the 128.55 and 130.73 ppm carbon signals as *C-23, 25* and *C-24*, respectively. No further confirmations by $^{2,3}J_{CH}$ correlations for these proton and carbon signals could, however, be obtained due to overlap of the signals.

The *H-4* proton signal showed a $^{2,3}J_{CH}$ correlation to the quaternary carbon signal at 156.07 ppm, which was, therefore, assigned as *C-31*. There was also a correlation between the *C-31* carbon signal and the proton signals at 6.90 and 7.14 ppm. There may be shielding and deshielding effects at the *ortho*- and the *meta*-substituted ring protons, respectively, by the imine nitrogen[60]. The 6.90 and 7.14 ppm proton signals were, therefore, assigned as *H-32, 36* and *H-33, 35*, respectively. Neither the corresponding carbon signals nor further $^{2,3}J_{CH}$ correlations could be determined in either the HSQC or HBBC experiment due to overlap of the signals in the aromatic region.

The *H-3* proton signal showed a $^{2,3}J_{CH}$ correlation to the quaternary carbon signal at 152.62 ppm in the HMBC experiment, which was, therefore, assigned as *C-11*. The other ring proton and carbon signals could not be determined because of overlap of the signals in the aromatic region.

The C≡O carbon signals were observed at 193.67 and 193.95 ppm with 1 : 2 intensity, respectively. As for the *trans*-isomer **13a**, the *N-Re-CO* carbon signals may appear as one signal at a higher chemical shift than the *C-Re-CO* carbon signal and the latter may, therefore, expect a half of the intensity of the former. The 193.67 and 193.95 ppm carbon signals were, therefore, assigned as *C-Re-CO* and *N-Re-CO*, respectively.

For the *cis*-isomer **13b**, the chemical shifts of the *N-Re-CO* and *C-Re-CO* carbon signals were very similar, while the former was by 6 ppm higher than the latter for the *trans*-isomer **13a**, indicating that the tricarbonyl carbons in the *cis*-isomer **13b** were almost chemically equivalent. As for the *trans*-isomer **13a**, the *H-2*, *3* and *4* proton signals showed a correlation to the C≡O carbon signals in the HMBC experiment. The *H-3* proton signal showed a correlation to the *C-Re-CO* signal, the *H-2* signal to both *C-Re-CO* and *N-Re-CO* signals, and the *H-4* signal to the *N-Re-CO* signal. The correlations between the *H-2* and *3* proton and the carbonyl carbon signals were consistent in both isomers. The *H-4* proton signal in the *cis*-isomer **13b**, however, showed a correlation to the *N-Re-CO* carbon signal, while it was to the *C-Re-CO* carbon signal in the *trans*-isomer **13a**.

2.2.2.1.2.4 X-Ray Crystallography

The structure of **12** was determined by X-ray crystallography (Figure 2-10). The table below shows the selected bond lengths for the complex **12**.

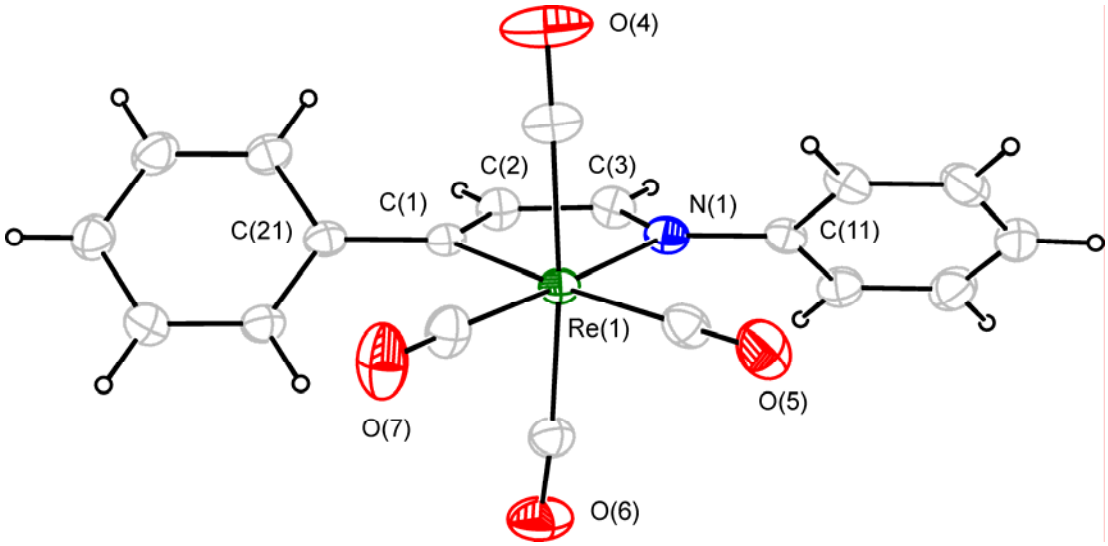

Figure 2-10: X-ray Single Crystal Structure of **12**

Table 2-12: Selected Bond Lengths for the Complex **12**

12 / Å	
Re(1)-C(1)	2.1877(16)
Re(1)-N(1)	2.1852(15)
C(1)-C(2)	1.343(2)
C(2)-C(3)	1.427(3)
N(1)-C(3)	1.319(2)
Re(1)-C(4)	1.9859(19)
Re(1)-C(5)	1.951(2)
Re(1)-C(6)	1.9949(19)
Re(1)-C(7)	1.9356(19)

The Re(1), C(1), C(2), C(3) and N(1) form a five-membered ring to give a cyclorheniated azabutadiene. The five-membered ring is planar with the two phenyl groups twisted out of the plane. There are two axial CO ligands and two equatorial ones *trans* to C(1) and N(1), respectively. Carbon has higher *trans*-influence than nitrogen, so the Re(1)-C(5) distance expects to be longer than the Re(1)-C(7) one. The Re(1)-C(5) distance of 1.951(2) Å was longer by 0.015 Å than the Re(1)-C(7) distance of 1.936(19) Å. The two equatorial CO ligands are equivalent, competing for the dπ-electron density of the rhenium, so the Re(1)-C(4) and Re(1)-C(6) distances expect to be the same and those of 1.9859 and 1.9949 Å were essentially the same with the standard deviation of 0.0019 Å.

X-ray crystal structure determinations were also carried out on the single crystals of the two isomers of the substituted derivatives **13a** and **13b**. The figures illustrate the structure of **13a** and **13b** and the table summarises the selected bond lengths for the *trans*- and *cis*-isomer **13a** and **13b**, respectively.

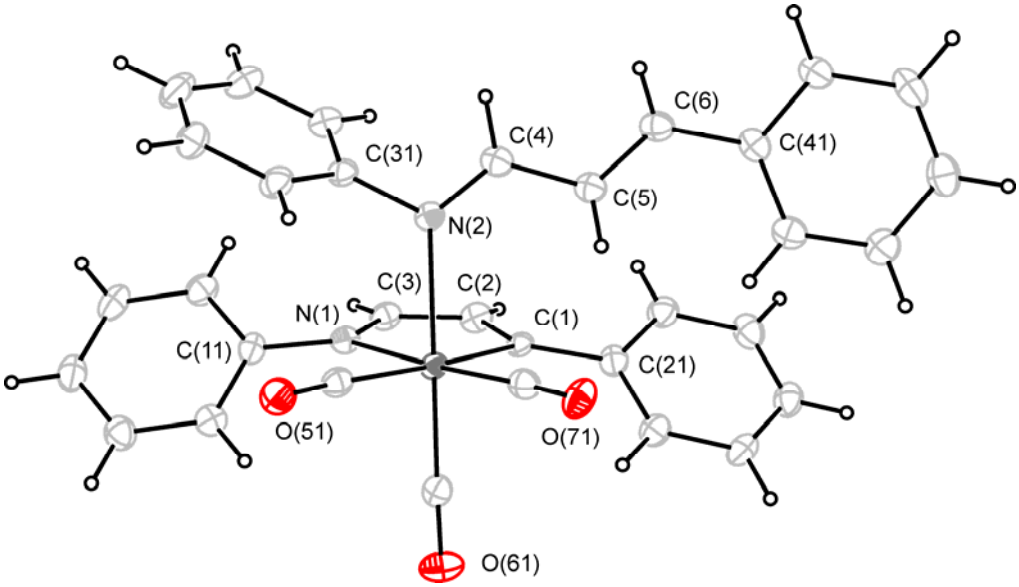

13a

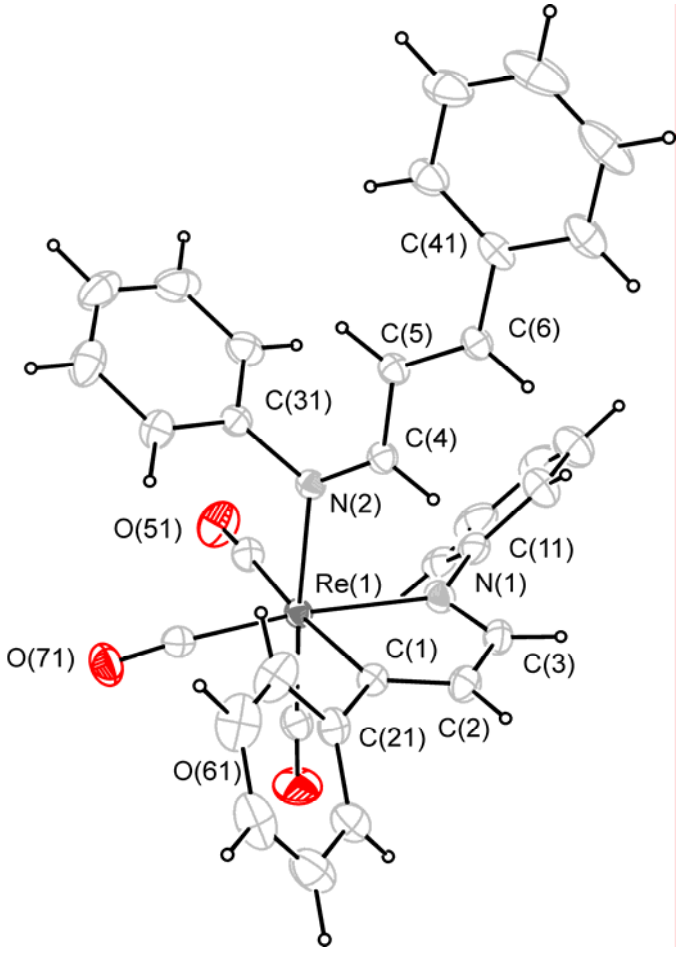

13b

Figure 2-11: X-ray Single Crystal Structures of **13a** and **13b**

Table 2-13: Selected Bond Lengths for the Complexes **13a** and **13b**

/ Å	**13a***	**13b**
Re(1)-C(1)	2.187(3)	2.178(2)
Re(1)-N(1)	2.186(2)	2.183(2)
Re(1)-N(2)	2.238(2)	2.188(2)
Re(1)-C(51)	1.953(3)	1.949(3)
Re(1)-C(61)	1.916(3)	1.925(3)
Re(1)-C(71)	1.922(3)	1.922(3)
C(1)-C(2)	1.352(4)	1.346(4)
C(2)-C(3)	1.423(4)	1.423(4)
C(4)-C(5)	1.437(4)	1.443(3)
C(5)-C(6)	1.342(4)	1.341(3)
N(1)-C(3)	1.313(4)	1.315(4)
N(2)-C(4)	1.295(4)	1.294(3)

*Data adapted from the undergraduate laboratory report[57]

Again, there is a cyclorheniated ring which has the same geometry and bond length in both the complexes **13a** and **13b** as in the complex **12**. In the complex **13a**, one *axial* CO is replaced by a *trans*-azabutadiene coordinated to the rhenium through the imine nitrogen. That is a *cis*-azabutadiene which replaces one *axial* CO in the complex **13b**.

The Re(1)-N(2) distance of 2.238(2) Å in the *trans*-isomer **13a** was longer than that of 2.188(2) Å in the *cis*-isomer **13b**, indicating stronger coordination of the latter to the rhenium. In the *trans*-isomer **13a**, the bulky phenyl groups of the cyclorheniated azabutadiene and the ligand are facing each other, creating steric crowding around the Re(1)-N(2) bond. While, in the *cis*-isomer **13b**, the *cis*-azabutadiene coordinates at 90° with respect to Re, so the bulky phenyl groups are away from those of the cyclorheniated azabutadiene and, hence, there is less steric crowing around the Re(1)-N(2) bond, making the N(2) possible to coordinate more closely and, hence, strongly to the metal. The Re(1)-N(2) distance of 2.188 Å in the *cis*-isomer **13b** was essentially the same as the Re(1)-N(1) of 2.183(2) within the standard deviation, suggesting that the coordination of the N(2) to the rhenium is as strong as that of the N(1) in the cyclorheniated ring.

Trans-influence was also observed in both isomers **13a** and **13b**. The Re(1)-C(51) bond length was longer than the Re(1)-C(61) and Re(1)-C(71) ones which are both *trans* to nitrogen.

In both isomers, the C(1)-C(2) distances of 1.352(4) and 1.346 Å were slightly longer than the C(5)-C(6) of 1.342(4) and 1.341(3) Å. The N(1)-C(3) distances of 1.313(4) and 1.315(4) Å were also longer than the N(2)-C(4) of 1.295(4) and 1.294(3) Å. The C(2)-C(3) distances of 1.423(4) and 1.423(4) Å were, on the other hand, shorter than the C(4)-C(5) distance of 1.437(4) and 1.443(3) Å. The longer C(1)-C(2) and C(3)-N(1) and shorter C(2)-C(3) bond distances in the cyclorheniated rings than the formal π- and σ-bonds in the ligands may suggest that the five-membered ring has some degree of aromaticity, a pseudo-aromatic system, as generally expected for cyclometallated compounds[16].

No previous examples of *cis*-azabutadienes acting as a ligand towards a metal have been reported, while there are many of *trans*-ones. The complex **13b** appears, therefore, to be the first example of *cis*-azabutadiene metal complexes that has ever been isolated and the structure of which was determined by X-ray crystallography.

2.2.2.2 Reaction of $PhCH_2Re(CO)_5$ with the Azabutadienes *17* and *18*

To further investigate, reaction of $PhCH_2Re(CO)_5$ with azabutadienes, the azabutadienes **17** and **18** were prepared and reacted under the same conditions. The basicity of the imine nitrogen was reduced in the azabutadiene **17** and those of the *C-1* carbon and imine nitrogen were enhanced in the azabutadiene **18** with respect to those in the azabutadiene **16**. The reactions were summarised in the schemes below.

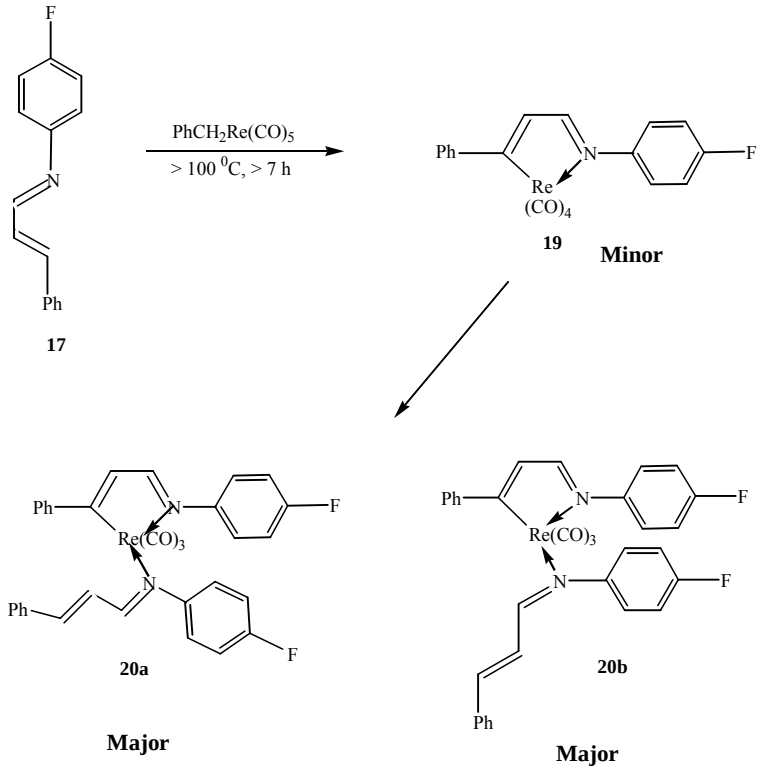

Scheme 2-4: Reaction with the Azabutadiene **17**

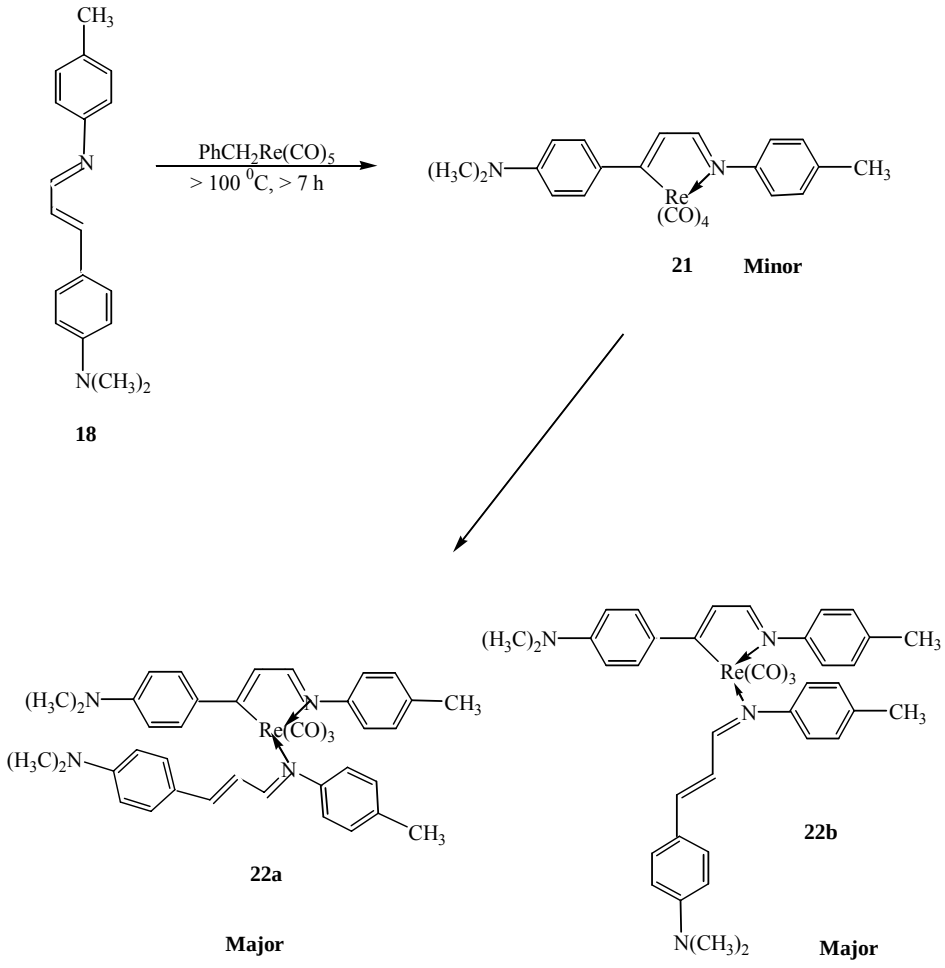

Scheme 2-5: Reaction with the Azabutadiene **18**

2.2.2.2.1 Reaction

When a mixture of $PhCH_2Re(CO)_5$ and the azabutadienes **17** and **18** was heated at > 100 ºC for 7 hours, analogues of the cyclorheniated azabutadiene tetracarbonyl complex **12**, and the substituted derivatives **13a** and **13b**, **19** and **21**, and **20a**, **20b**, **22a** and **22b**, respectively, were obtained.

The IR spectra of the reactions in CH_2Cl_2/heptane indicated that both reactions could be initiated at > 95 ºC, which was consistent with the reaction with the azabutadiene **16**, by the development of the e bands at 1900 and 1890 cm^{-1} for the reactions with the azabutadienes **17** and **18**, respectively. A_1 band could also be observed at 2003 and 1996 cm^{-1} for the reactions with the azabutadienes **17** and **18**, respectively, as the reaction continued. The mixtures turned intense red and precipitation of the products as a red solid were also observed in both reactions as in the reaction with the azabutadiene **16**.

The products could, again, easily be purified by PLC, eluting with CH_2Cl_2/petroleum spirits and crystallised from CH_2Cl_2/petroleum spirits at –20 ºC. The cyclorheniated azabutadiene tetracarbonyl complexes **19** and **21** could be obtained as yellow and red plates, respectively, the latter of which was different in colour from the other two analogues which were both yellow. The substituted derivatives **20a** and **20b**, and **22a** and **22b** were obtained again as a mixture of red plates and needles. X-ray crystal determinations on the single crystals of **20a** and **20b** confirmed that the plate-shaped crystal was the *trans*- and the needle was the *cis*-isomer as for the *trans*- and *cis*-isomers of the substituted derivatives **13a** and **13b**. The plates and needles obtained from the reaction with the azabutadiene **18** were, therefore, assumed to be the *trans*- and *cis*-isomer, respectively, of the substituted derivative **22**. The two isomers were, again, not possible to isolate by PLC.

The substituted derivatives were the main products in both reactions and the cyclorheniated tetracarbonyl complexes were obtained again in minor yields as in the reaction of the azabutadiene **16**. The table below summarises the yields of the cyclorheniated tetracarbonyl complexes and the substituted derivatives prepared from 1 : < 1 and 1 : > 2 mole ratio reactions ($PhCH_2Re(CO)_5$: azabutadiene), using the

approximately 0.30 moles of $PhCH_2Re(CO)_5$. The yields from 1 : < 1 and 1 > 2 mole ratio reactions were calculated based on the number of moles of the azabutadienes and the $PhCH_2Re(CO)_5$, respectively. The stated yields for the substituted derivatives were as the mixture of the two isomers.

Table 2-14: Yields (%) of the Complexes **12, 13**, **19**, **20**, **21** and **22** from 1 : < 1 and 1 : > 2 Mole Ratio Reactions

Mole Ratio[*1]	**12**	**19**	**21**	**13**[*2]	**20**[*2]	**22**[*2]
1 : < 1	29	15	32	57	73	67
1 : > 2	7	8	-	93	77	-

[*1] $PhCH_2Re(CO)_5$: Azabutadienes; [*2] As the mixture of the two isomers.

The yields of the substituted derivatives were always good to excellent e.g. 57 – 93% in all the reactions. The yield of the cyclorheniated azabutadiene **19** could be improved in 1 : 1 mole ratio reaction, which was consistent with that of the cyclorheniated complex **12**.

On 1 : 1 mole ratio, using ~0.30 moles of $PhCH_2Re(CO)_5$, it required four hours for the C≡O bands corresponding to the starting material of $PhCH_2Re(CO)_5$ to completely shift to the product bands in the reaction with the azabutadiene **16**, while it was seven and half hours and three hours in the reactions with the azabutadienes **17** and **18**, respectively. In the azabutadiene **17**, the basicity of the imine was reduced by the electron-withdrawing fluorine and was enhanced in the azabutadiene **18** by the electron-donating methyl group at the *para*-sites of the aniline rings. The cyclometallated azabutadiene is believed to form via initial coordination of the imine nitrogen to the metal followed by formation of a new σ-bond between the *C-1* carbon and the metal to give the metallocycle. The longer and shorter reaction times for the reactions with the azabutadienes **17** and **18**, respectively, may, therefore, be due to the reduced or enhanced basicity of the imine nitrogen and/or the *C-1* carbon in the azabutadienes **17** and **18**. It may also be assumed that the reactions both occur by the same route and give the same products as in the reaction with the azabutadiene **16**, so are the same reactions.

2.2.2.2.2 Characterisation

2.2.2.2.2.1 IR

IR analysis was carried out in CH_2Cl_2. The table below summarises the υ(C≡O) frequencies for the complexes **12**, **13**, **19**, **20**, **21** and **22**. The data for the substituted derivatives were as the mixture of the two isomers.

Table 2-15: C≡O Frequencies for the Complexes **12**, **13**, **19**, **20**, **21** and **22**

υ(C≡O) / cm^{-1}	**12**	**19**	**21**	**13**	**20**	**22**
	2092 (w)	2092 (vw)	2089 (vw)	2002 (s)	2003 (s)	1996 (s)
	1992 (s)	1994 (s)	1988 (s,br)	1896 (s,br)	1900 (s,br)	
		1983 (s)	1973 (s,br)	1890 (s,br)	1890 (s,br)	1890 (s,br)
	1934 (m)	1935 (w)	1925 (w)			

Cis-$L_2Re(CO)_4$ molecules expect four carbonyl bands[61]. The four bands were observed at 2092 (w), 1994 (s), 1983 (s), 1935 (w) cm^{-1} for the complex **19** and at 2089 (vw), 1988 (s,br), 1973(s, br) and 1925 (w) cm^{-1} for the complex **21** in CH_2Cl_2. The υ(C≡O) frequencies for the complexes **12** and **19** were consistent. The 1992 cm^{-1} band which could not be resolved for the complex **12**, was also clearly observed as a strong band at 1983 cm^{-1} in the spectrum of the azabutadiene **19**. The υ(C≡O) bands for the complex **21** were observed at lower frequencies by 3 – 10 cm^{-1} from those for the complexes **12** and **19**.

$LRe(CO)_3$ molecules with L which has low symmetry, expect a_1 and e bands with the splitting of the latter[61]. The three bands were clearly observed at 2003 (s), 1900 (s, br) and 1893 (s, br) cm^{-1} in the spectrum of the complex **20**, but only two bands for the complex **22** at 1996 (s) and 1890 (s, br) with the latter containing the unresolved bands. Again, the υ(C≡O) frequencies for the complexes **13** and **20** were consistent. The a_1 band for the complex **22** was shifted by 7 cm^{-1} to a lower frequency from the corresponding frequencies for the complexes **13** and **20**, but that of the e band was consistent with the other two complexes, which, however, appeared as unresolved bands.

FTIR in transmission mode using a microscope attachment was also carried out on the single crystals of **20a**, **20b** and **22a**. The table below summarises the υ(C≡O) frequencies for the single crystals of **13a**, **20a**, **20b** and **22a**.

Table 2-16: υ(C≡O) Frequencies for the Single Crystals of **13a**, **20a**, **20b**, and **22a**

υ(C≡O) / cm^{-1}		A_1	E
13a	3984, 3860, 3756 (m)	1983 (vs,br)	1875 (vs,br)
20a	3990, 3875, 3773 (s)	1994 (vs)	1881 (vs,br)
20b	3991, 3874, 3773 (s)	1994 (vs)	1884 (vs,br)
22a	3981, 3871, 3745 (w)	1994 (s)	1871 (s,br)

The e bands for all the complexes appeared as unresolved bands. The a_1 bands for the complexes **20a**, **20b** and **22a** all shifted by 11 cm^{-1} to a higher frequency from that for the complex **13a**. The e bands for the complexes **20a** and **20b** also shifted by 6 – 9 cm^{-1} to higher frequencies and that for the complex **22a** was, on the other hand, shifted by 4 cm^{-1} to a lower frequency from the corresponding frequency for the complex **13a**. There was no significant difference in the frequencies of the υ(C≡O) bands in the *trans*- and *cis*-isomers **20a** and **20b**, suggesting that the two isomer were indistinguishable by IR spectroscopy.

The unusually strong overtones of the υ(C≡O) bands were also observed in the spectra of the complexes **20a**, **20b** and **22a** at similar frequencies and there was no sign of those in the normal IR spectrum as for the complex **13a**. The overtone bands for the isomer **22a** were very weak compared to the other complexes. This may, however, be only due to the quality of the single crystal, which of the complex **22a** was not as good as the other isomers.

2.2.2.2.2.2 ESI-MS

ESI-MS analysis was carried out at a cone voltage of 20 V in MeOH/NaOMe. The table below summarises the *m/z* corresponding to the parent molecules for the complexes **19**, **20**, **21**, and **22**.

Table 2-17: *M/z* Corresponding to the Parent Molecules for the Complexes **19**, **20**, **21**, and **22**

m/z (%)	$[M + H]^+$	$[M + Na]^+$	$[M + OMe]^-$
19			553(100)
21	562(100)[*1]	584(100)	593(100)
20[*2]		742(56)	750(100)
22[*2]	799(100)[*1]	821(100)	829(100)

[*1]In MeOH ; [*2]The mixture of the two isomers

For the complex **19**, the parent molecule was observed at *m/z* 553 as $[M + OMe]^-$ in the negative ion mode. For the complex **21**, it was observed at *m/z* 562, 584 and 593 as $[M + H]^+$, $[M + Na]^+$ and $[M + OMe]^-$, for the complex **20**, at m/z 742 and 750 as $[M + Na]^+$ and $[M + OMe]^-$ and for the complex **22**, at m/z 799, 821 and 829 as $[M + H]^+$, $[M + Na]^+$ and $[M + OMe]^-$, respectively. For the complex **22**, the observed *m/z* of 821.243 on HR-MS in MeOH/NaOMe closely agree with the mass of 821.247 calculated for the formulae $C_{39}H_{39}N_4NaO_3Re$, which can be assigned as $[M + Na]^+$ (M = **22**), further supporting the assignment. The *m/z* of 837.221 corresponding to the $[M + K]^+$ ion was also observed on HR-MS and showed a close agreement with the calculated mass for the formulae.

Loss of CO ligands at a cone voltage of 20 V, was also observed in the spectra of the complexes **19** and **21** as for the complex **12**. The *m/z* corresponding to the loss of CO ligands are summarised in the table below.

Table 2-18: *M/z* Corresponding to the Loss of CO Ligands from the Parent Molecules of **12**, **19** and **21** in ESI-MS at a Cone Voltage of 20 V

m/z(%)	$[M + OMe]^-$	$[M + OMe - CO]^-$	$[M + OMe - 2CO]^-$
12	535(100)	507(30)	479(10)
19	553(100)	525(40)	497(13)
21	592(100)	565(34)	536(30)

The peaks corresponding to one and two CO ligands losses were *m/z* 28 and 56, respectively, apart from the *m/z* of the parent molecules of **19** and **21** at *m/z* 553 and 592, respectively, as $[M + OMe]^-$ in the negative ion mode. At 20 V, the peaks corresponding to the parent molecules with no loss of a CO ligand appeared with 100

% intensity and those corresponding to loss of one and two CO ligands were observed with ~30 and ~10 % intensity, respectively. The cyclorheniated tetracarbonyl complexes **12**, **19** and **21** all showed loss of CO ligands at cone voltage of 20 V in ESI-MS. While, loss of CO ligands was not observed for the substituted tricarbonyl species at all, suggesting that the CO ligands in the tetracarbonyl species were more labile than those in the tricarbonyl species.

2.2.2.2.2.3 ^{1}H and ^{13}C NMR

NMR experiments were carried out on samples in $CDCl_3$ at 400 MHz. For the substituted derivatives, the experiments were carried out on the mixture of the two isomers. The *J* value of 160 Hz was used to optimise signals for aromatic and other sp^2 and sp carbons in the DEPT, HSQC and HMBC experiments and the d9 value of 0.03 seconds was used in the SELCTOSY experiment. The assignments for the complexes **12**, **19** and **21** are summarised in the table below and the figures show the selected ^{1}H-^{1}H couplings and $^{2,3}J_{CH}$ correlations in the complex **21**.

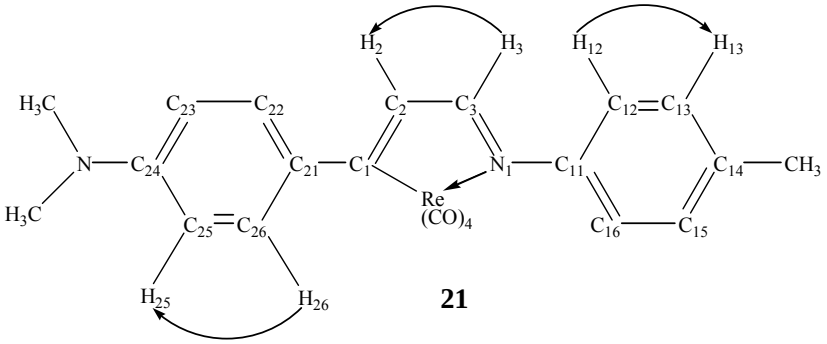

Figure 2-12: ^{1}H-^{1}H Couplings in the Cyclorheniated Azabutadiene **21**

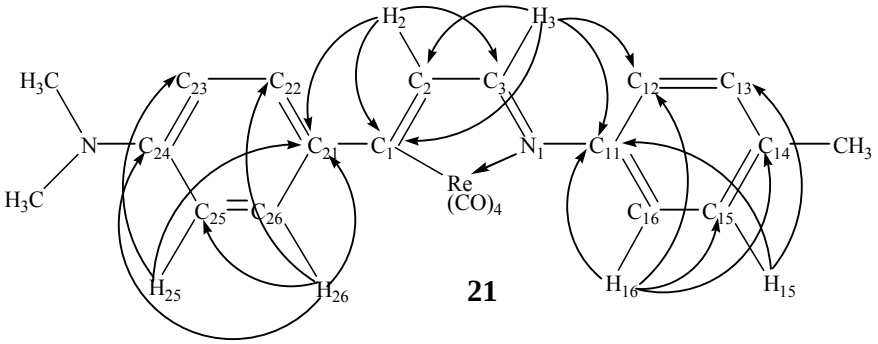

Figure 2-13: $^{2,3}J_{CH}$ Correlations in the Cyclorheniated Azabutadiene **21**

Table 2-19: NMR Assignments for the Complexes **12**, **19** and **21**

δ / ppm	**12**	**19**	**21**
^{1}H NMR			
H-2	7.24 (d, $^{3}J_{HH}$ = 2.24 Hz, 1 H)	7.23 (d, $^{3}J_{HH}$ = 2.32 Hz, 1 H)	7.25 (d, $^{3}J_{HH}$ = 2.52 Hz, 1 H)
H-3	8.26 (d, $^{3}J_{HH}$ = 2.28 Hz, 1 H)	8.23 (d, $^{3}J_{HH}$ = 2.32 Hz, 1 H)	8.16 (d, $^{3}J_{HH}$ = 2.52 Hz, 1 H)
H-12, 16	7.23 (m)	7.20 (m)	7.10 (d, $^{3}J_{HH}$ = 8.28 Hz, 2 H)
H-13, 15	7.44 (m)	7.12 (m, 3 H)	7.19 (m)
H-14	7.31 (m)	-	-
H-22, 26	7.38 – 7.45 (m)	7.43 (m, 7 H)	7.56 (d, $^{3}J_{HH}$ = 8.88 Hz, 2 H)
H-23, 25	7.43 (m)	7.43 (m)	6.75 (d, $^{3}J_{HH}$ = 8.88 Hz, 2 H)
H-24	7.38 – 7.45 (m)	7.30 (m, 1 H)	-
N(CH_3)$_2$			3.04 (s, 6 H)
CH_3			2.39 (s, 3 H)
^{13}C NMR			
C-1	218.45 (C)	219.47	216.99 (C)
C-2	137.03 (CH)	136.91	133.77 (CH)
C-3	177.85 (CH)	178.02	176.72 (CH)
C-11	153.62 (C)	149.93 (d, $^{4}J_{CF}$ = 3.30 Hz)	151.71 (C)
C-12, 16	122.25 (2 CH)	123.75 (d, $^{3}J_{CF}$ = 8.49 Hz)	122.23 (2 CH)
C-13, 15	129.38 (2 CH)	116.17 (d, $^{2}J_{CF}$ = 22.86 Hz)	129.72 (4 CH)
C-14	127.27 (CH)	161.45 (d, $^{1}J_{CF}$ = 246.92 Hz)	136.48 (C)
C-21	151.28 (C)	151.21	138.87 (C)
C-22, 26	128.28 (2 CH)	128.28 (2 CH)	129.72 (4 CH)
C-23, 25	126.64 (2 CH)	126.58 (2 CH)	111.52 (2 CH)
C-24	128.15 (CH)	128.23 (CH)	151.26 (C)
CO-Re-CO	187.49 (2 C)	187.37	188.24 (2 C)
N-Re-CO	191.69 (C)	191.43	192.55 (C)
C-Re-CO	191.05 (C)	190.99	191.41 (C)
N(CH_3)$_2$			40.39 (CH_3)
CH_3			21.02 (CH_3)

In the complex **21**, the *H-3* proton signal appeared at 8.16 ppm as a doublet with a $^{3}J_{HH}$ coupling constant of 2.52 Hz. The coupling constant was consistent, but the signal was shifted by 0.1 ppm up-field from the corresponding signal for the complex **12**. The *H-3* proton signal showed a $^{1}J_{CH}$ correlation to the tertiary carbon signal at 176.72 ppm in the HSQC experiment, which was, therefore, assigned as *C-3* and the chemical shift of the carbon signal also agreed with the corresponding signal for the complex **12**. The *H-3* signal showed a ^{1}H-^{1}H coupling with the proton signal at 7.25 ppm in the SELTOCSY experiment, which was, therefore, assigned as *H-2*. The *H-2* proton signal showed a $^{1}J_{CH}$ correlation to the tertiary carbon signal at 133.77 ppm in the HSQC experiment and the carbon signal was, therefore, assigned as *C-2*. The $^{2,3}J_{CH}$ correlations between the *H-3* proton and the *C-2* carbon signals, and the *H-2* proton and the *C-3* carbon signals in the HMBC experiment further supported the assignments. The *C-1* carbon signal was determined by the $^{2\text{-}3}J_{CH}$ correlations from the *H-3* and *2* proton signals in the HMBC experiment. Both the *H-3* and *2* proton signals showed a $^{2,3}J_{CH}$ correlation to the quaternary carbon signal at 216.99 ppm. With respect to the *C-1* carbon signal for the complex **12** which appeared at 218.45 ppm, the 216.99 ppm signal was assigned as *C-1*.

The *H-3* proton signal showed $^{2,3}J_{CH}$ correlations to the quaternary and tertiary carbon signals at 151.71 and 122.23 ppm, respectively, in the HMBC experiment. The corresponding proton signal for the 122.23 ppm tertiary carbon was determined by the HSQC experiment and appeared at 7.10 ppm. The 7.10 ppm proton signal appeared as a doublet with a $^{3}J_{HH}$ coupling constant of 8.28 Hz and also could integrate for two protons. The proton signal showed $^{2,3}J_{CH}$ correlations to the tertiary carbon signals at 122.23 and 129.72 ppm and the quaternary carbon signals at 151.71 and 136.48 ppm in the HMBC experiment. The HSQC experiment showed the corresponding proton signal for the 129.72 ppm carbon signal at 7.19 ppm. Further $^{2,3}J_{CH}$ correlations between the proton and carbon signals (Figure 2-13) suggested that the 151.71, 122.23, 129.72 and 136.48 ppm carbon signals could be assigned as *C-11*, *C-12, 16, C-13, 15* and *C-14*, respectively, and the corresponding protons as *H-12, 16* and *H-13, 15*.

The *H-2* proton signal showed a $^{2,3}J_{CH}$ correlation to the quaternary carbon signal at 138.87 ppm in the HMBC experiment. The proton signals at 7.56 and 6.75 ppm which

were both doublet with a $^{3}J_{HH}$ coupling constant of 8.88 Hz, showed a $^{2,3}J_{CH}$ correlation to the 138.87 carbon signal in the HMBC experiment. The 7.56 signal showed a ^{1}H-^{1}H coupling to the 6.75 ppm signal in the SELTOCSY experiment. The 7.56 and 6.75 ppm proton signals showed a $^{1}J_{CH}$ correlation to the carbon signals at 129.72 and 111.52 ppm, respectively, in the HSQC experiment. Further $^{2,3}J_{CH}$ correlations between the proton and carbon signals (Figure 2-13) suggested that the 138.87, 129.72 and 111.52 ppm carbon signals could be assigned as *C-21*, *C-22*, *26* and *C-23, 25*, respectively, and their corresponding proton signals as *H-22, 26* and *H-23, 25*. The *C-24* carbon signal could also be determined by the $^{3}J_{CH}$ correlation from the *H-22, 26* proton signals. The signal appeared at 151.26 ppm and was also confirmed as a quaternary carbon signal by the DEPT experiment.

The C≡O carbon signals appeared at 188.24, 192.55 and 191.41 ppm with 2 : 1 : 1 intensity, respectively, which were, therefore, assigned as *CO-Re-CO*, *N-Re-CO* and *C-Re-CO*, respectively. The chemical shifts were consistent with the corresponding signals for the complex **12**. As for the complex **12**, the *H-3* and *2* proton signals showed correlations to the C≡O carbon signals in the HMBC experiment. The *H-3* proton signal showed a correlation to the *N-Re-CO* and *CO-Re-CO* signals and the *H-2* signal to the *C-Re-CO* and *CO-Re-CO* signals.

The overall chemical shifts for the complexes **12** and **21** were consistent. The differences in the chemical shifts could be accounted by the substituent increments for CH_3 and $N(CH_3)_2$ groups.

The assignments for the complex **19** were made by comparison with those for the complexes **12** and **21**. In the complex **19**, the *H-3* proton appeared at 8.23 ppm as a doublet with a $^{3}J_{HH}$ coupling constant of 2.32 Hz. The *H-2* proton signal was observed at 7.23 ppm as a doublet with a $^{3}J_{HH}$ coupling constant of 2.32 Hz. Their corresponding carbons appeared at 178.02 and 136.91 ppm, respectively. The *C-1* carbon signal was observed at 219.47 ppm. The chemical shifts of the cinnamaldehyde ring proton and carbon signals closely agreed with the corresponding signals for the complex **12** and were, therefore, assigned accordingly. The signals for the *para*-fluorinated benzene ring protons and carbons were shifted by the substituent increments for a fluoride from the corresponding signals for the complex **12**. For the

ring carbon signals, ^{13}C-^{19}F couplings were also observed and the concerned carbon signals all appeared as a doublet with a descendent coupling constant with distance from the fluoride. The *C-14* carbon signal appeared at 161.45 ppm with a $^{1}J_{CF}$ coupling constant of 246.92 Hz, the *C-13, 15* signal at 116.17 ppm with a $^{2}J_{CF}$ coupling constant of 22.86 Hz, the *C-12, 16* signal at 123.75 ppm with a $^{3}J_{CF}$ coupling constant of 8.49 Hz and the *C-11* signal at 149.93 ppm with a $^{4}J_{CF}$ coupling constant of 3.30 Hz. The chemical shifts and intensity pattern of the C≡O carbon signals were also consistent with those for the complexes **12** and **21**. The two *axial* CO carbons appeared as one signal at 187.37 ppm and the *equatorial* CO carbons were observed at 191.43 and 190.99 ppm, which were assigned as *N-Re-CO* and *C-Re-CO*, respectively.

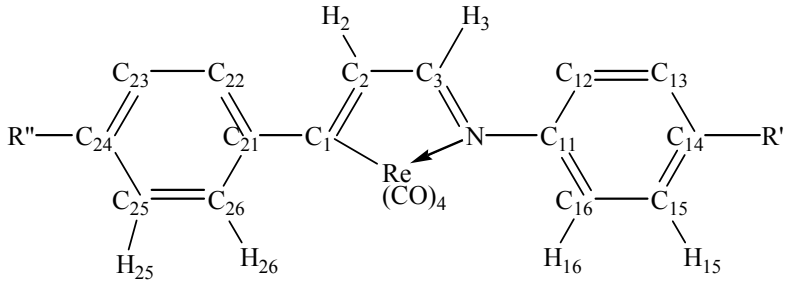

R' = F, CH_3 ; R" = $N(CH_3)_2$

Figure 2-14: Cyclorheniated Azabutadiene Tetracarbonyl Complex

In a cyclorheniated azabutadiene tetracarbonyl complex of the type above, a signal for the *H-3* proton appears at ~8.2 ppm as a doublet or a doublet of doublet with a $^{3}J_{HH}$ coupling constant of ~2.3 Hz. Signal for the *H-2* proton can be determined by SELTOCSY experiment irradiating at the *H-3* proton signal. The *H-2* signal usually appears at ~7.2 ppm as a doublet with a $^{3}J_{HH}$ coupling constant of ~2.4 Hz. The corresponding carbon signals can be determined by HSQC experiment. The *C-3* and *2* carbon signals appear at ~177 and ~136 ppm, respectively. $^{2,3}J_{CH}$ correlations between the *H-3* proton and *C-2* carbon signals, and the *H-2* proton and *C-3* carbon signals are usually observed in HMBC experiment and further support the assignments. The *C-1* carbon signal can be determined by the $^{2,3}J_{CH}$ correlations from the *H-3* and *2* proton signals in HMBC experiment and appears at ~217 ppm. The chemical shifts of the central ring proton signals remain consistent upon cyclometallation with $PhCH_2Re(CO)_5$, with the corresponding signals for the free azabutadiene. The

coupling constants of the *H-3* and *2* proton signals, however, decrease from ~8.0 to ~2.3 Hz upon the cyclometallation as expected[63]. Cyclorheniation shifts the central ring carbon signals by 8 – 16 ppm down-field. Rheniation also significantly shifts the *C-1* carbon signal to ~217 ppm from 144 ppm for the free azabutadiene, indicating rhenium is strongly deshielding.

Signals for the carbonyl carbons appear at ~191.6, 191.0 and 187.4 ppm with intensity of 1 : 1 : 2, respectively. The two *axial* C≡O carbons appear as one signal as they are in the same chemical environments. The signal for the *equatorial* C≡O carbon *trans* to nitrogen is observed at a higher chemical shift than that for the *equatorial* C≡O carbon *trans* to carbon as nitrogen is more deshielding than carbon.

For the substituted derivatives **20a**, **20b**, **22a** and **22b**, NMR experiments were carried out on the mixture of the two isomers in $CDCl_3$ at 400 MHz. The table below summarises the assignments for the substituted derivatives **22a** and **22b** and the figures show the selected ^{1}H-^{1}H couplings and $^{2,3}J_{CH}$ correlations in the *trans*-isomer **22a**.

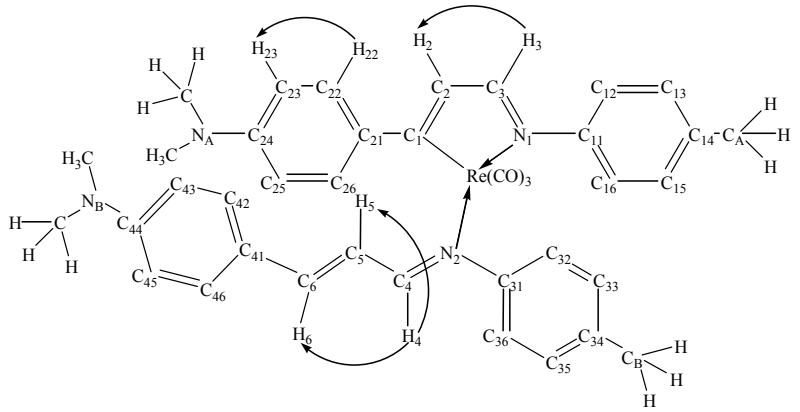

Figure 2-15: Selected ^{1}H-^{1}H Couplings in the Complex **22a**

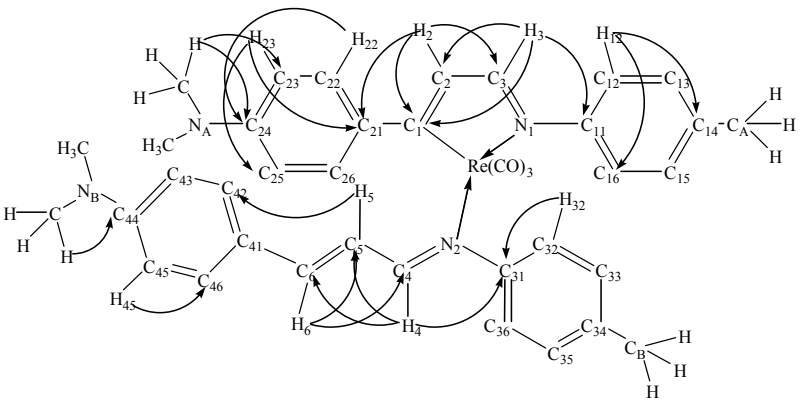

Figure 2-16: Selected $^{2,3}J_{CH}$ Correlations in the Complex **22a**

Table 2-20: NMR Assignments for the Substituted Derivatives **22a** and **22b**

δ / ppm	**22a**	**22b**		**22a**	**22b**
^{1}H NMR			**^{13}C NMR**		
			C-1	201.84 (C)	201.08 (C)
H-2	7.24 (d, $^{3}J_{HH}$ = 2.44 Hz)	7.04 (d, $^{3}J_{HH}$ = 2.56 Hz)	*C-2*	132.12 (CH)	132.67 (CH)
H-3	8.30 (d, $^{3}J_{HH}$ = 2.44 Hz, 0.5 H)	8.05 (d, $^{3}J_{HH}$ = 2.56 Hz)	*C-3*	175.08 (CH)	174.61 (CH)
H-4	8.00 (d, $^{3}J_{HH}$ = 10.12 Hz)	7.74 (d, $^{3}J_{HH}$ = 9.92 Hz)	*C-4*	171.68 (CH)	174.10 (CH)
H-5	6.02 (m)	6.98 (m)	*C-5*	116.07 (CH)	123.72 (CH)
H-6	6.82 (d, $^{3}J_{HH}$ = 13.60 Hz)	6.81 (d, $^{3}J_{HH}$ = 13.44 Hz)	*C-6*	147.72 (CH)	150.30 (CH)
			C-11	151.52 (C)	150.76 (C)
H-12, 16	7.02 (m)		*C-12, 16*	122.53 (CH)	122.10 (CH)
H-13, 15			*C-13, 15*		128.77 (CH)
			C-14	135.38 (C)	135.64 (C)
			C-21	139.77 (C)	140.43 (C)
H-22, 26	7.58 (d)	7.59 (m)	*C-22, 26*	129.34 (CH)	129.30 (CH)
H-23, 25	????	6.70 (m)	*C-23, 25*	111.67 (CH)	111.95 (CH)
			C-24	150.81 (C)	150.50 (C)
			C-31	150.05 (C)	154.36 (C)
H-32, 36	6.96 (m)		*C-32, 36*	123.7?	122.96 (CH)
H-33, 35			*C-33, 35*		128.80 (CH)
			C-34	135.52 (C)	134.88 (C)
			C-41		
H-42, 46			*C-42, 46*	122.1?	123.04 (CH)
H-43, 45	6.55 (d, $^{3}J_{HH}$ = 8.92 Hz)	6.45 (d, $^{3}J_{HH}$ = 8.88 Hz)	*C-43, 45*	111.67 (CH)	111.41 (CH)
			C-44	151.99 (C)	151.75 (C)
C_AH_3	2.36 (s)	2.28 (s)		20.98 (CH_3)	20.78 (CH_3)
C_BH_3	2.35 (s)	2.26 (s)		21.03 (CH_3)	20.78 (CH_3)
$N_A(CH_3)_2$	3.02 (s)	3.00 (s)			
$N_B(CH_3)_2$	2.98 (s)	3.02 (s)			
			N-Re-CO	199.80 (2 C)	199.91 (2 C)
			C-Re-CO	194.80 (C)	194.91 (C)

A study[62] on the lanthanide shift reagents induced *cis-trans* isomerisation using ultra-violet spectroscopy showed that substituents on the aniline ring would not affect the isomerisation process, so isomerisation of azabutadienes can be expected for the reactions with the azabutadienes **17** and **18**. As for the substituted derivatives **13a** and **13b**, two sets of the signals corresponding to each isomer were observed with 2 : 1

intensity in the ^{1}H and ^{13}C spectra of the substituted derivatives **22a** and **22b**. The set of the signals with a greater intensity was assigned to the *cis*-isomer **22b** and the other to the *trans*-isomer **22a** with respect to the consistency of the chemical shifts with those for the derivatives **13a**, **13b**, **20a** and **20b** as the chemical shifts of the corresponding signals for the cyclorheniated azabutadiene tetracarbonyl species **12**, **19** and **21** were quite consistent (Table 2-19). The signals for the *trans*-isomers, however, appeared with greater intensities for the derivatives **13** and **20**. The greater intensity of the *cis*-isomer signals than that of the *trans*-isomer ones for the derivatives **22** may be explained by the fact that the derivatives were prepared from 1 : 1 mole ratio reaction, while the derivatives **13** and **20** were both prepared from 1 : > 2 mole ratio reactions ($PhCH_2Re(CO)_5$: azabutadiene). The literature[62] stated that "*Cis/trans* ratio depends on the molar ratio of LSR" [62]. The *cis*-isomers of the azabutadienes may, therefore, be favoured in 1 : 1 mole ratio reactions, while the *trans*-isomers may be the favoured product in 1 : > 2 mole ratio reactions.

The intensity of the signals for the *trans*-isomer **22a** was always about the half of that of the corresponding signals for the *cis*-isomer **22b**. The *H-3* proton signal appeared at 8.30 ppm as a doublet with a $^{3}J_{CH}$ coupling constant of 2.44 Hz. The *H-3* proton signal showed a $^{1}J_{CH}$ correlation to the tertiary carbon signal at 175.08 ppm in the HSQC experiment, which was, therefore, assigned as *C-3*. The *H-3* proton signal showed a ^{1}H-^{1}H coupling with the proton signal at 7.24 ppm in the SELTOCSY experiment, which was, therefore, assigned as *H-2*. The *H-2* proton signal appeared as a doublet with a $^{3}J_{CH}$ coupling constant of 2.44 Hz in the ^{1}H NMR spectrum, which was consistent with that of the *H-3* proton signal. The *H-2* proton signal showed a $^{1}J_{CH}$ correlation to the tertiary carbon signal at 132.12 ppm in the HSQC experiment and the carbon signal was, therefore, assigned as *C-2*. In the HMBC experiment, the $^{2}J_{CH}$ correlations between the *H-3* proton and the *C-2* carbon signals and the *H-2* proton and the *C-3* carbon signals further support the assignments. The *H-3* and *2* proton signals both showed a $^{2,3}J_{CH}$ correlation to the quaternary carbon signal at 201.84 ppm in the HMBC experiment and, which was , therefore, assigned as *C-1*.

The *H-4* proton signal appeared at 8.00 ppm as a doublet with a $^{3}J_{CH}$ coupling constant of 10.12 Hz. The *H-4* proton signal showed a $^{1}J_{CH}$ correlation to the tertiary carbon signal at 171.68 ppm in the HSQC experiment. The signal was, therefore,

assigned as *C-4*. The *H-4* proton signal showed ^{1}H-^{1}H couplings with the proton signals at 6.02 and 6.82 ppm in the SELTOCSY experiment. The former appeared as a multiplet and the latter as a doublet with a $^{3}J_{CH}$ coupling constant of 13.60 Hz in the ^{1}H NMR spectrum. The 6.02 and 6.82 ppm proton signals showed a $^{1}J_{CH}$ correlation to the tertiary carbon signals at 116.07 and 147.72 ppm, respectively, in the HSQC experiment. The $^{2,3}J_{CH}$ correlations (Figure 2-16) in the HMBC experiment suggested that the 116.07 and 147.72 ppm carbon signals could be assigned as *C-5* and *6*, respectively, and the corresponding proton signals as *H-5* and *6*.

The *H-3* proton signal showed a $^{2,3}J_{CH}$ correlation to the quaternary carbon signal at 151.52 ppm in the HMBC experiment. The carbon signal was assigned as *C-11*. The methyl protons at the *C-14* carbon showed correlations to the *C-11* carbon signal and the tertiary carbon signal at 122.53 ppm in the HMBC experiment (Figure 2-16). The corresponding proton signal for the 122.53 ppm carbon was determined by the HSQC experiment and observed at 7.02 ppm. The 7.02 ppm proton signal showed a $^{2,3}J_{CH}$ correlation to the quaternary carbon at 135.38 ppm, which was, therefore, assigned as *C-14* and the 122.53 ppm tertiary carbon signal was assigned as *C-12*, *16* by reference to the chemical shift of the corresponding signals for the *cis*-isomer **22b** and the corresponding proton signals as *H-12*, *16*.

The *H-2* proton signal showed a $^{2,3}J_{CH}$ correlation to the quaternary carbon signal at 139.77 ppm in the HMBC experiment. The carbon signal was assigned as *C-21*. The dimethylamino protons at the *C-24* carbon showed a $^{2,3}J_{CH}$ correlation to the quaternary and tertiary carbon signals at 150.81 and 111.67 ppm, respectively. The corresponding proton signal for the 111.67 ppm tertiary carbon signal showed a $^{2,3}J_{CH}$ correlation to the *C-21* carbon signal in the HMBC experiment. The proton signal at 7.58 ppm showed a correlation to the *C-24* carbon signal in the HMBC experiment. The corresponding carbon signal for the 7.58 ppm proton signal was determined by HSQC experiment and observed at 129.34 ppm. The 150.81, 111.67 and 129.34 ppm carbon signals were, therefore, assigned as *C-24*, *C-23, 25* and *C-22, 26*, respectively, and the corresponding protons as *H-23, 25* and *H-22, 26*.

The *H-4* proton signal showed a $^{2,3}J_{CH}$ correlation to the quaternary carbon signal at 150.05 ppm in the HMBC experiment. The 150.05 ppm carbon signal was, therefore,

assigned as *C-31*. The proton signal at 6.96 ppm also showed a correlation to the *C-31* carbon signal in the HMBC experiment. The corresponding carbon signal for the 6.96 ppm proton signal was determined by HSQC experiment and observed at 123.7 ppm. The chemical shift of the *C-13*, *15* carbon signals can be expected at ~128 ppm by reference to the corresponding shift for the *trans*-isomer **22a**. The 123.7 ppm carbon and 6.96 ppm proton signals were, therefore, assigned as *C-12, 16* and *H-12, 16*, respectively.

The dimethylamino proton signals at the *C-44* carbon showed a $^{2,3}J_{CH}$ correlation to the quaternary carbon at 151.99 in the HMBC experiment. The carbon signal was assigned as *C-44*. The *H-43, 45* proton signals appeared at 6.55 ppm as a doublet with a $^{3}J_{CH}$ coupling constant of 8.92 Hz and the corresponding carbon was also observed at 111.67 ppm in the HSQC experiment. The 6.55 ppm proton signal showed a $^{2,3}J_{CH}$ correlation to the tertiary carbon signal at 122.1 ppm in the HMBC experiment and the carbon signal also showed a $^{2,3}J_{CH}$ correlation to the *H-5* proton signal in the HMBC experiment. The carbon signal was, therefore, assigned as *C-42, 46*.

As for the complexes **13a**, **13b** and **22b**, correlations between the *H-2* proton and *N-Re-C≡O* carbon signals and the *H-4* proton and *C-Re-C≡O* carbon signals were observed in the HMBC experiment.

The proton signals for the *trans*-isomer **22a** were shifted slightly down-field from the corresponding signals for the *cis*-isomer **22b**, which was consistent with the isomers **13a** and **13b**. The overall chemical shift of the carbon signals were consistent with the corresponding signals for the derivatives **13a** and **13b** except for the *C-2* and *5* carbon signals which shifted by 3 and 4 ppm up-field for the derivatives **22a** and **22b**, respectively. The chemical shifts of the corresponding signals for the derivatives **13**, **20** and **22** are discussed more in details later in this section.

The figure below shows the selected ^{1}H-^{1}H couplings and $^{2,3}J_{CH}$ correlations in the *cis*-isomer **22b**.

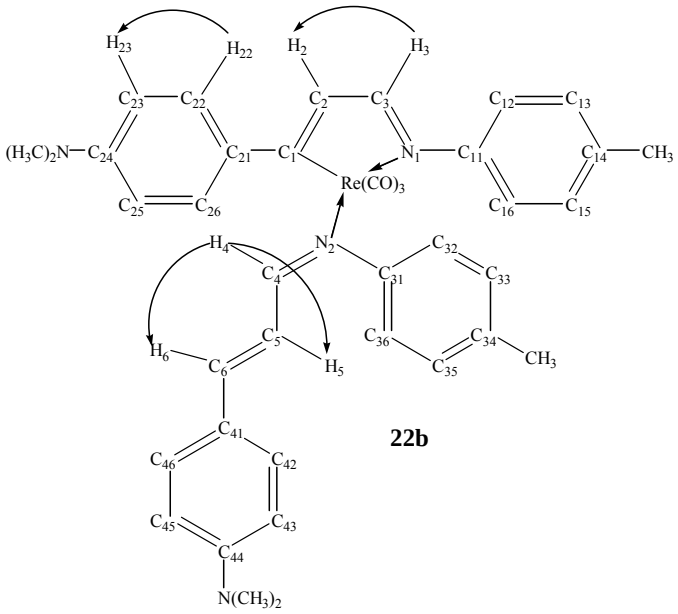

Figure 2-17: Selected ^{1}H-^{1}H Couplings in the Complex **22b**

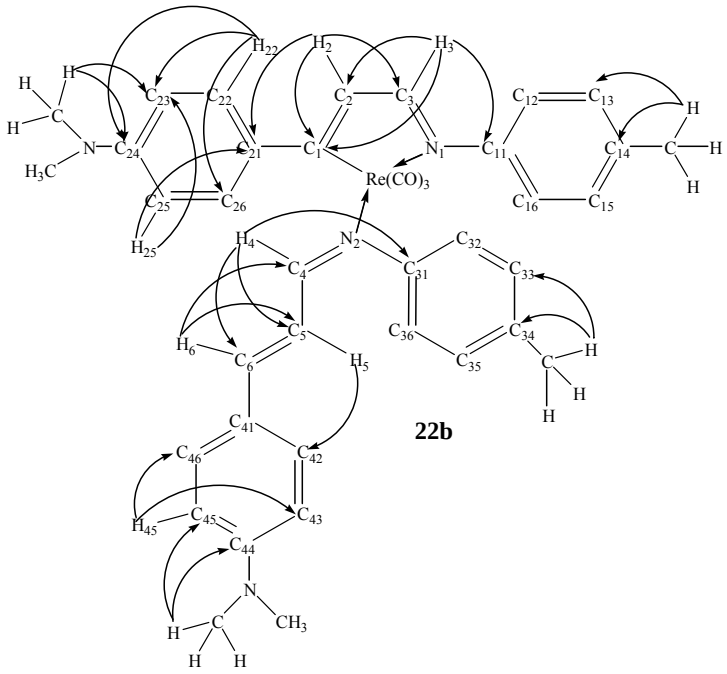

Figure 2-18: Selected $^{2,3}J_{CH}$ Correlations in the Complex **22b**

For the *cis*-isomer **22b**, the *H-3* proton signal appeared at 8.05 ppm as a doublet with a $^{3}J_{CH}$ coupling constant of 2.56 Hz. The *H-3* carbon signal showed a $^{1}J_{CH}$ correlation to the tertiary carbon signal at 174.61 ppm in the HSQC experiment, which was, therefore, assigned as *C-3*. In the SELTOCSY experiment, the *H-3* proton signal showed a ^{1}H-^{1}H coupling with the proton signal at 7.04 ppm. In the ^{1}H NMR spectrum, the 7.04 ppm proton signal appeared as a doublet with a $^{3}J_{CH}$ coupling

constant of 2.56 Hz. The 7.04 ppm proton signal showed a $^{1}J_{CH}$ correlation to the tertiary carbon signal at 132.67 ppm in the HSQC experiment. The 7.04 ppm proton and the corresponding carbon signals were, therefore, assigned as *H-2* and *C-2*, respectively. The $^{2}J_{CH}$ correlations between the *H-3* proton and the *C-2* carbon signals, and the *H-2* proton and the *C-3* carbon signals further supported the assignments. The *C-1* carbon signal could be determined by the $^{2,3}J_{CH}$ correlations in the HMBC experiment. Both the *H-3* and *2* proton signals showed a $^{2,3}J_{CH}$ correlation to the quaternary carbon signal at 201.08 ppm (Figure 2-18), which was, therefore, assigned as *C-1*.

The *H-4* proton signal appeared at 7.74 ppm as a doublet with a $^{3}J_{CH}$ coupling constant of 9.92 Hz. The *H-4* carbon signal showed a $^{1}J_{CH}$ correlation to the tertiary carbon signal at 174.10 ppm in the HSQC experiment, which was, therefore, assigned as *C-4*. In the SELTOCSY experiment, the *H-4* proton signal showed ^{1}H-^{1}H couplings to the proton signals at 6.98 and 6.81 ppm. The former appeared as a multiplet and the latter as a doublet with a $^{3}J_{CH}$ coupling constant of 13.44 Hz in the ^{1}H NMR spectrum. The 6.98 and 6.81 ppm proton signals showed a $^{1}J_{CH}$ correlation to the tertiary carbon signals at 123.72 and 150.30 ppm, respectively. The $^{2,3}J_{CH}$ correlations in the HMBC experiment suggested that the 123.72 and 150.30 ppm carbon signals could be assigned as *C-5* and *C-6* and the corresponding protons as *H-5* and *H-6*, respectively.

The signals for the aromatic protons and carbons were difficult to assign with supporting $^{2,3}J_{CH}$ correlations due to overlap of the signals, so detailed assignments were not made. The *H-3* proton signal showed a $^{2,3}J_{CH}$ correlation to the quaternary carbon signal at 150.76 ppm, which was assigned as *C-11*. The methyl proton signals also showed $^{2,3}J_{CH}$ correlations to the quaternary carbon signal at 135.64 and the tertiary carbon signal at 128.77 ppm, which were, therefore, assigned as *C-14* and *C-13, 15*, respectively.

The *H-2* proton signal showed a $^{2,3}J_{CH}$ correlation to the quaternary carbon signal at 140.43 ppm. The proton signal at 6.70 ppm also showed a correlation to the 140.43 carbon signal in the HMBC experiment. In the SELCTOSY experiment, the 6.70 ppm proton signal showed a ^{1}H-^{1}H coupling with the proton signal at 7.59 ppm. The 6.70 and 7.59 ppm proton signals showed a $^{1}J_{CH}$ correlation to the tertiary carbon signals at

111.95 and 129.30 ppm, respectively. The $^{2,3}J_{CH}$ correlations in the HMBC experiments (Figure 2-18) suggested that the 129.30 and 111.95 ppm carbon signals could be assigned as *C-22, 26* and *C-23, 25*, respectively, and the corresponding protons as *H-22, 26* and *H-23, 25*. The *C-24* carbon signal was determined by the $^{2,3}J_{CH}$ correlations from the *H-23, 25* and dimethylamino proton signals and observed at 150.50 ppm.

The *H-4* proton signal showed a $^{2,3}J_{CH}$ correlation to the quaternary carbon signal at 154.36 ppm, which was assigned as *C-31*. The methyl protons at *C-34* showed a $^{2,3}J_{CH}$ correlation to the quaternary carbon signal at 134.88 ppm and the tertiary carbon signal at 128.80 ppm, which were, therefore, assigned as *C-34* and *C-33, 35*, respectively.

The dimethylamino protons at *C-44* showed a $^{2,3}J_{CH}$ correlation to the quaternary and tertiary carbon signals at 151.75 and 111.41 ppm which were assigned as *C-44* and *C-43, 45*, respectively. The HSQC experiment showed the corresponding proton signals for the *C-43, 45* carbon signals at 6.45 ppm, which were, therefore, assigned as *H-43, 45*. The *H-43, 45* proton signals showed $^{2,3}J_{CH}$ correlations to the tertiary carbon signals at 111.41 and 123.04 ppm in the HMBC experiment. The *H-5* proton signal showed a $^{2,3}J_{CH}$ correlation to the 123.04 ppm carbon signal in the HMBC experiment, which was, therefore, assigned as *C-42, 46*.

A correlation between the *H-2* proton and the *N-Re-C≡O* carbon signals and the *H-4* proton and the *C-Re-C≡O* carbon signals were also observed in the HMBC experiment as for the *cis*-isomer **22b**.

The table below summarises the assignments for the substituted derivatives **20a** and **20b** and the ^{1}H-^{1}H couplings and $^{2,3}J_{CH}$ correlations in the *trans*- and *cis*-isomers **20a** and **20b**, respectively, were shown in the following figures.

Table 2-21: NMR Assignments for the Substituted Derivatives **20a** and **20b**

δ / ppm	**20a**	**20b**		**20a**	**20b**
^{1}H NMR			**^{13}C NMR**		
			C-1	200.54 (C)	199.86 (C)
H-2	7.25 (d, $^{3}J_{HH}$ = 2.40 Hz)	7.08 (m)	*C-2*	135.26 (CH)	135.85 (CH)
H-3	8.35 (d, $^{3}J_{HH}$ = 2.12 Hz)	8.11 (d, $^{3}J_{HH}$ = 2.28 Hz)	*C-3*	176.39 (CH)	175.99 (CH)
H-4	8.15 (d, $^{3}J_{HH}$ = 10.04 Hz)	7.86 (d, $^{3}J_{CH}$ = 9.64 Hz)	*C-4*	172.67 (CH)	174.84 (CH)
H-5	6.25 (m)	7.11 (m)	*C-5*	120.61 (CH)	127.86 (CH)
H-6	7.00 (d, $^{3}J_{CH}$ = 13.60 Hz)	7.00 (d, $^{3}J_{CH}$ = 14.08 Hz)	*C-6*	148.41 (CH)	151.05 (CH)
			C-11	149.43 (d, $^{4}J_{CF}$ = 2.90 Hz, C)	148.73 (d, $^{4}J_{CF}$ = 2.70 Hz, C)
H-12, 16			*C-12, 16*	123.91 (d, $^{3}J_{CF}$ = 8.08 Hz, 2 CH)	123.52 (d, $^{3}J_{CF}$ = 7.90 Hz, 2 CH)
H-13, 15			*C-13, 15*	115.32 (d, $^{2}J_{CF}$ = 22.85 Hz, 2 CH)	115.79 (d, $^{2}J_{CF}$ = 22.63 Hz, 2 CH)
			C-14	161.24 (d, $^{1}J_{CF}$ = 246.38 Hz, C)	161.24 (d, $^{1}J_{CF}$ = 246.38 Hz, C)
			C-21		
H-22, 26	7.44 (m)		*C-22, 26*		
H-23, 25			*C-23, 25*		
			C-24		
			C-31	147.50 (d, $^{4}J_{CF}$ = 2.90 Hz, C)	152.26 (C)
H-32, 36	7.01 (m)	7.10 (m)	*C-32, 36*	123.52 (d, $^{3}J_{CF}$ = 7.90 Hz, 2 CH)	124.18 (d, $^{3}J_{CF}$ = 7.82 Hz, 2 CH)
H-33, 35	6.23 (m)		*C-33, 35*		
			C-34	160.95 (d, $^{1}J_{CF}$ = 246.36 Hz, C)	161.04 (d, $^{1}J_{CF}$ = 246.25 Hz, C)
			C-41	134.07 (C)	
H-42, 46	7.45 (m)	7.52 (m)	*C-42, 46*	128.14 (2 CH)	
H-43, 45	7.40 (m)	7.31 (m)	*C-43, 45*		
H-44	7.28 (m)	7.19 (m)	*C-44*		
			N-Re-CO	199.40 (2 C)	199.40 (2 C)
			C-Re-CO	193.48 (C)	193.73 (C)

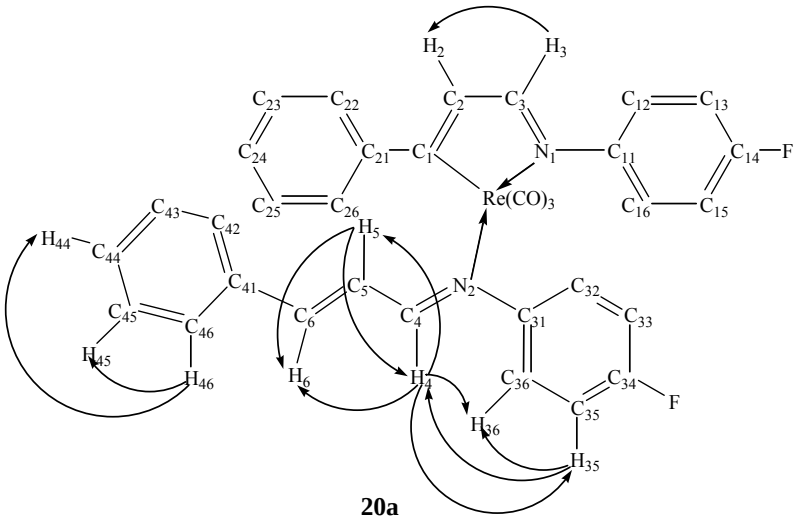

20a

Figure 2-19: ^{1}H-^{1}H Couplings in the Complex **20a**

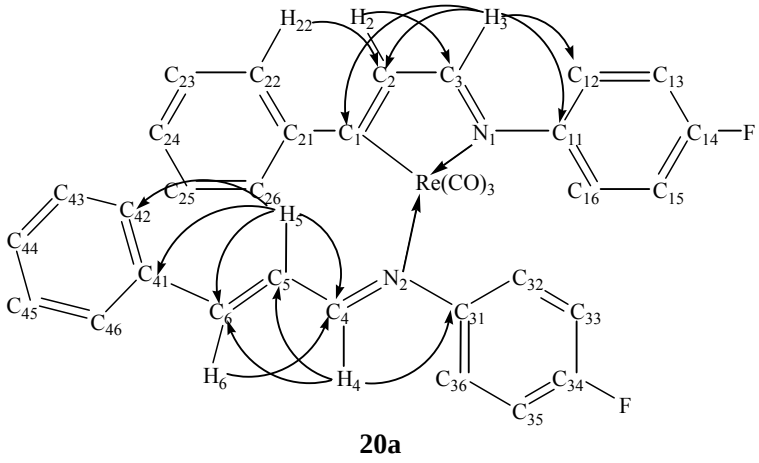

20a

Figure 2-20: $^{2,3}J_{CH}$ Correlations in the Complex **20a**

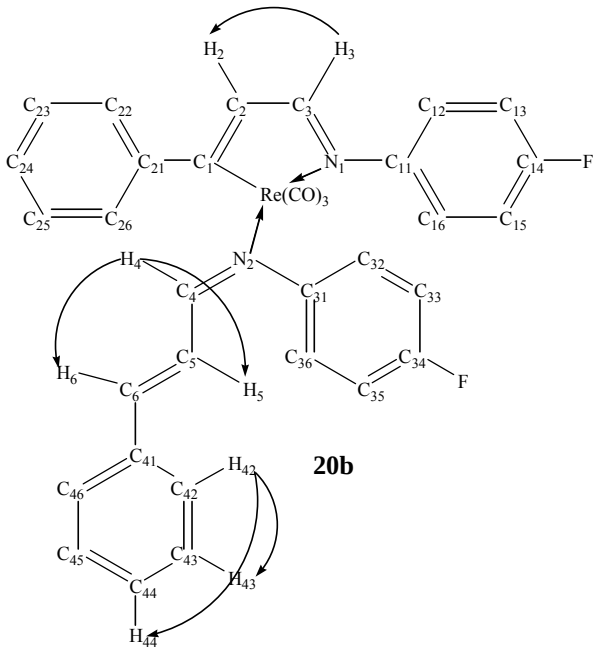

20b

Figure 2-21: ^{1}H-^{1}H Couplings in the Complex **20b**

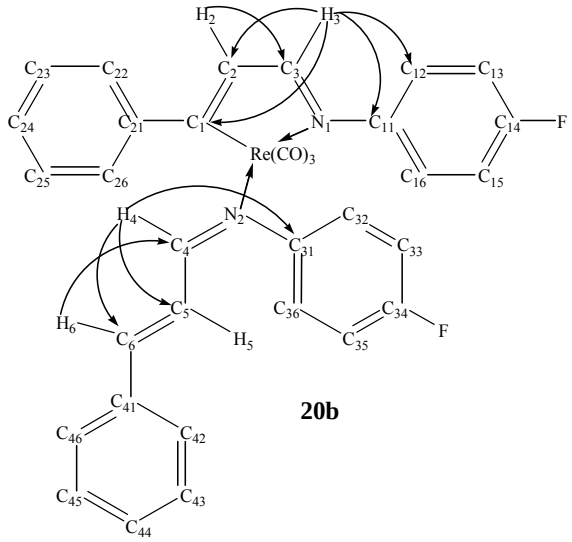

Figure 2-22: $^{2,3}J_{CH}$ Correlations in the Complex **20b**

As for the complexes **13a**, **13b**, **22a** and **22b**, the ^{1}H and ^{13}C signals for the complexes **20a** and **20b** were assigned in accordance with the ^{1}H-^{1}H couplings (Figure 2-19, 21), $^{1}J_{CH}$ and $^{2,3}J_{CH}$ (Figure 2-20, 22) correlations observed in the SELTOCY, HSQC and HMBC experiments, respectively, and also with reference to those for the complexes **13a**, **13b**, **22a** and **22b** where appropriate.

The tables below summarises the assignments for the derivatives **13a**, **13b**, **20a**, **20b**, **22a** and **22b**.

Table 2-22: NMR Assignments for the Substituted Derivatives **13a**, **13b**, **20a**, **20b**, **22a** and **22b**

δ / ppm	**13a**	**20a**	**22b**	**13b**	**20b**	**22a**
^{1}H NMR						
H-2	7.28 (d, $^{3}J_{HH}$ = 2.16 Hz)	7.25 (d, $^{3}J_{CH}$ = 2.40 Hz, 1 H)	7.24 (d, $^{3}J_{CH}$ = 2.44 Hz)	7.10 (d, $^{3}J_{HH}$ = 2.44 Hz)	7.08 (m)	7.04 (d, $^{3}J_{CH}$ = 2.56 Hz)
H-3	8.40 (d, $^{3}J_{HH}$ = 2.28 Hz, 1 H)	8.35 (d, $^{3}J_{CH}$ = 2.12 Hz, 1 H)	8.30 (d, $^{3}J_{CH}$ = 2.44 Hz, 0.5 H)	8.15 (d, $^{3}J_{HH}$ = 2.40 Hz, 0.3 H)	8.12 (d, $^{3}J_{CH}$ = 2.28 Hz, 0.5 H)	8.05 (d, $^{3}J_{CH}$ = 2.56 Hz)
H-4	8.17 (d, $^{3}J_{HH}$ = 10.00 Hz, 1 H)	8.15 (d, $^{3}J_{CH}$ = 10.04 Hz, 1 H)	8.00 (d, $^{3}J_{CH}$ = 10.12 Hz)	7.88 (d, $^{3}J_{HH}$ = 9.80 Hz, 0.3 H)	7.86 (d, $^{3}J_{CH}$ = 9.64 Hz, 0.5 H)	7.74 (d, $^{3}J_{CH}$ = 9.92 Hz)
H-5	6.25 (m, 1 H)	6.25 (d, $^{3}J_{CH}$ = Hz, 1 H)	6.02 (m)	6.87 (m)	7.11 (m)	6.98 (m)
H-6	6.98 (d, $^{3}J_{HH}$ = 15.65 Hz, 1 H)	7.00 (d, $^{3}J_{CH}$ = 13.60 Hz, 1 H)	6.82 (d, $^{3}J_{CH}$ = 13.60 Hz)	6.98 (d, $^{3}J_{HH}$ = 15.65 Hz, 0.3 H)	7.00 (d, $^{3}J_{CH}$ = 14.08 Hz)	6.81 (d, $^{3}J_{CH}$ = 13.44 Hz)
^{13}C NMR						
C-1	200.71 (C)	200.54 (C)	201.84 (C)	200.11 (C)	199.86 (C)	201.08 (C)
C-2	135.25 (CH)	135.26 (CH)	132.12 (CH)	135.90 (CH)	135.85 (CH)	132.67 (CH)
C-3	176.31 (CH)	176.39 (CH)	175.08 (CH)	176.04 (CH)	175.99 (CH)	174.61 (CH)
C-4	171.82 (CH)	172.67 (CH)	171.68 (CH)	174.57 (CH)	174.84 (CH)	174.10 (CH)
C-5	120.69 (CH)	120.61 (CH)	116.07 (CH)	122.70 (CH)	127.86 (CH)	123.72 (CH)
C-6	147.55 (CH)	148.41 (CH)	147.72 (CH)	150.42 (CH)	151.05 (CH)	150.30 (CH)
C-Re-CO	193.67 (C)	193.48 (C)	194.80 (C)	193.95 (C)	193.73 (C)	194.91 (C)
N-Re-CO	199.45 (2 C)	199.40 (2 C)	199.80 (2 C)	193.67 (2 C)	199.40 (2 C)	199.91 (2 C)

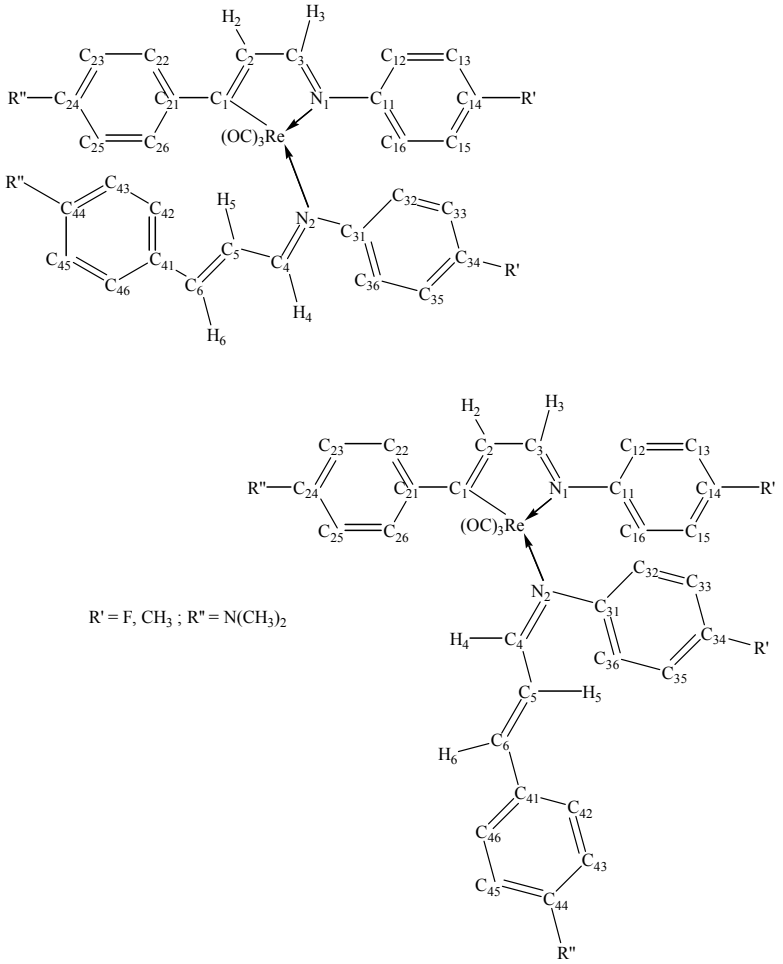

Figure 2-23: *Trans*- and *Cis*-Isomers of Substituted Derivatives

The intensity of the signals corresponding to *trans*- and *cis*-isomers of the derivatives **13a** and **13b**, **20a** and **20b**, and **22a** and **22b**, was 3 : 1, 2 : 1 and 1 : 2 respectively. The signals corresponding to the *cis*-isomer appeared with greater intensities for the substituted derivatives **22**, while those to the *trans*-isomers were observed with greater intensities for the derivatives **13** and **20**. The cyclorheniated ring proton and carbon signals were quite consistent for the corresponding isomers. The corresponding signals also show the same $^{2,3}J_{CH}$ correlation patterns in the HMBC experiments, so the pattern can be used to assign the corresponding signals. For the *trans*-isomers, the *H-3* proton signals appeared at 8.30 – 8.40 ppm as a double with a $^{3}J_{HH}$ coupling constant of 2.1 – 2.4 Hz and the *H-2* proton signals at 7.28 – 7.24 ppm as a doublet with a $^{3}J_{HH}$ coupling constant of 2.2 – 2.4 Hz. The *H-3* and *2* proton signals for the *cis*-isomers shifted by ~0.2 ppm up-field and appeared at 8.05 – 8.15 ppm and 7.04 – 7.10 ppm, respectively. The chemical shifts of the *C-3* and *2* carbon

signals were consistent for both isomers and observed at ~175 and 135 ppm, respectively. The *C-1* carbon signals appeared at ~200 ppm for all the derivatives.

For the *trans*-isomers, the *H-4* proton signals appeared at 8.00 – 8.17 ppm and, for the *cis*-isomers, the signal shifted by 0.29 – 0.26 ppm up-field and appeared at 7.86 – 7.74 ppm. The *H-4* signals appeared as a doublet with a $^{3}J_{HH}$ coupling constant of ~10 Hz which slightly decreased to ~9.8 Hz for the *cis*-isomers. The *C-4* carbon signals appeared at ~171 ppm for the *trans*-, shifted by 3 ppm down-field and appeared at ~174 ppm for the *cis*-isomers. The *H-5* proton signals appeared as a multiplet at 6.24 – 6.02 ppm for the *trans*-isomers, shifted by 0.62 – 0.96 ppm down-field and appeared at 7.11 – 6.87 ppm for the *cis*-isomers, which was also the greatest shifts observed for the corresponding proton signals for the *trans*- and *cis*-isomers. The *C-5* carbon signals appeared at 120 – 116 ppm for the *trans*-, shifted by 2 – 7 ppm down-field and appeared at ~123 ppm for the *cis*-isomers. The *H-6* proton signals were consistent for both isomers and appeared at 7.00 – 6.81 ppm as a doublet with a $^{3}J_{HH}$ coupling constant of 13 – 15 Hz. The *C-6* carbon signals appeared at 148 – 147 ppm for the *trans*-isomers, shifted by 3 ppm down-field and appeared at 151 – 150 ppm for the *cis*-isomers.

Signals for the C≡O carbons for both *trans*- and *cis*-isomers appeared in the range from 193 – 199 ppm as two signals with 2 : 1 intensity. The two C≡O carbons *trans* to nitrogen appeared as one signal and the one *trans* to carbon appeared as one signal with about half of the intensity of the *N-Re-C≡O* carbons. The *N-Re-C≡O* carbon signals appeared at a higher chemical shift than the *C-Re-CO* one, which were consistent for all the derivatives.

For all the derivatives, correlations between the *H-2*, *3* and *4* proton and the C≡O carbon signals were observed in the HMBC experiments. For the derivative **13a**, the *H-2* proton signal showed a correlation to both C≡O signals and the *H-3* and *4* proton signals to the *C-Re-C≡O* carbon signal. For the derivative **13b**, the *H-2* proton signal showed a correlation to both C≡O signals and the *H-3* and *4* proton signal to the *C-Re-C≡O* and *N-Re-C≡O* carbon signals, respectively. In the derivative **22a** and **22b**, correlations between the *H-2* proton and *N-Re-C≡O* carbon signals and the *H-4* proton and *C-Re-C≡O* signals were observed. For the complex **20a**, the *H-3* and *4*

proton signals showed a correlation to the *C-Re-C≡O* carbon signal and the *H-2* signal to both carbonyl signals. For the complex **20b**, the *H-3* and *4* proton signals showed a correlation to the *C-Re-C≡O* carbon signal and the *H-2* proton signal to the *N-Re-C≡O* carbon signal. There was no obvious trend for these correlations, but the *H-2* proton signal appeared to show a correlation to both carbonyl signals. The correlations are all beyond $^{2,3}J_{CH}$ distances. The protons and carbons may, therefore, be in the positions due to the geometry of the molecules, which allow them to correlate and show a signal in HMBC experiments.

2.2.2.2.2.4 X-Ray Crystallography

An X-ray crystal structure determination was carried out on the single crystal of **20a**. The table below shows the selected bond lengths for the complexes **13a** and **20a**, and the figure illustrates the crystal structure of **20a**.

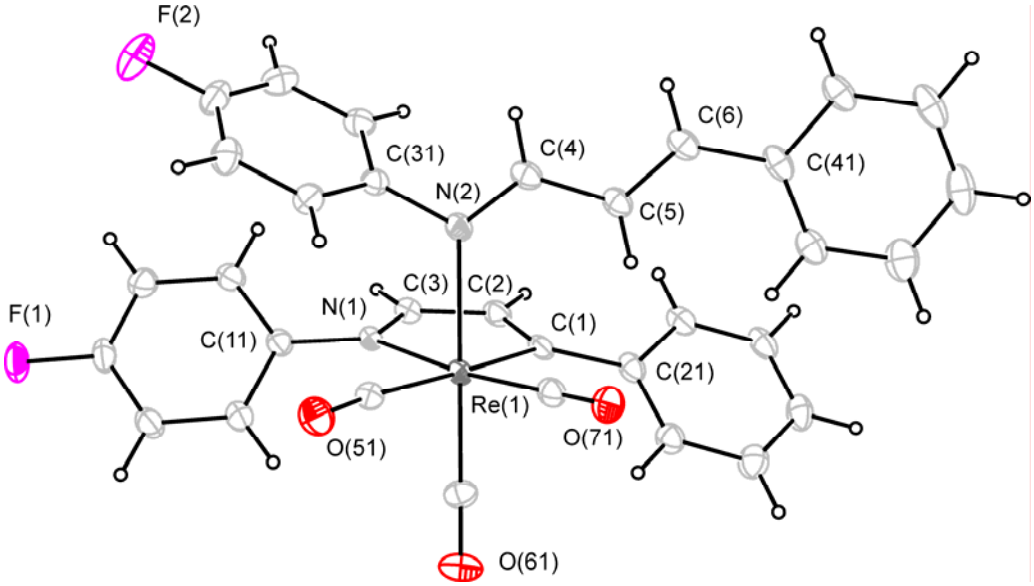

20a

Figure 2-24: Crystal Structure of **20a**

Table 2-23: Selected Bond Lengths for the Complexes **13a** and **20a**

/ Å	**13a**[*]	**20a**
Re(1)-C(1)	2.187(3)	2.183(2)
Re(1)-N(1)	2.186(2)	2.186(2)
Re(1)-N(2)	2.238(2)	2.238(2)
Re(1)-C(51)	1.953(3)	1.956(3)
Re(1)-C(61)	1.916(3)	1.918(3)
Re(1)-C(71)	1.922(3)	1.926(3)
C(1)-C(2)	1.352(4)	1.362(4)
C(2)-C(3)	1.423(4)	1.429(4)
C(4)-C(5)	1.437(4)	1.437(4)
C(5)-C(6)	1.342(4)	1.340(4)
N(1)-C(3)	1.313(4)	1.303(3)
N(2)-C(4)	1.295(4)	1.297(3)

[*]Adapted from the undergraduate laboratory report[57]

The structure of **20a** is analogous to that of **13a**. There is a cyclorheniated ring which has the same geometry and bond lengths as in the complex **13a**. One *axial* CO is replaced by a *trans*-azabutadiene coordinating through the imine nitrogen.

Trans-influence was also observed in the complex **20a** as in the complex **13a** The Re(1)-C(51) distance of 1.956(3) Å, which is *trans* to carbon, is longer than the Re-C(61) and Re-C(71) distances of 1.918(3) and 1.926(3) Å , respectively, which are both *trans* to nitrogen.

The C(1)-C(2) distance of 1.362(4) Å is slightly longer than the C(5)-C(6) distance of 1.340(4) Å. The N(1)-C(3) distance of 1.303(4) Å is also longer than the N(2)-C(4) distance of 1.297(3) Å. The C(2)-C(3) distance of 1.429(4) Å is, on the other hand, shorter than the C(4)-C(5) distance of 1.437(4) Å. The longer C(1)-C(2) and C(3)-N(1) and shorter C(2)-C(3) bond distances in the cyclorheniated ring than the corresponding formal π-bond C(5)-C(6) and C(3)-N(1) and σ-bond C(4)-C(5) distances, respectively, in the ligand suggest that the central five-membered ring in the complex **20a** is also a pseudo-aromatic system.

2.3 Conclusion

The cyclometallated azabutadiene tetracarbonyl species of the type **23** could be prepared from the reaction of $PhCH_2Re(CO)_5$ with azabutadienes, including their single crystals which were suitable for X-ray crystal structure determinations. The reaction tolerated substituents of different electronic properties e.g. electron-withdrawing and electron-donating, on the phenyl rings and gave the analogues in similar yields. Cyclometallation of 1-azabutadienes to give the cyclometallated azabutadiene **23**, appeared be a general process with $PhCH_2Mn(CO)_5$ and $PhCH_2Re(CO)_5$ although the cyclometallated azabutadiene **23** of the former could never be isolated. The tetracarbonyl species **23** appeared to be unstable in both Re and Mn systems, so rapidly undergoes the subsequent reactions to give the further reacted products as the main reaction products in good-to-excellent yield. In the Mn system, a CO insertion into the Mn-C σ-bond occurs and the CO insertion product **10**[48] is obtained, while, in the Re system, the substituted derivatives **25** are formed via substitution of a second azabutadiene to Re. The Re analogues of the cyclorheniated azabutadiene tetracarbonyl species **23** were always obtained in minor yields even under the modified conditions to optimise the yield, which may also support that the species **23** is a reactive intermediate.

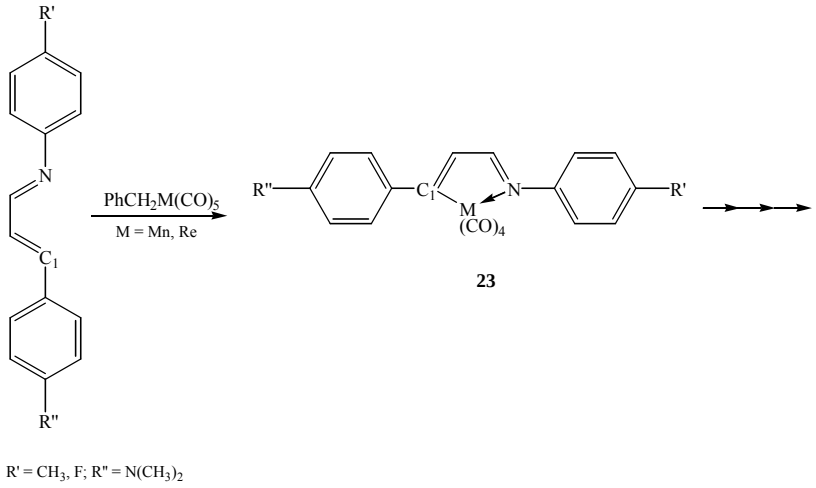

Scheme 2-6: Cyclometallation of Azabutadienes with $PhCH_2M(CO)_5$ (M = Mn or Re)

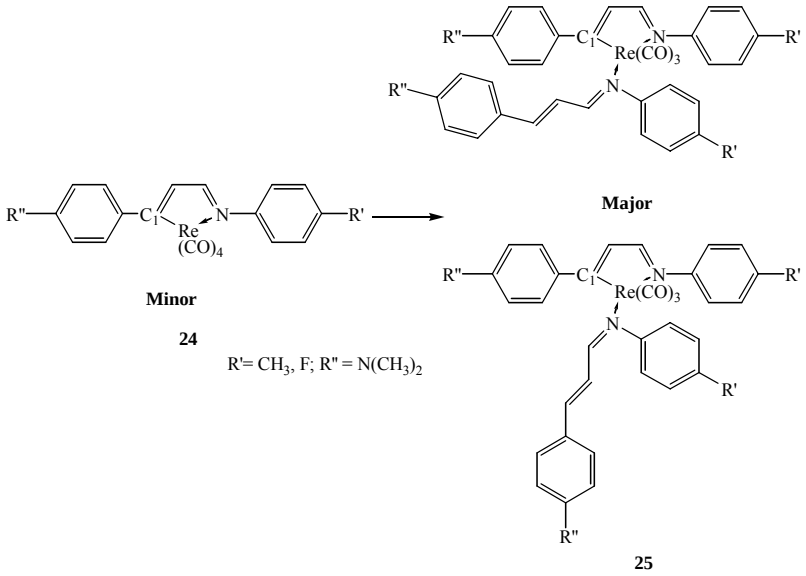

Scheme 2-7: Cyclorheniated Azabutadienes **24** and Substituted Derivatives **25**

Modification on the basicity of the N and *C-1* carbon atoms of the azabutadienes did not interfere with cyclometallation reaction, but affected the reaction time. Reduction in the basicity of the imine nitrogen appeared to result in a slower reaction and need a longer reaction time to go completion. The increased basicity of the imine nitrogen and *C-1* carbon atoms, on the other hand, seemed to enhance the reaction and a shorter reaction time would be required for completion. These were all consistent with the general cyclometallation mechanism[2, 7]. Enhancement in the basicity of the N and *C-1* carbon atoms hastens cyclometallation and also substitution reactions and vice versa.

Isomerisation of azabutadienes occurs in the Re system and provides the *cis*-azabutadiene metal complexes no other examples of which can be found in the literatures. Substitutions on the aniline and cinnamaldehyde rings of the azabutadienes did not appear to affect the isomerisation, but gave the analogues of the *trans*- and *cis*-isomers. Whether the *trans*- or *cis*-isomer of the azabutadienes and, hence, of the substituted derivatives would be favoured appeared to depend on the molar ratio of the rhenium in the reaction as stated in the literature[62]. In a lower molar concentration, the *cis*-isomers seemed to be the favoured product and it is the *trans*-isomers in a higher concentration.

All the complexes prepared in this chapter could be characterised well by IR, ESI-MS, HR-MS, NMR, XRD and also micro analysis and the spectroscopic data were all consistent for the analogues.

The study may be extended to reactions with other azabutadienes of different reactivity and/or other metals which may be less expensive and have potentials to yield novel compounds with 1-azabutadienes.

2.4 Experimental

2.4.1 Preparation of Starting Materials

2.4.1.1 Preparation of $PhCH_2Re(CO)_5$

Experimental: The method was adapted from the literature[5].

Mercury (~ 70 g, 5 mL) was placed in a Schlenk flask. The flask was connected to the Schlenk line, degassed and filled with N_2 several times. Small pieces of a clean sodium metal (~ 0.5 g) were added to the flask, letting each dissolve before adding the next. The amalgam was allowed to cool. Distilled tetrahydrofuran (thf) (~30 mL), $[Re_2(CO)_{10}]_2$ (2.00 g, 3.1 mmol) and a stirrer bar were added to the flask. The reaction mixture was strongly stirred at room temperature for 24 hours and then left to settle. Using a nitrogen-flushed syringe, the resulting solution of $Na[Re(CO)_5]$ (~6 mmol) was transferred to another nitrogen-flushed Schlenk flask, containing a well-stirred solution of $PhCH_2Br$ (0.69 mL, 1.0 g, 5.9 mmol). Precipitation of NaBr as an orange/yellow solid was immediately observed. The mixture was gently stirred for 1 – 2 hours. The solvent was removed under vacuum and the residue was extracted with petroleum spirits/CH_2Cl_2 (10 : 1, 25 mL × 3). The extract was filtered to remove the cloudiness of the solution. The yellow filtrate, which was still a little cloudy, was concentrated to ~10 mL under vacuum. Crystallisation of the filtrate at –20 °C provided a yellow-brown solid **14** (1.62 g, 66 %). Purification was attempted by sublimation, but it was still obtained as a dark yellow solid, while a pure product should form a white solid at –20 °C. The complex **14** was stored in the freezer until needed unless, otherwise, it would slowly oxidise in the air and faster when liquid.

Crystallisation of the filtrate at –20 °C also provided a very small amount of a red solid **15** as by-product. The by-product was isolated by transferring the complex **14** when it was liquid at room temperature by a nitrogen-flushed syringe to a round-bottomed flask under normal atmosphere. The solid was dried under vacuum for 1½ hours and then characterised only by ESI- and HR-MS.

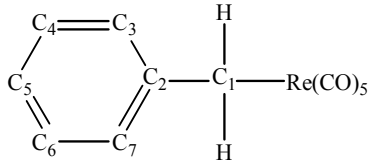

14

Description:		Dark yellow/brown solid
Empirical Formula:		$C_{12}H_7O_5Re$
Mr:		417.39
IR:	(Hexane)	υ (C≡O) 2127 (w), 2018 (vs, br), 1986 (s) cm^{-1}
^{1}H NMR:	(400 MHz, $CDCl_3$)	δ 7.17 (m, 2 H), 7.06 (m, 2 H), 6.85 (t, 1 H), 2.44 (s, 2 H) ppm
^{13}C NMR:	(300 MHz, DEPT*, $CDCl_3$)	δ 185.01 (4 C), 180.98 (C), 155.04 (C), 128.33 (2 CH), 125.44 (2 CH), 122.44 (CH), –2.20 (CH_2) ppm
ESI-MS:		
	(MeOH/NaOMe, cone 20 V, -ve ion)	*m/z* 448 (97 %, $[M + OMe]^-$), 392 (100 %, $[M + OMe – 2CO]^-$)
	(cone 11 V, -ve ion)	*m/z* 448 (100 %, $[M + OMe]^-$), 392 (5 %, $[M + OMe – 2CO]^-$)

*At 400 MHz

15

Description:		Red solid
Formula:		$C_{13}H_9O_6Re_2$
Mr:		633.62
HR-MS:	(MeOH/NaOMe, -ve ion)	*m/z* 632.957 (100 %, *m/z* 632.948 calcd. for $Re_2O_6C_{13}H_9$, $[M – H]^-$ ($M = Re_2O_6C_{13}H_{10}$))

2.4.1.2 Preparation of Azabutadienes

All the azabutadienes were stored in the freezer until needed unless, otherwise, would slowly decompose in the air.

2.4.1.2.1 Preparation of 1, 4-Diphenyl-1-Azabuta-1, 3-Diene *16*

Experimental: The method was adopted from the literature[58].

Na_2SO_4 (3.03 g) was added to a solution of cinnamaldehyde (2.00 mL, 15.9 mmol) and freshly distilled aniline (1.40 mL, 15.1 mmol) in distilled Et_2O (30 mL) in a round-bottomed flask under normal atmosphere. The clear yellow reaction mixture was gently stirred at room temperature for 1 hour 10 minutes. The mixture was filtered through a filter paper into another round-bottomed flask, the residue was washed with Et_2O (20 mL), the extract was collected in the same flask containing the filtrate. Crystallisation of the filtrate at –20 °C for 48 hours provided pale yellow needles of **16**. The needles were collected on a Buchner funnel, washed with CH_2Cl_2 (~2 mL) and dried on the funnel by suction for 20 minutes. Yield: 1.57 g, 50 %.

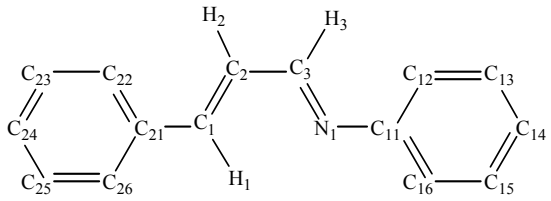

16

Description:		Pale-yellow needle
Empirical Formula:		$C_{15}H_{13}N$
Mr:		207.27
^{1}H NMR:	(400 MHz, $CDCl_3$)	δ 8.28 (dd, $^{3,4}J_{CH}$ = 7.02, 1.12 Hz, 1 H), 7.55 (m, 2 H), 7.39 (m, 5 H), 7.15 (m, 5 H) ppm
^{13}C NMR:	(400 MHz, DEPT, $CDCl_3$)	δ 161.63 (CH), 151.82 (C), 144.01 (CH), 135.67 (C), 129.62 (CH), 129.21 (2 CH), 128.96 (2 CH), 128.70 (CH), 127.54 (2 CH), 126.14 (CH), 120.95 (2 CH)

ppm

ESI-MS: (MeOH, cone 20 V, +ve ion) *m/z* 208 (100 %, $[M + H]^+$)

HR-MS: (MeOH, +ve ion) *m/z* 208.1129 (*m/z* 208.1121 calcd. for $C_{15}H_{14}N$)

2.4.1.2.2 Preparation of 1-(4-Fluorophenyl)-4-Phenyl-1-Azabuta-1, 3-Diene *17*

Experimental: The literature method[58] was used.

In a nitrogen-flushed Schlenk flask, Na_2SO_4 (3.01 g) was added to a solution of cinnamaldehyde (1.91 mL, 15.1 mmol) and 4-fluoroaniline (1.45 mL, 15.3 mol) in Et_2O (30 mL). The clear yellow reaction mixture was stirred at room temperature for 3½ hours. The mixture was filtered through a filter paper into a bottom-round flask under normal atmosphere, the residue was washed with Et_2O (30 mL) and the extract was collected in the same flask containing the filtrate. Crystallisation of the filtrate at –20 °C for 24 hours gave the azabutadiene **17** as a white precipitate. The precipitate was collected on a Buchner funnel, washed with Et_2O (1 – 2 mL) and dried on the funnel by suction for 1 hr. The azabutadiene **17** was obtained as a pale-white powder (1.70 g, 50 %).

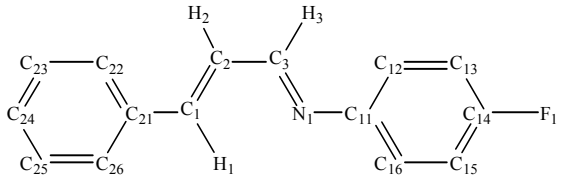

17

Description: Pale-white powder

Empirical Formula: $C_{15}H_{12}NF$

Mr: 225.26

IR: (KBr) υ 1627 (m), 1607 (m), 1586 (w), 1502 (s), 1298 (w), 1240 (m), 1152 (w), 1095 (w), 981 (m), 953 (w), 837 (m), 774 (w), 747 (m), 692 (m), 504 (w), 434 (w) cm^{-1}

ESI-MS: (MeOH, cone 20 V, +ve ion) *m/z* 226 (100 %, $[M + H]^+$)

HR-MS:	(MeOH, +ve ion)	*m/z* 226.1021 (*m/z* 226.1027 calcd. for $C_{15}H_{13}NF$)
^{1}H NMR:	(400 MHz, $CDCl_3$)	δ 8.25 (d, $^{3}J_{CH}$ = 8.08 Hz, 1 H), 7.53 (m, 2 H), 7.40 (m, 4 H), 7.15 (m, 5 H) ppm
^{13}C NMR:	(400 MHz, $CDCl_3$)	δ 161.35 (d, $^{1}J_{CF}$ = 245.06 Hz), 161.34, 147.86 (d, $^{4}J_{CF}$ = 3.00 Hz), 144.11, 135.60, 129.67, 128.97, 128.51, 127.53, 122.30 (d, $^{3}J_{CF}$ = 8.21 Hz), 115.90 (d, $^{2}J_{CF}$ = 22.59 Hz) ppm

2.4.1.2.3 Preparation of 1-(4-Tolyl)-4-(4-*N*, *N*-Dimethylaminophenyl)-1-Azabuta-1, 3-Diene *18*

Experimental: Two literature methods [A][58] and [B][59] were attempted.

[A] The method was adapted from the literature[58]. In a nitrogen-flushed Schlenk flask, Na_2SO_4 (3.12 g) was added to a solution of 4-dimethylaminocinnamaldehyde (2.66 g, 15.2 mmol) and *p*-toluidine (1.63 g, 15.2 mmol) in Et_2O (30 mL). The clear yellow reaction mixture was stirred at room temperature for 4½ hours. The mixture was filtered through a filter paper into a round-bottomed flask under normal atmosphere, the residue was washed with Et_2O (4 × 20 mL) and the extract was collected in the same flask containing the filtrate. Crystallisation of the filtrate at –20 °C for 24 hours provided the azabutadiene **18** as a yellow precipitate. The precipitate was collected on a Buchner funnel, washed with Et_2O (10 mL) and dried on the funnel by suction for 1 hour. Yellow powder **18**: 0.19 g, 4.7 %.

[B] The method was adapted from the literature[59]. Under normal atmosphere, 4-dimethylaminocinnamaldehyde (1.00 g, 5.73 mmol) was added to a solution of *p*-toluidine (0.61 g, 5.68 mmol) in MeOH (HPLC grade)/distilled CH_2Cl_2 (15 : 6 mL) in a round-bottomed flask. The clear yellow-red reaction mixture was stirred gently in an oil bath at 20 – 24 ºC for 24 hours. Precipitation of a yellow solid was observed. Stirring was continued for another 48 hours. The precipitate was collected on a Buchner funnel, washed with MeOH (HPLC grade, 2 – 3 mL) and dried on the funnel by suction for 1 hour 20 minutes. A yellow powder was obtained (0.38 g, 25 %). Recrystallisation of the yellow powder from CH_2Cl_2/EtOH (Analytical grade) gave the azabutadiene **18** as a yellow powder (88 mg, 6 %).

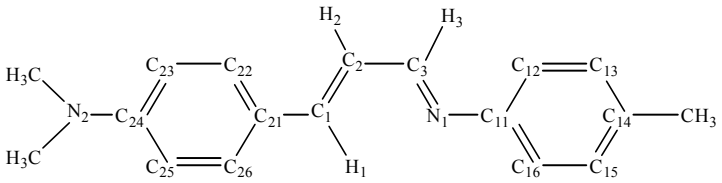

18

Description:		Yellow powder
Empirical Formula:		$C_{18}H_{20}N_2$
Mr:		264.36
IR:	(KBr)	υ 2905 (m, br), 2802 (m), 2739 (m), 1665 (s), 1605 (s), 1528 (m), 1449 (w), 1374 (m), 1266 (w), 1192 (w), 1140 (m), 1068 (w), 1008 (w), 972 (m), 810 (s), 587 (vw), 524 (w) cm^{-1}
ESI-MS:	(MeOH, cone 20 V, +ve ion)	*m/z* 265 (100 %, $[M + H]^+$)
HRMS:	(MeOH, +ve ion)	*m/z* 287.1524 (*m/z* 287.1519 calcd. for $C_{18}H_{20}N_2Na$), *m/z* 265.1701 (*m/z* 265.1699 calcd. for $C_{18}H_{21}N_2$)
^{1}H NMR:	(400 MHz, $CDCl_3$)	δ 8.24 (d, $^3J_{CH}$ = 8.84 Hz, 1 H), 7.43 (d, $^3J_{CH}$ = 8.84 Hz, 2 H), 7.10 (m, 6 H), 6.70 (d, $^3J_{CH}$ = 8.88 Hz, 2 H), 3.02 (s, 6 H), 2.36 (s, 3H) ppm
^{13}C NMR:	(400 MHz, DEPT, $CDCl_3$)	δ 161.57 (CH), 151.31 (C), 149.68 (C), 144.35 (CH), 135.32 (C), 129.74 (2 CH), 129.00 (2 CH), 124.25 (CH), 123.87 (C), 120.84 (2 CH), 112.09 (2 CH), 40.21 (2 CH_3), 20.99 (CH_3) ppm

2.4.2 Reactions of $PhCH_2Re(CO)_5$ with Azabutadienes

2.4.2.1 Reaction of $PhCH_2Re(CO)_5$ with the Azabutadiene *16*

Experimental: The method was adopted from the unpublished undergraduate laboratory report[57]. The reaction was carried out on 1 : 1 and also 1 : 4 mole ratio ($PhCH_2Re(CO)_5$:

azabutadiene). The progress of the reaction was monitored by IR spectroscopy in heptane/CH_2Cl_2.

[On 1 : 1 Mole Ratio] In a nitrogen-flushed Schlenk flask, the azabutadiene **16** (45 mg, 0.22 mmol) was added to a solution of $PhCH_2Re(CO)_5$ **14** (94 mg, 0.23 mmol) in distilled heptane (20 mL). With continuous stirring, the temperature of the oil bath was slowly raised to 95 ºC at which the clear yellow reaction mixture started turning red and new υ(C≡O) bands were observed in the IR spectrum. Since no further progress of the reaction was observed in the IR spectrum, the temperature was raised to 100 ºC and heating was continued at 100 – 110 ºC for 7 hours. The resulting clear red mixture was cooled to room temperature and precipitation of a red solid was observed. The solvent was removed and the residue was dried under vacuum for 30 minutes. The residue was chromatographed on a PLC plate, eluting with CH_2Cl_2/petroleum spirits (9 : 11), giving a strong yellow and orange band at R_F 0.90 and 0.59, respectively. The bands were collected individually in a sintered glass funnel, extracted with CH_2Cl_2, the dichloromethane was removed and the residue was dried under vacuum for 2 hours. Crystallisation from CH_2Cl_2/petroleum spirits at –20 ºC provided the complex **12** as yellow plates (32 mg, 29 %) and **13a** and **13b** as a mixture of red plates and needles (42 mg, 56 %), from the yellow and orange fraction, respectively. The yield of the complexes **12** and, **13a** and **13b** as combined, was calculated based on the number of moles of the azabutadiene **16**.

[On 1 : 4 Mole Ratio] In a nitrogen-flushed Schlenk flask, the azabutadiene **16** (1.40 g, 6.75 mmol) was added to a solution of $PhCH_2Re(CO)_5$ **14** (0.69 g, 1.65 mmol) in distilled heptane (20 mL). With continuous stirring, the reaction mixture was heated in an oil bath at 100 – 105 °C for 4½ hours and cooled to room temperature. Precipitation of a red solid was already observed during the course of the reaction. The solvent was removed and the residue was dried under vacuum for 2 hours. The residue was chromatographed on a PLC plate, eluting with CH_2Cl_2/petroleum spirits (2 : 3), giving a strong yellow and orange band at R_F 0.86 and 0.57, respectively. The bands were collected individually in a sintered glass funnel, extracted with CH_2Cl_2, the dichloromethane was removed and the residue was dried under vacuum for 4 hours. Crystallisation from CH_2Cl_2/petroleum spirits at –20 °C provided the complex **12** as yellow plates (55.6 mg, 7 %) and **13a** and **13b** as a mixture of red plates needles (1.11 g, 98 %) from the yellow and orange band, respectively. The yield of the complexes **12** and, **13a**

and **13b** as combined, was calculated based on the number of moles of $PhCH_2Re(CO)_5$. The weight of $PhCH_2Re(CO)_5$ is only rough weight, so the number of moles may not be exact, accounting for the > 100% yield.

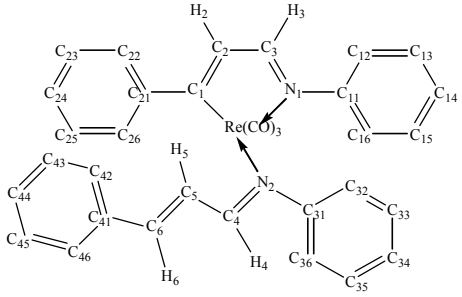

13a

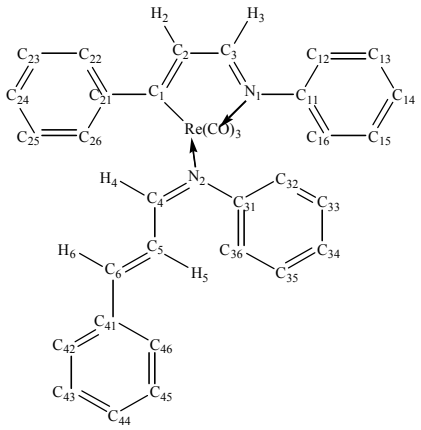

13b

Description:		Red plates **13a** and red needles **13b**
Empirical Formula:		$C_{33}H_{25}N_2O_3Re$
Mr:		683.77
IR*[1]:	(KBr)	υ(C≡O) 1997 (s), 1876 (s, br) cm^{-1}
	(CH_2Cl_2)	υ(C≡O) 2002 (s), 1897, 1891 (s, br) cm^{-1}
	(Hexane)	υ(C≡O) 2008 (s), 1913, 1897 (s) cm^{-1}
	(Transmission mode*[2], **13a**)	υ(C≡O) 3984 (m), 3860 (m), 3756 (m), 1983 (vs), 1875 (vs, br) cm^{-1}
^{1}H NMR*[1]:	(400 MHz, $CDCl_3$)	δ 8.40 (d, $^3J_{CH}$ = 2.28 Hz, 1 H), 8.17 (d, $^3J_{CH}$ = 10.00 Hz, 1 H), 8.15 (d, $^3J_{CH}$ = 2.40 Hz, 0.3 H), 7.88 (d, $^3J_{CH}$ = 9.80 Hz, 0.3 H), 6.86 – 7.34 (m, 30 H) ppm
^{13}C NMR*[1]:	(400 MHz, DEPT, $CDCl_3$)	δ 200.71 (C), 200.11 (C), 199.45 (C), 193.95 (C), 193.67 (C), 176.31 (CH), 176.04 (CH), 174.57 (CH), 171.82 (CH), 156.07 (C), 153.30 (C), 152.62 (C), 151.91 (C), 151.73 (C), 151.54 (C), 150.42 (CH), 147.55 (CH), 135.90 (CH), 135.25 (CH), 134.54 (C), 134.29 (C), 131.10 (CH), 130.73 (CH), 129.06 (CH), 129.01 (CH), 128.91

(C), 128.76 (CH), 128.65 (CH), 128.58 (CH), 128.55 (CH), 128.34 (CH), 128.22 (CH), 128.12 (CH), 128.04 (CH), 127.47 (CH), 127.02 (CH), 126.73 (CH), 126.61 (CH), 126.58 (CH), 126.10 (CH), 122.70 (CH), 122.61 (CH), 122.21 (CH), 121.80 (CH), 120.95 (CH), 120.69 (CH) ppm

ESI-MS: (MeOH, cone 20 V, +ve ion) *m/z* 707 (3 %, $[M + Na]^+$), 685 (100 %, $[M + H]^+$)

(MeOH/NaOMe, cone 20 V, +ve ion) *m/z* 1391 (7 %, $[2M + Na]^+$), 707 (83 %, $[M + Na]^+$)

(MeOH, cone 20 V, -ve ion) *m/z* 715 (5 %, $[M + OMe]^-$), 684 (65 %, $[M]^-$)

(MeOH/NaOMe, cone 20 V, -ve ion) *m/z* 715 (100 %, $[M + OMe]^-$)

HR-MS: (MeOH/NaOMe, +ve ion) *m/z* 707.1372 (*m/z* 707.1315 calcd. for $C_{33}H_{25}N_2NaO_3Re$)

Elemental Analysis: Found: C 57.23 %, H 3.81 %, N 3.97 %

Required: C 57.97 %, H 3.69 %, N 4.10 %

*[1] Mixture of the two isomers **13a** and **13b**; *[2] Single Crystal FTIR.

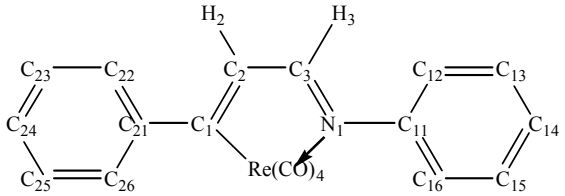

12

Description: Yellow plates

Empirical Formula: $C_{19}H_{12}N_1O_4Re$

Mr: 504.51

m.p.: 170 ºC

IR: (KBr) υ(C≡O) 2093 (w), 1998 (s), 1981 (vs), 1916 (s) cm^{-1}

(CH_2Cl_2) υ(C≡O) 2092 (w), 1992 (s), 1934 (m) cm^{-1}

(Hexane) υ(C≡O) 2091 (w), 1990 (s, br), 1948 (sh, m) cm^{-1}

^{1}H NMR: (400 MHz, $CDCl_3$) δ 8.26 (d, $^3J_{CH}$ = 2.28 Hz, 1 H), 7.44 (m, 4 H), 7.31 (m, 4 H), 7.26 (m, 3 H) ppm

^{13}C NMR:	(400 MHz, DEPT, $CDCl_3$)	δ 218.45 (C), 191.69 (C), 191.05 (C), 187.49 (2 C), 177.85 (CH), 153.62 (C), 151.28 (C), 137.03 (CH), 129.38 (CH), 128.38 (CH), 128.28 (CH), 128.15 (CH), 127.27 (CH), 126.64 (CH), 122.25 (CH) ppm
ESI-MS:	(MeOH, cone 20, +ve ion)	*m/z* 505 (3 %, $[M + H]^+$)
	(MeOH/NaOMe, cone 20, -ve ion)	*m/z* 535 (100 %, $[M + OMe]^-$), 507 (30 %, $[M + OMe – CO]^-$), 479 (10 %, $[M + OMe – 2\ CO]^-$)
Elemental Analysis:	Found:	C 45.45 %, H 2.30 %, N 2.87 %
	Required:	C 45.23 %, H 2.40 %, N 2.78 %

2.4.2.2 Reaction of $PhCh_2Re(CO)_5$ with the Azabutadiene *17*

Experimental: The same experimental procedure[57] was used. Two reactions, one on 1 : 1 and the other on 1 : 2 mole ratio ($PhCH_2Re(CO)_5$: azabutadiene), were carried out under the same reaction conditions. The progress of the reactions was monitored by IR spectroscopy in CH_2Cl_2/heptane.

In a nitrogen-flushed Schlenk flask, the azabutadiene **17** ((1 : 1) 0.08 g, 0.35 mmol; (1 : 2) 0.17 g, 0.74 mmol) was added to a solution of $PhCH_2Re(CO)_5$ **14** ((1 : 1) 0.15 g, 0.36 mmol; (1 : 2) 0.13 g, 0.31 mmol) in distilled heptane (15 mL). With continuous stirring, the clear yellow reaction mixtures were heated in an oil bath at 100 – 110 °C for 7½ hours. Both mixtures started turning red at 100 °C and precipitation of a red solid was observed during the course of the reaction. The resulting clear red mixtures with the red precipitates were cooled to room temperature, the solvents were removed and the residues were dried under vacuum for 2 hours. The residues were chromatographed on PLC plates, eluting with CH_2Cl_2/petoroleum spirits (2 : 3). A strong yellow and orange band at R_F 0.78 and 0.47, respectively, were collected individually in a sintered glass funnel, extracted with CH_2Cl_2, the dichloromethane was removed and the residues were dried under vacuum for 2 hours. Yellow fraction: (1 : 1) 28 mg, 15 %; (1 : 2) 12 mg, 8 %. Orange fraction: (1 : 1) 93 mg, 73%; (1 : 2) 172 mg, 77 %. Crystallisation from CH_2Cl_2/petroleum spirits at –20 ºC (or at room temperature) provided a yellow plate **19** and a mixture of a red plate **20a** and needles **20b**

from the yellow and orange fractions, respectively. Single crystals of the complexes **19**, **20a** and **20b** were prepared by vapour diffusion from CH_2Cl_2/*n*-pentane at –20 °C.

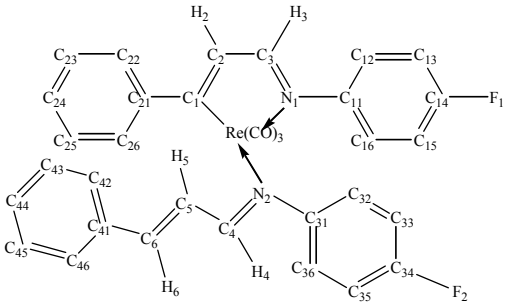

20a

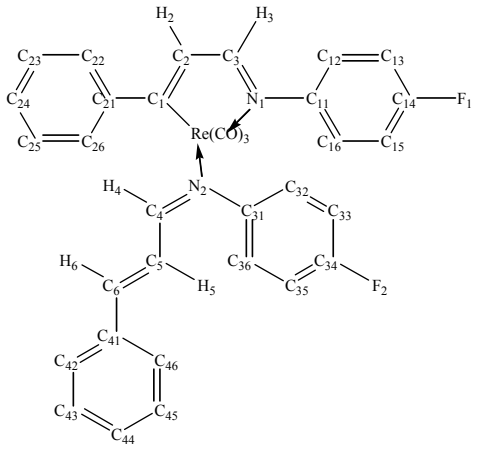

20b

Description: Red plates **20a** and red needles **20b**

Empirical Formula: $C_{33}H_{23}F_2N_2O_3Re$

Mr: 719.75

IR[*1]: (CH_2Cl_2) υ(C≡O) 2003 (s), 1899, 1892 (s, br) cm^{-1}

(Transmission mode[*2], **20a**) υ(C≡O) 3990 (s), 3875 (s), 3773 (s), 1994 (vs), 1881 (vs, br) cm^{-1}

(Transmission mode[*2], **20b**) υ(C≡O) 3991 (s), 3874 (s), 3773 (s), 1994 (vs), 1884 (vs, br) cm^{-1}

ESI-MS:

(MeOH/NaOMe, cone 20 V, +ve ion) *m/z* 742 (56 %, $[M + Na]^+$)

(-ve ion) *m/z* 750 (100 %, $[M + OMe]^-$)

^{1}H NMR[*1]: (400 MHz, $CDCl_3$) δ 8.35 (d, $^3J_{CH}$ = 2.12 Hz, 1 H), 8.15 (d, $^3J_{CH}$ = 10.04 Hz, 1 H), 8.12 (d, $^3J_{CH}$ = 2.28 Hz, 0.5 H), 7.86 (d, $^3J_{CH}$ = 9.64 Hz, 0.5 H), 7.31 (m, 32 H), 6.99 (m, 26 H) ppm

^{13}C NMR[*1]: (400 MHz, $CDCl_3$) δ 200.54, 199.86, 199.40, 193.73, 193.48, 177.21, 176.52, 176.39, 176.26, 176.17, 175.99, 175.79, 175.69, 175.55, 175.10, 174.84, 173.49, 172.86, 172.67, 172.47, 171.83, 161.24 (d, $^1J_{CF}$ = 246.38 Hz), 161.04 (d, $^1J_{CF}$ = 246.25 Hz), 160.95 (d, $^1J_{CF}$

= 246.36 Hz), 152.25, 151.65, 151.43, 151.05, 149.43, 148.73, 148.41, 148.12, 147.50, 144.00, 136.14, 135.85, 135.57, 135.26, 134.97, 134.36, 134.07, 131.75, 131.43, 131.04, 129.49, 129.17, 128.84, 128.57, 128.46, 128.31, 128.14, 127.85, 127.74, 127.48, 127.12, 126.85, 126.72, 126.42, 124.18 (d, $^{3}J_{CF}$ = 7.82 Hz), 123.91 (d, $^{3}J_{CF}$ = 8.08 Hz), 123.52 (d, $^{3}J_{CF}$ = 7.90 Hz), 120.61, 120.30, 120.00, 115.79 (d, $^{2}J_{CF}$ = 22.63 Hz), 115.32 (d, $^{2}J_{CF}$ = 22.85 Hz) ppm

Elemental Analysis: Found: C 55.07 %, H 3.07 %, N 3.91 %

Required: C 55.07 %, H 3.22 %, N 3.89 %

[*1] Mixture of the two isomers **20a** and **20b**; [*2] Single crystal FTIR

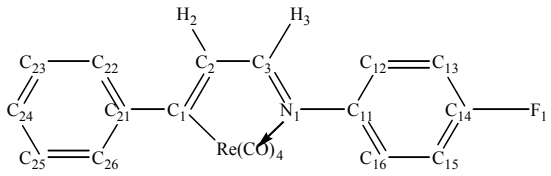

19

Description: Yellow plates

Empirical Formula: $C_{19}H_{11}F_1N_1O_4Re$

Mr: 522.50

m.p.: 145 ºC

IR: (CH_2Cl_2) υ(C≡O) 2092 (vw), 1995 (s), 1983 (vs), 1936 (w) cm^{-1}

ESI-MS:

(MeOH/NaOMe, cone 20 V, -ve ion) *m/z* 553 (100 %, $[M + OMe]^-$), 525 (40 %, $[M + OMe - CO]^-$), 497 (13 %, $[M + OMe – 2 CO]^-$)

^{1}H NMR: (400 MHz, $CDCl_3$) δ 8.23 (d, $^{3}J_{CH}$ = 2.32 Hz, 1 H), 7.43 (m, 7 H), 7.30 (m, 1 H), 7.23 (d, $^{3}J_{CH}$ = 2.32 Hz, 1 H), 7.20 (m, 3 H), 7.12 (m, 3 H) ppm

^{13}C NMR: (400 MHz, $CDCl_3$) δ 219.47, 191.43, 190.99, 187.37, 178.02, 161.45

(d, $^{1}J_{CF}$ = 246.92 Hz), 149.93 (d, $^{4}J_{CF}$ = 3.30 Hz), 136.91, 128.28, 128.23, 126.58, 123.75 (d, $^{3}J_{CF}$ = 8.49 Hz), 116.17 (d, $^{2}J_{CF}$ = 22.86 Hz) ppm

Elemental Analysis: Found: C 44.40 %, H 2.13 %, N 2.70 %

Required: C 43.68 %, H 2.12 %, N 2.68 %

2.4.2.3 Reaction of $PhCH_2Re(CO)_5$ with the Azabutadiene *18*

Experimental: The same experimental procedure[57] was used. The progress of the reaction was monitored by IR spectroscopy in heptane/CH_2Cl_2.

In a nitrogen-flushed Schlenk flask, the azabutadiene **18** (74 mg, 0.28 mmol) was added to a solution of $PhCH_2Re(CO)_5$ **14** (122 mg, 0.29 mmol) in distilled heptane (20 mL). With continuous stirring, the clear yellow reaction mixture was heated in an oil bath at 100 – 110 ºC for 7 hours. The mixture started turning red at 85 ºC and precipitation of a red solid was observed during the course of the reaction. The resulting very dark red mixture with the red precipitate was cooled to room temperature, the solvent was removed and the residue was dried under vacuum for 2 hours. The residue was chromatographed on a PLC plate, eluting with CH_2Cl_2/petroleum spirits (3 : 2), giving a strong orange and red band at R_F 0.92 and 0.67, respectively. The bands were collected individually in a sintered glass funnel, extracted with CH_2Cl_2, the dichloromethane was removed and the residue was dried under vacuum for 1 hour. Crystallisation from CH_2Cl_2 at –20 ºC provided the complex **21** as red plates (50 mg, 32 %) and **22a** and **22b** as a mixture of red blocks and needles (75 mg, 67 %) from the orange and red band, respectively.

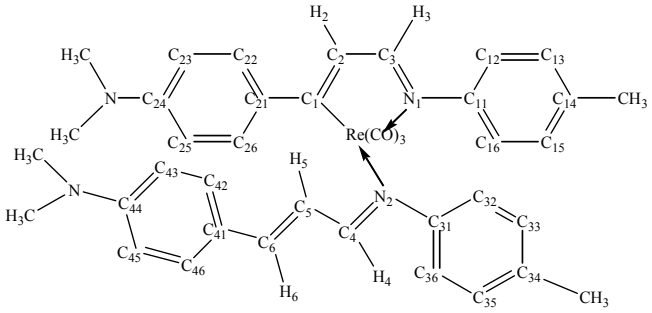

22a

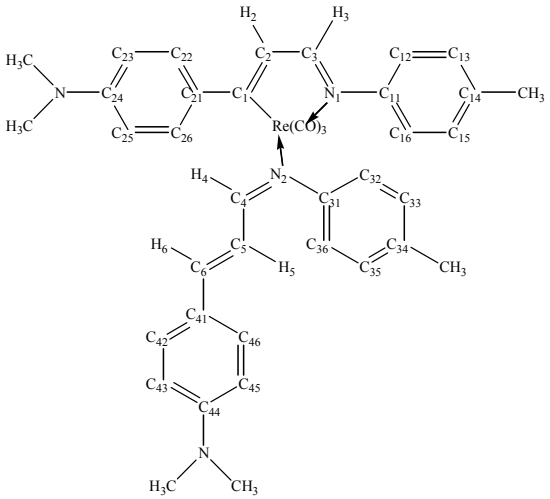

22b

Description:		Red blocks **22a** and red needles **22b**
Empirical Formula:		$C_{39}H_{39}N_4O_3Re$
Mr:		797.96
m.p.:		180 ºC
IR[*1]:	(KBr)	υ(C≡O) 1993 (s), 1880 (vs, br) cm^{-1}
	(CH_2Cl_2)	υ(C≡O) 1997 (s), 1891 (s, br) cm^{-1}
	(Transmission mode[*2], **22a**)	υ(C≡O) 3981 (w), 3871 (w), 3745 (w), 1994 (s), 1871 (s, br) cm^{-1}
ESI-MS:	(MeOH, cone 20 V, +ve ion)	*m/z* 799 (100 %, $[M + H]^+$)
	(MeOH/NaOMe, cone 20 V, +ve ion)	*m/z* 821 (100 %, $[M + Na]^+$)
	(-ve ion)	*m/z* 829 (100 %, $[M + OMe]^-$)
HRMS:	(MeOH/NaOMe, +ve ion)	*m/z* 837.218 (*m/z* 837.221 calcd. for $C_{39}H_{39}N_4KO_3Re$), 821.243 (*m/z* 821.247 calcd. for $C_{39}H_{39}N_4NaO_3Re$)
^{1}H NMR[*1]:	(400 MHz, $CDCl_3$)	δ 8.30 (d, $^3J_{CH}$ = 2.44 Hz), 8.25 (d, $^3J_{CH}$ = 8.92 Hz), 8.05 (d, $^3J_{CH}$ = 2.56 Hz), 8.00 (d, $^3J_{CH}$ = 10.12 Hz), 7.74 (d, $^3J_{CH}$ = 9.92 Hz), 7.59 (m), 7.44 (d, $^3J_{CH}$ = 8.92 Hz), 6.80 (m), 6.55 (d, $^3J_{CH}$ = 8.92 Hz), 6.45 (d, $^3J_{CH}$ = 8.88 Hz), 3.02 (m), 2.36 (d, *J* = 5.40 Hz), 2.27 (d, *J* = 9.04 Hz) ppm
^{13}C NMR[*1]:	(400 MHz, DEPT, $CDCl_3$)	δ 201.84 (C), 201.08 (C), 199.91 (C), 199.80 (C), 194.91 (C), 194.80 (C), 175.08 (CH), 174.61 (CH),

174.10 (CH), 171.68 (CH), 161.65 (C), 154.36 (C), 151.99 (C), 151.75 (C), 151.52 (C), 150.81 (C), 150.76 (C), 150.50 (C), 150.30 (CH), 150.05 (C), 147.72 (CH), 140.43 (C), 139.77 (C), 135.64 (C), 135.52 (C), 135.38 (C), 134.88 (C), 132.67 (CH), 132.12 (CH), 130.53 (CH), 130.23 (CH), 129.89 (CH), 129.80 (CH), 129.53 (CH), 129.34 (CH), 129.30 (CH), 129.11 (CH), 128.80 (CH), 128.77 (CH), 123.72 (CH), 123.04 (CH), 122.96 (CH), 122.53 (CH), 122.20 (CH), 122.10 (CH), 121.65 (CH), 120.86 (CH), 116.07 (CH), 112.05 (CH), 111.95 (CH), 111.67 (CH), 111.41 (CH), 40.54 (CH_3), 40.27 (CH_3), 40.09 (CH_3), 21.03 (CH_3), 20.98 (CH_3), 20.78 (CH_3) ppm

Elemental Analysis: Found: C 58.88 %, H 4.94 %, N 7.01 %

Required: C 58.70 %, H 4.93 %, N 7.02 %

[*1] Mixture of the two isomers; [*2] Single Crystal FTIR.

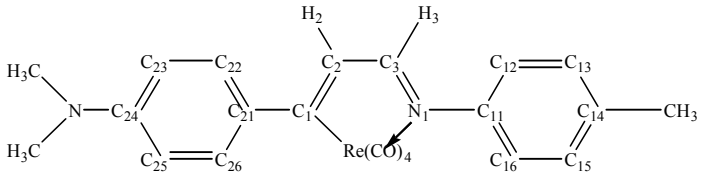

21

Description: Red blocks

Empirical Formula: $C_{22}H_{19}N_2O_4Re$

Mr: 561.60

m.p.: 210 ºC

IR: (CH_2Cl_2) υ(C≡O) 2089 (vw), 1989, 1974 (s), 1926 (w) cm^{-1}

ESI-MS: (MeOH, cone 20 V, +ve ion) *m/z* 562 (100 %, $[M + H]^+$)

(MeOH/NaOMe, cone 20 V, +ve ion) *m/z* 584 (100 %, $[M + Na]^+$), 562 (30 %, $[M + H]^+$)

(-ve ion) *m/z* 592 (100 %, $[M + OMe]^-$), 564 (34 %, $[M + OMe – CO]^-$), 536 (30 %, $[M + OMe – 2\ CO]^-$)

^{1}H NMR:	(400 MHz, $CDCl_3$)	δ 8.16 (d, $^{3}J_{CH}$ = 2.52 Hz, 1 H), 7.56 (d, $^{3}J_{CH}$ = 8.88 Hz, 2 H), 7.24 (d, $^{3}J_{CH}$ = 2.5 Hz, 1 H) 7.19 (m, 4 H), 7.10 (d, $^{3}J_{CH}$ = 8.28 Hz, 2 H), 6.75 (d, $^{3}J_{CH}$ = 8.88 Hz, 2 H), 3.04 (s, 6 H), 2.39 (s, 3 H) ppm
^{13}C NMR:	(400 MHz, DEPT, $CDCl_3$)	δ 216.99 (C), 192.55 (C), 191.41 (C), 188.24 (2 C), 176.72 (CH), 151.71 (C), 151.26 (C), 138.87 (C), 136.48 (C), 133.77 (CH), 129.72 (4 CH), 122.23 (2 CH), 111.52 (2 CH), 40.39 (CH_3), 21.02 (CH_3) ppm
Elemental Analysis:	Found:	C 47.51 %, H 3.53 %, N 4.92 %
	Required:	C 47.05 %, H 3.41 %, N 4.99 %

2.4.3 X-Ray Crystallography

Table 2-24: Crystal Data and Refinement Details for **13a***, **13b**, **12** and **20a**

	13a*	**13b**	**12**	**20a**
Empirical Formula	$C_{33}H_{25}N_2O_3Re$	$C_{33}H_{25}N_2O_3Re$	$C_{19}H_{12}NO_4Re$	$C_{33}H_{23}F_2N_2O_3Re$
M_r	683.75	683.75	504.50	719.73
T / K	84(2)	93(2)	93(2)	97(2)
Wavelength / Å	0.71073	0.71073	0.71073	0.71073
Crystal System	Monoclinic	Monoclinic	Monoclinic	Orthorhombic
Space Group	P2(1)/c	P2(1)/c	P2(1)/c	Pbca
***a* / Å**	12.0281(2)	9.3259(3)	12.4902(3)	13.8048(3)
***b* / Å**	14.4460(2)	10.0899(3)	17.5205(4)	14.8172(3)
***c* / Å**	15.7868(2)	29.4933(9)	8.1233(2)	27.0507(6)
α / °	90	90	90	90
β / °	97.690(1)	95.066(1)	106.365(1)	90
γ / °	90	90	90	90
V / Å^3	2718.41(7)	2764.40(15)	1705.64	5533.2(2)
Z	4	4	4	8
ρ / g cm^{-3}	1.671	1.643	1.965	1.728
μ / mm^{-1}	4.507	4.432	7.147	4.444
F (000)	1344	1344	960	2816
Crystal Size / mm^3	0.28 × 0.28 × 0.12	0.26 × 0.22 × 0.02	0.30 × 0.25 × 0.15	0.43 × 0.37 × 0.34
θ range / °	1.71 to 26.42	2.70 to 34.88	1.70 to 35.06	1.51 to 28.04
Limiting Indices	$-13 \le h \le 15$, $-18 \le k \le 17$, $-19 \le l \le 17$	$-13 \le h \le 14$, $-15 \le k \le 15$, $-45 \le l \le 43$	$-19 \le h \le 18$, $-25 \le k \le 25$, $-11 \le l \le 12$	$-14 \le h \le 18$, $-19 \le k \le 16$, $-32 \le l \le 35$
Reflection Collected	15836	45919	39116	60010
Unique Reflections	5543 (R_{int} 0.0239)	9871 (R_{int} 0.0322)	6436 (R_{int} 0.0266)	6693 (R_{int} 0.0317)
Completeness to θ ° (%)	26.42 (99.4)	27.50 (99.3)	27.50 (99.9)	28.04 (99.8)
Absorption Correction	Multiscan	Semi-empirical from equivalents	Semi-empirical from equivalents	Multiscan
T_{max} and T_{min}	0.413 and 0.292	0.9166 and 0.3920	0.4136 and 0.2230	0.3134 and 0.2510
Refinement Method	Full-matrix least-squares on F^2	Full-matrix least-squares on F^2	Full-matrix least-squares on F^2	Full-matrix least-squares on F^2
Data / Restraints / Parameters	5543 / 0 / 368	9871 / 0 / 352	6436 / 0 / 226	6693 / 0 / 370
GoF on F^2	1.087	1.261	1.073	1.080
Final R Indices [I > 2σ(I)]	R_1 0.0215, wR_2 0.0502	R_1 0.0312, wR_2 0.0594	R_1 0.0163, wR_2 0.0361	R_1 0.0207, wR_2 0.0521

R Indices (all data)	R_1 0.0265, wR_2 0.0530	R_1 0.0378, wR_2 0.0607	R_1 0.0213, wR_2 0.0379	R_1 0.0251, wR_2 0.0549
Largest Diff. Peak and Hole / eÅ^{-3}	1.410 and -0.984	1.679 and -3.258	0.953 and -0.559	1.403 and -1.030

* From the undergraduate laboratory report[57].

Chapter 3 Reactions of the Cyclometallated Azabutadiene with Unsaturated Molecules

3.1 Introduction

3.1.1 Reaction of Cyclometallated Azabutadienes with Unsaturated Molecules

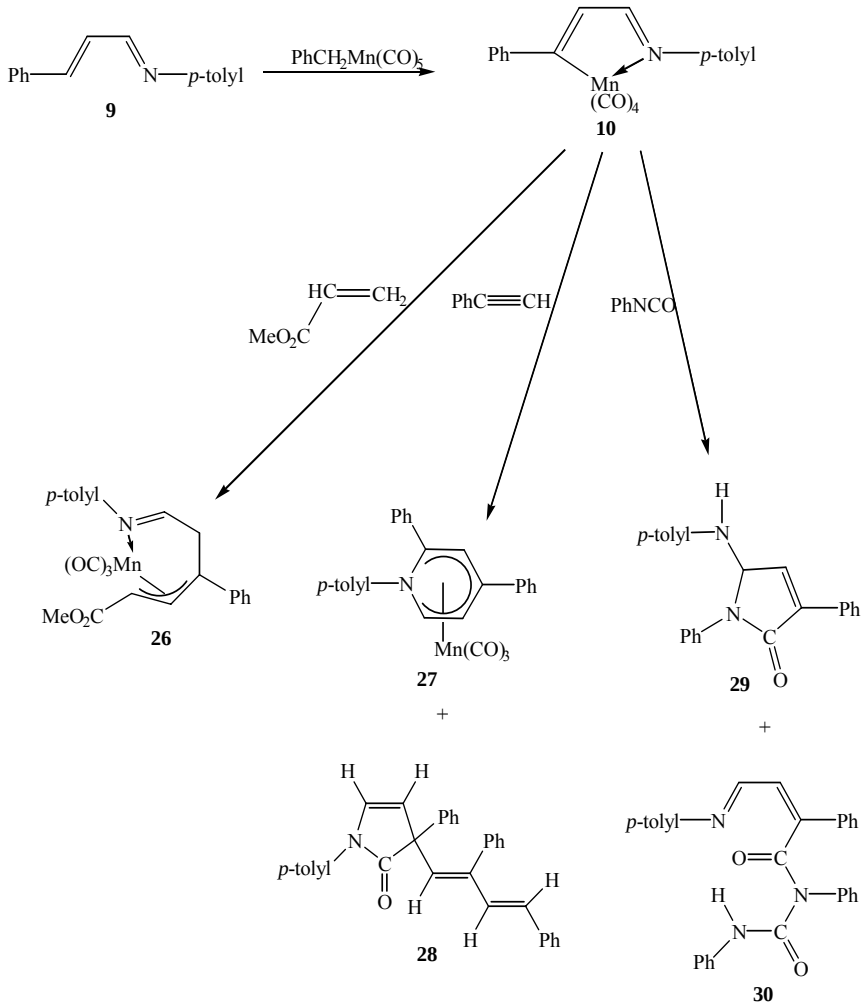

Scheme 3-1: *In situ* Reactions of 1,4-Diaryl-1-aza-1,3-butadienes with $PhCH_2Mn(CO)_5$ in the Presence of Unsaturated Reagents[48]

Previously, *in situ* reactions of 1,4-diaryl-1-aza-1,3-butadienes with $PhCH_2Mn(CO)_5$ in the presence of unsaturated reagents including PhC≡CH, CH_2=CHCOOMe and PhNCO, have been examined[48]. The scheme above summarises the reactions.

In situ reaction of an azabutadiene with $PhHCH_2Mn(CO)_5$ in the presence PhC≡CH gave a tri-aryl-η^5-azacyclohexadienyl-$Mn(CO)_3$ complex **27**. The complex is the *N*-analogue of the η^5-pyranyl complexes **6** obtained in reaction of cyclomanganated chalcones with alkynes[5]. The scheme below shows the proposed mechanism of the reaction[48]. The reaction first undergoes cyclometallation of an azabutadiene to give the cyclomanganated azabutadiene **11**. As in the reaction of cyclomanganated aryl ketones and chalcones with alkynes[5], the reaction then proceeds by insertion of PhC≡CH into the Mn-C σ-bond followed by cyclisation, involving the N=C bond, leading to a tri-aryl-η^5-azacyclohexadienyl ring with the $Mn(CO)_3$ group attaching to one face of the heteroaromatic ring **27** (Scheme 3-2)[48]. The tri-aryl-η^5-azacyclohexadienyl-$Mn(CO)_3$ complex **27** could be obtained in an excellent yield e.g. > 80 %[48].

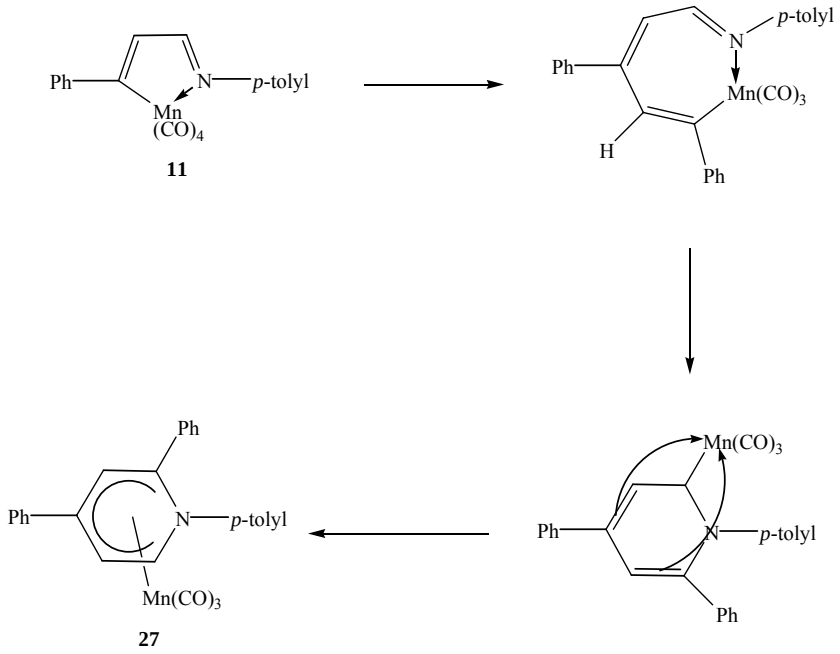

Scheme 3-2: Route to the Tri-aryl-η^5-azacyclohexadienyl-$Mn(CO)_3$ Complex **27**

Coupling reaction of CH_2=CHCOOMe with the azabutadiene through the Mn-C carbon gives the methyl 7-azahepta-3,6-dien-2-yloate ligand and this coordinates to the $Mn(CO)_3$ group via an η^3-allyl interaction with the two electron donation from the N atom[48].

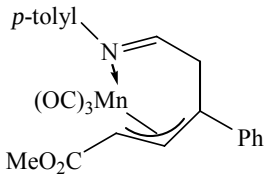

26

Figure 3-1: Methyl 7-Azahepta-3,6-dien-2-yloate-$Mn(CO)_3$ Complex **26**

The reaction in the presence of PhNCO gave two purely organic products **29** and **30** in a moderate yield (Figure 3-2)[48]. Cyclometallation of an azabutadiene and insertion of PhNCO into the Mn-C bond of the pre-formed cyclomanganated azabutadiene followed by cyclisation involving the C=N bond and subsequent protio-demetallation gave the CO inserted complex **29**. The other product **30** formed via a double insertion of PhNCO[48].

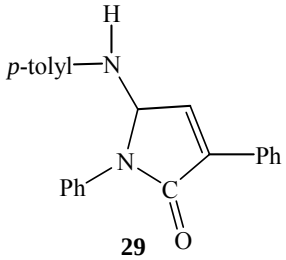

29

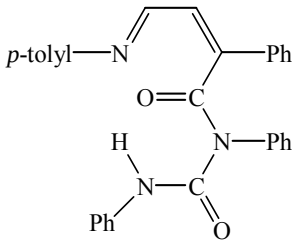

30

Figure 3-2: Products **29** and **30** from the Reaction in the Presence of PhNCO

All reactions appear to first undergo cyclometallation of an azabutadiene followed by insertion of the unsaturated substrate into the Mn-C bond of the pre-formed cyclomanganated azabutadiene, leading to a seven-membered metallocyclic ring intermediate. Subsequent reactions differ depending on the substrate[48]. The alkyne-intermediate cyclises by attack at the imine nitrogen to give a six-membered ring, the PhNCO-intermediate attacks at the imine

carbon atom, leading to a five-membered ring, while the alkene-derived species does not undergo a cyclisation reaction at all[48].

Reaction of azabutadiene and $PhCH_2Mn(CO)_5$ with Bu^tNC gave no azabutadiene derived product[48]. Isonitriles were too effective as Lewis bases and interfered with cyclometallation of azabutadiene by reacting with $PhCH_2Mn(CO)_5$ before the reaction could take place[48].

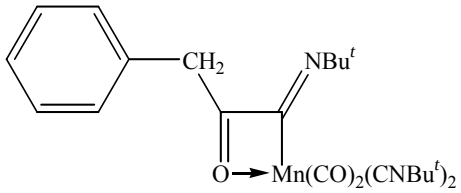

31

Figure 3-3: Complex **31**

This complex formed via first an insertion of a CO ligand followed by a Bu^tNC one into the Mn-C bond followed by further replacement of two terminal carbonyl groups by isonitriles[48].

In situ reaction of an azabutadiene with $PhCH_2Mn(CO)_5$ in the presence of unsaturated reagents, presumably via the cyclomanganated azabutadiene **11**, has shown interesting reactions and products[48]. The corresponding reactions of the substituted derivatives **13** with unsaturated reagents were, therefore, investigated. This chapter will report the investigations. For the isocyanide reaction, *para*-methoxyphenyl isocyanide was used instead of Bu^tNC[48].

3.2 Results and Discussion

3.2.1 Reaction of Cyclorheniated Azabutadiene with CO and Unsaturated Reagents

The scheme summarises the reactions discussed in this chapter. The complex **13** was used as the mixture of the two isomers.

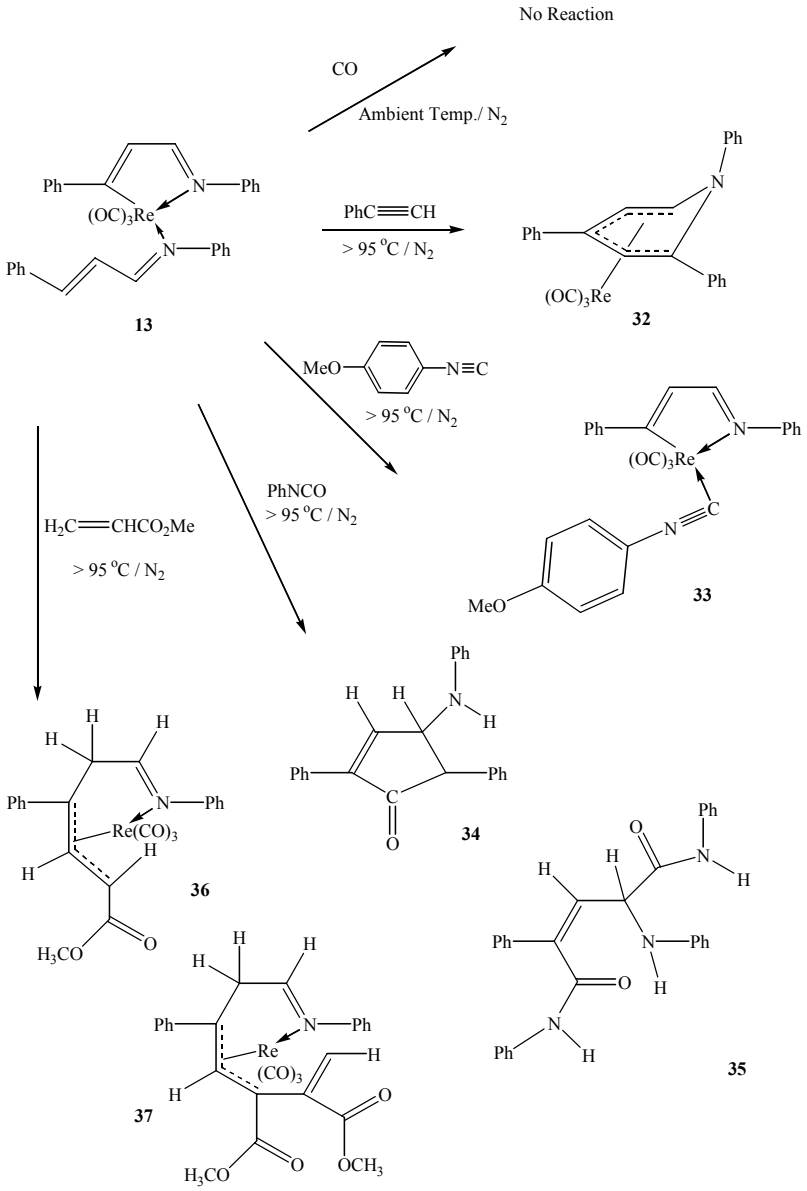

Scheme 3-3: Reactions of **13** with CO and Unsaturated Molecules

3.2.1.1 Reaction with CO

The complex **13** was reacted with CO (g) in CH_2Cl_2 to investigate if the η^1-azabutadiene ligand would be displaced by a CO and the tetracarbonyl complex **12** form. Stirring at room temperature for 24 hours under a CO atmosphere showed no reaction indicated by the same υ(C≡O) bands observed at the start of the reaction in the IR spectrum. No further investigation was, therefore, carried out.

3.2.1.2 Reaction with Phenyl Acetylene, PhC≡CH

3.2.1.2.1 Reaction

The scheme below summarises the reaction.

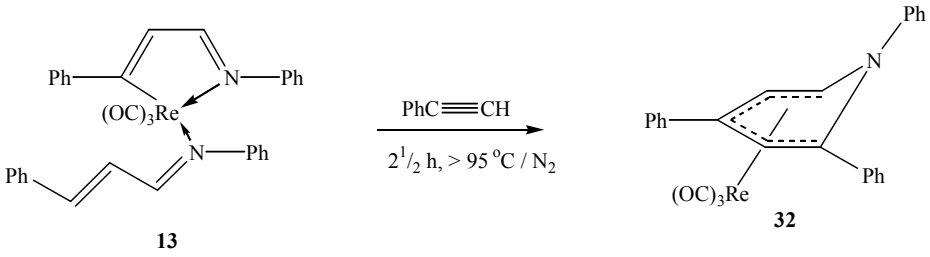

Scheme 3-4: Reaction of **13** with PhC≡CH

When the complex **13** and PhCCH (ca. 1 : 2 – 3) in distilled heptane were heated above 95 °C for 2½ hours, the Re analogue of a tri-aryl-η^5-azacyclohexadienyl-$Mn(CO)_3$ complex **32** could be obtained. The η^5-azacyclohexadienyl ring coordinates to the $Re(CO)_3$ group in the same manner as in the Mn complex **38** (Figure 3-4)[48].

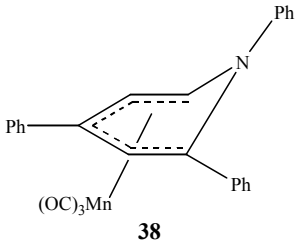

Figure 3-4: Complex **38**

The yield of the complex **32** was low compared to that of the complex **27**, which could be prepared in an excellent yield e.g. 87 %[48] cf. 49 % in the Re system. The IR spectrum of the reaction mixture, however, indicated that all the complex **13** was reacted and the υ(C≡O) bands corresponding to the product appeared with strong intensities. There was a streak during the chromatography process on a PLC plate. The yield may, therefore, have been reduced during the isolation process.

The reaction could be initiated at 35 ºC, indicated by the development of a new peak at 2029 cm^{-1} in the υ(C≡O) region of the IR spectrum in CH_2Cl_2/heptane. No further growth of the 2029 cm^{-1} peak was observed by stirring further at 35 ºC. The temperature of the oil bath was, therefore, raised to 85 ºC and the development of the peak was, again, observed. The υ(C≡O) bands corresponding to the complex **13** completely shifted after 2 hours at > 85 ºC which indicated the reaction needed to be heated at > 85 ºC to complete. The reaction mixture turned yellow and new bands at 2028, 1953 and 1937 cm^{-1} were observed in the υ(C≡O) region of the IR spectrum. Crystallisation from petroleum spirits/CH_2Cl_2 at –20 ºC gave the complex **32** as yellow crystals from the yellow fraction collected at R_F 0.66 on PLC.

3.2.1.2.2 Characterisation

3.2.1.2.2.1 IR

IR analysis was carried out in CH_2Cl_2. Symmetrical $LRe(CO)_3$ molecules expect a_1 and e υ_{CO} bands, with splitting of the latter if the L group has low symmetry[61]. The a_1 and e bands were observed at 2026 (s), 1949 (m) and 1935 (m) cm^{-1}, respectively, in the υ(C≡O) region. The table below summarises the υ(C≡O) frequencies for the complexes **32** and **27** and also $CpM(CO)_3$ (M = Mn or Re)[61] for comparison.

Table 3-1: υ(C≡O) Frequencies for the Complexes **32**, **27** and $CpM(CO)_3$ (M = Mn or Re)

υ(C≡O) / cm^{-1}			
27 (in petroleum spirits)[48]	2025, s (A_1)	1965, m (E)	1946, m (E)
32 (in heptane)	2028, s (A_1)	1953, m (E)	1937, m (E)
$CpMn(CO)_3$ (in C_6H_{12})[61]	2028 (A_1)	1945 (E)	
$CpRe(CO)_3$ (CS_2, CCl_4)[61]	2041 (A_1)	1939 (E)	

The overall pattern of the tricarbonyl bands was the same for the complexes **32** and **27**. A_1 band appears at the highest and e bands at lower frequencies. The pattern was also consistent with that in $CpMn(CO)_3$ and $CpRe(CO)_3$ complexes[61] (Table 3-1). Splitting of the e band was also observed for both complexes **32** and **27**. The intensity pattern of the bands for the complexes **32** and **27** analogues were also consistent. A_1 band appears with strong and e bands with strong to medium to intensity, respectively.

3.2.1.2.2.2 ESI-MS

ESI-MS analysis was carried out at cone voltage of 20 V in MeOH with NaOMe. The parent molecule was observed at *m/z* 601, 577, 609 as $[M + Na]^+$, $[M - H]^-$ and $[M + OMe]^-$, (M = **32**), respectively, in the respective ion modes. At cone voltage of 20 V, the peak at *m/z* 308 dominates the spectrum in the positive ion mode. HR-MS showed that the observed *m/z* of 308.144 in the positive ion mode closely agreed with the mass of 308.1434 calculated for the formula of $C_{23}H_{18}N_1$ which was consistent with the mass of the azacyclohexadienyl ring itself and, therefore, could be assigned as $[M - Re(CO)_3]^+$. This may suggest that the coordination of the $Re(CO)_3$ group to the azacyclohexadienyl ring is fairly weak and the $Re(CO)_3$ group can be removed at a relatively low cone voltage e.g. 20 V, generating a very stable pyridinium cation. The demetallaion in the ESI-MS was also observed for the Mn analogue **27**[48].

3.2.1.2.2.3 ^{1}H and ^{13}C NMR

NMR experiments were carried out on samples in $CDCl_3$ at 400 MHz. The table below summarises the selected chemical shifts for the complex **32** and **27**.

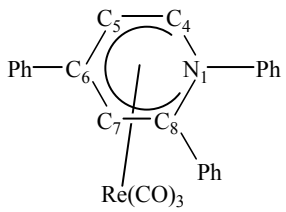

32

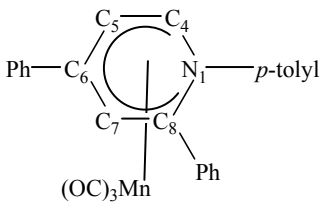

27

Table 3-2: Selected Chemical Shifts for the Complexes **32** and **27**[48]

δ / ppm	**32**	**27**[48]		**32**	**27**[48]
^{1}H NMR			**^{13}C NMR**		
H-4	5.26 (d, $^{3}J_{HH}$ = 4.1 Hz)	5.01 (d, $^{3}J_{HH}$ = 4.2 Hz)	*C-4*	57.2	65.3
H-5	5.83 (d, $^{3}J_{HH}$ = 4.0 Hz)	5.52 (d, $^{3}J_{HH}$ = 4.2 Hz)	*C-5*	93.9	91.7
			C-6	101.0	102.4
H-7	6.63 (s)	6.29 (s)	*C-7*	90.68	88.7
			C-8	79.8	81.4
			M(CO)$_3$	193.0	221.5

The *H-4*, *5* and *7* proton signals for the complex **32** were shifted by 0.25 – 0.34 ppm down-field than the corresponding signals for the complex **27**. The azacyclohexadienyl ring protons were more deshielded in the complex **32** than in the Mn analogue. The chemical shifts of the corresponding ring carbon signals were, however, quite similar with a slight shifts either down- or up-field (there was no obvious trend). The greatest shift was observed for the *C-4* carbon signals. The *C-4* carbon signal for the complex **32** was shifted by 8.1 ppm up-field from the corresponding signal for the complex **27**. The ^{3}J coupling constants of the *H-4* and *5* protons in the complexes **32** and **27** were consistent, but slightly smaller in the former. Coupling constant strongly depends on the electronegativity of the substituents[60]. The more electronegative the substituent is, the smaller the coupling constant will be. The smaller coupling constants and further down-field chemical shifts for the complex **32** may, therefore, suggest the stronger electron-withdrawal from the azacyclohexadienyl ring by Re than Mn.

The metal carbonyl carbon signals in the complex **32** appeared at 193.0 ppm which was further up-field than those in the Mn analogue at 221.5 ppm. The carbonyl carbons are more strongly shielded in the complex **32** than **27**.

3.2.1.2.2.4 X-Ray crystal Structure

X-ray crystal structure determination of the yellow plate crystal elucidated the structure of **32** (Figure 3-5). The table lists the selected bond lengths and angles for the complex **32** and also **27**[48].

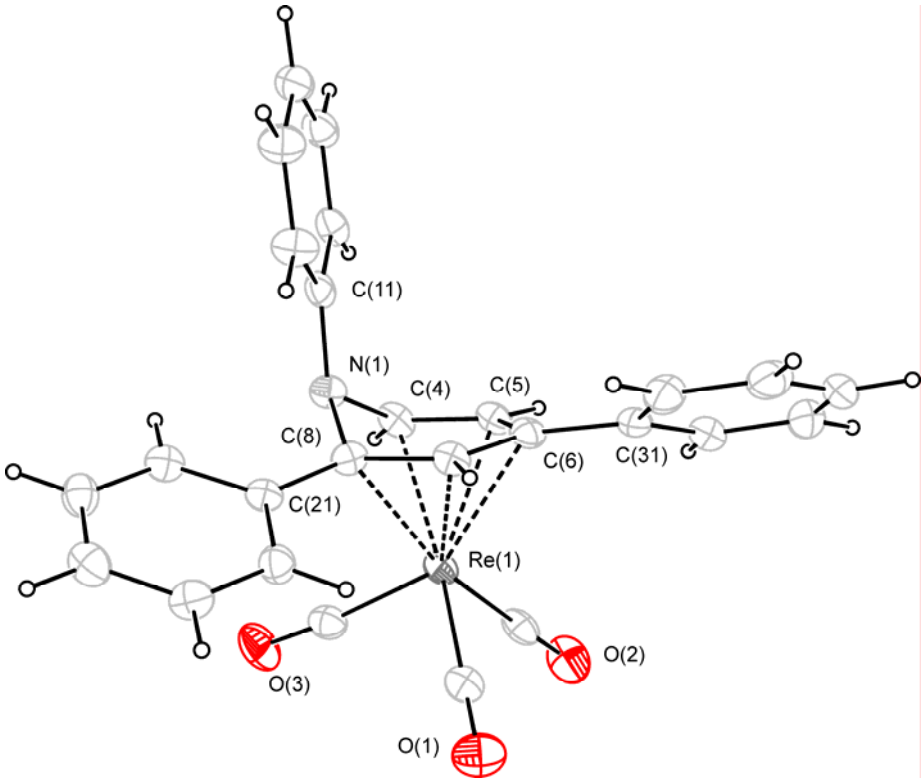

Figure 3-5: Crystal Structure of **32**

Table 3-3: Selected Bond Lengths for the Complexes **32** and **27**

	M-C(4)	**M-C(5)**	**M-C(6)**	**M-C(7)**	**M-C(8)**	**C(8)-N(1)**	**C(4)-N(1)**	**C(11)-N(1)**
27	2.142(3)	2.107(3)	2.160(3)	2.212(2)	2.202(2)	1.453(3)	1.429(3)	1.420(3)
32	2.298(3)	2.271(3)	2.329(3)	2.276(3)	2.344(3)	1.462(3)	1.450(4)	1.417(4)
	M-C(1)	**M-(2)**	**M-(3)**	**Av.**				
27	1.803(3)	1.793(3)	1.792(3)	1.796				
32	1.939(3)	1.919(4)	1.919(3)	1.926				

The complex **32** crystallises in a monoclinic system with space group *C*2/*c*. It is isomorphous with the Mn analogue[48]. The azacyclohexadienyl ring has the same geometry as in the Mn analogue. The C(4)-C(8) atoms are planar within ± 0.025 Å, forming a dihedral angle with the C(8)-N(1)-C(4) plane of 131.3º. In the Mn analogue, the ring carbons are planar within ± 0.024 Å, forming a dihedral angle with

the C(8)-N(1)-C(4) plane of 130.0º [48]. The distances between the rhenium and ring carbons range from 2.271(3) to 2.344(3) Å with an average of 2.304 Å. Those in the Mn analogue are from 2.107(2) to 2.202(3) with an average of 2.146 Å[48]. The difference in the average M-C bond distances of 0.158 Å is greater than that that in the average M-CO bond distances of 0.130 Å[48]. This may suggest that the coordination of the $Re(CO)_3$ group to the ring is weaker than the $Mn(CO)_3$ in the Mn analogue.

3.2.1.2.3 Mechanism

A route to the complex **32** was proposed by analogy to the Mn system[48]. The scheme below shows the proposed mechanism.

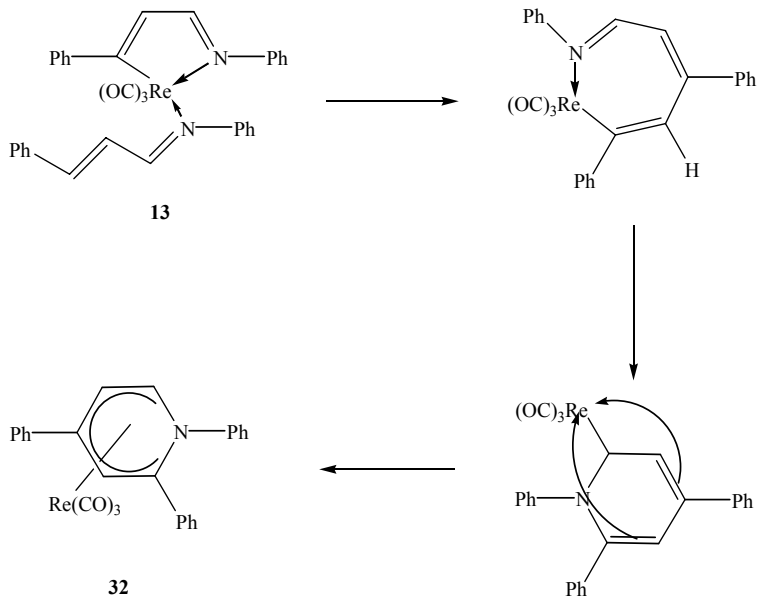

Scheme 3-5: Proposed Route to the Complex **32**

The first step of the reaction is the removal of the η^1-azabutadiene ligand, leaving a vacant coordination site on the rhenium. Phenyl acetylene inserts into the Re-C bond forming a seven-membered metallocycle followed by addition of the new Re-C bond across the N=C and rearrangements, leading to the azacyclohexadienyl ligand coordinating to the $Re(CO)_3$ group in a η^5 manner which achieves eighteen-electron configuration on the rhenium.

3.2.1.3 Reaction with *p*-Methoxyphenyl Isocyanide, $MeOC_6H_4N{\equiv}C$

3.2.1.3.1 Reaction

The scheme below summarises the reaction.

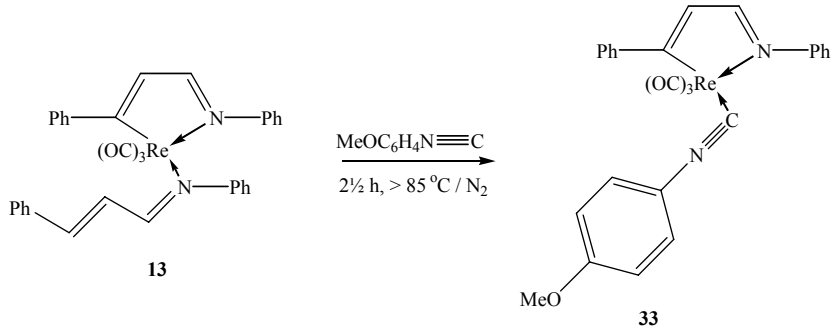

Scheme 3-6: Reaction of **13** with $MeOC_6H_4N{\equiv}C$

When the complex **13** and *p*-methoxyphenyl isocyanide (ca. 1 : 7) in distilled hexane were heated at 85 – 90 °C for 2½ hours, displacement reaction of the azabutadiene ligand by the isocyanide occurred and the derivative **33** could be obtained.

The reaction could be initiated between 40 – 85 °C, indicated by the development of a new band at 2010 cm^{-1} in the υ(C≡O) region of the IR spectrum in CH_2Cl_2/heptane. The reaction went to completion in an hour above 85 °C. The reaction mixture turned yellow and precipitation of the product as a red solid was observed during the course of the reaction. New bands were observed at 2010, 1943 and 1907 cm^{-1} in the υ(C≡O) region, indicating a new $Re(CO)_3$ complex. The reaction mixture was also heated above 100 °C with monitoring by IR spectroscopy to investigate if insertion of the isocyanide into the Re-C σ-bond which normally occur in the reactions of the cyclomanganated azabutadiene with the unsaturated reagents[48], would take place at a higher temperature. There was no sign of a C≡N inserted product, but only the displacement product **33** was indicated in the IR spectrum.

Attempts were made to prepare single crystals of **33**, but could not be achieved. Crystallisation from petroleum spirits at –20 °C, however, could provide a pure crystal of the complex **33** as a red block in a reasonable yield from the orange fraction collected at R_F 0.69 on chromatography.

3.2.1.3.2 Characterisation

3.2.1.3.2.1 IR

IR analysis was carried out in CH_2Cl_2. The tricarbonyl bands were observed at 2009 (s), 1939 (m), and 1904 (m) cm^{-1}.

3.2.1.3.2.2 ESI-MS

ESI-MS analysis was carried out at cone voltage of 20 V in MeOH with NaOMe. The parent molecule was observed at *m/z* 610, 632 and 640 as $[M + H]^+$, $[M + Na]^+$ and $[M + OMe]^-$, respectively, in the appropriate ion mode. The peaks suggested that the parent molecule had a mass of 609 which agreed with the combined mass of one cyclorheniated azabutadiene tricarbonyl rhenium complex and one *p*-methoxyl phenyl isocycanide. A structure of the complex **33** was, therefore, proposed (Figure 3-6).

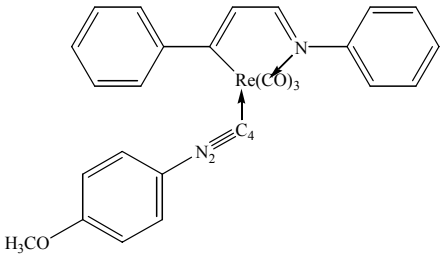

Figure 3-6: Proposed Structure of **33**

3.2.1.3.2.3 ^{1}H and ^{13}C NMR

NMR analyses were carried out on samples in $CDCl_3$ at 400 MHz. The NMR data support the proposed structure. Assignments were made in accordance with the 1D and 2D NMR data including ^{1}H and ^{13}C, DEPT, SELTOCSY, HSQC and HMBC

experiments. The table below summarises the assignments and the figure shows the selected SELTOCSY and HMBC correlations in the complex **33**.

Table 3-4: NMR Assignments for the Complex **33**

δ ppm		**33**	
^{1}H NMR		**^{13}C NMR**	
		C-1	225.15, C
H-2	7.20, 1 H	*C-2*	135.61, CH
H-3	8.27, d ($^{3}J_{HH}$ = 2.28 Hz), 1 H	*C-3*	176.29, CH
		C-4	???
		C-11	154.23??, C
H-12, 16	7.40?, q ($^{3}J_{HH}$ = 7.40 Hz), 2 H	*C-12, 16*	122.45?, 2 CH
H-13, 15	7.28?, d ($^{3}J_{HH}$ = 7.76 Hz), 2 H	*C-13, 15*	129.3??, 2 CH
H-14	~ 7.28?	*C-14*	126.64??, CH
		C-21	???
H-22, 26	7.50, d ($^{3}J_{HH}$ = 7.36 Hz), 2 H	*C-22, 26*	126.52, 2 CH
H-23, 25	7.40?, q ($^{3}J_{HH}$ = 7.40 Hz), 2 H	*C-23, 25*	128.09??, 2 CH
H-24	7.28?, d ($^{3}J_{HH}$ = 7.76 Hz), 2 H	*C-24*	127.46??, CH
		C-31	152.43??, C
H-32, 36	7.19, d ($^{3}J_{HH}$ = 8.64 Hz), 2 H	*C-32, 36*	127.93, 2 CH
H-33, 35	6.85, d ($^{3}J_{HH}$ = 8.80 Hz), 2 H	*C-33, 35*	114.77, 2 CH
		C-34	160.13, C
OCH_3	3.81, s, 3 H	*OCH_3*	55.71, CH_3
		Re-C≡O	195.77, 194.78, 190.62

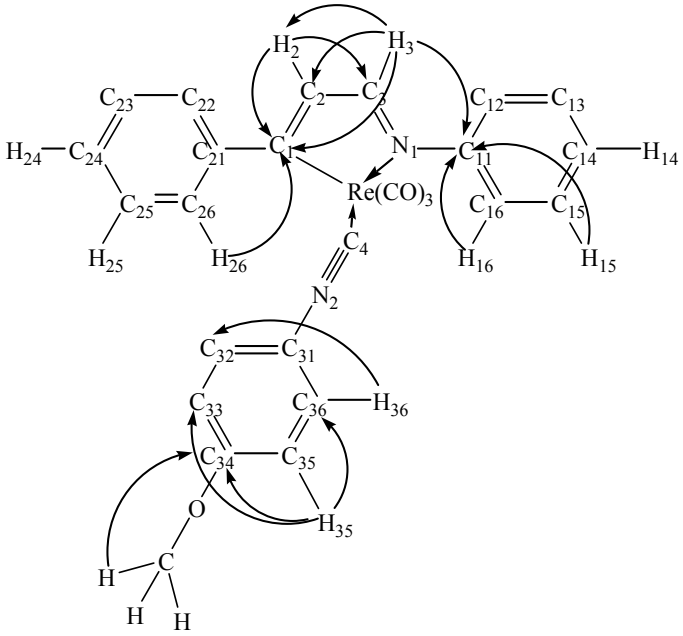

Figure 3-7: Selected ^{1}H-^{1}H Couplings and $^{2,3}J_{CH}$ Correlations in the Complex **33**

The *H-3* proton signal appeared at 8.27 ppm as a doublet with a coupling constant of 2.28 Hz. The shift and coupling constant were consistent with those in the related cyclorheniated azabutadienes e.g. **12** and **13**. The SELTOCSY experiment showed that the signal coupled with the proton signal at 7.20 ppm. The 7.20 ppm signal was, therefore, assigned as *H-2*. The coupling constant of the *H-2* proton signal could not be determined because it overlapped with the signal at 7.19 ppm. Their corresponding carbon was determined by HSQC experiment. The *H-3* and *2* protons showed a correlation with a carbon signal at 176.29 and 135.62 ppm, respectively, which were, therefore, assigned as *C-3* and *C-2*. The assignments were further confirmed by HMBC correlations. The $^{2}J_{CH}$ correlations between the *H-3* proton and *C-2* carbon, and the *H-2* proton and *C-3* carbon signals are observed (Figure 3-7). The DEPT experiment also confirmed that they were tertiary carbon signals.

The signal for the *C-1* carbon was determined by $^{3}J_{CH}$ correlations in the HMBC experiment. The *H-3*, *2* and *26* protons all showed a $^{3}J_{CH}$ correlation to the carbon signal at 225.2 ppm (Figure 3-7). The further down-field shift was also expected for a rheniated carbon as seen in the other cyclorheniated azabutadienes. The signal also arises from a quaternary carbon as confirmed by the DEPT experiment.

The *H-32, 36* and *33, 35* protons appeared at 7.19 and 6.85 ppm, respectively, as a doublet with an average coupling constant of 8.72 Hz. The $^{3}J_{HH}$ coupling of the protons was shown by the SELTOCOSY experiment. Both peaks also integrated as two protons. The coupling constant of about 8.7 Hz was also different from those for the *H-12 – 16* and *H-22 – 26* aromatic protons. These had a coupling constant of about 7.4 Hz. In the HSQC experiment, the 6.85 and 7.19 ppm signals showed $^{1}J_{CH}$ correlations to the carbon signals, which were also determined as tertiary carbons, at 114.77 and 127.93 ppm, respectively. The former was assigned as the *C-33*, *35* and the latter as the *C-32*, *36* according to substituent effects on an aromatic ring by a methoxyl or an isocyanide group at the respective positions. The *C-34* carbon was determined by HMBC correlations. The *H-35* and methoxyl protons showed a correlation to a carbon signal at 160.3 ppm, so the signal was assigned as the *C-34* carbon. The signal was also confirmed as a quaternary carbon by the DEPT experiment.

The *H-22* and *26* protons appeared at 7.50 ppm as a doublet with a coupling constant of 7.4 Hz. In the SELTOCSY experiment, the protons showed a strong coupling with the signal at 7.40 ppm and a weak one with one at 7.28 ppm. The former appeared as a quartet with a coupling constant of 7.4 Hz and the latter as a doublet with a $^{3}J_{HH}$ of 7.8 Hz. Both could be integrated as approximately four protons, indicating overlap with other proton signals. The HSQC experiment showed a $^{1}J_{CH}$ correlation to a carbon signal at 126.52 ppm, so was assigned as the *C-22, 26* carbons.

Both the 7.40 and 7.28 ppm signals also showed a correlation to the quaternary carbon signal at 154.23 ppm. This signal was also seen by the *H-3* proton, so could be the *C-11* carbon, leaving the 7.40 and 7.28 ppm protons as either *ortho*- or *meta*-protons. These assignments could, however, not be confirmed with further NMR data as the signals were overlapped. The signals of other aromatic protons and carbons were tentatively assigned, but could not be confirmed further with 2D NMR data because of overlap of the signals, especially in the aromatic region.

The *C-4*, *21* and *31* quaternary carbons were also difficult to assign because they were overlapped in the aromatic region or not on $^{2\text{-}3}J_{CH}$ HMBC distances.

The signals of the metal-carbonyl carbons appeared at 195.77, 194.78 and 190.62 ppm with the same intensity. They were confirmed as quaternary carbons by the DEPT experiment and showed no correlations in the HMBC experiment as expected.

NMR data supported the displacement product, but not the insertion one.

3.2.1.4 Reaction with Phenyl Isocyanate, PhNCO

3.2.1.4.1 Reaction

The scheme below summarises the reaction.

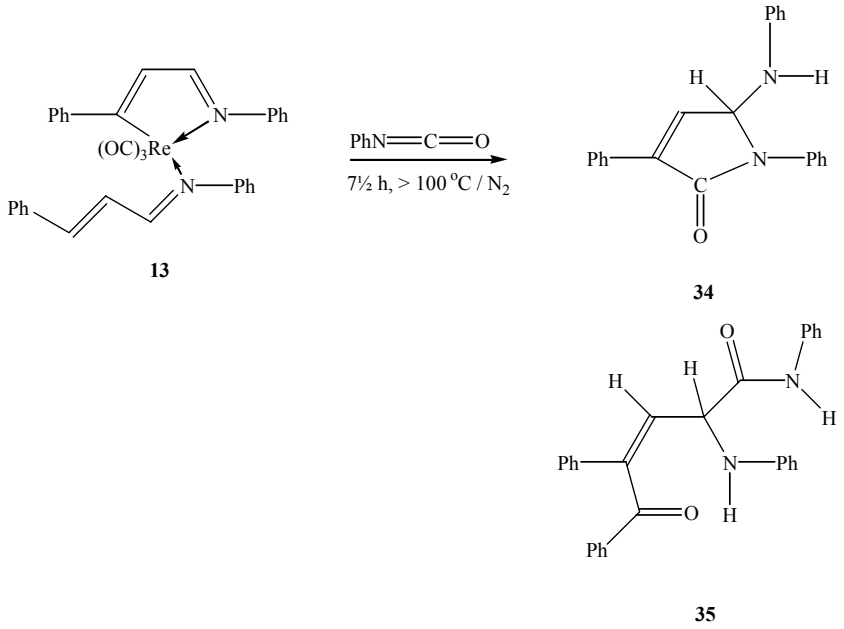

13 **34** **35**

Scheme 3-7: Reaction of **13** with PhNCO

When the complex **13** and phenyl isocyanate (ca. 1 : 2.5) in distilled heptane were heated at 100 – 110 ºC for 7½ hours, the compounds **34** and **35**, which were the analogues of the compounds **29** and **30** (Figure 3-8), respectively, in the corresponding Mn reaction[48], could be obtained.

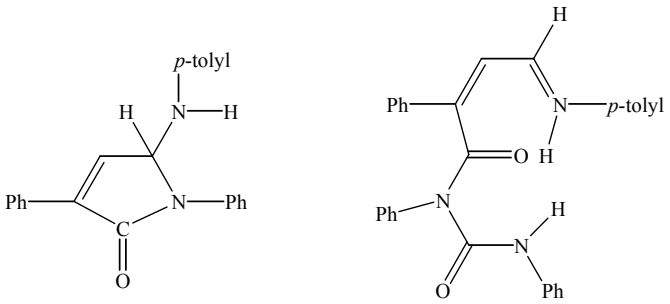

29 **30**

Figure 3-8: Proposed Products **29** and **30** in the Corresponding Mn Reaction[48]

The reaction could be initiated at 100 ºC, indicated by the development of a new peak at 2022 cm^{-1} in the υ(C≡O) region of the IR spectrum in CH_2Cl_2/heptane. The mixture turned yellow and precipitation of a yellow (major) and red (minor) solid with a small amount of a brown oil was observed. The absence of the original υ(C≡O) bands and new bands at 2022 (s) and 1900 (s) cm^{-1} indicated that all the complex **13** reacted with PhNCO. Crystallisation from CH_2Cl_2/petroleum spirits 40 – 60 ºC at –20 ºC gave a mixture of yellow and red solids with a brown oil from the crude product. Attempts were made to grow single crystals of the yellow and red solids by vapour diffusion from CH_2Cl_2/petroleum spirits (or *n*-pentane) at –20 ºC, but could not be achieved.

Purification of the products was difficult. Chromatography on a PLC plate showed a streak up to the solvent front, indicating decomposition of the products. Streaks were observed even with the much diluted samples. The different solvent combinations did not give any better separation either. The solvents attempted included CH_2Cl_2/petroleum spirits (1 : 1, 2 : 1) and ethyl acetate/petroleum spirits (1 : 1, 2 : 3, 1 : 2, 3 : 7, 1 : 3, 1 : 4) and all gave a streak. Although there was a still streak, the solvent combination of ethyl acetate/petroleum spirits (1 : 4) gave a slightly better separation than the others, so was attempted on a PLC plate.

The yellow band (3rd yellow) collected at R_F 0.71 showed IR, ESI-MS and NMR evidence for the compounds **34** and **35**. Attempts were made to prepare single crystals of the compounds **34** and **35** to carry out an XRD determination. Vapour diffusion from CH_2Cl_2 at –20 °C gave a clear yellow block from the 3rd yellow fraction, but the crystals were twinned and not suitable for XRD determination. Different solvents were also attempted including CH_2Cl_2/*n*-pentane, $CHCl_3$/hexane, benzene/petroleum

spirits and the vials were kept at room temperature, in the refrigerator and in the freezer, which were all not successful. Single crystals could not be prepared, so the compounds were characterised spectroscopically only.

3.2.1.4.2 Characterisation

3.2.1.4.2.1 IR

IR analysis was carried out on the 3rd yellow fraction in CH_2Cl_2. The table summarises the υ(C=O) and υ(C=N) frequencies for the 3rd yellow fraction and also the complexes **29** and **30**[48].

Table 3-5: υ(C=O) and υ(C=N) Frequencies for the **3rd Yellow Fraction** and the Compounds **29** and **30**[48].

CH_2Cl_2 / cm^{-1}	υ(C=O)	υ(C=N)
3rd Yellow	1715, m, br, 1712, s	1676
29	1715, br	
30	1718, 1703	1676

The compound **29** showed the υ(C=O) band at ~1715 (br) cm^{-1} and, for the compound **30**, the υ(C=O) and υ(C=N) bands were observed at 1718, 1703 and 1676 cm^{-1}, respectively[48]. New bands were observed at 1715 (m, br), 1712 (s) and 1676 cm^{-1} in the spectrum of the 3rd fraction. A υ(C=O) band for a cyclic ketone incorporated into a five-membered ring is expected at ~1750 cm^{-1} [60]. The frequency can be lowered by unsaturation at α, β positions and also incorporation of N atom into the ring[60]. The 1715 cm^{-1} band could, therefore, be assigned as the υ(C=O) band for the complex **34** and the 1712 and 1676 cm^{-1} bands might correspond to the υ(C=O) and υ(C=N) bands, respectively, for the compound **35**.

3.2.1.4.2.2 ESI-MS

ESI-MS analysis was carried out on the 3rd yellow fraction at cone voltage of 20 V in MeOH with NaOMe. For the compound **34**, the parent molecule was observed at *m/z* 327 and 349 as $[M_1 + H]^+$ and $[M_1 + Na]^+$ (M_1 = **34**), respectively, in the positive ion

mode and at *m/z* 325 and 357 as $[M_1 - H]^-$ and $[M_1 + OMe]^-$ in the negative ion mode. An additional peak of $[2M_1 + Na]^+$ was also observed at *m/z* 675. The corresponding peaks were also observed in the spectrum of the compound **29**.

For the compound **35**, the parent molecule was observed at m/z 447 as $[M_2 + H]^+$ (M_2 = **35**) in the positive ion mode. The accurate mass of 447.189 on HR-MS in MeOH was consistent with the mass of 447.194 calculated for the formula of $[(Ph_2C_3NH_3)(PhNCO)_2H + H]^+$.

A peak at *m/z* 235.090 on HR-MS suggested the presence of another product **34a**.

The observed mass of 235.090 in the positive ion mode closely agreed with a calculated mass of 235.099 for $[Ph_2C_4NOH_3]^+$. However, no sensible structure can be assigned to this.

3.2.1.4.2.3 ^{1}H and ^{13}C NMR

NMR experiments were carried on samples in $CDCl_3$ at 400 MHz. NMR analysis was carried out on the yellow solid recrystallised from the crude product from CH_2Cl_2/petroleum spirits at –20 ºC. The supernatant was removed by a syringe, the residue was dried under vacuum and then dissolved in $CDCl_3$. The spectra were dominated by the signals of the azabutadiene **16**, indicating that there was a significant amount of the ligand in the sample. There were, however, signals which were not consistent with those for the azabutadiene **16**, but appeared to be consistent with those for the compound **29**[48]. Since the purification of the sample was difficult, the signals for the azabutadiene **16** were subtracted in the spectrum by means of superimposition of the spectra of the sample and the azabutadiene **16** itself and only the residual peaks were used in the assignment. Assignments were made first by reference to that for **29**[48] and then further confirmed, where possible, by 1D and 2D NMR investigations including DEPT, SELTOCSY, HSQC and HMBC experiments. The *J* value of 160 Hz was used in the HSQC and HMBC experiments to optimise signals for sp^2 and sp aromatic and other unsaturated carbons.

The table below summarises the selected assignments for the compound **34** and **29**[48]. The figures show the selected ^{1}H-^{1}H couplings and $^{2,3}J_{CH}$ correlations in the SELTOCSY and HMBC experiments, respectively.

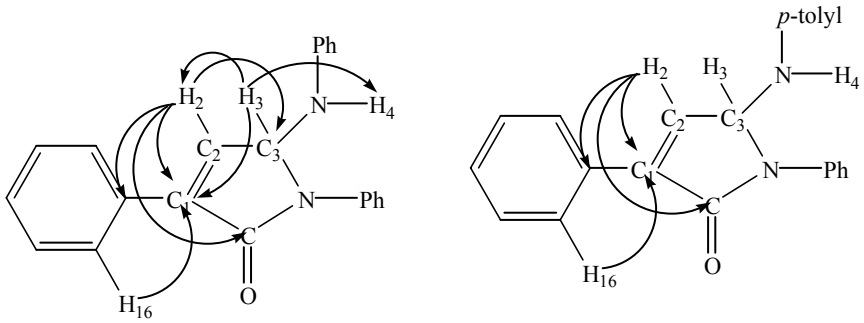

34 **29**

Figure 3-9: Selected ^{1}H-^{1}H Couplings and $^{2,3}J_{CH}$ Correlations in the Compounds **34** and **29**[48]

Table 3-6: Selected Assignments for the Compounds **34** and **29**[48].

δ ppm	*H-2*	*H-3*	*H-4*	*C-1*	*C-2*	*C-3*	*CO*
29[48]	7.30 ($^{3}J_{HH}$ = 2.0 Hz)	6.05 ($^{3}J_{HH}$ = 2.0 Hz)	3.90 , s	137.9	138.2	70.9	168.2
34	7.30, d ($^{3}J_{HH}$ = 2.6 Hz)	6.10, dd, ($^{3}J_{HH}$ = 1.72, 9.39 Hz), 1 H	3.98, d ($^{3}J_{HH}$ = 10.6 Hz), 1 H	138.1	137.8	70.1	168.0

The signals for the five-membered ring protons and carbons were selected as were indicative for the compound **34**. The signals for the *H-2*, *3* and *4* protons were observed at the expected shifts for the compound **34**. A slight difference in shift may arise from the different concentration of the samples used for the NMR determinations or substituent effects by the methyl group on the *p*-tolyl ring in the compound **29**[48].

The *H-3* proton appeared at 6.10 ppm as a doublet of a doublet. The signal showed a ^{1}H-^{1}H coupling with the proton signals at 7.30 and 3.98 ppm in the SELTOCSY experiment. The former had a coupling constant of about 2 Hz and the latter 10 Hz.

The coupling constant of 2 Hz of the 7.30 ppm signal was very close to that of the *H-2* proton signal in the compound **29**. The signals were, therefore, assigned as *H-2*, *3* and *4* and also each could integrate as one proton. Their corresponding carbons were identified by the HSQC experiment. The *H-2* and *H-3* proton signal showed a $^{1}J_{CH}$ correlations to the carbon signal at 137.8 and 70.1 ppm, which were, therefore, assigned as *C-2* and *C-3*, respectively. The chemical shifts also closely agreed with those in the compound **29**. No $^{1}J_{CH}$ correlation for the *H-4* proton signal was observed in the HSQC spectrum as expected. The *C-1* carbon was identified by the HMBC experiment. The $^{2}J_{CH}$ and $^{3}J_{CH}$ correlations to the *C-1* carbon are shown in the figures above. The *H-2* proton signal showed correlations to the carbon signals at 168.0, 138.1, 130.6 and 70.1 ppm. The *H-3* proton signal also showed correlations to the carbon signals at 138.1 and 144.7 ppm and the *H-16* proton signal to the carbon signals at 138.1 and 128.9 ppm. These correlations indicated that the signal at 138.1 ppm could be assigned as *C-1* and were consistent with the other assignments.

The chemical shifts of the signals for the aromatic protons and carbons were also consistent with those in the analogue **29**, except for those for the *p*-tolyl ring protons and carbons because of the electron-donating CH_3 group at the *para*-site of the ring. A full assignment is summarised in the table below. Since there were intense signals of the azabutadiene **16** in the spectrum, some aromatic proton and carbon signals could not be confirmed with the supporting 2D NMR evidence due to overlap of the signals.

Table 3-7: Full NMR Assignments for the Compounds **34** and **29**[48]

δ ppm	*H-2*	*H-3*	*H-4*	*H-12*	*H-13*	*H-14*	*H-32*
29[48]	7.30, d ($^3J_{HH}$ = 2.0 Hz)	6.05, d ($^3J_{HH}$ = 2.0 Hz)	3.90 , s	7.95, d ($^3J_{HH}$ = 6.3 Hz)	7.43, m	7.46, m	7.58, d ($^3J_{HH}$ = 7.6 Hz)
34	7.30, d ($^3J_{HH}$ = 2.6 Hz)	6.10, dd, ($^3J_{HH}$ = 1.72, 9.39 Hz), 1 H	3.98, d ($^3J_{HH}$ = 10.6 Hz), 1 H	7.92, dd ($^3J_{HH}$ = 6.52 Hz), 2 H	7.41, m	7.44, m	7.52, d
	H-33	*H-34*	*H-22*	*H-23*	*H-24*		
29[48]	7.39, m	7.22, t ($^3J_{HH}$ = 7.4 Hz)	6.67, d ($^3J_{HH}$ = 8.4 Hz)	7.01, d ($^3J_{HH}$ = 8.3 Hz)	-		
34	7.39, m	7.19, t ($^3J_{HH}$ = 7.3 Hz)	6.68, d ($^3J_{HH}$ = 7.8 Hz), 2 H	7.17, m	6.82, t ($^3J_{HH}$ = 7.30 Hz), 1 H		
	C-1	*C-2*	*C-3*	*C-11*	*C-12*	*C-13*	*C-14*
29[48]	137.9	138.2	70.9	131.0	127.9	128.9	129.5
34	138.1	137.8	70.1	130.6	127.6	128.9	129.5
	C-31	*C-32*	*C-33*	*C-34*	*C-21*	*C-22*	*C-23*
29[48]	136.8	123.4	129.4	125.8	129.7	115.9	130.3
34	136.6	123.2	129.3	125.7	144.7?	115.0	129.5?
	C-24	*CO*					
29[48]	142.5	168.2					
34	119.9	168.0					

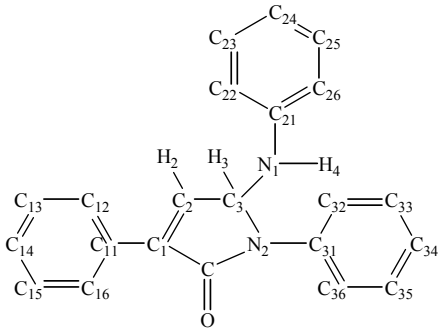

34

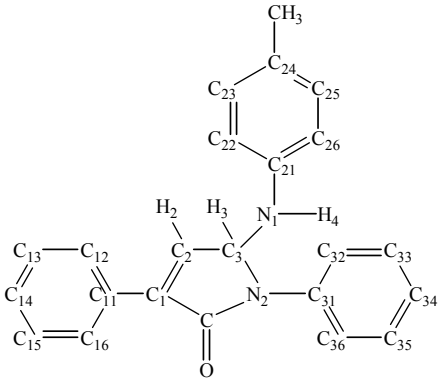

29

Figure 3-10: Compounds **34** and **29**

The figure below shows the HMBC correlations for the aniline ring protons and carbons. The *C-21* carbon appeared at 144.7 ppm. The signal was determined as a quaternary carbon by the DEPT experiment. The HMBC experiment showed correlations of the signal with those of the *H-3*, *25* and *26* protons as shown in the figure below. In the SELTOCSY experiment, the signals of *H-25* and *26* protons at 7.17 and 6.68 ppm, respectively, showed a coupling to a proton signal at 6.82 ppm, which was, therefore, assigned as *H-24*. The *H-24* and *26* proton signals could also be integrated as one and two protons, respectively. Their corresponding carbon signals were determined by the HSQC experiment. The *C-24*, *25* and *26* carbons appeared at 119.9, 129.5 and 115.0 ppm, respectively. The $^{1}J_{CH}$ correlation for the *H-25* proton in the HSQC spectrum could not be readily identified as the signal was overlapped in the aromatic region with those for the azabutadiene **16**. It could, however, be determined by $^{2\text{-}3}J_{CH}$ correlations in the HMBC experiment. The assignments were further confirmed by the HMBC experiment. The *H-24* proton showed $^{2\text{-}3}J_{CH}$ correlations to the *C-25* and *26* carbons. The *H-26* proton could be correlated with the *C-22* and *24* carbons. The *H-25* proton showed $^{2\text{-}3}J_{CH}$ correlations with the *C-24* and *26* carbons.

The *H-4* imine proton also showed a $^{3}J_{CH}$ correlation to the *C-26* carbon as illustrated below.

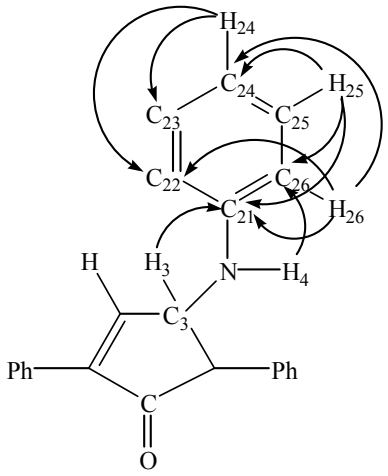

Figure 3-11: $^{2,3}J_{CH}$ Correlations in the Compound **34**

The figures below illustrate the proposed structure of the compounds **30**[48] and **35a** and the table shows the NMR data reported for the compound **30**[48].

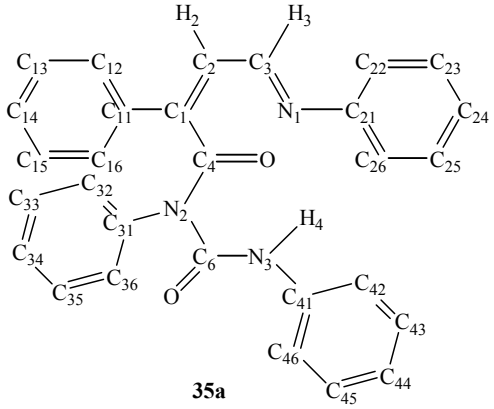

35a

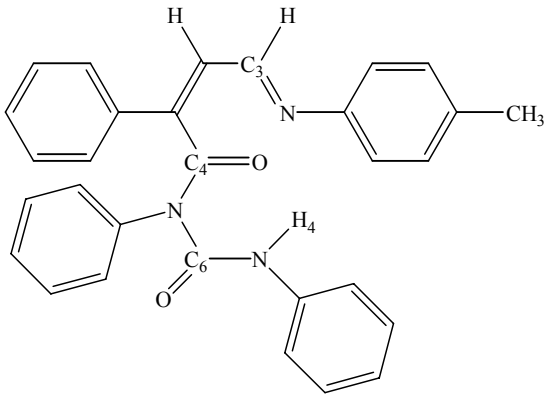

30

Figure 3-12: Proposed Structures of the Compounds **30** and **35a**

Table 3-8: Reported NMR Data for the Compound **30**[48].

δ ppm		**30**[48]	
^{1}H NMR		**^{13}C NMR**	
H-4	8.96	*C-3*	153.8
CH	6.07	*C-4*	154.6
Aryl-H	6.78 – 7.82	*C-6*	168.0
		CH	67.6
		Aryl-CH	120.2 – 140.4

Signals corresponding to the compounds **35a** and **30** were not observed in the present study.

NMR analysis was, therefore, carried out on the third yellow fraction. The experiment was carried out in $CDCl_3$ at 400 MHz. The experiments included ^{1}H, ^{13}C, DEPT, SELCOSY, HSQC and HMBC. The *J* values of 160 and 145 Hz were used in the DEPT, HSQC and HMBC experiments to optimise signals for aromatic and other sp^2 and sp, and oxygenated sp^3 carbons, respectively. There was no difference in the spectrum between the two *J* values.

There were still the intense azabutadiene **16** signals in the spectrum, but the signals for the compound **34** were not observed. There were new signals which were not observed in the previous NMR spectrum. Subtraction of the azabutadiene signals by superimposition of the spectra was, again, carried out and the residual signals were listed and assigned for the proposed structure **35a**. The signals were not, however, consistent with the structure. A new structure was, therefore, proposed. The figure below shows the proposed structure **35** and the table summarises a tentative assignment for the structure **35**.

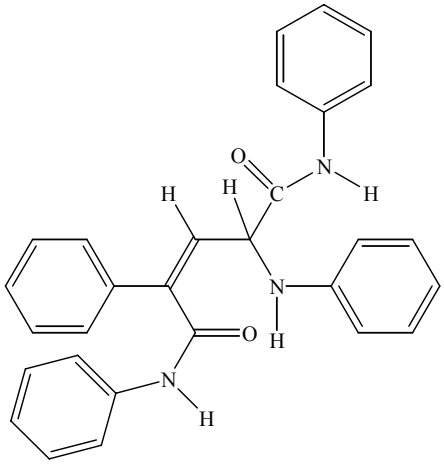

35

Figure 3-13: Proposed Structure **35**

Table 3-9: Tentative Assignments for the Structure **35**

δ ppm		**35**	
^{1}H NMR		**^{13}C NMR**	
		C-1	140.51
H-2	7.07	*C-2*	118.86
H-3	7.15?	*C-3*	129.68
		C-4	154.83?
		C-5	169.37?
		C-11	133.11
H-12, 16	7.96, m	*C-12, 16*	128.38
H-13, 15	7.43, m	*C-13, 15*	128.39
H-14		*C-14*	130.58
		C-21	148.21
H-22, 26	6.98	*C-22, 26*	121.93
H-23, 25	7.37	*C-23, 25*	
H-24	7.19	*C-24*	124.83
		C-31	
H-32, 36		*C-32, 36*	
H-33, 35		*C-33, 35*	
H-34		*C-34*	
		C-41	
H-42, 46		*C-42, 46*	
H-43, 45		*C-43, 45*	
H-44		*C-44*	

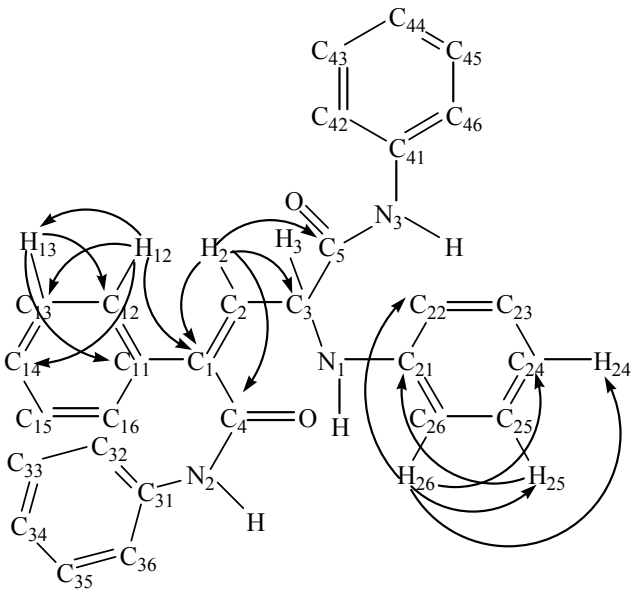

35

Figure 3-14: $^{2,3}J_{CH}$ Correlations in the Compound **35**

The proton signal at 7.07 ppm was assigned as *H-2*. The signal appeared as a singlet, suggesting that there were no adjacent protons. The SELTOCSY experiment, irradiating the 7.07 ppm signal, also supported that by showing no ^{1}H-^{1}H couplings of the signal. There was, however, a weak signal at 7.15 ppm that could a coupling, but also a noise. The SELTOCSY experiment, irradiating at the 7.15 ppm signal was not possible because the signal was overlapped in the aromatic region. The *C-2* carbon signal could be determined by HSQC experiment and appeared at 118.86 ppm. In the HMBC experiment, the *H-2* proton showed correlations to the carbon signals at 129.8 (CH), 140.6 (C), 154.9 (C) and 169.6 (C) ppm. The *H-12* proton signal showed a correlation to the 140.6 ppm signal, so was assigned as *C-1*. No correlations were observed for the other three signals, indicating that they were not within $^{2-3}J_{CH}$ distances of any proton. The 169.6 and 154.9 ppm quaternary carbon signals could be assigned for the carbonyl carbons of the isocyanate as they were consistent with the carbonyl signals observed for the compound **30**[48]. This leaves the 129.68 ppm tertiary carbon to be assigned as *C-3*. These assignments agree with the proposed structure **35**. The signal for the *H-3* proton could, however, not be identified by either the SELTOCSY experiment irradiating at the *H-2* proton, or the HSQC experiments searching for the tertiary proton for the 129.68 ppm carbon signal. Neither the signals nor correlations to the NH protons were observed, which might be due to rapid

exchange of NH protons with deuterium of the solvent, $CDCl_3$, so no signal could be expected. They could, therefore, not be used to determine the signals for the neighbouring protons and carbons, which might, otherwise, further support the assignments discussed earlier. No further NMR evidences to support the proposed structure **35** could be obtained.

The *H-12, 16* proton signals showed a ^{1}H-^{1}H coupling with a proton signal at 7.43 ppm in the SELTOCSY experiment. Both signals could integrate as two protons. The 7.43 ppm signal was, therefore, assigned as *H-13, 15*. The corresponding *C-12, 16* and *13, 15* carbons were determined in the HSQC experiment. The former appeared at 128.38 ppm and the latter at 128.39 ppm. In the HMBC experiment, the *H-12, 16* proton signals showed a correlation with the carbon signals at 128.39 and 130.58 ppm as in the figure. The DEPT experiment confirmed that they were both tertiary proton signals. The *H-13, 15* proton signals also showed a $^{2\text{-}3}J_{CH}$ correlation to the carbon signals at 130.58 and 133.11 ppm. The DEPT experiment indicated that the 133.11 ppm carbon signal arose from a quaternary carbon. The 130.58 ppm signal was, therefore, assigned as *C-12, 14* and the 133.11 ppm signal as *C-11*.

The doublet at 6.98 ppm showed a strong coupling with the proton signal at 7.37 and a weak one with the one at 7.19 ppm in the SELTOCSY experiment. The 6.98 ppm signal showed a $^{1}J_{CH}$ correlation to the carbon signal at 121.93 in the HSQC experiment. In the HMBC experiment, the proton signal showed a $^{2\text{-}3}J_{CH}$ correlation to the carbon signals at 121.93 and 124.83 ppm. The DEPT experiment indicated that both were tertiary carbons. The 7.37 ppm signal showed a $^{2\text{-}3}J_{CH}$ correlation to the carbon signal at 148.21 ppm in the HMBC experiment. The DEPT experiment indicated that the signal was a quaternary carbon signal. These suggest that the signals arise from an aromatic ring. A tentative assignment was made and is shown in the table above. Due to overlap of the signals, no further confirmation could be obtained.

3.2.1.4.3 Mechanism

A route to the compound **34** could be proposed by analogy to that to the compound **29**[48] in the corresponding Mn reaction. The diagram below illustrates the proposed mechanism.

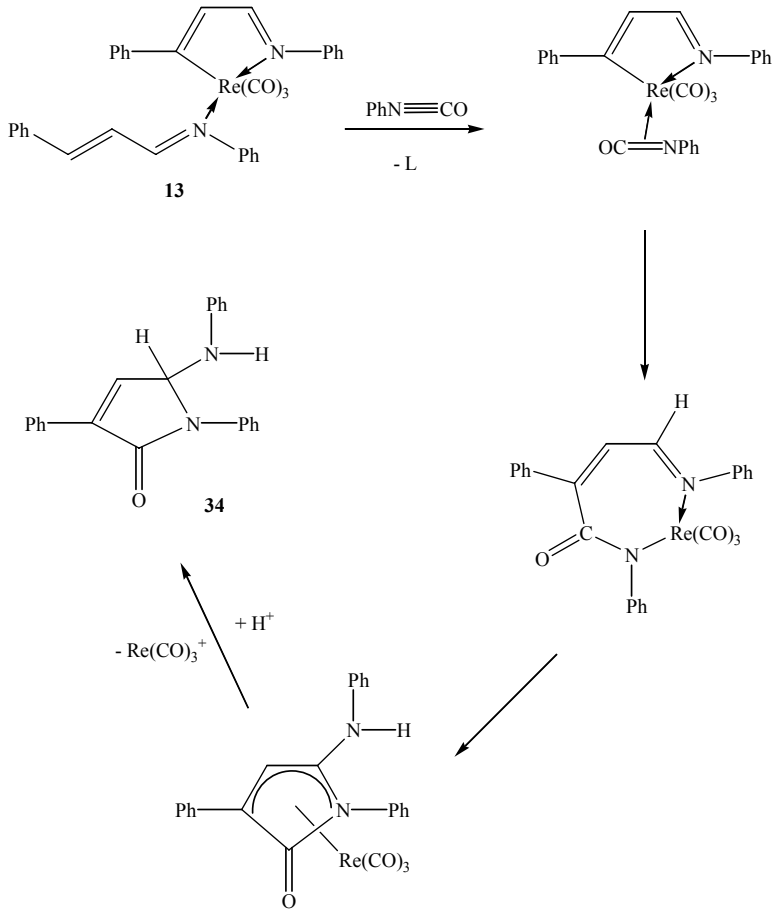

Scheme 3-8: Route to the Compound **34**

The azabutadiene ligand is first lost, leaving a vacant coordination site for reaction. Insertion of PhNCO into the Re-C bond places the bulky phenyl group adjacent to the rhenium metal due to steric pressure, giving the seven-membered ring intermediate. Nucleophilic attack by the amine nitrogen to the imine α-carbon forms the five-membered ring with the $Re(CO)_3$ attaching to one face of the pyrrolidonyl ring. Loss of the $Re(CO)_3^+$ and protonation during work-up gives the compound **34**.

The compound **35** may have formed via another insertion of PhNCO into the new Re-C bond added across the N=C bond after the seven-membered ring intermediate had formed instead of undergoing nucleophilic attack by the amine nitrogen to the imine α-carbon. Demetallation of the $Re(CO)_3$ and protonation during work-up gives the compound **35**.

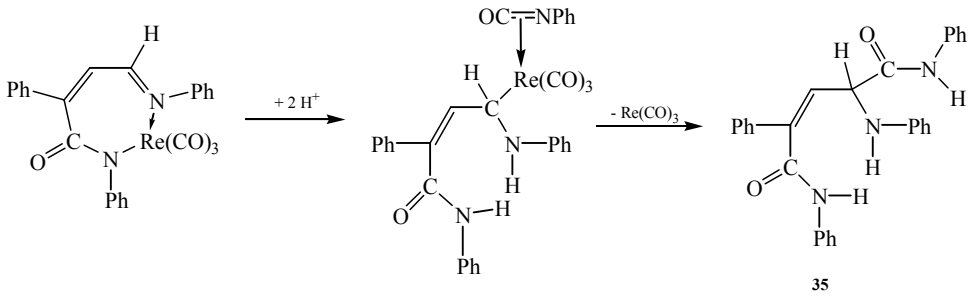

Scheme 3-9: Route to the Compound **35**

3.2.1.5 Reaction with Methyl Acrylate, CH_2=$CHCO_2Me$

3.2.1.5.1 Reaction

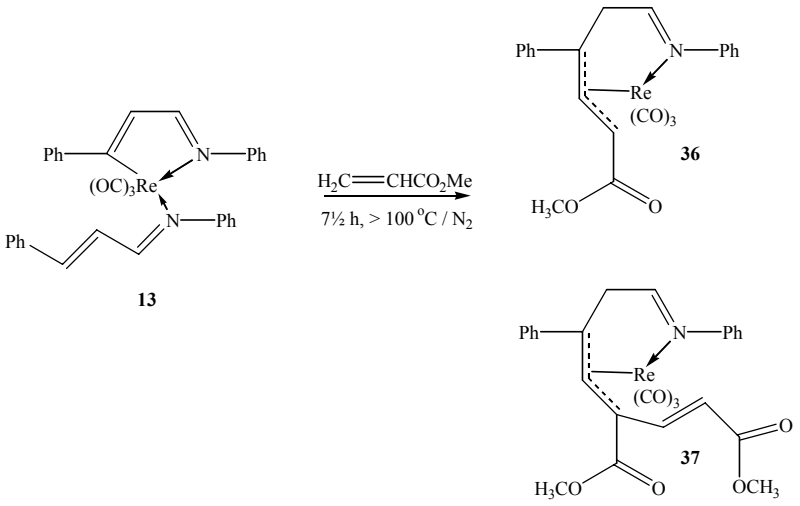

Scheme 3-10: Reaction of **13** with H_2C=$CHCO_2Me$

When the complex **13** and methyl acrylate (ca. 1 : 2.5) in distilled heptane were heated at 100 – 110 °C for 7½ hours, a mixture of the complexes **36** and **37** could be obtained.

The reaction was investigated with monitoring by IR spectroscopy in CH_2Cl_2/heptane. The reaction could be initiated at 100 °C, indicated by the development of a new peak at 2017 cm^{-1} in the υ(C≡O) region. The metal-carbonyl bands at 2003 (s), 1897 and 1891 (s, br) cm^{-1} corresponding to the complex **13** disappeared and new peaks at 2017

(s), 1897 (s, br) cm^{-1} and 1727 cm^{-1} were observed. The mixture turned very dark red and precipitation of a red and black solid was observed as the reaction continued.

The ESI-MS spectrum of the mixture indicated that it was a mixture of more than one product. The peaks observed were, however, all of minor intensity, and the main reaction product could not be identified. Some peaks showed a rhenium isotope pattern, suggesting a rhenium complex as a product. The peaks at *m/z* 208 and 230 corresponding to $[L + H]^+$ and $[L + Na]^+$ (L = **16**), respectively, were also observed in the positive ion mode with a great intensity, e.g. 100 %.

Purification of the mixture was difficult. Chromatography on a PLC plate only gave a streak regardless of the sample concentration and the solvent combinations and also no clear band was observed. Although a satisfactory separation could not be achieved, the residue after the solvent was removed was chromatographed on a PLC plate, eluting with CH_2Cl_2/petroleum spirits (3 : 2). The yellow and orange bands collected at R_F 0.92 and 0.78, respectively, showed evidence for the complexes **36** and **37**, respectively, in their IR and ESI-MS spectrum. Crystallisation of the yellow and orange fraction from CH_2Cl_2/*n*-pentane at –20 °C provided a very small amount of a yellow and red solid, respectively.

Since isolation of the products in a satisfactory yield by PLC was difficult, attempts were made to crystallise the products directly from the mixture after the solvent was removed under vacuum. The solvent combinations attempted included Et_2O/petroleum spirits 40 – 60 °C, $CHCl_3$, $CDCl_3$ or CH_2Cl_2/petroleum spirits 60 – 80 or 40 – 60 °C at –20 °C. Crystals could, however, not be prepared. Only brown oil with a minor amount of a red and black solid were obtained and were not suited for XRD determination either. It appeared that a mixture of CH_2Cl_2, $CHCl_3$ or $CDCl_3$ and petroleum spirits always gave a brown oil regardless of the solvent ratio and addition of an excess amount of petroleum spirit also caused a sudden precipitation of the brown oil and red solid. Crystallisation was, therefore, carried out only from petroleum spirits. The oil was first dissolved in CH_2Cl_2 or $CHCl_3$ and petroleum spirits (20 – 30 mL) was added. Dichloromethane was then evaporated away in a warm water bath at 45 °C and the mixture was concentrated to ~5 mL. It was then placed in the freezer to crystallise. A red solid and brown oil could be obtained. NMR

analysis was carried out on the red solid and suggested that it was the compound **37** as the main product.

Attempts were made to grow single crystal of the yellow and orange fraction and red solid for XRD determination, by vapour diffusion from CH_2Cl_2/*n*-pentane at –20 °C, but they could not be prepared. The compounds were, therefore, characterised spectroscopically only.

3.2.1.5.2 Characterisation

3.2.1.5.2.1 IR

IR analysis was carried out on the yellow and orange fraction in CH_2Cl_2. The table below shows the frequencies of the C≡O and C=O stretches for the yellow **36** and orange fraction **37** and the compound **26**[48]. The figure illustrates the proposed structures of **26**[48].

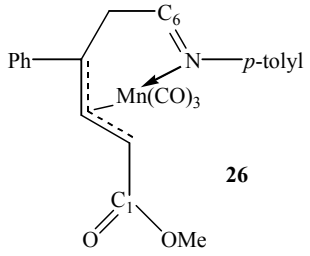

26

Figure 3-15: Structure of the Complex **26**[48]

Table 3-10: Frequencies for υ(C≡O) and υ(C=O) bands in the Complexes **36**, **37** and **26**[48]

CH_2Cl_2 / cm^{-1}	$M(CO)_3$	C=O
26[48]	2017, s, 1933, m, br	1734
36	2016, s, 1895, s, br	1724, m
37	2016, s, 1895, s, br	1724, m

The IR spectrum of the yellow and orange fraction showed the same bands. The υ(C≡O) bands were observed at 2016 (s) and 1895 (s) cm^{-1} with the latter containing the unresolved bands. The pattern was consistent with that in the complex **26**[48] and for a $LRe(CO)_3$ complex with symmetric L. The highest frequency υ(C≡O) band

appeared at the same frequency as in the complex **26**[48], but the lower bands were shifted by 38 cm^{-1} to a lower frequency in the Re complexes. The υ(C=O) band was also shifted by 10 cm^{-1} to a lower frequency in the Re complexes and observed at 1724 (w) cm^{-1}. The C=O stretch of methyl acrylate is expected at 1745 – 1750 cm^{-1} if the carbon is bonded to a saturated carbon and at 1720 cm^{-1} if bonded to an unsaturated carbon (Table 3-11). The υ(C=O) band at 1724 cm^{-1}, therefore, suggests that the C=O is more likely to be bonded to an unsaturated carbon.

Table 3-11: υ(C=O) Frequencies in Methyl Acrylate

υ(C=O) / cm^{-1}	
$-CH_2-C(O)OCH_3$	~1745 – 1750
$=CH-C(O)OCH_3$	~1720

The presence of the C=N bond was also indicated by the 1586 cm^{-1} band.

3.2.1.5.2.2 ESI-MS

ESI-MS analysis was carried out at cone voltage of 20 V in MeOH/NaOMe. The ESI-MS spectrum of the yellow fraction showed the parent molecule at *m/z* 562 as $[M_1 - H]^-$ (M_1 = **36**) (Figure 3-16) in the negative ion mode with the isotope pattern for one rhenium. An additional peak was also observed at *m/z* 291 in the negative ion mode which could be assigned as $[M_1 - Re(CO)_3 - H]^-$.

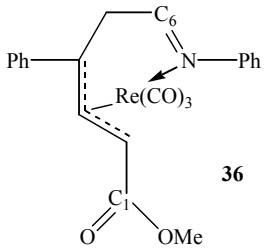

36

Figure 3-16: Complex **36**

The ESI-MS spectrum of the orange fraction showed a peak at *m/z* 677 in the negative ion mode with the isotope pattern for one rhenium. The mass of *m/z* 677 peak was consistent with the combined mass of an azabutadiene with a $Re(CO)_3$ group, two

methyl acrylate and a OMe to give an anion $[M_2 + OMe]^-$ (M_2 = **37**) . The figure below illustrates a possible structure of **37**.

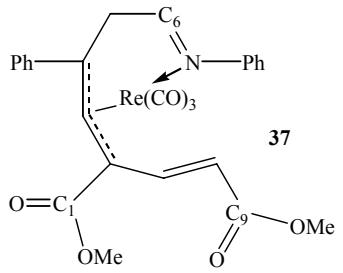

Figure 3-17: Possible Structure of **37**

There was also a peak at *m/z* 1027 in the negative ion mode which could be assigned as $[2M_3 + OMe]^-$ (M_3 = **36b**). Under strong basic condition, the compound **36b** may form via removal of a C_5 proton by OMe^- after loss of the $Re(CO)_3$ group, followed by substitution of an azabutadiene to the C_5 carbon (Scheme 3-11).

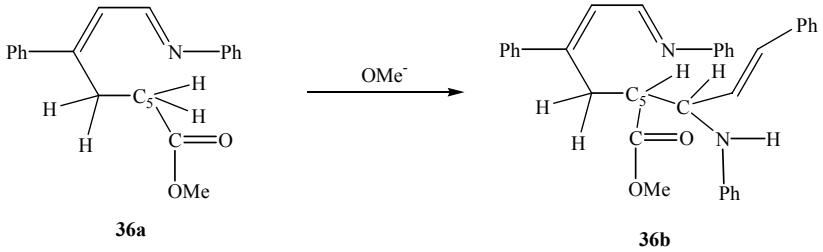

Scheme 3-11: Formation of the Compound **36b**

3.2.1.5.2.3 ^{1}H and ^{13}C NMR

NMR experiments were carried out on the residue after the solvent was removed under vacuum, in $CDCl_3$ at 400 MHz. The *J* value of 160 Hz was used to optimise signals for aromatic and other sp^2 and sp carbons. The spectra showed intense signals of the azabutadiene **16** as well as new signals of minor intensity. The intense signals of the azabutadiene **16** were, therefore, subtracted by means of superimposition of the spectra of the residue and the azabutadiene **16** itself. The structure of **36** and **37** was proposed by analogy to the complex **26**[48] in the corresponding Mn reaction with reference to the IR and ESI-MS data of the products suggesting the presence of N=C bond and that they were a combination of an azabutadiene, a $Re(CO)_3$ unit and either one or two methyl acrylate molecules. Assignments were made by reference to those

for the complex **26**[48] and further confirmed, where possible, by 1D and 2D NMR experiments including SELTOCSY, DEPT, HSQC and HMBC experiments. Detailed assignments, especially for aromatic protons and carbons were not made due to overlap of the signals. The figures below show the ^{1}H-^{1}H couplings in the SELCOSY experiments (d9 = 0.03 seconds) and $^{2,3}J_{CH}$ correlations in the HMBC experiment. The table below summarises the assignments for the sample and the complex **26**[48].

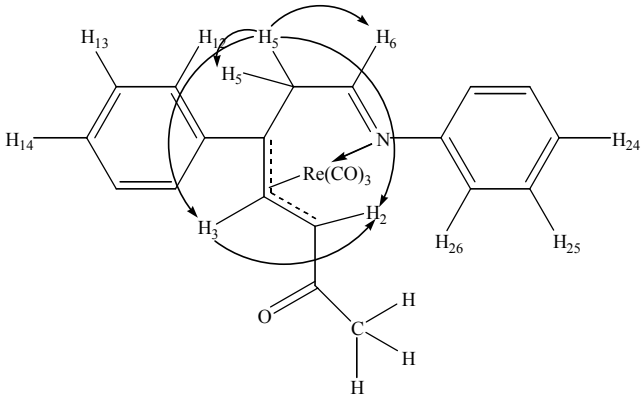

36

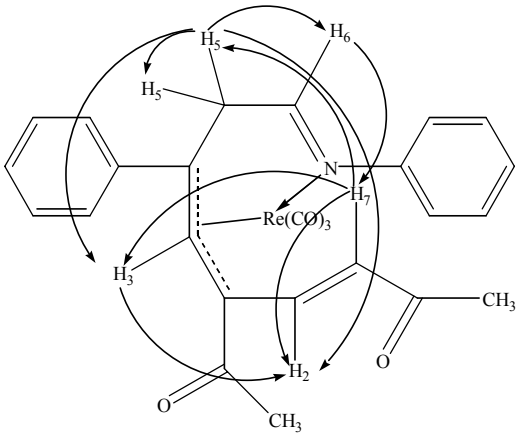

37

Figure 3-18: ^{1}H-^{1}H Couplings in the Complex **36** or **37**

Table 3-12: NMR Assignments for the Complexes **36** or **37** and **26**[48]

δ / ppm	**36** or **37**	**26**[48]		**36** or **37**	**26**[48]
^{1}H NMR			**^{13}C NMR**		
			C-1	171.78?, C?	174.7
H-2	4.01 (d, $^{3}J_{HH}$ = 7.6 Hz, 1 H)	2.23 (d, $^{3}J_{HH}$ = 11.8 Hz)	*C-2*	53.99	59.9
H-3	6.17 (d, $^{3}J_{HH}$ = 2.3 Hz, 1 H)	6.43 (d, $^{3}J_{HH}$ = 11.7 Hz)	*C-3*	121.57? (CH)	102.2
			C-4	144.57? (C)	90.5
H-5	2.89 (dd, $^{2,3}J_{HH}$ = 21.7, 7.44 Hz, 1 H) 3.14 (dd, $^{2,3}J_{HH}$ = 22.9, 7.24 Hz, 1 H)	3.33 (d, $^{2}J_{HH}$ = 22.3 Hz) 3.72 (d, $^{2}J_{HH}$ = 22.2 Hz)	*C-5*	39.84 (CH_2)	44.7
H-6	4.63 (m, br, 1 H)	7.53 (s)	*C-6*	55.42 (CH)	176.4
H-7	4.38 (d, $^{3}J_{HH}$ = 10 Hz, 1 H)		*C-7*	??	
			C-11	134.60? (C)	145.7
H-12, 16	6.73? (m)	7.66 (m)	*C-12, 16*	115.42 (2 CH)	126.5
H-13, 15	7.18? (m)	7.39 (m)	*C-13, 15*	128.39 (2 CH)	128.7
H-14	7.50? (d, $^{2}J_{HH}$ = 16? Hz, 1 H?)	7.23 (m)	*C-14*	119.01 (CH)	126.5
			C-21	133.7? (C)	150.6
H-22, 26	6.68 (d, $^{3}J_{HH}$ = 8.2 Hz, 2 H)	7.04 (d, $^{3}J_{HH}$ = 8.1 Hz)	*C-22, 26*	113.79 (2 CH)	120.7
H-23, 25	7.19? or 6.73? (m, 2 H)	7.22 (d, $^{3}J_{HH}$ = 8.1 Hz)	*C-23, 25*	128.3?	129.9
H-24	6.78 (m, 1 H)	-	*C-24*	117.97 (CH)	137.6
OCH_3	3.58 (s, 3 H)	3.83 (s)	*OCH_3*	51.84 (CH_3)	51.6
Re-CO				197.16 (C)	

The two *H-5* protons appeared at 2.89 ppm and 3.14 ppm as a doublet of doublet with a $^{2,3}J_{HH}$ coupling constant of 22 and 7 Hz, respectively. The signals were shifted by 0.44 – 0. 58 ppm to up-field from the corresponding signals in the complex **26**, but the $^{2}J_{HH}$ coupling constant of 22 Hz was consistent with that of the signals. The HSQC experiment showed that the corresponding carbon appeared at 39.84 ppm and the DEPT experiment also confirmed the signal was a secondary carbon signal. The 2.89 ppm signal showed ^{1}H-^{1}H couplings to the other *H-5* proton and the signals at 4.01, 6.17 and 4.63 ppm in the SELTOCSY experiment. The 4.01, 6.17 and 4.63 ppm signal showed a $^{1}J_{CH}$ correlation to the carbon signal at 53.99, 121.57 and 55.42 ppm, respectively, in the HSQC experiment and were all confirmed as tertiary carbon signals by the DEPT experiment. The $^{2-3}J_{CH}$ correlations in the HMBC experiment suggested that the 4.01, 6.17 and 4.63 ppm proton signals could be assigned as *H-2, 3* and *6* and the corresponding carbons as *C-2, 3* and *6*, respectively. The $^{2-3}J_{CH}$ correlations also suggested that the signal at 144.57 ppm could be assigned as *C-4*. The signals could, however, not distinguish between the complexes **36** and **37** as the sample was the mixture and the observed correlations were also consistent in both structures as shown in the figures above. The signals might also arise from both complexes as the complexes were of a very similar structure so that the signals might appear at the same chemical shifts.

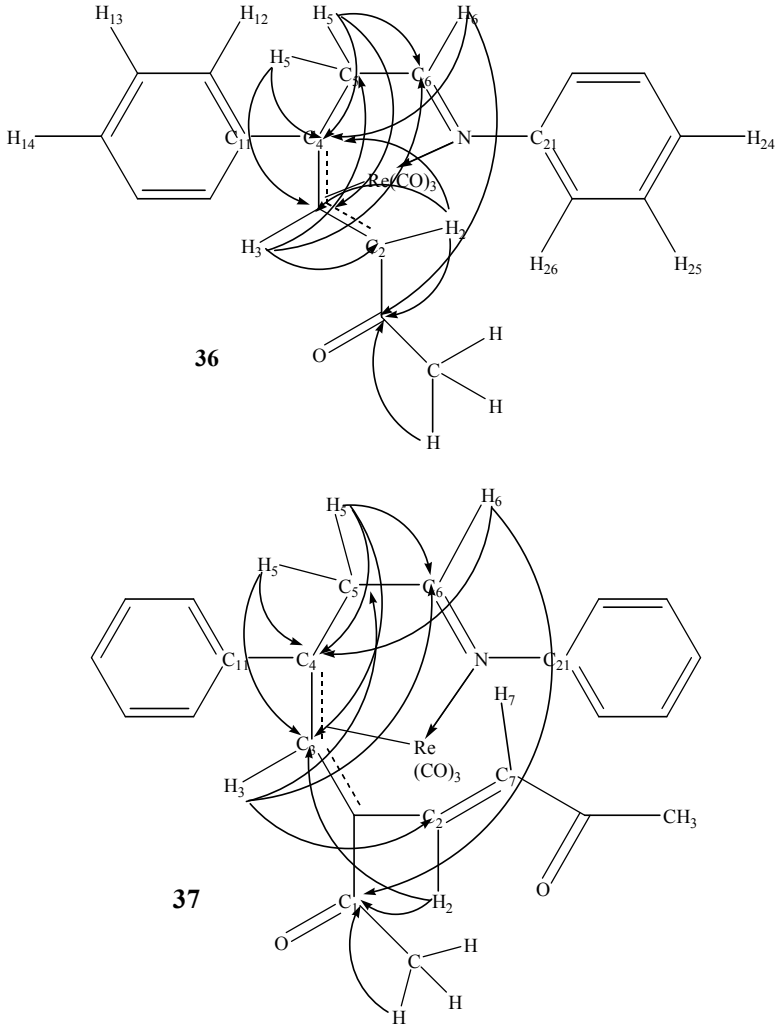

Figure 3-19: $^{2,3}J_{CH}$ Correlations in the Complex **36** or **37**

The *C-2* and *5* carbon signals were shifted by 5 – 6 ppm to up-field and the *C-3* carbon signal by 19 ppm to down-field from the corresponding signals in the Mn analogue **26**. The shifts may be accounted by the different metal carbonyl groups coordinating to the disubstituted methyl azaheptadienyloate ligand. The *C-4* and *6* carbon signals were quite different. The *C-4* carbon signal at 144.57 ppm was shifted by 54 ppm to further down-field from the corresponding signal at 90.5 ppm in the Mn analogue **26**[48]. The *C-4* quaternary carbon signal showed $^{2,3}J_{CH}$ correlations with the two *H-5, 6* and *2* proton signals in the HMBC experiment. The correlations suggest that the signal is likely to be for the *C-4* position. The *C-6* carbon signal at 55.42 ppm was, on the other hand, shifted by 121 ppm to further up-field from the corresponding signal at 176.4 ppm in the Mn analogue **26**. The carbon signal was confirmed as a tertiary carbon signal by DEPT experiment. The HSQC experiment showed a clear $^{1}J_{CH}$ correlation with the 4.63 ppm proton signal which could be assigned for the *H-6*

proton. In the HMBC experiment, the *C-6* carbon signal showed a $^{2}J_{CH}$ correlation with the *H-5* proton signal at 2.89 ppm. The 55.42 ppm carbon signal can, therefore, be the *C-6* carbon. No further $^{2,3}J_{CH}$ correlations or NMR evidences to confirm the assignments could, however, be obtained.

The *H-6* proton signal showed a ^{1}H-^{1}H coupling with the proton signal at 4.38 ppm in the SELTOCSY experiment. The proton signal appeared as a doublet with a coupling constant of 10 Hz, which could be expected for a *Jcis* coupling for an alkene, in the ^{1}H NMR spectrum. Since there was no proton to assign in the complex **36**, the proton could be the *H-7* proton in the complex **37**. It, however, showed no $^{1}J_{CH}$ and $^{2,3}J_{CH}$ correlation to any proton signal either in the HSQC or HMBC experiment. No further confirmation could, therefore, be obtained.

The figure below shows the ^{1}H-^{1}H couplings and $^{2\text{-}3}J_{CH}$ correlations for aromatic protons and carbons. Because of the intense azabutadiene signals and overlap of the signals, some assignments could not be confirmed with further correlations.

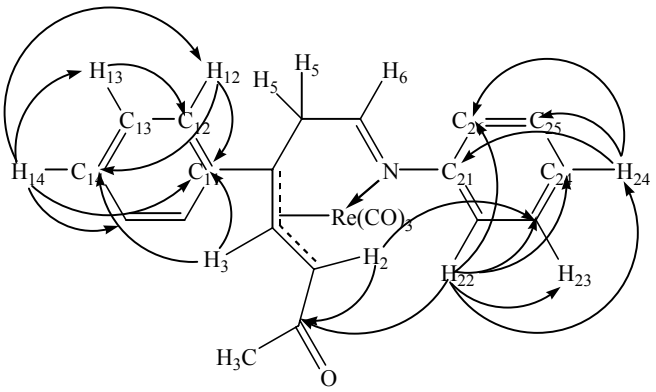

Figure 3-20: ^{1}H-^{1}H Couplings and $^{2\text{-}3}J_{CH}$ Correlations for Aromatic Protons and Carbons

The *H-3* proton signal showed a correlation to the quaternary carbon signal at 134.60 and the tertiary carbon signal 119.01 ppm in the HMBC experiment. The 119.01 ppm signal showed a $^{1}J_{CH}$ correlation to the proton signal at ~7.50 ppm in the HSQC experiment. The 7.50 ppm proton signal showed ^{1}H-^{1}H couplings with the proton signals at ~6.73 and 7.18 ppm in the SELTOCSY experiment. Their corresponding carbon appeared at 115.42 and 128.39 ppm, respectively, in the HSQC experiment. The $^{2,3}J_{CH}$ correlations between the proton and carbon signals (Figure 3-20) in the

HMBC experiment suggested that the 6.73, 7.18 and 7.50 ppm proton signals could be assigned as *H-12, 16*, *H-13, 15* and *H-14*, respectively, the corresponding carbons as *C-12, 16*, *C-13, 15* and *C-14* and the 134.60 ppm quaternary carbon signal as *C-11*.

The *H-2* proton signal showed a correlation to the tertiary carbon signal at 128.3 ppm in the HMBC experiment. The proton signal at 6.68 ppm showed ^{1}H-^{1}H couplings with the proton signals at 7.19(6.73?) and 6.78 ppm. The 6.68 ppm signal also showed a correlation to the *C-1* carbon signal in the HMBC experiment. The 6.68, 7.19(6.73?) and 6.78 ppm signals could integrate as 2 : 2 : 1 and were, therefore, assigned as *H-22, 26, H- 23, 25* and *H-24*, respectively. The *C-22, 26* and *C-24* carbon signals could be determined by the HSQC experiment. The *H-22, 26* and *H-24* proton signal showed a $^{1}J_{CH}$ correlation to the tertiary carbon signal at 113.79 and 117.97 ppm, which were, therefore, assigned as *C-22, 26* and *C-24*, respectively. The *H-22, 26* and *H-24* proton signals showed a $^{2}J_{CH}$ and $^{3}J_{CH}$ correlation, respectively, to the tertiary carbon signal at 128.3 ppm and the signal was, therefore, assigned as *C-23, 25*. The *H-24* proton signal also showed a correlation to the quaternary carbon signal at 133.7 ppm in the HMBC experiment. This could be the *C-21* carbon signal, but not be confirmed with further correlations.

3.3 Conclusion

The reaction of the complex **13** with the selected unsaturated reagents gave the Re analogues of the products in the corresponding Mn reactions with some new others which may be formed via further reaction with the unsaturated molecules. Reaction with CO gave no new product as was found in the Mn reaction[48]. Reaction with phenyl acetylene, phenyl isocyanate and methyl acrylate gave the Re analogues of the compounds **27**, **29** and **26,** respectively, in the corresponding Mn reactions. The other products in the reaction with phenyl isocyanate and methyl acrylate which also appeared to be the main product were characterised spectroscopically only as no pure product could be isolated. A new structure of the compound **35** was proposed based on the NMR analyses, which may be formed via insertion of PhNCO into the Re-C_3 bond instead of the N-H bond of the PhNCO which gave the compound **30**. Further characterisation, is, however, needed to confirm the structure. The compound **37** was also tentatively assigned for the product from the reaction with methyl acrylate according to the spectroscopic data including IR, ESI-MS and NMR experiments and also appeared to be the main product of the reaction rather than the compound **36**. The compounds **36** and **37**, were however, very similar in structure, so the spectroscopic data could not be assigned for either of the products with further evidences. Further characterisation may, therefore, be needed to confirm the products. With *p*-methoxyphenyl isocyanide, simple displacement of the ligand with the isocyanide occurred, but there was no sign of the insertion product as seen in the other reactions.

Purification of the products from the present reactions, except for the one from the isocyanide reaction, was difficult by PLC or fractional crystallisation. It appeared that the reactions all proceeded in the same manner and gave the analogous or similar products as in the corresponding Mn reactions, but the products in the present studies could not easily be purified because of the excess amount of the azabutadiene **16** dissociating from the starting material **13** during the course of the reactions, interfering with isolation and crystallisation of the products. The products may be isolated in a pure crystal form if the cyclorheniated azabutadiene tetracarbonyl complex **12** or the analogues were used as the starting material.

However, since the products of the Mn and Re reactions with unsaturated molecules seem to give the same products (despite their different behaviour in the initial cyclometallation reactions), the one of the Re substrates offers no advantages.

3.4 Experimental

3.4.1 Reaction of Cyclorheniated Azabutadiene with CO (g) and Unsaturated Reagents

3.4.1.1 Reaction with CO (g)

Experimental: In a nitrogen-flushed Schlenk flask, a small amount of the complex **13** in CH_2Cl_2 was bubbled with CO (g). Under a CO atmosphere, the reaction mixture was gently stirred at room temperature for 24 hours. The IR spectrum indicated that no reaction had occurred, showing the υ(C≡O) bands seen at the start of the reaction. The reaction was, therefore, discontinued.

3.4.1.2 Reaction with Phenyl Acetylene, PhC≡CH

Experimental: The progress of the reaction was monitored by IR spectroscopy in heptane/CH_2Cl_2.

In a nitrogen-flushed Schlenk flask, PhC≡CH (0.11 mL, 1.00 mmol) was added to a solution of the complex **13** (0.21 g, 0.31 mmol) in distilled heptane (15 mL). With continuous gentle stirring, the clear red reaction mixture was heated in an oil bath at 95 – 100 °C for 2 hours 40 minutes. The mixture turned yellow and precipitation of a red solid and brown oil were observed. The development of new peaks at 2026 (s), 1950 (m) and 1935 (m) cm^{-1} in the υ(C≡O) region of the IR spectrum was observed. The mixture was cooled to room temperature with stirring. The solvent was removed and the residue was dried for 3 hours under vacuum. The residue was chromatographed on a PLC plate, eluting with CH_2Cl_2/petroleum spirits (2 : 3). A weak yellow and strong yellow and orange bands at R_F 0.77, 0.66, and 0.51, respectively, were collected individually in a sintered glass funnel, extracted with CH_2Cl_2, the solvent was removed and the residue was dried under vacuum for 30 minutes. Crystallisation from CH_2Cl_2/petroleum spirits at –20 °C provided the

complex **12** as a yellow plate from the weak yellow band, which was carried on from the preparation of the complex **13** and the unreacted complex **13** as red needles from the strong orange band (10 mg, 5%). The crystals were characterised spectroscopically by IR and ESI-MS. Crystallisation from CH_2Cl_2/petroleum spirits at –20 °C gave the complex **32** as a yellow plate (31.5 mg, 18 %) from the strong yellow band. Single crystals of the complex **32** were grown by vapour diffusion from CH_2Cl_2 or CH_2Cl_2/petroleum spirits at –20 °C.

Chromatography, eluting with CH_2Cl_2/petroleum spirits (7 : 5) could give a better separation. The complex **32** was obtained as a yellow solid (29.1 mg, 49 %) from the yellow fraction at R_F 0.91.

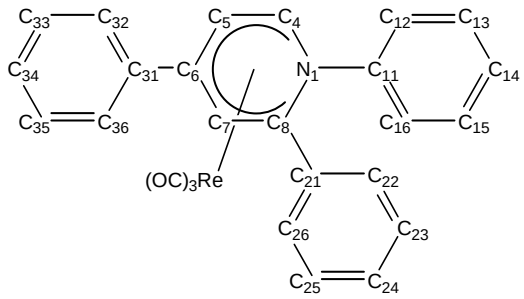

32

Description: Yellow plates

Formula*:* $C_{26}H_{18}N_1O_3Re$

Mr: 578.63

IR: (CH_2Cl_2) υ (C≡O) 2026 (s), 1949 (m), 1935 (m) cm^{-1}

ESI-MS:

(MeOH/NaOMe, cone 20 V, +ve ion) *m/z* 601 (4 %, $[M + Na]^+$), 308 (100 %, $[M – Re(CO)_3]^+$)

(-ve ion) *m/z* 610 (100 %, $[M + OMe]^-$), 578 (15 %, $[M – H]^-$)

HR-MS: (MeOH, +ve ion) *m/z* 308.144 $[M – Re(CO)_3]^+$ (calcd. *m/z* 308.1434 for $C_{23}H_{18}N_1$)

^{1}H NMR: (400 MHz, $CDCl_3$) δ 7.51 (t, $^3J_{HH}$ = 9.34 Hz, 4 H), 7.35 (m, 6 H), 7.24 (dd, $^{3,4}J_{HH}$ = 9.76, 2.48 Hz, 2 H), 7.12 (t, $^3J_{HH}$ = 7.90 Hz, 2 H), 6.85 (t, $^3J_{HH}$ = 7.30 Hz, 1 H), 6.70 (d, $^3J_{HH}$ = 8.36 Hz, 2 H),

		6.63 (s, 1 H), 5.83 (d, $^3J_{HH}$ = 4.04 Hz, 1 H), 5.26 (d, $^3J_{HH}$ = 4.08 Hz, 1 H) ppm
^{13}C NMR:	(400 MHz, $CDCl_3$)	δ 193.04, 157.85, 138.00, 135.81, 129.11, 129.03, 128.56, 128.27, 127.56, 127.44, 123.05, 121.13, 115.01, 101.03, 93.92, 90.68, 79.78, 57.23 ppm

3.4.1.3 Reaction with *p*-Methoxyphenyl Isocyanide, $MeOC_6H_4N{\equiv}C$

Experimental: The progress of the reaction was monitored by IR spectroscopy in hexane/CH_2Cl_2.

In a nitrogen-flushed Schlenk flask, $MeOC_6H_4N{\equiv}C$ (0.19 g, 1.43 mmol) was added to a solution of the complex **13** (0.15 g, 0.22 mmol) in distilled hexane (15 mL). With continuous stirring, the clear red reaction mixture was heated in an oil bath at 85 – 90 °C for 2½ hours. The mixture turned yellow and precipitation of a brown solid was observed during the course of the reaction. The development of new peaks at 2009 (s), 1941 (m), 1906 (m) cm^{-1} was observed in the υ(C≡O) region of the spectrum. The mixture was cooled to room temperature with stirring and then placed at –20 °C to crystallise. A mixture of a yellow and red solid and a brown oil was obtained after 24 hours. The solvent was removed and the residue was dried for 2 hours under vacuum. The residue was then chromatographed on a PLC plate, eluting with CH_2Cl_2/petroleum spirits (1 : 1). A strong yellow and orange band at R_F 0.92 and 0.69, respectively, were collected individually in a sintered glass funnel and extracted with CH_2Cl_2, the solvent was removed and the residue was dried under vacuum for 1 hour. Crystallisation from CH_2Cl_2/petroleum spirits at –20 ºC afforded the complex **12** carried on from the preparation of the complex **13** as a yellow plate from the strong yellow and the complex **33** as a red twinned crystal from the strong orange bands.

The reaction was repeated at 100 – 105 °C to see if insertion of the N≡C into the Re-C bond would occur at a higher temperature. In a nitrogen-flushed Schlenk flask, a mixture of the complex **13** (0.19 g, 0.28 mmol) and $MeOC_6H_4CN$ (0.19 g, 1.43 mmol)

in distilled heptane (15 ml) was heated at 100 - 105 °C for 5 hours. After the solvent was removed under vacuum, the residue was chromatographed on a PLC plate, eluting with CH_2Cl_2/petroleum spirits (1 : 1). The major orange band was collected and extracted with CH_2Cl_2, the solvent was removed under vacuum and a red oil **33** (0.136 g, 80 %) was obtained. Crystallisation from petroleum spirits in the refrigerator provided a pure crystal of the complex **33** as a red block. Attempts were made to grow a single crystal of **33** by vapour diffusion, but were not successful. The solvents attempted included CH_2Cl_2/petroleum spirits, $CHCl_3$/petroleum spirits, $CDCl_3$/hexane, Et_2O/petroleum spirits and CH_2Cl_2/*n*-pentane and crystallisation both in the refrigerator and in the freezer was attempted.

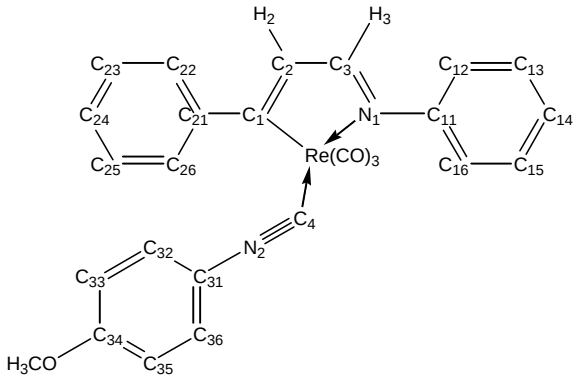

33

Description: Red blocks

Formula*:* $C_{26}H_{19}N_2O_4Re$

Mr: 609.65

IR: (CH_2Cl_2) υ (C≡O) 2009 (s), 1939 (m), 1904 (m) cm^{-1}

ESI-MS:

(MeOH/NaOMe, cone 20 V, +ve ion) *m/z* 632 (100 %, $[M + Na]^+$), 610 (10 %, $[M + H]^+$)

(-ve ion) *m/z* 640 (100 %, $[M + OMe]^-$)

^{1}H NMR: (300 MHz, $CDCl_3$) δ 8.29 (d, $^3J_{HH}$ = 2.28 Hz, 1 H), 7.52 (dd, $^{3,4}J_{HH}$ = 7.02, 1.38 Hz, 2 H), 7.43 (m, 5 H), 7.29 (m, 4 H), 7.22 (dd, $^{3,4}J_{HH}$ = 9.18, 2.16 Hz, 2 H), 6.88 (dd, $^{3,4}J_{HH}$ = 9.0, 2.1 Hz, 2 H), 3.84 (s, 3 H) ppm

^{13}C NMR: (300 MHz, $CDCl_3$) δ 225.37, 195.73, 194.76, 190.65, 176.30, 174.58, 160.21, 154.31, 152.51, 150.44,

135.59, 129.15, 128.10, 127.94, 127.46,
126.65, 126.51, 122.47, 114.84, 55.72 ppm

3.4.1.4 Reaction with Phenyl Isocyanate, PhNCO

Experimental: The progress of the reaction was monitored by IR spectroscopy in CH_2Cl_2/heptane.

In a nitrogen-flushed Schlenk flask, PhNCO (0.03 mL, 0.28 mmol) was added to a solution of the complex **13** (152 mg, 0.22 mmol) in distilled heptane (20 mL). With continuous stirring, the clear red reaction mixture was heated in an oil bath at 100 – 110 ºC for 7½ hours. The development of new peaks at 2022 (s) and 1902 (s, br) cm^{-1} was observed in the υ(C≡O) region of the IR spectrum. After 4 hours above 100 ºC, extra PhNCO (approximately 0.03 mL) was added as no further reaction progress was observed in the IR spectrum. Heating was continued for another 3 hours. The mixture turned yellow and precipitation of a mixture of a yellow (major) and red solid (minor) and brown oil (minor) was observed during the course of the reaction. The mixture was cooled to room temperature with stirring. The solvent was removed and the residue was dried under vacuum for 11 hours. The residue was chromatographed on a PLC plate, eluting with ethyl acetate/petroleum spirits (5 : 17). Two minor yellow (1st and 2nd yellow), a major yellow (3rd yellow) and orange (orange) bands at R_F 0.89, 0.83, 0.71 and 0.63, respectively, were collected individually in a sintered glass funnel and extracted with CH_2Cl_2, the solvent was removed and the residues were dried under vacuum for 4 hours. Crystallisation from CH_2Cl_2/petroleum spirits at –20 °C afforded a white from the 1st, yellow from the 2nd yellow and red crystals from the orange bands. The yellow needle obtained from the 2nd yellow band was identified as the azabutadiene **16** by XRD. The melting point was also determined and was ~100 °C. The orange band was identified as the unreacted complex **13** by IR, ESI and NMR analyses. Crystallisation by vapour diffusion from CH_2Cl_2/*n*-pentane at –20 °C gave the compounds **34** and **35** as a mixture of yellow crystals from the 3rd yellow band.

Crystallisation from petroleum spirits (20 mL) at –20 °C provided a yellow solid from the crude yellow solid (not chromatographed), which was, again, the mixture of the

compounds **34** and **35** and the azabutadiene **16** shown by NMR analysies. Attempts were made to grow single crystals of the compound **34** and **35** by vapour diffusion from CH_2Cl_2/*n*-pentane at –20 ºC from the crude product, but could not be obtained. The solvent combinations attempted included CH_2Cl_2/*n*-pentane, $CHCl_3$/hexane, benzene/petroleum spirits and the samples were kept at room temperature, in the refrigerator or in the freezer. Single crystals which were suitable for XRD determination could not, however, be prepared.

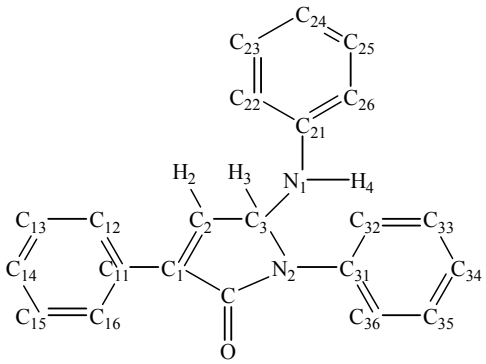

34

Description:		Yellow blocks
Formula*:*		$C_{22}H_{18}N_2O_1$
Mr:		326.39
IR:	(CH_2Cl_2)	υ(C=O) 1712 (s) cm^{-1}
ESI-MS:		
(MeOH/NaOMe, cone 20 V, +ve ion)		*m/z* 675 (10 %, $[2M + Na]^+$), 349 (100 %, $[M + Na]^+$), 327 (5 %, $[M + H]^+$)
	(-ve ion)	*m/z* 357 (70 %, $[M + OMe]^-$), 325 (100 %, $[M – H]^-$)
^{1}H NMR:	(400 MHz, $CDCl_3$)	δ 7.92 (dd, $^3J_{HH}$ = 6.52 Hz, 2 H), 7.30 (d, $^3J_{HH}$ = 2.6 Hz), 7.52 (d), 7.44 (m), 7.41 (m), 7.39 (m), 7.19 (t, $^3J_{HH}$ = 7.3 Hz), 7.17 (m), 6.82 (t, $^3J_{HH}$ = 7.30 Hz, 1 H), 6.68 (d, $^3J_{HH}$ = 7.8 Hz, 2 H), 6.10 (dd, $^{3,4}J_{HH}$ = 9.39, 1.72 Hz, 1 H), 3.98 (d, $^3J_{HH}$ = 10.6 Hz, 1 H) ppm
^{13}C NMR:	(400 MHz, $CDCl_3$)	δ 168.0, 138.1, 137.8, 136.6, 130.6, 129.5, 129.3, 128.9, 127.6, 125.7, 123.2, 123.2, 119.9, 118.8, 115.0, 70.1 ppm

Formula*:*		$C_{29}H_{23}N_3O_2$
Mr:		445.51
IR:	(CH_2Cl_2)	υ(C=O) 1715 (m, br, as a shoulder of the 1712 cm^{-1} peak)
		υ(C=N) 1676 (m), 1629 (s) cm^{-1}
ESI-MS:		
(MeOH/NaOMe, cone 20 V, +ve ion)		*m/z* 447 (100 %, $[M + H]^+$)
HR-MS:	(MeOH, +ve ion)	*m/z* 447.189 (calcd. *m/z* 447.194 for $[(Ph_2C_3NH_3)(PhNCO)_2H + H]^+$), 235.0896 (calcd. *m/z* 235.099 for $[(Ph_2C_3NH_2)(CO) + H]^+$)
^{1}H NMR:	(400 MHz, $CDCl_3$)	δ 7.96 (m), 7.43 (m), 7.37, 7.19, 7.15, 7.07, 6.98 ppm
^{13}C NMR:	(400 MHz, $CDCl_3$)	δ 169.37, 154.83, 148.21, 140.51, 133.11, 130.58, 129.68, 128.39, 128.38, 124.83, 121.93, 118.86 ppm

3.4.1.5 Reaction with Methyl Acrylate, CH_2=$CHCO_2Me$

Experimental: The progress of the reaction was monitored by IR spectroscopy in CH_2Cl_2/heptane.

In a nitrogen-flushed Schlenk flask, CH_2=$CHCO_2Me$ (0.024 mL, 0.27 mmol) was added to a solution of the complex **13** (153 mg, 0.22 mmol) in distilled heptane (20 mL). With continuous stirring, the clear red reaction mixture was heated in an oil bath at 100 – 110 °C for 7½ hours. The development of new peaks at 2017, 1897 and 1727 $cm^{-1}$was observed in the υ(C≡O) region of the IR spectrum. After 4 hours above 100 °C, extra MeO_2CCH=CH_2 (approx. 0.02 mL) was added as no further reaction progress was observed in the IR spectrum. Heating was continued for another 3 hours 15 minutes. The mixture turned dark red and precipitation of a black (major) and dark red solid (minor) was observed. The mixture was cooled to room temperature with

stirring. The solvent was removed and the residue was dried under vacuum for 11 hours. NMR analyses on the residue in $CDCl_3$ indicated that it was a mixture of products (minor signals) and the azabutadiene **16** (major signals). The residue was, therefore, chromatographed on a PLC plate, eluting with CH_2Cl_2/petroleum spirits (3 : 2). It, however, streaked and no satisfactory separation was achieved. Although the separation was not satisfactory, weak yellow and orange bands at R_F 0.92 and 0.78, respectively, were collected individually in a sintered glass funnel and extracted with CH_2Cl_2. The fractions were analysed by IR and ESI-MS analysis. Crystallisation by vapour diffusion from CH_2Cl_2/petroleum spirits at –20 °C provided a very small amount of yellow solid **36** and red solid **37** from the yellow and orange bands, respectively.

Crystallisation from Et_2O/petroleum spirits 40 – 60 °C at –20 °C provided a brown oil with a small amount of red and black solids from the crude product. Crystallisation from petroleum spirits (20 mL) in the refrigerator, which was concentrated to ~ 5 mL after dichloromethane was evaporated away, provided a red solid with a minor amount of a brown oil. Less intense signals for the azabutadiene **16** and slightly stronger signals corresponding to the products were observed in the NMR spectra of the red solid (red solid) in $CDCl_3$.

36

Description: Yellow fraction

IR: (CH_2Cl_2) υ(C≡O) 2016 (s), 1895 (s) cm^{-1}
υ(C=O) 1724 (w), 1585 (m) cm^{-1}

ESI-MS:

(MeOH/NaOMe, cone 20 V, -ve ion) *m/z* 562 (97 %, $[M_1 - H]^-$), 291 (50 %, $[M_1 - Re(CO)_3 - H]^-$), ($M_1 = Ph_2C_3H_3N + Re(CO)_3 + C_2H_2C(O)OMe$)

37

Description: Orange fraction

IR: (CH_2Cl_2) υ(C≡O) 2016 (s), 1895 (s) cm^{-1}
υ(C=O) 1724 (w), 1585 (m) cm^{-1}

ESI-MS:

(MeOH/NaOMe, cone 20 V, -ve ion) *m/z* 648 (50 %, $[M_2 - H]^-$), 677 (100 %, $[M_2 + OMe]^-$) ($M_2 = Ph_2C_3H_3N + Re(CO)_3 + 2 \times C_2H_2C(O)OMe - H$)

Crude product

^{1}H NMR: (400 MHz, $CDCl_3$) δ 7.50? (d), 7.18 (m), 6.78 (m, 1 H), 6.73 (m, 2 H), 6.68 (d, $^3J_{HH}$ = 8.2 Hz, 2 H), 6.17 (d, $^3J_{HH}$ = 2.3 Hz, 1 H), 4.63 (m, br, 1 H), 4.38 (d, $^3J_{HH}$ = 10 Hz, 1 H), 4.01 (d, $^3J_{HH}$ = 7.6 Hz, 1 H), 3.58 (s, 3 H), 3.14 (dd, $^{2,3}J_{HH}$ = 22.9, 7.24 Hz, 1 H), 2.89 (dd, $^{2,3}J_{HH}$ = 21.7, 7.44 Hz, 1 H) ppm

^{13}C NMR: (400 MHz, DEPT, $CDCl_3$) δ 197.16 (C), 171.78 (C), 144.57 (C), 134.60 (C), 133.7 (C), 128.58 (CH), 128.39 (CH), 128.30 (CH), 121.57 (CH), 119.01 (CH), 117.97 (CH), 115.52 (CH), 115.42 (CH), 113.83 (CH), 113.79 (CH), 55.45 (CH), 55.42 (CH), 54.04 (CH), 53.99, 51.85 (CH), 51.84 (CH_3), 39.87 (CH_2) 39.84 (CH_2) ppm

3.4.2 X-Ray Crystallography

Table 3-13: Crystal Data and Refinement Details for the Complex **32**

	32
Empirical Formula	$C_{26}H_{18}NO_3Re$
M_r	578.61
T / K	83(2)
Wavelength / Å	0.71073
Crystal System	Monoclinic
Space Group	C2/c
***a* / Å**	22.3672(8)
***b* / Å**	10.9716(4)
***c* / Å**	17.0784(6)
α / º	90
β / º	93.127(1)
γ / º	90
V / Å^3	4184.9(3)
Z	8
ρ / g cm^{-3}	1.837
μ / mm^{-1}	5.836
F (000)	2240
Crystal Size / mm^3	0.40 × 0.18 × 0.15
θ range / º	2.41 to 31.75
Limiting Indices	-32 ≤ h ≤ 32, -15 ≤ k ≤ 15, -23 ≤ l ≤ 14
Reflection Collected	13176
Unique Reflections	6166 (R_{int} 0.0274)
Completeness to θ º (%)	31.75 (86.6)
Absorption Correction	Empirical
T_{max} and T_{min}	0.4748 and 0.2036
Refinement Method	Full-matrix least-squares on F^2
Data / Restrains / Parameters	6166 / 0 / 280
GoF on F^2	1.015
Final R Indices [I > 2σ(I)]	R_1 0.0273, wR_2 0.0470
R Indices (all data)	R_1 0.0465, wR_2 0.0515
Largest Diff. Peak and Hole / eÅ^{-3}	0.925 and -0.893

Chapter 4

4.1 General Experimental Procedures and Materials

4.1.1 General Experimental Techniques

Oxygen or moisture-sensitive compounds were handled under an inert atmosphere of dry nitrogen using the standard Schlenk line techniques[64]. Unless otherwise, specified, the compounds prepared in the present study were handled without any special precautions at room temperature under normal atmosphere.

The reactions were heated in a silicone oil bath with a thermostatted heating coil.

Melting points were determined on a Reichert Thermovar apparatus.

Elemental analyses were performed at the University of Otago at the Campbell Microanalytical Laboratory.

4.1.1.1 Schlenk Lines

Schlenk line was performed following an established Schlenk line procedure. The solvents were degassed by inducing boiling at low pressures and introducing dry gaseous nitrogen several times. The solvents were removed and concentrated by inducing boiling at low pressures and the samples were dried at the low pressures for the appropriate duration of time.

4.1.1.2 Chromatography

Thin layer chromatography was performed on a 70 × 15 mm TLC strip cut out from a 200 × 200 mm TLC aluminium sheet of Merck Kieselgel 60 F_{254} silica gel purchased from Merck and eluted in a beaker containing the solvent mixture of the appropriate ratio.

Preparative layer chromatography (PLC) plates were prepared by the established method as follows. Silica gel (140 g, Merck Kieselgel 60 PF_{254}, weighed on a Triple Beam Balance) was mixed with distilled water (250 mL, measured in a 500 mL glass cylinder) and the mixture was shaken vigorously to make a smooth slurry. The slurry was deposited on a 200 × 200 mm glass plate to a depth of 1 – 1.5 mm, allowed to air dry overnight and then activated in an oven at 120 ºC for at least 24 hours. The plate was removed for atmospheric equilibration at least 18 hours before use. A UV lamp employing the wavelengths of 254 and 312 nm was used to view the colourless fractions which were not, otherwise, visible under a room light.

The samples were dissolved in CH_2Cl_2 and applied at the bottom of the PLC plate as a thin line by a glass pipette. The plate was developed in a tank containing the solvent mixture of the appropriate ratio. The bands were removed by scraping with a steel knife and the products were extracted with CH_2Cl_2 in a sintered glass (SINTA GLASS 2), which was dried overnight in an oven at 120 ºC and allowed to cool for 2 – 3 hours before use, and collected in a round-bottomed flak under normal atmosphere.

4.1.2 Instrumentation

4.1.2.1 FTIR

Fourier Transform Infrared Spectroscopy (FTIR) was performed on a Digilab Scimitar FTS 2000 series spectrometer using Varian Resolution software version 4.1.0.101. Solution IR was carried out in an IR cell with 0.1 mm path length between two KBr windows. Solid state IR was obtained as a KBr disc prepared by finely grinding sample with a KBr powder dried in an oven at 100 ºC and pressured in a device at 8 tons for several minutes.

FTIR of single crystals was obtained on a Spectrum Spotlight 200 Spectrometer FT-IR Microscope using Spectrum version 6.3.1. The sample was placed on a CaF_2 window which had the spectral cut off of 1100 cm^{-1} and the spectra were recorded in transmission mode using a microscope attachment in the air as background.

4.1.2.2 ESI-MS

Electrospray ionisation mass spectrometry was performed on a Fisons Instruments VG Platform II spectrometer using MassLynx software version 2.0. The samples were run in MeOH as mobile phase at 60 ºC as the source temperature and also cone voltage of 20 V unless, otherwise, specified, in both positive and negative ion modes. The isotope pattern spectra were obtained with a low and high mass resolution (LM and HM resolution) of 13.5 – 15 and a gain of 4000 in the spectral window of *m/z* 20 within the desired peak.

High-resolution mass spectrometry (HR-MS) was carried out on a Bruker Daltonics MicrOTOF spectrometer using DataAnalysis software version 3.3. The samples were run in MeOH and with NaOMe as required.

A few drops of dichloromethane (drum grade) before addition of MeOH and sodium methoxide/methanol solution were added to the samples when the compounds were not very soluble in MeOH or to enhance ionisation[65]. The methanol solution of NaOMe was prepared by adding a small piece of sodium metal in methanol (drum grade) and used within two weeks or freshly prepared as required.

4.1.2.3 NMR

Nuclear magnetic resonance (NMR) was performed on either a Bruker Avance DRX 300 or a Bruker Avance DRX 400 spectrometer using Topspin software version 1.3. Chemical shifts were reported in ppm relative to tetramethylsilane (Me_4Si). The samples were run in $CDCl_3$ (Chloroform-*d*, 99.8 atom % D, Aldrich) which was used as received. The *J* and d values used for the 1D and 2D experiments used for the samples were specified in the appropriate results and discussion sections.

4.1.2.4 XRD

A full X-ray crystal structure determination (XRD) was performed at the University of Auckland or the University of Canterbury. The X-ray intensity data were collected on a Siemens SMART CCD diffractometer using standard procedures and softwares. The structures were solved by direct methods, developed and refined on F^2 using the SHELX program[66] running under the WINGX[67].

Preliminary investigations were also carried out by precession photography using nickel-filtered Cu-Kα X-ray radiation which allowed the determination of space group and unit cell dimensions and also an indication of crystal quality.

4.1.3 Chemicals

Unless, otherwise, specified below, the solvents were all drum grade and the solvents and chemicals were used as received. The purified and HPLC grade solvents were listed in the table below with the methods of the purification and the commercial suppliers, respectively.

Table 4-1: Purification Methods and Commercial Suppliers

Solvent	**Method of Purification & Commercial Suppliers**
Tetrahydrofuran (thf)	SPS
Distilled Heptane	Distilled from CaH_2
Hexane	SPS
Diethyl ether	SPS
Ethyl acetate	Ajax Finechem
Petroleum spirits 60 – 80 ºC	Ajax Finechem
Petroleum spirits 40 – 60 ºC	Ajax Finechem
n-Pentane	Ajax Finechem
Chloroform	Ajax Finechem
Methanol	Ajax Finechem
Ethanol	Ajax Finechem

Distillation was carried out under a nitrogen atmosphere. SPS refers to the PureSolv solvent purification system model SP-SD-5 which supplies dry deoxygenated solvents suitable for the moisture and oxygen sensitive chemical reactions. The HPLC grade solvents were used as received.

The table below lists the reagents used in the present study with the names of the commercial suppliers if commercial, and the methods of storage.

Table 4-2: Chemical Suppliers and Methods of Storage

Chemicals	**Storage**	**Supplier**
$[Re_2(CO)_{10}]_2$	Room temperature	Strem Chemicals
$PhCH_2Br$	In the Solvent Cabinet	Sigma-Aldrich
Na_2SO_4	Room temperature	Sigma-Aldrich
Cinnamaldehyde	Room temperature	Sigma-Aldrich
Aniline	Room temperature	Sigma-Aldrich
4-Fluoroaniline	Room temperature	Sigma-Aldrich
4-Dimethyl aminocinnamaldehyde	In the Freezer	Sigma-Aldrich
p-Toluidine	Room temperature	Sigma-Aldrich
PhC≡CH	In the Refrigerator	Sigma-Aldrich
$MeOC_6H_4N{\equiv}C$	In the Freezer	Prepared by Corry[68]
PhNCO	In the Refrigerator	Sigma-Aldrich
$CH_2{=}CHCO_2Me$	In the Refrigerator	Sigma-Aldrich

Aniline was freshly distilled at 184 – 190 ºC (lit.[69] 184 ºC) prior to use. The other reaction precursors including $PhCH_2Re(CO)_5$, the compound **13** and the azabutadienes **16**, **17** and **18** were stored at –20 ºC until needed.

All the compounds prepared in this study were also stored at –20 ºC until needed.

References

[1] Martinho Somões, J. A.; Minas da Piedade, M. E. In *Comprehensive Organometallic Chemistry III*; Parkin, G, Ed.; Elsevier: Amsterdam, London, 2007; pp 625-628.

[2] Bruce, M. I., *Angew. Chem. Int. Ed. Engl*. **1977**, 16, 73-86.

[3] Wikipedia. http://en.wikipedia.org/wiki/Metallocycle (accessed November 2008).

[4] Wikipedia. http://en.wikipedia.org/wiki/Carbon-hydrogen_bond_activation (accessed November 2008).

[5] Main, L.; Nicholson, B. K., In *Advances in Metal-Organic Chemistry*, Liebeskind, L. S., (Ed.) 1994; Vol. 3, pp 1-50.

[6] Hanusa, T. P. In *Encyclopedia of Inorganic Chemistry*; King, R. B, (Ed.); Wiley: New York, 2005; pp 1242.

[7] Omae, I., *Organometallic Intramolecular-Coordination Compounds*; Elsevier: Amsterdam, 1986 (*J. Organomet. Chem. Library, 18*).

[8] Ryabov, A. D., *Chemical Reviews* **1990**, 90, 403-424,

[9] Omae, I., *Coord. Chem. Rev.*, **1988**, 83, 137-167.

[10] Omae, I., *Coord. Chem. Rev.*, **2004**, 248, 995-1023.

[11] Dehand, J.; Pfeffer, M., *Coord. Chem. Rev.*, **1976**, 18, 327-352.

[12] Parshall, G. W., *Acco. Chem. Res.*, **1970**, 3, 139-144.

[13] Lindner, E.; Starz, K. A.; Hoehne, S., *Zeits. Naturforsch Teil B* **1982**, 37b, 1301.

[14] Ng, J. K.-P.; Tan, G.-K.; Vittal, J. J.; Leung, P.-H., *Inorg. Chem.*, **2003**, 42, 7674-7682.

[15] Depree, G. J.; Childerhouse, N. D.; Nicholson, B. K., *J. Organomet. Chem*. **1996**, 533, 143-151.

[16] DeShong, P.; Slough, G. A.; Sidler, D. R.; Rybczynski, P. L., *Organometallics*. **1989**, 8, 1381-1388.

[17] Revell, J. B., M.Sc. Thesis, University of Waikato, Hamilton, N.Z., 2008.

[18] Brown, S. D. J.; Henderson, W.; Kilpin, K. J.; Nicholson, B. K., *Inorg. Chimi. Acta*. **2006**, 360, 1310-1315.

[19] Leeson, M. A.; Nicholson, B. K.; Olsen, M. R., *J. Organomet. Chem*. **1999**, 579, 243-251.

[20] Morris III, W. H.; Sullivan, L. M.; Wellons, M. S.; Lukehart, C. M., In *Encyclopedia of Inorganic Chemistry*; King, R. B., (Ed.); Wiley: New York, 2005; pp 3936.

[21] Constable, E. C., *Polyhedron*. **1984**, 3, 1037.

[22] Trofimenko, S., *Inorg. Chem*. **1973**, 12, 1215.

[23] Bruce, M. I.; Liddell, M. J.; Snow, M. R.; Tiekink, E. R. T., *Aust. J. Chem*. **1988**, *41*, 1407.

[24] Bennett, R. L.; Bruce, M. I.; Goodall, B. L.; Stone, F. G. A., *Aust. J. Chem*. **1974**, *27*, 2131.

[25] Bennett, R. L.; Bruce, M. I.; Matsuda, I., *Aust. J. Chem*. **1975**, *28*, 1265.

[26] Little, R. G.; Doedens, R. J., *Inorg. Chem*. **1973**, *12*, 840; 844.

[27] McKinney, R. J.; Hoxmeier, R.; Kaesz, H. D. *J. Amer. Chem. Soc.*, **1975**, *97*, 3059.

[28] McKinney, R. J.; Kaesz, H. D. *J. Amer. Chem. Soc*., **1975**, *97*, 3066.

[29] McKinney, R. J.; Firestein, G.; Kaesz, H. D. *Inorg. Chem.*, **1975**, *14*, 2057.

[30] Knobler, C. B.; Crawford, S. S. Kaesz, H. D., *Inorg. Chem.*, **1975**, *14*, 2062. See also McKinney, R. J.; Crawford, S. S., *Inorg. Syntheses.*, **1989**, *26*, 155.

[31] Crawford, S. S.; Kaesz, H. D., *Inorg. Chem.*, **1977**, 16, 3193.

[32] Cabral, A. W., PhD. Thesis, University of California, Los Angeles. 1981.

[33] Haupt, H. J.; Lohmann, G.; Florke, U. Z., *Anorg. Allg. Chemie.*, **1985**, 526, 103.

[34] DeShong, P.; Slough, G. A.; Sidler, D. R.; Rybczynski, P. J.; von Philipsborn, W.; Kunz, R. W.; Bursten, B. E.; Clayton, T. W., *Organometallics*, **1989**, 8, 1381.

[35] Verboom, W.; Reinhoudt, D. N. *Rev. Trav. Chim. Pays-Bas*, **1986**, 105, 199.

[36] Liebeskind, L. S.; Johnson, S. A.; McCallum, J. S. *Tetrahedron Letters*, **1990**, 31, 4397.

[37] DeShong, P.; Sidler, D. R.; Rybczynski, P. J.; Slough, G. A.; Rheingold, A. L., *J. Amer. Chem. Soc.*, **1988**, 110, 3575.

[38] Depree, G. J.; Main, L.; Nicholson, B. K., *J. Organomet. Chem*. **1998**, 551, 281.

[39] Cooney, J. M.; Depree, C. V.; Main, L.; Nicholson, B. K., *J. Organomet. Chem*. **1996**, 515, 109.

[40] Harbourne, D. A.; Stone, F. G. A., *J. Chem. Soc. (A)*, **1968**, 1765.

[41] Booth, B. L.; Hargreaves, R. G. *J. Chem. Soc. (A)*, **1969**, 2766.

[42] Booth, B. L.; Hargreaves, R. G. *J. Chem. Soc. (A)*, **1970**, 308.

[43] Tully, W.; Main, L.; Nicholson, B. K., *J. Organomet. Chem.*, **1996**, *507*, 103.

[44] (a) DeShong, P.; Slough, G. A. *Organometallics*., **1984**, *4*, 636; (b) DeShong, P.; Slough, G. A.; Elango, V., *J. Amer. Chem. Soc.*, **1985**, *107*, 7788; (c) DeShong, P.; Slough, G. A.; Rheingold, A. L., *Tetrahedron Lett*., **1987**, *28*, 2229; (d) DeShong, P.; Sidler, D. R.; Slough, G. A., *Tetrahedron Lett*., **1987**, *28*, 2232.

[45] Tully, W.; Main, L.; Nicholson, B. K., *J. Organomet. Chem.*, **1995**, *503*, 75.

[46] Tully, W. M. Sc. Thesis, University of Waikato, Hamilton, 1990.

[47] Mace, W. J., Ph.D. Thesis, University of Waikato, Hamilton, 2003.

[48] Mace, W. J.; Main, L.; Nicholson, B. K.; Van de Pas, D. J., *J. Organomet. Chem*. **2004**, *689*, 2523-2530.

[49] Groenendaal, B.; Ruijter, E.; Orru, R. V. A., *Chem. Commun*. **2008**, 5474-5489.

[50] Heller, B.; Hapke, M., *Chem. Soc. Rev*. **2007**, *36*, 1085-1094.

[51] Stamp, L.; Dieck, H. T., *Inorg. Chim. Acta*., **1988**, *147*, 199-206.

[52] Otsuka, S.; Yoshida, T.; Nakayama, A. *Inorg. Chem*. **1967**, *6*, 20.

[53] Adams, R. D.; Huang, M. Organometallics. **1995**, *14*, 506.

[54] Homrighausen, C. L.; Alexander, J. A.; Krause Bauer, J. A., *Inorg. Chim. Acta*., **2002**, *334*, 419.

[55] Polm, L. H.; Mul, W. P.; Elsevier, C. J.; Vrieze, K.; Christopherson, M. J. N.; Stam, C. H.,

Organometallics. **1988**, *7*, 423; Mul, W. P.; Elsevier, C. J.; Smeets, W. J. J.; Spek, A. L., *Inorg. Chem.*, **1991**, *30*, 4152; Elsevier, C. J.; Mul, W. P.; Vrieze, K.; *Inorg. Chim. Acta*., **1992**, *198*, 689.; Imhofm W, *J, Chem. Soc*., Dalton Trans. **1996**, 1429.

[56] Tenreiro, S.; Alberdi, G.; Martinez, J.; Lopez-Torres, M.; Ortigueira, J. M.; Pereira, M. T.; Vila, J. M., *Inorg. Chim. Acta*., **2003**, *342*, 145-150.

[57] Nielson, J. Unpublished data, Undergraduate Project, University of Waikato, Hamilton, N.Z., 2006.

[58] Knölker, H.-J.; Baum, G.; Foitzik, N, Goesmann, H.; Gonser, P.; Jones, P. G.; Röttele, H., *Eur. J. Inorg. Chem.*, **1998**, 993-1007.

[59] Derinkuyu, S.; Ertekin, K .; Oster, O.; Denizalti, S.; Cetinkaya, E., *Ana. Chimi. Acta*. **2007**, 588, 42-49.

[60] Fresenius, W.; Huber, J. F. K.; Pungor, E.; Rechnitz, G. A.; Simon, W.; West, Th. S. (Eds.), *Tables of Spectral Data for Structure Determination of Organic Compounds*, 2nd ed.; Springer-Verlag: Berlin; New York, 1989.

[61] Braterman, P. S., *Metal Carbonyl Spectra*; Academic Press: London; New York, 1975.

[62] Al-Rawi, J. M. A.; Saleem, L. M. N., *Spect. Lett.* **1991**, 24(1), 161-171.

[63] Silverstein, R. M., *Spectrometric Identification of Organic Compounds*; John Wiley & Sons: Hoboken, NJ, 2005.

[64] Shriver, D. F.; Drezdzon, M. A., *The Manipulation of Air-Sensitive Compounds*; 2nd Ed., John Wiley & Sons: New York, 1986.

[65] Henderson, W.; McIndoe, J. S.; Nicholson, B. K.; Dyson, P. J., *J. Chem. Soc.*, Dalton Trans., **1998**, 519.

[66] Sheldrick, G. M, SHELX-97 Programs for the Solution and Refinement of Crystal Structures, University of Goettingen, Germany, 1997. (Release 97-2).

[67] Farrugia, L. J., WinGX – Version 1.64.05, Department of Chemistry, University of Glasgow; Farrugia, L. J., *J. Appl. Cryst*., **1999**, *32*, 837.

[68] Decker, C., Ph.D. Thesis, University of Waikato, Hamilton, 2002.

[69] O'Neil, M. J.; Merck Research Laboratories. *The Merck Index: An Encyclopedia of Chemicals, Drugs, and Biologicals*; Whitehouse Station, N.J.; Merck Research Laboratories. 2001.

List of Numbered Compounds

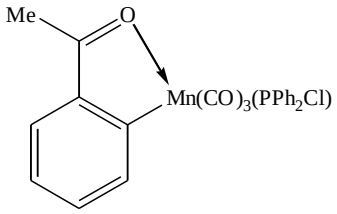

1

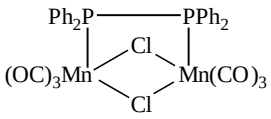

2

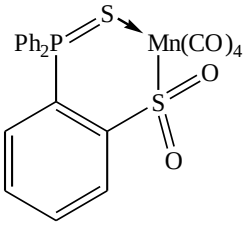

3

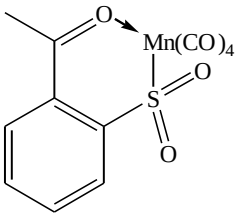

4

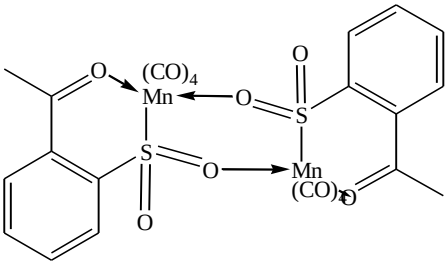

5

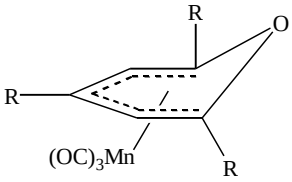

6

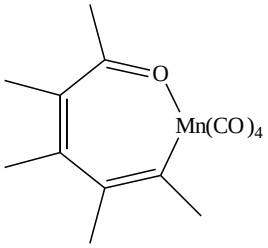

7

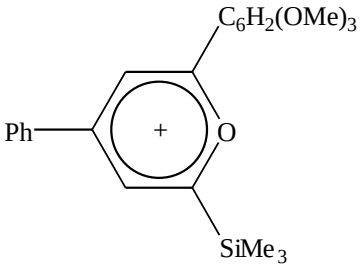

8

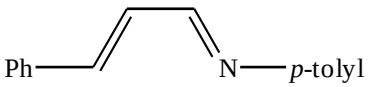

9

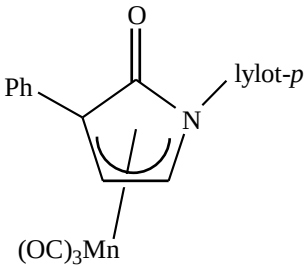

10

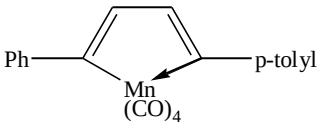

11

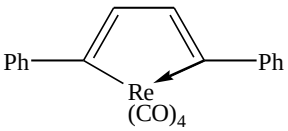

12

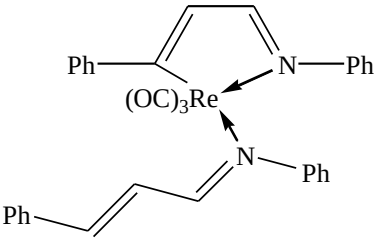

13

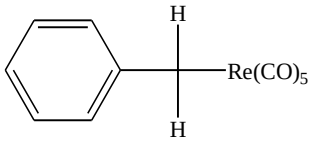

14

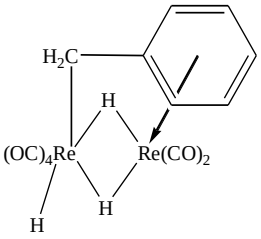

15

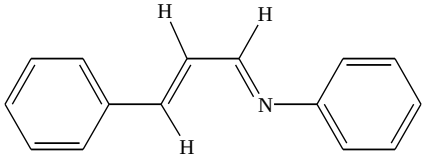

16

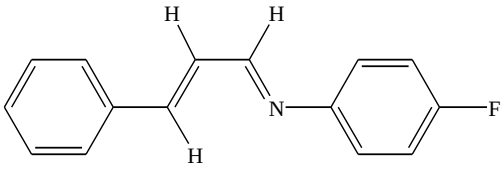

17

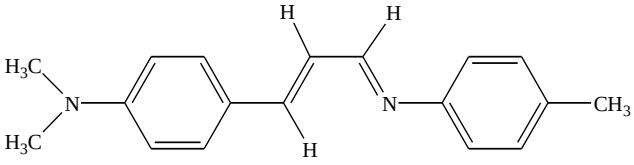

18

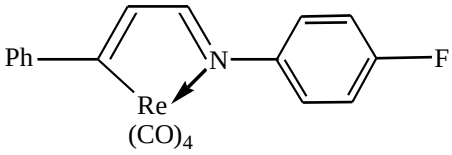

19

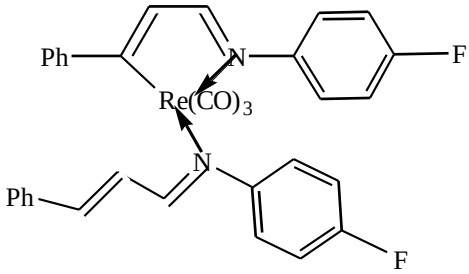

20a

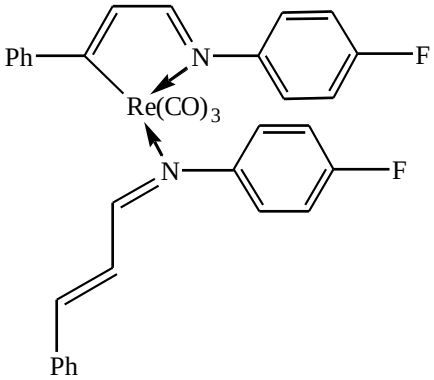

20b

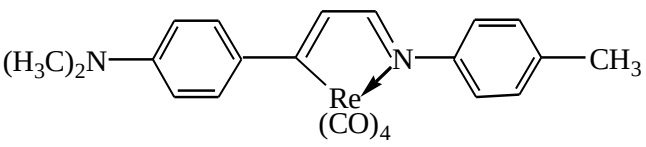

21

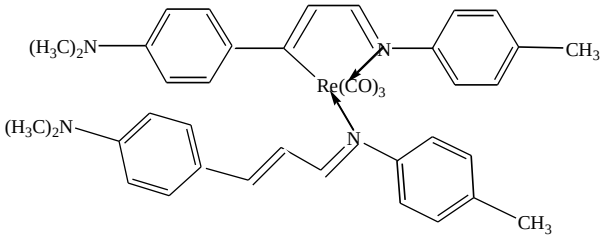

22a

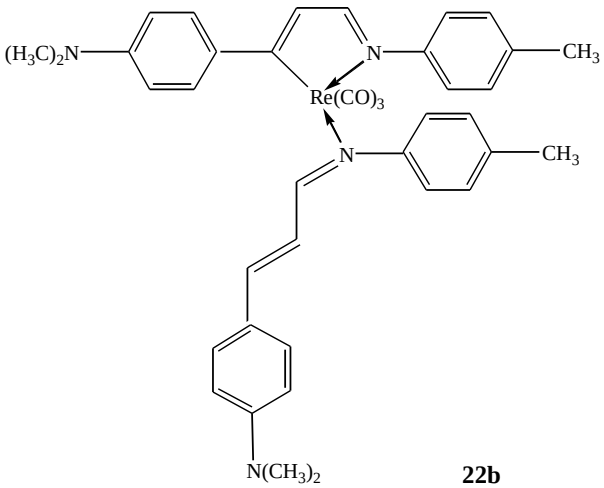

22b

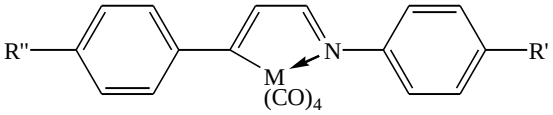

23

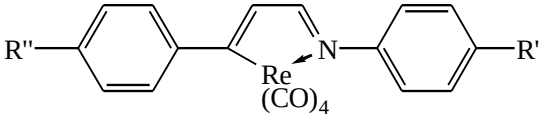

R'= CH_3, F; R" = $N(CH_3)_2$

24

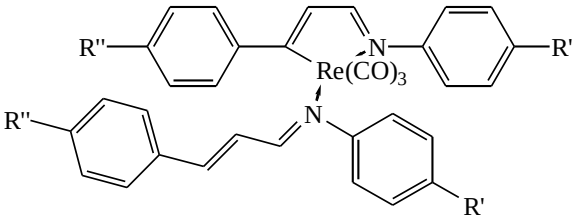

R'= CH_3, F; R" = $N(CH_3)_2$

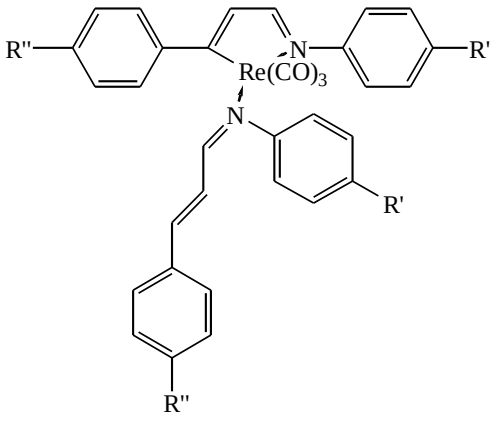

25

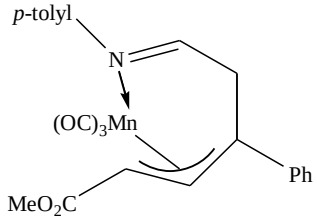

26

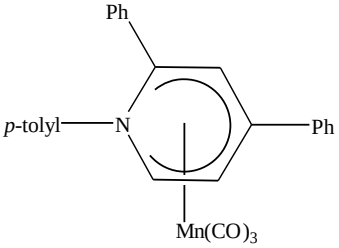

27

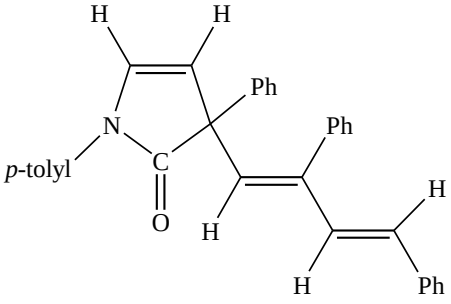

28

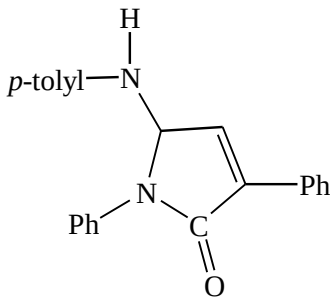

29

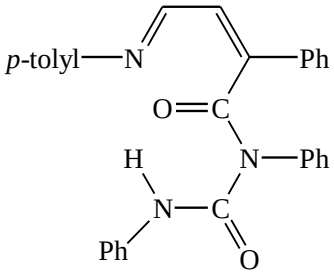

30

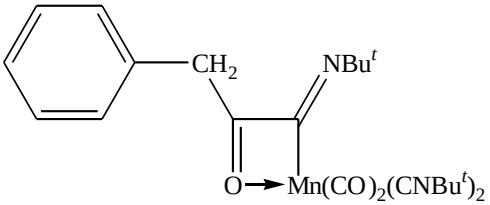

31

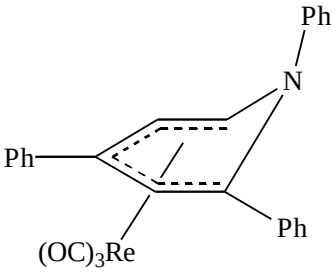

32

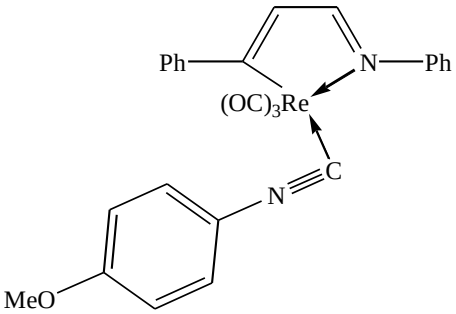

33

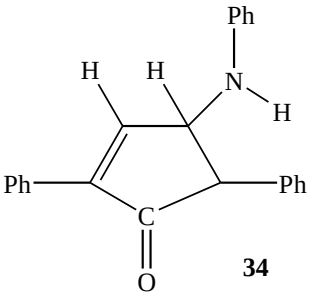

34

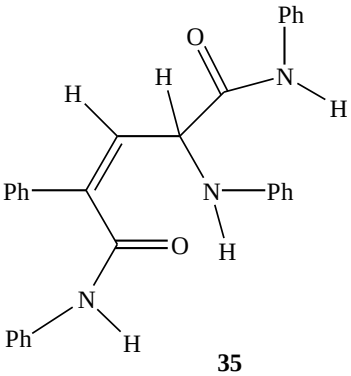

35

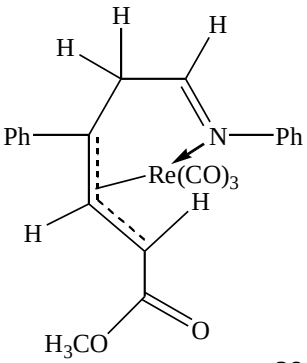

36

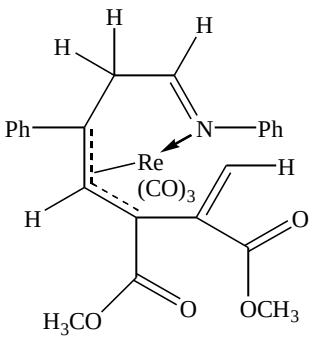

37

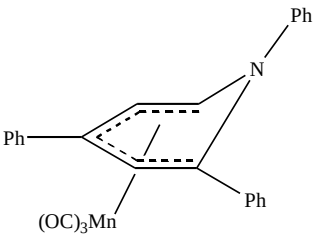

38